UNIVERSITÉ DE STRASBOURG

ÉCOLE DOCTORALE DE SCIENCES CHIMIQUES (ED 222)

INSTITUT CHARLES SADRON (UPR22-CNRS)

THÈSE présentée par :

Yali ZENG

soutenue le : **06 Juillet 2020**

pour obtenir le grade de : **Docteur de l'université de Strasbourg**

Discipline/ Spécialité : Chimie supramoléculaire

Vers une efficace mise en œuvre de la ligation chimique native dynamique

THÈSE dirigée par :

M. GIUSEPPONE Nicolas Professeur, Université de Strasbourg – ICS - CNRS

RAPPORTEURS :

M. BARBOIU Mihail DR-CNRS, Institut Européen des Membranes, Montpellier

M. COLOMBANI Olivier MCF, Institut des Molécules et Matériaux du Mans

---

AUTRES MEMBRES DU JURY :

Mme CHAN-SENG Delphine CR-CNRS, Institut Charles Sadron, Strasbourg

RESUME

La chimie combinatoire dynamique (DCC) est une approche évolutive permettant de générer de la diversité chimique à la fois aux niveaux moléculaires et supramoléculaires (Figure 1).[1,2] La DCC met ainsi en jeu aussi bien des interactions non-covalentes intermoléculaires que des interactions covalentes intramoléculaires. Au niveau intermoléculaire, le concept de la chimie supramoléculaire (dynamique non covalente) dont la dynamique permet l'association et la dissociation réversibles entre molécules, a été proposé. Cependant, la présence de liaisons non covalentes faibles empêche son utilisation dans de nombreuses applications qui nécessitent une grande robustesse. La chimie covalente dynamique (DCvC) est apparue comme une alternative, qui permet l'échange réversible de liaisons covalentes au niveau moléculaire en mettant en jeu des énergies libres plus importantes que celles nécessaires à la rupture de liaisons supramoléculaires.[3–5]

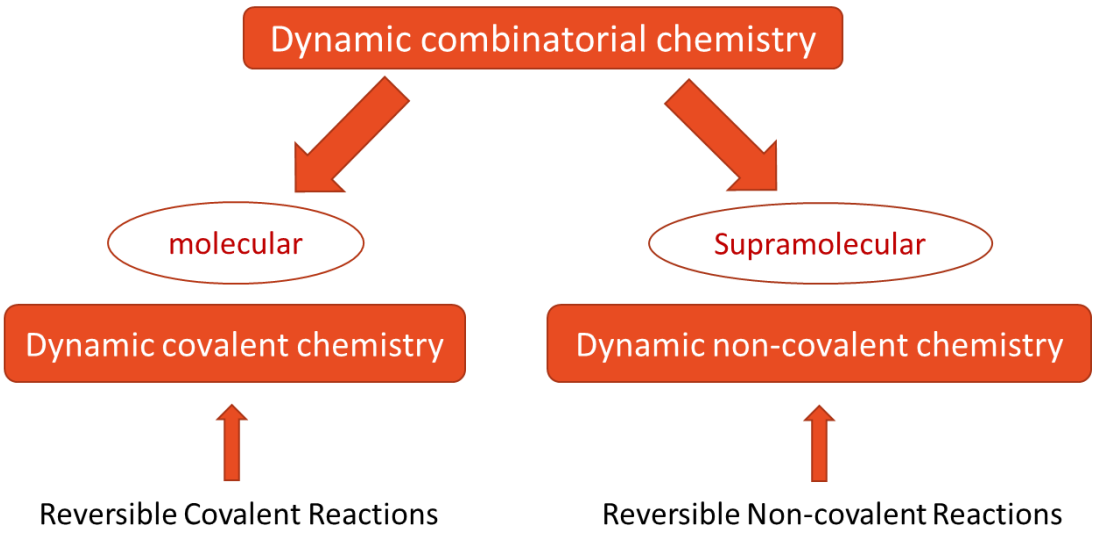

Figure 1 | Représentation schématique des différents concepts mis en jeu en chimie combinatoire dynamique.

La DCvC s'appuie sur des liaisons covalentes dynamiques qui permettent le libre échange de briques de base qui constituent la bibliothèque combinatoire dynamique (DCL)[6]. En pratique, de nombreuses liaisons covalentes dynamiques existent comme par exemple, la liaison disulfure qui confère des structures tertiaires/quaternaires bien définies aux protéines,[7] l'échange thiol-thioester qui joue un rôle

primordial dans la biosynthèse des polycétides[8] , ou encore la liaison imine qui s'avère essentielle dans la chimie de la vision.[8] La découverte de nouvelles méthodologies permettant d'accéder à divereses réactions covalentes dynamiques a conduit au développement rapide de la DCvC.[9]

En 2014, en se fondant sur la ligation chimique native (NCL), notre équipe a mis au point une nouvelle méthodologie permettant d'accéder à la liaison amide réversible dans des conditions douces et à des échelles de temps raisonnables afin de concevoir des bibliothèques des peptides dynamiques (dynPL) (Figure 2a).[10] La méthode développée, intitulée ligation chimique native covalente dynamique (dcNCL), implique l'utilisation de résidus de *N*-alkyl Cysteine (Cys) qui permettent à des fragments peptidiques de s'échanger dynamiquement. Par exemple, en présence de dithiothréitol (DTT) à pH compris entre 6 et 9, le résidu *N*-thioéthyl Cys (Daa1) présent au sein du peptide **P1**-Daa1-**P2** et sur la partie C-terminale du peptide Daa1-**P3** confère la dynamique nécessaire pour accéder aux dérivés peptidiques **P1**-Daa1-**P3** et Daa1-**P2** (Figure 2b) selon le mécanisme décrit en Figure 2a. De plus, afin d'envisager l'utilisation de cette méthodologie pour des peptides présentant un intérêt biologique, nous avons démontré que la *N*-méthyl-cystéine (***N*MeCys,** Daa2), qui est un acide aminé non ribosomal se trouvant dans les produits naturels, permet également l'échange de segments peptidiques (Figure 2b).

Cependant, la méthodologie développée initialement implique plusieurs contraintes : i) la bibliothèque de peptides doit être maintenue sous atmosphère inerte et en présence des tampons dégazés pour limiter l'oxydation du groupe thiol ; ii) la préparation des échantillons peut nécessiter 3-4 heures et la période d'équilibration (half-time) est d'au moins 10 heures ; iii) la présence d'hydrolyse au niveau de la liaison thioester limite le rendement d'échange. Afin de pouvoir mettre en œuvre la dcNCL au sein de matériaux dynamiques, le premier objectif de mon doctorat a consisté à optimiser la réaction d'échange aussi bien en solutions aqueuses et qu'en solvants organiques. En particulier, nous avons étudié comment mieux contrôler la dynamique des dynPL et améliorer

l'efficacité de la réaction d'échange. De plus, l'utilisation d'un solvant organique a été envisagée afin de limiter le phénomène d'hydrolyse observé au cours de la dcNCL. Enfin, l'application de cette méthodologie à des systèmes polymères capables de produire de phases ordonnées a constitué un deuxième objectif de mon doctorat.

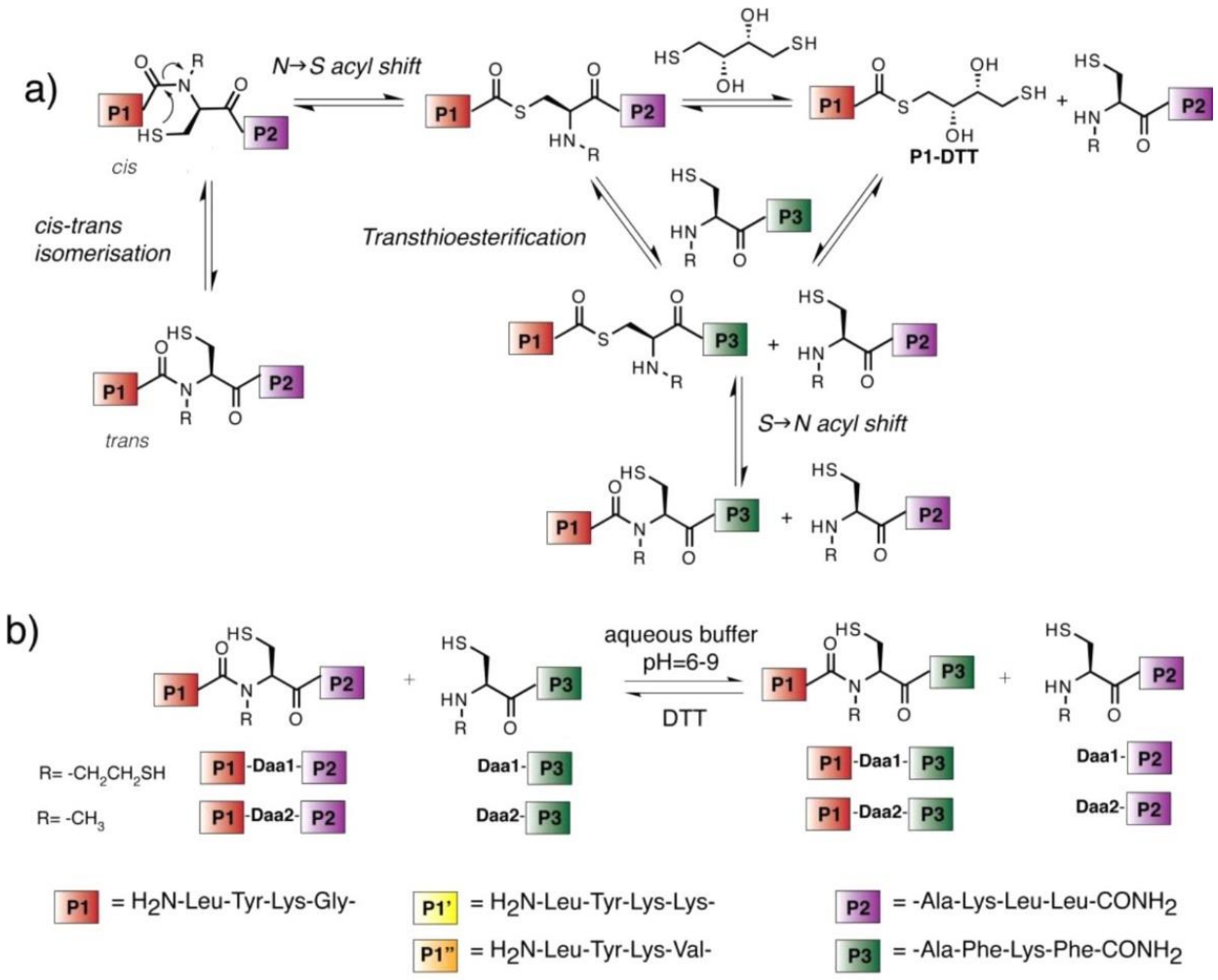

Figure 2 | a) Mécanisme complet de la ligation chimique native covalente dynamique (dcNCL) développée par notre équipe. b) Exemples d'échange de fragments peptidiques selon le mécanisme de dcNCL mettant en jeu l'utilisation de la *N*-thioéthyl-cystéine (Daa1) et de la *N*-méthyl-cystéine (Daa2). Tous les peptides présentent une fonction carboxamide à leur extrémité C-terminale.

Résultats et discussion

Dans un premier temps, nous avons étudié l'influence de différents paramètres tels que la nature de l'agent réducteur ou encore l'influence de la température sur des segments peptidiques incorporant des résidus ***N*MeCys** en positions N- ou C-terminales (Figure 3). Les différentes séquences peptidiques ont été synthétisées en phase solide assistée par micro-ondes.[11] L'utilisation d'un couplage simple a permis d'insérer la ***N*MeCys** au sein de la chaine peptidique. Cependant, lorsque la ***N*MeCys** devait être greffée initialement sur la résine (extrémité C terminale de la chaîne peptidique) ou pour l'insertion de l'acide aminé suivant la ***N*MeCys**, des doubles couplages (70°C, 35W) ont été privilégiés. Les séquences étudiées pour améliorer la méthodologie dcNCL correspondent aux peptides **P1** (NH_2-LYRAG-***N*MeCys**) et **P2** (***N*MeCys**-RANYLA-$CONH_2$). A l'équilibre thermodynamique, le peptide **P3** (NH_2-LYRAG-***N*MeCys**-RANYLA-$CONH_2$) et la ***N*MeCys** ont été identifiés dans le mélange.

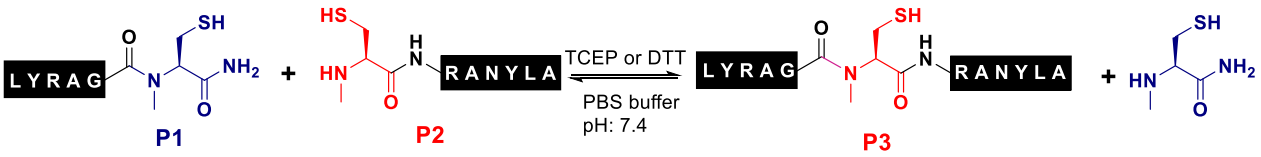

Figure 3 | Réaction d'échange modèle étudiée afin d'optimiser les paramètres de dcNCL dans l'eau.

Notre étude a permis de démontrer un comportement équivalent pour les différents réducteurs testés, notamment le DTT et le TCEP, ce qui nous offre une versatilité de choix en fonction de l'application envisagée. Nous avons également mis en évidence qu'une température plus élevée permettait d'accélérer l'échange mais également l'oxydation du groupe thiol.

Parallèlement à ce travail, nous avons étudié les conditions optimales de dcNCL en milieu organique et organo-aqueux. Afin d'assurer une solubilité des différents composés aussi bien en solvants organiques qu'en milieux aqueux, la ***N*MeCys** a été substituée par une courte chaîne alkyle, une chaine diéthylène glycol ou encore un groupement aromatique (dérivés **S1-S4**, Figure 4a). Ces composés sont suffisamment simples pour pouvoir étudier les différents paramètres qui gouvernent

la dcNCL et ainsi proposer des conditions modèles, qui ont pu être ensuite validées lors d'une réaction de métathèse entre les composés **S1** et **S5** permettant d'accéder aux composés **S6** et **S4 (**Figure 4b).

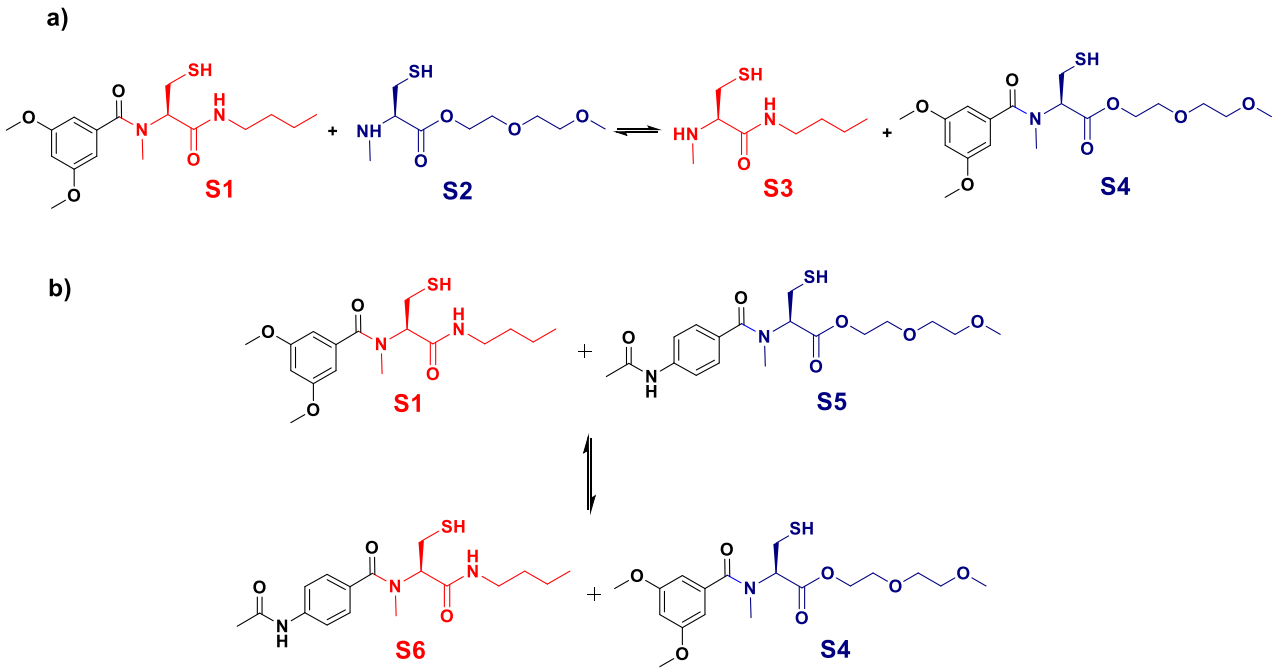

Figure 4 | a) Réaction d'échange modèle étudiée afin d'optimiser les paramètres de dcNCL en solvant organique. b) Réaction de métathèse étudiée afin de valider les conditions de dcNCL optimisées.

Notre étude a démontré que des solvants non polaires, tels que le dichlorométhane ou le THF, empêchent quasiment tout échange dynamique. Cependant, les solvants organiques polaires tels que le méthanol ou l'acétonitrile conduisent à une équilibration plus rapide, et s'avèrent donc plus appropriés pour stabiliser les composés intermédiaires chargés tout en améliorant également la solubilité de dérivés ***N*MeCys**.

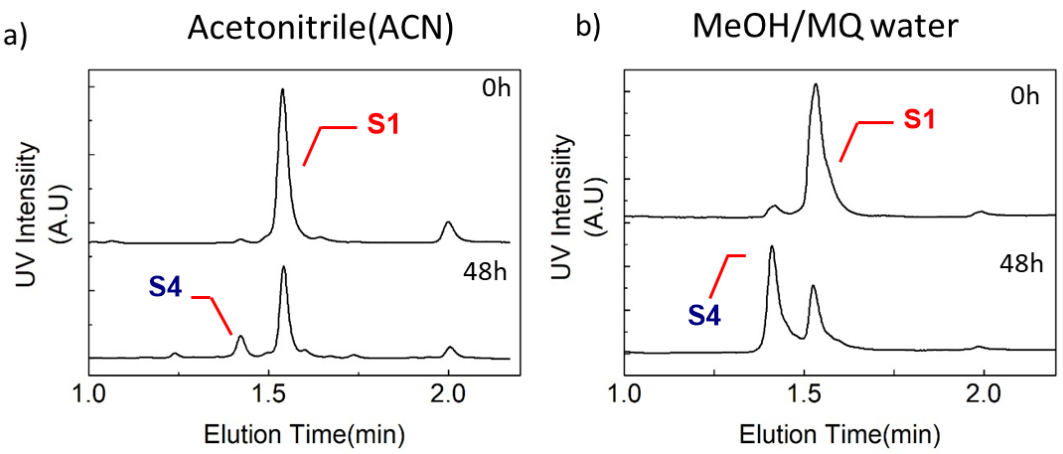

Figure 5 | Chromatogrammes en phase inverse (UPLC) obtenus pour la dynPL décrite en Figure 4a à t = 0 et 48 h. a) S1 (10 mM), S2 (10 mM), DTT (150 mM) dans l'acétonitrile à température ambiante; b) S1 (10 mM), S2 (10 mM), TCEP (150 mM), ascorbate de sodium (300 mM à pH 6) dans un mélange 1/1 méthanol/eau à température ambiante.

Nous avons également démontré que des systèmes mixtes de solvants miscibles tels qu'un mélange 1/1 (v/v) méthanol/eau permettaient des échanges plus rapides sans risque d'hydrolyse même à température ambiante (Figure 5b). Nous avons étudié l'influence du pH de la solution de TCEP sur la dcNCL dans ce mélange méthanol/eau et observé l'efficacité des échanges pour des pHs situés entre 4 et 7. Du fait de la présence du résidu ***N*MeCys**, le déplacement acyle N → S s'avère être l'étape cinétiquement limitante de l'ensemble du processus dynamique. Sous l'influence de facteurs externes comme un changement de pH, la dcNCL montre son comportement adaptatif (Figure 6). De manière plus large, la dcNCL peut être réalisée rapidement sans ajout de catalyseurs dans un milieu réactionnel simple.

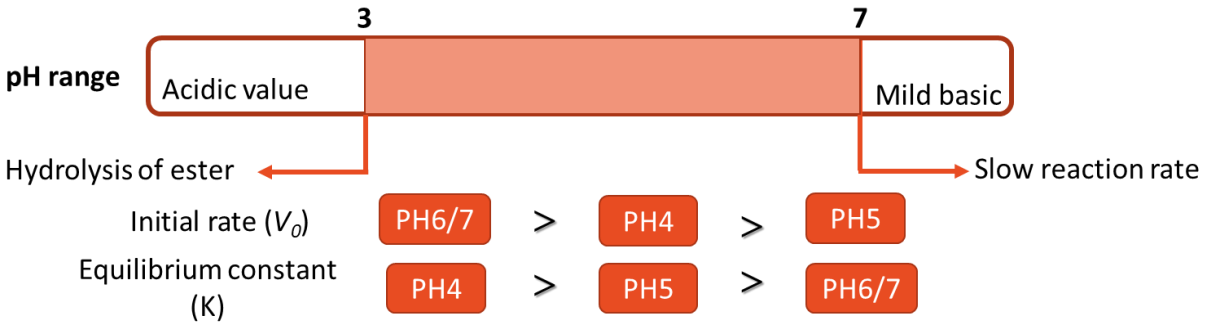

Figure 6 | Représentation schématique démontrant comment les valeurs du pH de la solution TCEP influencent la vitesse initiale V_0 et la constante d'équilibre K de la dcNCL.

Nous avons également appliqué notre méthodologie à d'autres dérivés incorporant un résidu ***N*MeCys** central (Figure 4b). Ainsi, les dérivés **S1** (10 mM) et **S5** (10 mM) ont subi une métathèse d'amide réversible conduisant à la formation des composés **S6** et **S4**. Cette réaction de métathèse a également été réalisée en partant des dérivés **S6** et **S4**. Après 72h, les deux réactions atteignent le même équilibre, démontrant ainsi le contrôle thermodynamique de notre système. Ces résultats démontrent l'intérêt de la dcNCL pour accéder à des nouvelles bibliothèques dynamiques constitutionnelles tout comme les autres liaisons covalentes dynamique. L'étude plus précise de la dcNCL entre composés incorporant une unité ***NMeCys*** nous a permis d'accéder un protocole plus facile à mettre en œuvre que le protocole initiale[10].

Afin de prouver l'intérêt de notre méthodologie, nous avons envisagé son application à des systèmes amphiphiles capable de transférer l'information de l'échelle moléculaire à l'échelle microscopique. Le système étudié repose sur un composé hydrophile (***N*MeCys**-PEG800) dérivé du polyéthylène glycol 800 (PEG800) et présentant une unité ***N*MeCys** N-terminale et un composé hydrophobe (C8BA-***N*MeCys** -C4) contenant une unité ***N*MeCys** interne. En conditions d'échange, le dérivé amphiphile C8BA-***N*MeCys**-PEG800 est obtenu, démontrant le comportement dynamique du processus (Figure 7).

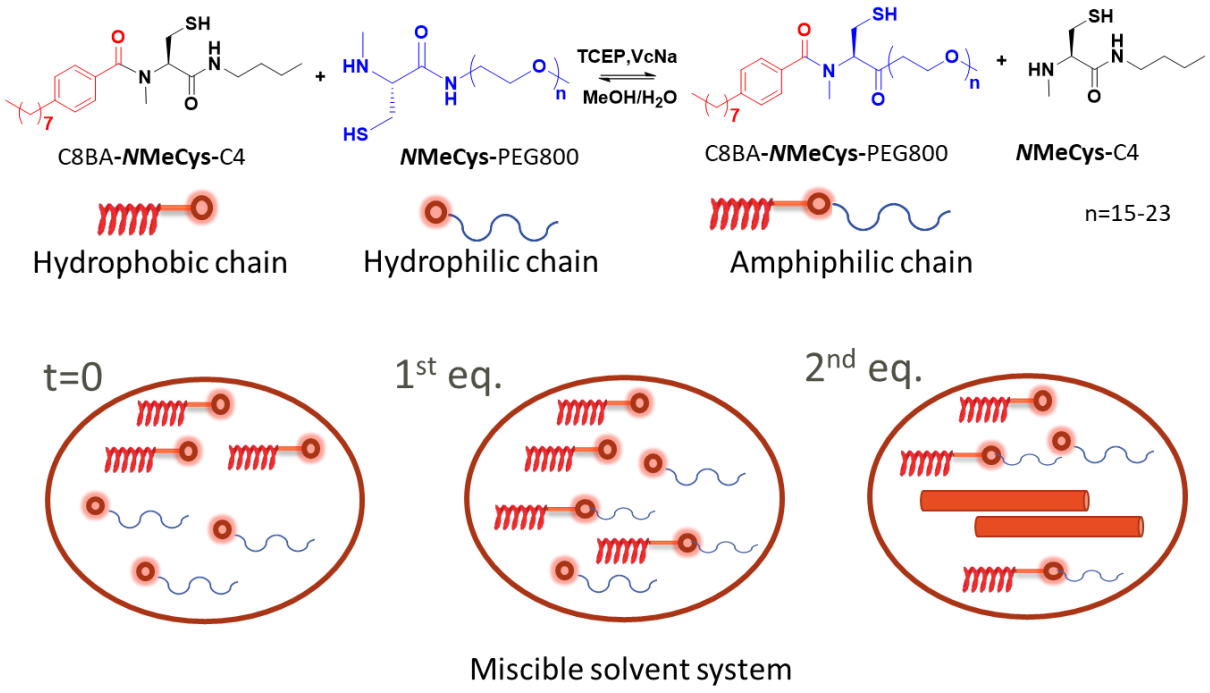

Figure 7 | Réaction d'échange et représentation schématique de l'évolution d'une dcNCL conduisant à la formation d'un dérivé amphiphile.

Pour un système de solvant impliquant un pourcentage d'eau faible (< 40%), les quatre composés (2 de départ et 2 d'échange) sont présents à l'équilibre thermodynamique. Par exemple, pour une dcNCL mettant en jeu ***N*MeCys**-PEG800 (10 mM) et C8BA-***N*MeCys**-C4 (10 mM) dans un mélange 3/1 (v/v) de méthanol/eau contenant TCEP (150 mM) comme agent réducteur, et l'ascorbate de sodium (300 mM) pour contrôler le pH, nous observons rapidement l'apparition du produit d'échange C8BA-***N*MeCys**-PEG800 (Figure 8a). 72h plus tard, l'équilibre thermodynamique de la réaction d'échange est atteint.

Cependant, lorsque le pourcentage d'eau dans le système augmente (mélange 3/1 (v/v) méthanol/eau), un caractère dynamique différent est observé (Figure 8b). Ainsi, nous avons mis en évidence la croissance sigmoïdale du dérivé C8BA-***N*MeCys**-PEG800 et la décroissance sigmoïdale du composé C8BA-***N*MeCys**-C4. Ce profil sigmoïdal d'évolution de la concentration en fonction du temps suggère que le composé amphiphile C8BA-***N*MeCys**-PEG800 présente une forte propension à l'auto-assemblage supramoléculaire. L'étude du comportement de ce composé (aussi bien pur qu'à l'issue du processus d'échange) par microscope électronique à la transmission (TEM) a démontré sa capacité

à former de longues micelles cylindriques d'environ 20 nm de diamètre. Cette dimension est en accord avec la longueur de deux chaînes amphiphiles simples qui se lient de façon non covalente entre elles. Enfin, le diagramme de phase associé à ce composé amphiphile a été établi à partir d'études de diffusion de la lumière (DLS) pour différentes concentrations et différents pourcentages d'eau dans le milieu réactionnel. Cette étude démontre qu'il est possible de déplacer l'équilibre de la dcNCL si le produit formé conduit à la formation de structures secondaires associées à la présence d'un second équilibre.

Elle indique également que la ligation chimique native covalente réversible est un outil permettant de transférer de l'information de l'échelle moléculaire au niveau microscopique.

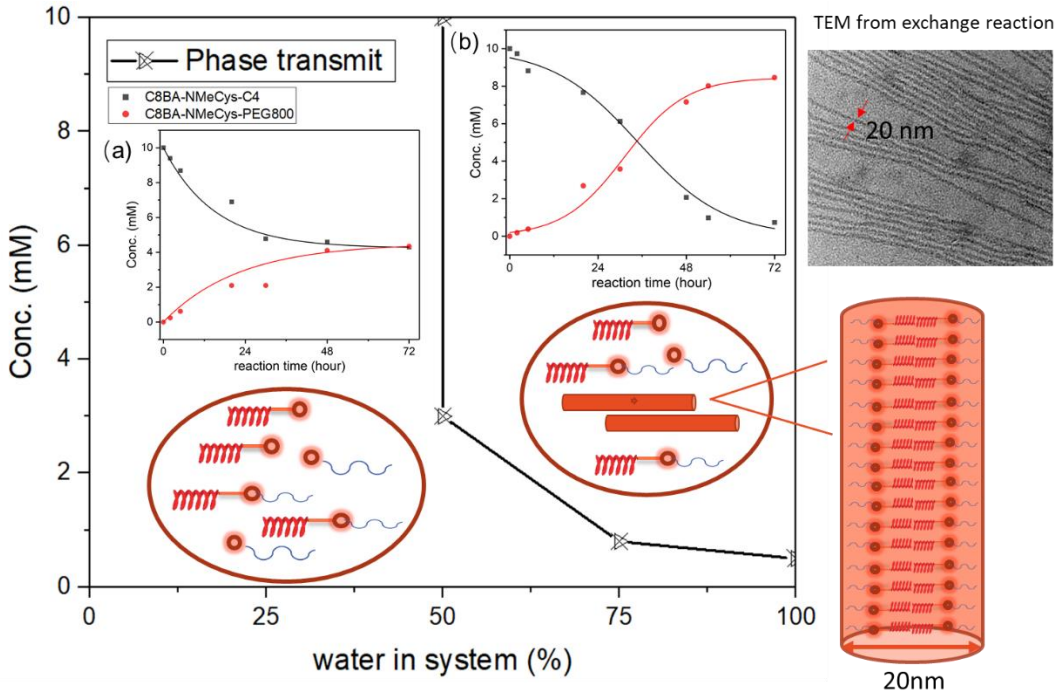

Figure 8 | Diagramme de phase obtenu pour la bibliothèque représentée en Figure 7 en fonction de la concentration et du pourcentgae d'eau présent dans le système. a) Evolution des concentrations des composés C8BA-*N*MeCys-C4 et C8BA-*N*MeCys-PEG800 en fonction du temps pour de faibles pourcentages d'eau. b) Evolution des concentrations des composés C8BA-*N*MeCys-C4 et C8BA-*N*MeCys-PEG800 en fonction du temps pour des pourcentages d'eau plus élevés.

Conclusions et perspectives

En conclusion, nous avons optimisé la dcNCL pour permettre son utilisation aussi bien en solvant organique qu'en phase organo-aqueuse. Nous avons mis au point un protocole efficace permettant d'effectuer la dcNCL en présence d'unités ***N*MeCys** aussi bien internes que C- ou N-terminales. Du point de vue applicatif, nous avons démontré que la dcNCL pouvait conduire à la formation de structures auto-assemblées, démontrant un transfert d'information de l'échelle moléculaire au niveau microscopique. Enfin, la possibilité de réaliser la dcNCL impliquant des unités ***N*MeCys** dans des conditions aérobies rend pertinent son utilisation en milieu biologique et devrait conduire aux premières applications en biologie chimique et en découverte de médicaments.

Références

1. Corbett, P. T. *et al.* Dynamic Combinatorial Chemistry. *Chem. Rev.* **106**, 3652–3711 (2006).
2. Ladame, S. Dynamic combinatorial chemistry: on the road to fulfilling the promise. *Org. Biomol. Chem.* **6**, 219–226 (2008).
3. Moulin, E., Cormos, G. & Giuseppone, N. Dynamic combinatorial chemistry as a tool for the design of functional materials and devices. *Chem. Soc. Rev.* **41**, 1031–1049 (2012).
4. Jin, Y., Yu, C., Denman, R. J. & Zhang, W. Recent advances in dynamic covalent chemistry. *Chem. Soc. Rev.* **42**, 6634 (2013).
5. Chakma, P. & Konkolewicz, D. Dynamic Covalent Bonds in Polymeric Materials. *Angew. Chem. Int. Ed.* **58**, 9682–9695 (2019).
6. Lehn, J.-M. Dynamic Combinatorial Chemistry and Virtual Combinatorial Libraries. *Chem. Eur. J,* **5**, 2455–2463 (1999).
7. Reuther, J. F. *et al.* Dynamic covalent chemistry enables formation of antimicrobial peptide

quaternary assemblies in a completely abiotic manner. *Nat. Chem.* **10**, 45–50 (2018).

8. Macpherson, L. J. *et al.* Noxious compounds activate TRPA1 ion channels through covalent modification of cysteines. *Nature* **445**, 541–545 (2007).
9. Wilson, A., Gasparini, G. & Matile, S. Functional systems with orthogonal dynamic covalent bonds. *Chem. Soc. Rev.* **43**, 1948–1962 (2014).
10. Ruff, Y., Garavini, V. & Giuseppone, N. Reversible Native Chemical Ligation: A Facile Access to Dynamic Covalent Peptides. *J. Am. Chem. Soc.* **136**, 6333–6339 (2014).
11. Pedersen, S. L., Tofteng, A. P., Malik, L. & Jensen, K. J. Microwave heating in solid-phase peptide synthesis. *Chem. Soc. Rev.* **41**, 1826–1844 (2012).

LISTE DES PRESENTATIONS

Poster Presentation :

14th International Symposium on Macrocyclic and Supramolecular Chemistry (ISMSC2019), Lecce, Italy.

Titre : Dynamic Covalent Chemistry: Playing With the Reversibility of N,S-acyl Migration Reaction

Auteurs: Yali Zeng, Cristian Rete, Manickasundaram Samiappan, Emilie Moulin, and Nicolas Giuseppone.

Acknowledgments

First of all, I would like to give the great thank to my supervisor, Prof. Nicolas Giuseppone. Your offer gives me a chance to join the big family, SAMS group. Your professional guidance in the academic area supported my research work and helped me get results with better quality. Your strict attitude toward science inspire me even for the rest of my life. The almost 4 year I spent in SAMS group is always happy and sweet which I will never forget.

I express my gratitude to my jury members, including Prof. Mihail D. Barboiu from Université de Montpellier, Dr. Olivier Colombani from Université du Maine and Dr. Delphine Chan-seng from ICS, for having accepted to evaluate my thesis.

My acknowledgment to Dr. Emilie Moulin is no less than my supervisor for her tremendous help to my project discussion and experimental support. Even during the terrible Covid-19 period, she still helps me timely with my manuscript as usual.

I would like to acknowledge our dear Odile, Marie-Celine, Andreas and Julie for their constant technological support, warm friendliness and care towards us. Odile, who work beside my fume hood for my time in SAMS, always provide me with friendly suggestions. Marie-Celine, even we meet with each other later but your positive attitude towards life and lab encourages me. Thanks for Julie with the technological support for HPLC and UPLC. Thanks for Andreas with TEM support and academic discussion.

I would like to thank all other current and former members in SAMS group: Gad, Mounir, Chris, Manic, petite Nicolas, Ting, Damien, Xuyang, Alexis, Qing, Melodie, Vasily, Flavio, Joakim, Xiaoqing, Wenzhi, Chuan, Raphael, Chris from Columbia and Junjun. The experiments may be boring and disappointing, but the time to spent with you is still very interesting and cheerful.

The same thanks to all other members of the Institut Charles Sadron, who have been of great help to me during the last 4 years.

To my friends who support me by “we chat” in China or who we met in France, especially Dr. Da Shi and his wife Yazhao, your selfless support help me a lot in the daily French life. Hope our friendship could overcome the time and distance.

I have to thank my family for their accepting and support to live so far away from home for 4 years by now. The same gratitude to the parents of my husband, who will miss and support me for the time I leave home.

Special thanks to Ruirui, my husband, my confidant. After April 2020, we already accompany with each other for 10 years. Because of you, I have the courage to leave home and study in France. Your daily companying, positive attitude and academic support help me to go through the good and bad time in my life. I have no idea how many decades our life will have, but I am happy the rest of decades we will spend with each other.

Table of Content

Abstract

Dynamic covalent chemistry (DCvC) has found various applications in diverse research areas, such as drug discovery, biotechnology, material science, etc, over the last twenty years. Although the scope of DCvC has expanded quickly, the development of new dynamic covalent reactions has been limited by the slow kinetics, and the need for catalysts to reach efficient equilibration. Based on a recent reversible amide exchange reaction reported by our group, this PhD project aims at optimizing the methodology of the dynamic covalent native chemical ligation (dcNCL), by establishing a convenient experimental protocol to construct dcNCL-based dynamic covalent libraries, which could undergo self-assembly at the mesoscopic scale by forcing the library to amplify specific constituents.

In the first chapter, we give a general introduction on DCvC, and highlight the most important dynamic covalent reactions and how to optimize them. We then describe their corresponding applications in dynamic combinatorial libraries with a particular focus on biosystems, for example involving peptides and proteins. Overall, this chapter provides a clear understanding of DCvC and aims to establish the necessary basis for this PhD project.

In the second chapter, we first recall the principles of dynamic covalent native chemical ligation (dcNCL) as initially reported by our group in 2014. Then, we focus on the various parameters which govern dcNCL in order to optimize the reaction conditions first on some model peptides and then on small molecules. In particular, we have designed and synthesized a series of building blocks to investigate how solvent, pH, concentration and temperature can influence the dcNCL. Overall, this chapter provides an optimum protocol to achieve dcNCL in various environmental conditions.

In the third chapter, we describe the first application of our methodological approach to complex DCvC systems. By designing and synthesizing dynamic libraries containing simultaneously hydrophilic and hydrophobic building blocks, we managed to achieve constitutional selectivity which induces the formation of a particular type of supramolecular self-assembly.

Overall, this thesis describes the methodological optimization of dcNCL and its use in DCLs for the selection of self-assembled nanostructures. It provides experimental evidences for the extension of this new dynamic covalent bond into various applications.

Abbreviations and symbols

Å	Ångstrom
aa	Amino acid
Boc	*tert*-butyloxycarbonyl
bpy	Bipyridine
PyBOP	Benzotriazol-1-yl-N-oxy-tris(pyrrolidino)phosphonium hexafluorophosphate
°C	Celsius degree
DA	Diels-Alder
DBU	1,8-Diazabicyclo[5.4.0]undec-7-ene
DCC	Dynamic Combinatorial Chemistry
DCC	Dicyclohexylcarbodiimide
DCvC	Dynamic Covalent Chemistry
DCL	Dynamic Combinatorial Library
DCM	dichloromethane
DIEA	*N*,*N*-diisopropylethylamine
DLS	Dynamic Ligation Screening
DMF	*N*,*N*-dimethylformamide
DMSO	dimethylsulfoxide
DNA	deoxyribonucleic acid
DTT	dithiothreitol
dcNCL	Dynamic covalent native chemical ligation
dynPL	Dynamic peptide library
EA	ethacrynic acid
EDC	1-ethyl-3-(3-dimethylaminopropyl)carbodiimide
EDTA	ethylenediaminetetraacetic acid
eq	equivalents
ESI	electrospray ionization
FDA	US Food and Drug Administration
Fmoc	9-fluorenylmethoxycarbonyl
g	gram
GC	gas chromatography

GSH	glutathione reduced
GST	glutathione S-transferase
h	hour
HATU	1-[bis(dimethylamino)methylene]-1H-1,2,3-triazolo[4,5-b]pyridinium 3-oxid hexafluorophosphate
HBTU	2-(1H-benzotriazol-1-yl)-1,1,3,3-tetramethyluronium hexafluorophosphate
HFIP	hexafluoro-2-propanol
HOBt	hydroxybenzotriazole
HPLC	high performance liquid chromatography
Hz	Hertz
K	equilibrium constant
kDa	kilodalton
µL	microliter
µM	micromolar
M	molar
Me	methyl
mg	milligram
MHz	megahertz
min	minutes
mL	milliliter
mM	millimolar
mmol	millimole
mol	mole
MPAA	4-mercaptophenylacetic acid
MS	mass spectrometry
MW	microwave
m/z	mass-to-charge ratio
o-NBS	4-nitrobenzylsulfonyl
NCL	native chemical ligation
NHS	*N*-hydroxysuccinimide
nM	nanomolar
NMP	N-methyl-2-pyrrolidinone
NMR	nuclear magnetic resonance

PBS	phosphate buffered saline
PEG	polyethylene glycol
PU	Polyurethane
SPPS	solid phase peptide synthesis
t	time
tBu	*tert*-butyl
TCEP	tris(2-carboxyethyl)phosphine
TEA	triethylamine
TES	triethylsilane
TFA	trifluoroacetic acid
TFET	trifluoroethanethiol
THF	tetrahydrofurane
TIPS	triisopropylsilane
TLC	thin layer chromatography
Trt	trityl
UPLC	ultra performance liquid chromatography
UV	ultra violet
v/v	volume per volume
Vis	visible
w/v	weight per volume
W	watt

General introduction and objectives

Dynamic covalent chemistry (DCvC), which unifies supramolecular and molecular chemistry, has evolved rapidly over the last 20 years in various fields of research. The key feature of DCvC relies on the use of dynamic covalent reactions that allow the free covalent exchange of building blocks to compose dynamic combinatorial libraries (DCLs). In particular, in 2014, our group reported a new methodology based on native chemical ligation (NCL) and *N*-methyl cysteine (*N*MeCys) to perform dynamic peptide exchanges. It allows the exchange of peptidic fragments in phosphate buffers at physiological pH and in the presence of a reducing agent. However, such dynamic peptide library (dynPL) requires long preparation time under inert atmosphere and is prompt to hydrolysis. The primary objective of this PhD project, as detailed in chapter 2, consisted in optimizing the methodology of dynamic covalent native chemical ligation (dcNCL). In particular, our efforts have targeted three main aims: (1) limiting the hydrolysis of the constituents in a dcNCL-based, (2) accelerating the reaction kinetics and shortening the equilibration time, and (3) extending the methodology to different environmental conditions, for example in organic solvents. The goal was thus to develop a refined experimental protocol for the dcNCL systems (Figure 1).

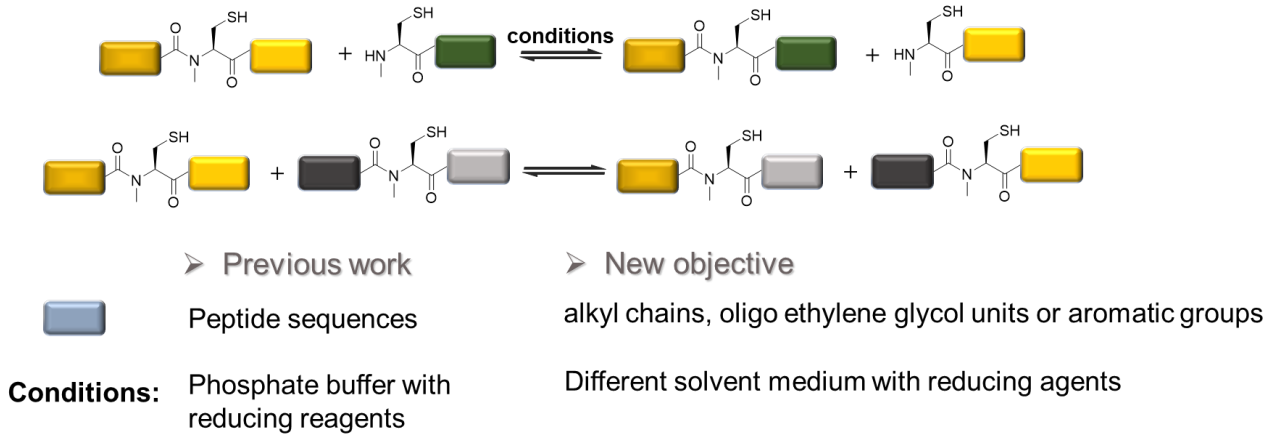

Figure 1| Schematic representation of the dcNCL systems in this thesis compared to previous work.

Based on this advanced protocol of dcNCL, we have considered the possible extension of our methodological approach to building blocks other than peptide sequences. For that, we have designed a DCL containing simultaneously hydrophilic and hydrophobic blocks which, could lead to the formation of supramolecular amphiphilic self-assemblies by reversible exchange of the constituents. We believe that the formed amphiphilic species may influence the kinetics of the dcNCL reaction and

potentially lead to self-assembly driven out-of-equilibrium system. By combining DCvC with supramolecular chemistry, we expect to extend the dcNCL from the molecular scale up to the microscopic level and to reach systems of increased complexity.

Overall, the objectives of my PhD project are two-fold: (1) developing an optimized protocol for dcNCL with the use of *N*MeCys residues and (2) applying the dcNCL to complex systems with transfer of information from the molecular scale up to the microscopic level. The ability of dcNCL with *N*MeCys residues to proceed efficiently in easy to use conditions could increase its intrinsic relevance for applications in chemical biology and drug discovery, but also in the field of material sciences.

Chapter 1. Research background

1.1 Dynamic covalent chemistry (DCvC)

Tracing the birth of dynamic covalent chemistry (DCvC), no one can ignore the concept of dynamic combinatorial chemistry (DCC) which has been developed since mid-1990's.[1] Compared to classical combinatorial chemistry, dynamic combinatorial chemistry (DCC) has been developed as a conceptually new approach which is established on the reversibility of covalent or non-covalent interactions between various building blocks that are able to generate a dynamic combinatorial library (DCL) under thermodynamic control.[2] DCC thus provides an evolutional method for the generation of chemical diversity at both the molecular and supramolecular levels by bringing together both ***inter***molecular noncovalent interactions and ***intra***molecular covalent bonds. The concept of supramolecular chemistry (i.e. dynamic non-covalent) is of particular interest to generate diversity at the intermolecular level, as its dynamic allows reversible dissociation and association between molecules. However, the presence of weak non-covalent interactions precludes its use in many applications where a high degree of robustness is required. Dynamic covalent chemistry (DCvC) has emerged as an alternative which allows for reversible exchange of covalent bonds at the molecular level by bringing into play higher free energies compared to the ones related to supramolecular interactions.[3–5] (Figure 1.1)

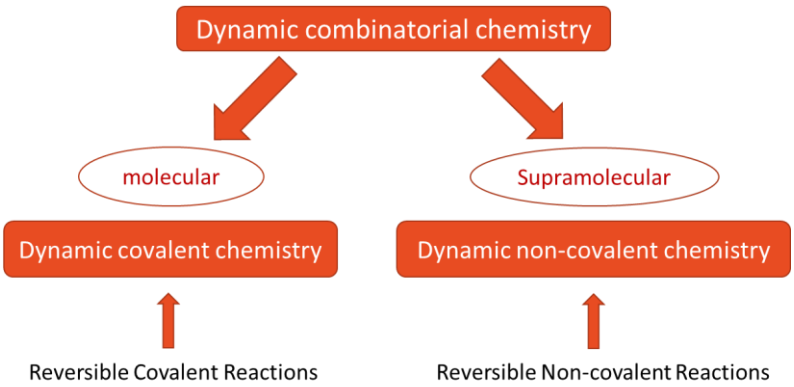

Figure 1.1 | Schematic representation of the different concepts related to dynamic combinatorial chemistry.

1.1.1 Basic concepts and significance the DCvC approach

Dynamic covalent chemistry (DCvC) rests on dynamic covalent bonds, which allow free exchange between building blocks at the ***intra***molecular level, thus extending reversible supramolecular chemistry into the molecular domain. Although the free energy required to break covalent bonds is higher than the free energy necessary for breaking ***inter***molecular interactions,[3] some distinguishing features of DCvC include: 1) dynamic process, as molecular components can exchange with each other to reach thermodynamic equilibrium within DCLs; and 2) constitutional adaptation to their surroundings, as DCLs can respond to changes in chemical environment (reaction medium, pH, presence of metal ions, molecular templates, concentration, *etc*) or physical conditions (temperature, irradiation, light, pressure, electric field, mechanical force, *etc*).[3]

The most common illustration of the characteristics of DCvC is Emil Fischer's key-and-lock metaphor (Figure 1.2).[6] A set of building blocks can covalently interact with each other by reversible covalent bonds leading to the formation of a DCL at thermodynamic equilibrium, but which still has the capacity to exchange its components. After adding a target selector so-called the "*lock"* which can selectively bind with one "*key"* constituent of the DCL, the thermodynamic equilibrium of the DCL is perturbed potentially leading to the amplification of the "fittest" *key- lock* by consuming all other possible *keys*. At the end of this process, the system will reach a new more favored thermodynamic equilibrium.

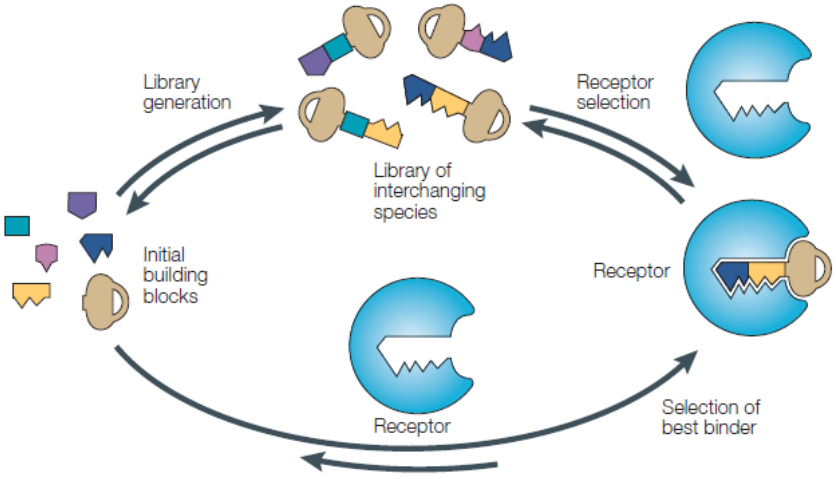

Figure 1.2 | Schematic representation of the characteristic behavior of DCvC and DCL. The building blocks interact with each other to form different "keys", and the key which best binds with the "lock" is amplified by consuming the other keys. Figure is adapted from ref. [6].

Over the last 20 years, the field of DCvC has expanded rapidly. Practically, nature has been a very important source of inspiration for this fast development,[7] as many processes occurring in nature are established on dynamic covalent bonds. For instance, dynamic disulfide bond plays a significant position in the folding of proteins, as they are very often responsible for the tertiary/quaternary structures which are very important for their proper functionning.[8] Besides, thioester exchange plays an important role in polyketide biosynthesis[9] while reversible imine bonds are essential for the chemistry of vision.[10]

Furthermore, DCvC offers new direction for the design and application of multi-component systems. Compared to individual molecular constituents, DCL may exhibit properties which emerges from its complexity at the molecular scale. The related functions become capable of continuous adaptation and evolution thanks to the presence of dynamic bonds. DCvC thus offers new possibility to develop systems presenting self-sorting, replicating, or self-healing behaviors.

1.1.2 Dynamic covalent reactions

The key feature of DCvC is the dynamic covalent reactions involved in the formation of the DCL and which allow free covalent exchange of its building blocks to reach thermodynamic equilibrium.[1,11] To do so, these reactions generally have to fit several characteristics:[1,6,12] (1) they should occur under reasonable time scale to avoid unfavorable side reactions; (2) they need to be easily controllable, in order to be turned on or off depending on the set of conditions used; (3) the reaction conditions have to ensure the solubility of all the DCL components, as insoluble members may induce thermodynamic or kinetic trap; and (4) in some particular cases, especially for drug discovery, they should operate under mild conditions to avoid degradation of the sensitive targets present in the system.

Hereafter, we present the most common types of dynamic covalent bonds that are used in DCvC and we intentionally will not be exhaustive. They are categorized according to their chemical functioning, namely acyl transfer exchange, C=N exchange, disulfide exchange, and other reversible covalent bonds.[1,5] We will conclude this part by highlighting the various parameters which need to be optimized in order to favor dynamic covalent exchanges.

1.1.2.1 Acyl transfer exchange

Acyl transfer, also called nucleophilic acyl substitution, includes diverse types of reactions such as amide, ester or aldol exchange, transthioesterification or thiol-Michael addition (Figure 1.3a)). They occur through a two-step mechanism: (1) nucleophilic attack of the carbonyl group to yield a tetrahedral intermediate and (2) displacement of the leaving group to form the new component. The different activation energies (E_a (1) or E_a (1')) necessary to achieve acyl transfer reflect the different energy barriers associated to the considered covalent bonds and define the thermal accessibility of the equilibrium of these exchange reactions (Figure 1.3b)).

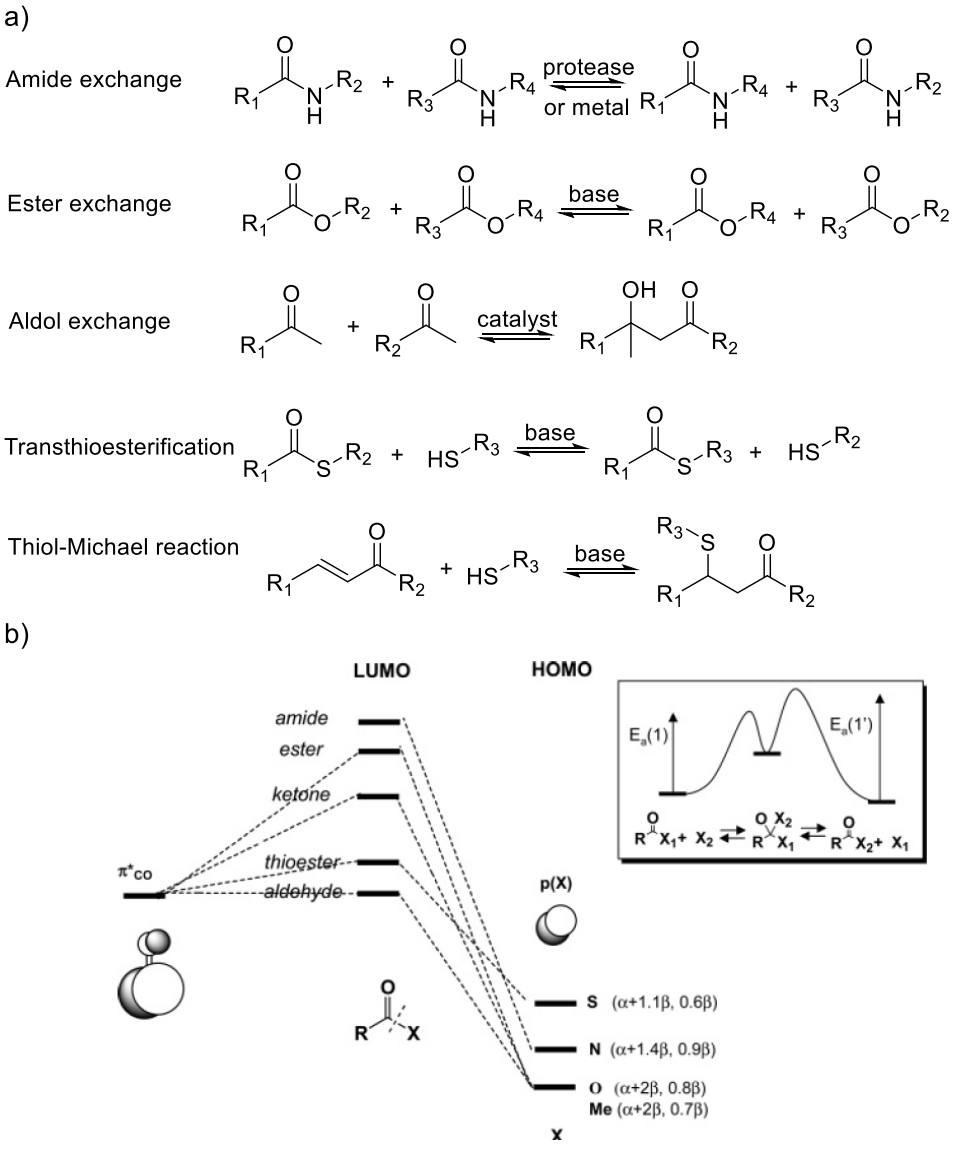

Figure 1.3 | a) Acyl transfer reactions used for DCvC and DCL and b) orbital categorization of activation energies for acyl transfer reactions. Figure is reproduced and adapted from ref. [1].

Therefore, amide exchange (including transamidation) and ester exchange (including transesterification) are more difficult to perform than other acyl transfer reactions.[1] They often require the use of a catalyst and high temperature. Transamidation is typically achieved using an enzyme, which has the limitation of long equilibrium time and biological instability.[13,14] Synthetic catalysts, like metal complexes as shown in Figure 1.4, have also been used for transamidation reactions in organic solvent at relatively high temperatures (90-120 °C).[15] In traditional (trans)esterifications, harsh conditions, like the use of strong acids or bases, are very common. For instance, Brønsted bases such as NaO*t*-Bu and DBU or Lewis acids such as $Ti(OBu)_4$ have been used for transesterification to increase the equilibration rates.[16] In principle, aldol exchange is more accessible than transamidation and transesterification. However, there are not many applications of aldol exchange in DCvC because of the absence of a suitable catalyst.

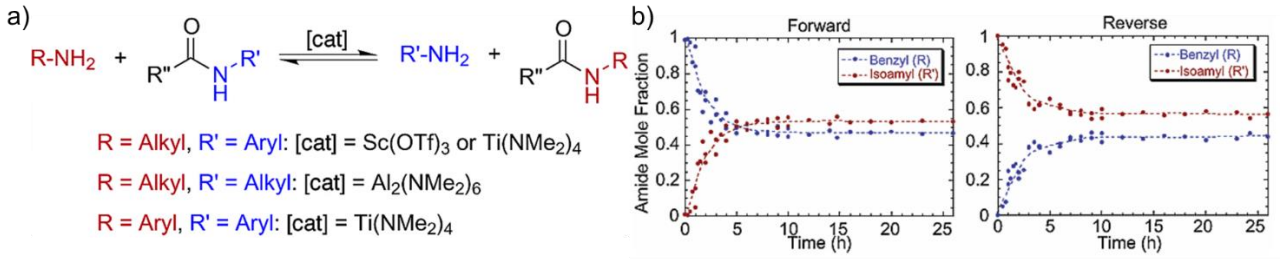

Figure 1.4 | a) Metal-catalyzed transamidation reaction. b) Evolution of the amide fraction with time as monitored by GC for the $Al_2(NMe_2)_6$-catalyzed equilibrium exchange between *N*-benzyl heptanamide and isoamylamine for the forward direction, and *N*-isoamyl heptanamide and benzylamine for the reverse direction. Figure is reproduced and adapted from ref. [15].

As sulfur is less electronegative, more nucleophilic and softer than nitrogen and oxygen, thiol-thioester exchange (also called transthioesterification) generally happens between a free thiol and a thioester at room temperature under neutral conditions without the need for any activation procedure. The possibility to perform efficiently this reaction in neutral aqueous media has propelled its wide use for biochemical applications. Ramström and coworkers reported a DCL made of five thioester substrates which could undergo transthioesterification by simply mixing its components with thiocholine under mild aqueous conditions. Upon addition of an enzyme, a new thermodynamic equilibrium was reached within 3 hours.[17] The transthioesterification exchange can also be accelerated by increasing the polarity of solvent media.[18] Applications of transthioesterification exchange, for instance in the field of materials science, are detailed in section 1.2.3.

Reversible thiol-Michael addition has a great potential in dynamic drug design due to the presence of surface-centered cysteine residues on proteins and has also been used in material science by its "click" nature.[19,20] In the presence of a nucleophile or a base, thiols add to α, β-unsaturated carbonyl compounds *via* 1,4-conjugated addition leading to the formation of a C-S bond. However, the long reaction time (over a week) has limited its application to DCvC. Some years ago, Anslyn and coworker reported that β-sulfido-α,β-unsaturated ketones can undergo rapid exchange with aliphatic thiols to produce vinyl sulfide carbonyls and β-dithiane carbonyls within 1 hour in DMSO in the presence of trimethylamine (Scheme 1.1).[21] The reaction was also shown to proceed efficiently in aqueous media (D_2O-DMSO, PBS buffer pH 7.7). Very recently, this methodology found applications in polymer science, allowing the fabrication of a healable and injectable hydrogel material.[22]

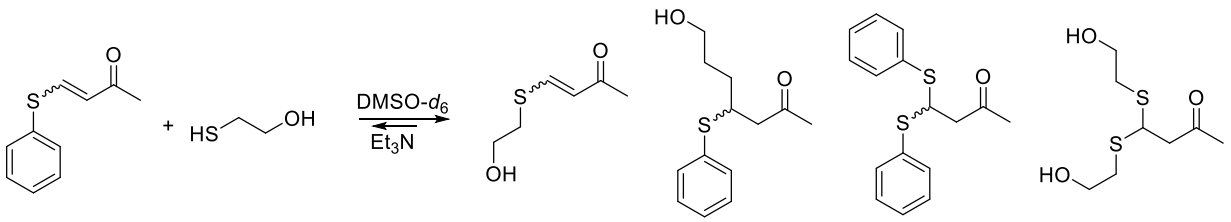

Scheme 1.1 | Reversible thiol-Michael addition on a β-sulfido-α,β-unsaturated ketones.

1.1.2.2 C=N exchange

One of the most widespread family of dynamic covalent bonds in DCvC is C=N bonds, such as imine, hydrazone or oxime.[5] The formation of these bonds comes from the condensation between an aldehyde and a primary amine to give an imine plus water (Scheme 1.2). Similar processes apply to form hydrazone, starting from an aldehyde and a hydrazine, or oxime, from an aldehyde and a hydroxylamine. The reversibility of these reactions comes from the possibility to hydrolyze them with water. Due to the relative thermodynamic instability of imine in the presence of water, DCLs made of imines have been mostly studied in organic solvents[23] or biphasic systems[24] and evolution of the DCL was, in most cases, monitored by NMR spectroscopy rather than HPLC. In anhydrous organic solvents, reversible transimination can occur between imines and amines with or without the addition of catalysts. For instance, Lehn and Giuseppone published a detailed study showing that Lewis acid $Sc(OTf)_3$ can universally catalyze transamination reactions in organic solvents and with an accelerated rate up to 6×10^5- fold.[25] Similarly, imine metathesis can occur between different imines under neutral conditions without additives and can be accelerated by the addition of acids or

nucleophilic catalysts.[4] For instance, Moore investigated the formation of poly(*m*-phenylene ethynylene imine)s *via* imine metathesis as a dynamic covalent reaction.[26] Addition of 10 mol % oxalic acid favored the formation of these polymers with high molecular weight over short trimers after several days thanks to the folding of the chains.

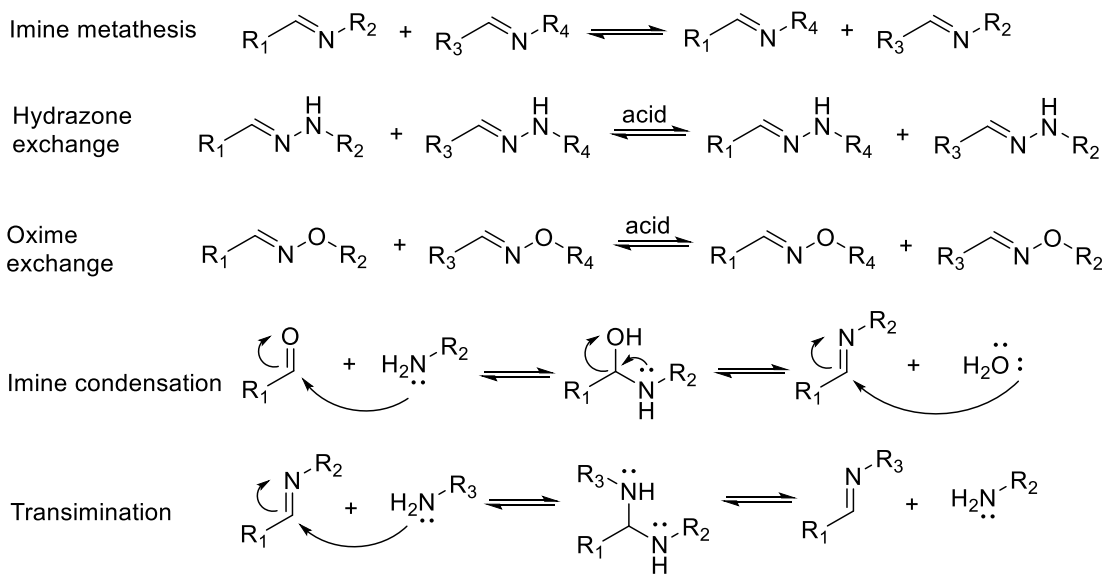

Scheme 1.2 | C=N exchange reactions used for DCvC and their mechanisms.

Compared with imines, hydrazones and oximes are more thermodynamically stable even at low pH in aqueous media. However, they suffer from low reaction rates at physiological pH, thus requiring the use of catalysts to enhance their reactivity. For instance, Dawson found out that the equilibrium between hydrazide-functionalized and glyoxylyl-functionalized unprotected peptides could be reached *via* hydrazone formation and transimination within a day at room temperature and at millimolar concentration using aniline as nucleophilic catalyst. One main advantage of using aniline as catalyst is the possibility to limit the use of a large amount of reactants to obtain an efficient exchange reaction.[27] They also proved that aniline could accelerate oxime ligation between aminooxyacetyl-functionalized and glyoxylyl-functionalized unprotected peptides in aqueous solution at pH 4.5 and pH 7. Their result demonstrates that the presence of aniline can help implementing dynamic hydrazones and oximes in DCLs with biological applications.[28]Besides, hydrazone exchange reaction using bi-functional building blocks (hydrazine and dimethoxyacetal units) can be triggered at room temperature using TFA and “switch off” upon addition of a base.[29] Furthermore, Dawson proved that stable bisaryl hydrazone bond could be cleaved under neutral condition (sodium phosphate buffer, 0.1M, pH 6.0) upon the addition of catalytic aniline. Specially,

as presented in Figure 1.5, CLB354 was found stable overnight in a solution of sodium phosphate buffer (0.1M, pH 6.0). However, after addition of aniline to the CLB354 solution, a decrease in the concentration of CLB354 to nearly 25% caused by the transamination and hydrolysis occurs. Then, upon synchronous addition of aniline and NH_2OH to the CLB354 solution, the free aldehyde produced via transamination and hydrolysis from the bisaryl hydrazone could trap NH_2OH to form a more stable oxime ligation. As a consequence, the stable hydrazone bond was disrupted and the equilibrium was shifted in the direction of oxime ligation. The methodological research presented by Dawson could be used in a wide range of biologically-relevant applications considering the mild exchange conditions and thus enrich the possible applications of DCvC.[30]

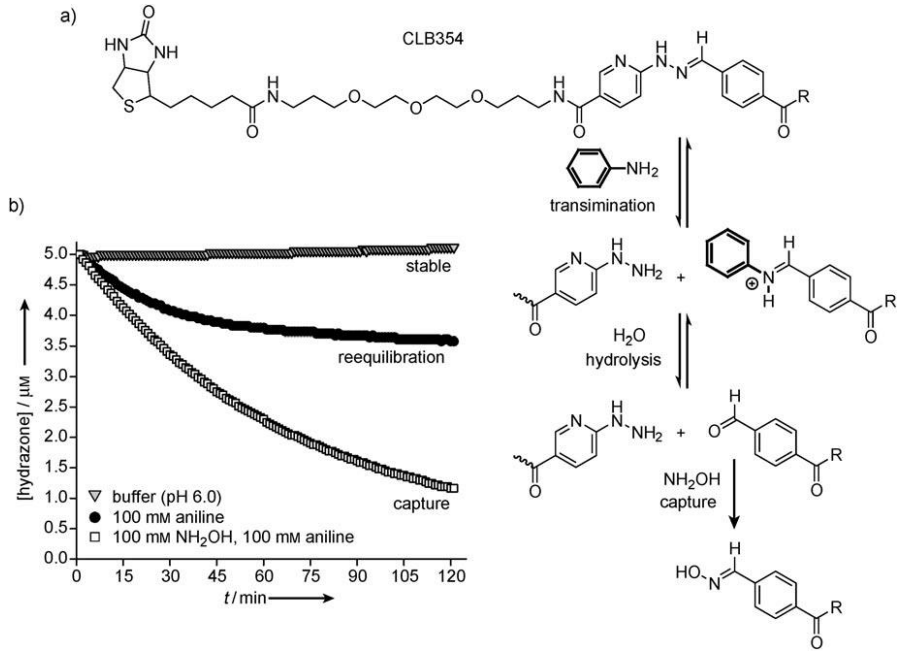

Figure 1.5 | Cleavage mechanism of CLB354 in the presence of aniline and NH_2OH; b) Graph showing the evolution of the concentration of CLB354 (started from 5 µM) with reaction time in buffer without aniline (stable line), after addition of aniline (100 mm, re-equilibration line), and upon synchronous addition of NH_2OH (100 mm) and aniline (100 mm, capture line). Figure is adapted from ref. [30].

So far, to the best of our knowledge, neither oxime nor hydrazone metathesis have been achieved probably due their high thermodynamic stability. Applications of C=N exchange, for instance in the field of materials science, are detailed in section 1.2.1.

1.1.2.3 Disulfide exchange

Disulfide exchange is another significant dynamic covalent bond widely employed in DCvC and, which is also known to play a significant role in biological processes. The mechanism of disulfide exchange reaction (Figure 1.6) can follow two main mechanistic pathways: either anionic or radical. The anionic mechanism is based on the formation of a thiolate anion which can then attack an original disulfide bond to create another disulfide moiety (Figure 1.6 A).[31] The radical pathway is initiated by radicals generated from light (Figure 1.6 B) or the addition of a radical initiator (Figure 1.6 C).[32] Interestingly, the chemical nature of the disulfide plays an important role in their reactivity. For instance, aromatic disulfide can easily undergo metathetic exchange (Figure 1.6 D) while aliphatic disulfide usually requires the use of a catalyst such as tri-*n*-butylphosphine or trimethylamine.[33–35]

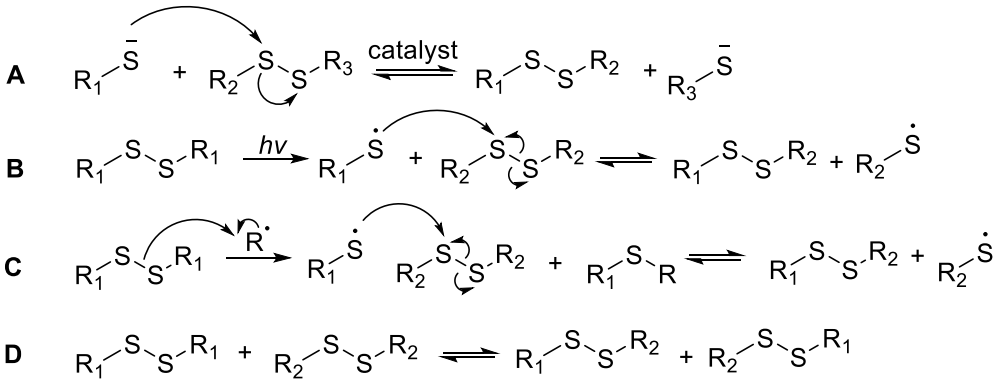

Figure 1.6 | Different mechanism of disulfide exchange reaction.

Since disulfide exchange can be triggered by a deprotonated thiol, the reaction can be controlled through the pH of the environmental media. Typically, for a pH ranging from 7 to 9, a sufficient amount of thiolate is generated for the exchange to occur. Correspondingly, lowering the pH of the media can quench the exchange. The presence of a catalytic quantity of reductants such as dithiothreitol (DTT) can also activate the exchange.[36] Recent studies have shown that new stimuli such as high pressure or ultrasound can also trigger dynamic disulfide exchange.[37,38] Applications of disulfide exchange, for instance in the field of materials science, are detailed in section 1.2.2.

1.1.2.4 Other reversible covalent reactions

Although many other dynamic covalent bonds have been considered for applications in DCvC such as alkene and alkyne metathesis, or acetal transfer[1], we will here focus only on Diels-Alder reaction

and dynamic boronic esters, as they have been particularly studied for applications in polymer science.[5] Diels-Alder reaction is the prototypical pericyclic reaction, which lead, through an exothermic [4+2] cycloaddition, to the formation of two σ-bonds at the expense of two weak π-bonds. Usually, either harsh temperatures or tailored dienes (electron-poor) and dienophiles (electron-rich) are necessary to favor the reversibility of Diels-Alder reaction.[39] Lehn and coworkers reported the possibility to perform reversible Diels-Alder reaction at room temperature (Scheme 1.3) by using 9,10-dimethylanthracene as diene and cyano-functionalized dienophiles.[40] The exchange reaction reached its equilibrium within 3 hours at room temperature in $CDCl_3$ and with a half reaction time ($t_{1/2}$) of 2.5 minutes. The reversibility of the reaction was confirmed by increasing the temperature to 50 °C, which shifts the equilibrium towards the starting materials.

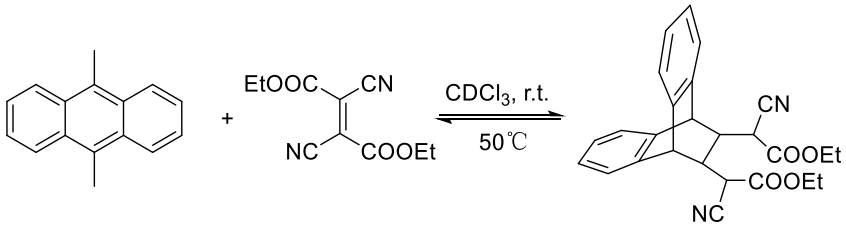

Scheme 1.3 | Dynamic covalent Diels–Alder reaction between anthracene and dienophile.

The Diels-Alder reaction between maleimide and furan is also of particular interest for DCvC. Northrop and coworkers have shown that the reversibility of this reaction rely mostly on the furan substitution while the maleimide moiety has only a minor influence.[41] Only mild electron-rich and neutral furans like 2-methylfuran are suitable for an efficient dynamic behavior in the Diels-Alder reaction.

In addition, Nguyen and coworkers have developed healable polyurethane (PU) networks at reasonable temperature (~60-70 °C) *via* reversible DA reactions and hydrogen bonds (Figure 1.7).[42] The DA bonds were incorporated at the interface between the hard and soft phases which is composed of a semicrystalline polycaprolactone while hydrogen bonds were located in the hard phase. These 2 dynamic moieties allowed the formation of PU materials with particular mechanical properties such as stiffness, toughness and mendability. Additional healing properties at mild temperature were obtained by melting the material in the soft phase. Interestingly, adjustment of the functional units involved in the reversible DA reaction could provide a way to optimize these PU materials. This work showed the combination of DCvC and supramolecular chemistry can lead to efficient heal ability and high mechanical properties in dynamic polymer networks, which is promising for the use of dynamic

covalent bonds in material science.

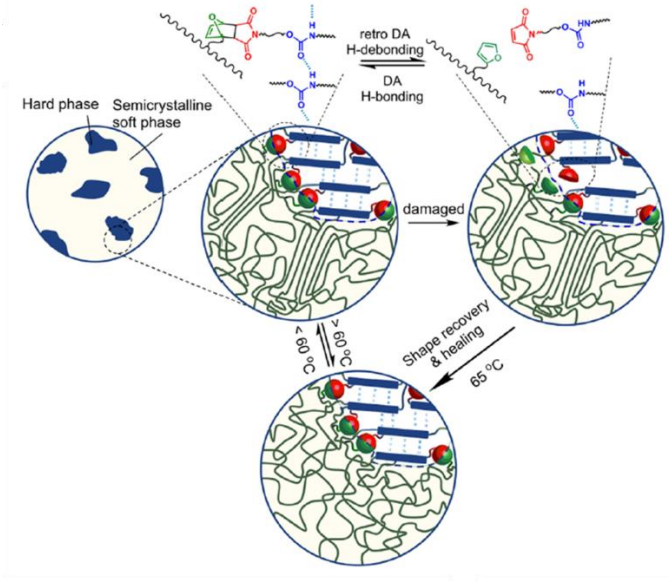

Figure 1.7 | Schematic representation of the healing process of PU materials containing both DA moieties at the hard-soft interface and hydrogen bonding interactions in the soft phase. Figure is adapted from ref. [42].

One more recent dynamic reaction is the formation of boronic esters performed between diols and boronic acids under ambient conditions. In aqueous solution, the reversibility of the boronic ester formation is controlled by the pH. Thus, when the pH value is higher than the pK_a of the boronic acids, the formation of boronate esters is favored, while the equilibrium is shifted to the starting materials for pH lower than this pK_a.[43] Formation of boronic esters can also be accomplished in organic solvents. For instance, the group of Iwasawa reported the dynamic formation of boronic ester depending on environmental conditions.[44] As shown in Figure 1.8, when equimolar amounts of polyol **1** and 1,4-benzenedi(boronic acid) **2** were mixed in methanol, the polymeric boronate, which was insoluble in the system, was formed *via* boronic ester linkages and precipitated from the solution. Precipitation of the insoluble products served as trigger for the selection process. When methanol was replaced by a 2:1 mixture of methanol and toluene in the same reaction, a tetrameric macrocycle (abbreviated as [2 + 2]) complexing one toluene molecule was synthesized with 90% yield. As [2 + 2] is soluble in several organic solvents, toluene acted as a template to trigger its selective formation. More interestingly, after replacing toluene with benzene in the same condition, a hexameric macrocycle (abbreviated as [3 + 3]) complexing two benzene rings was obtained with 94% yield. These results offer possibilities for future applications of boronic ester formation with selective functions.

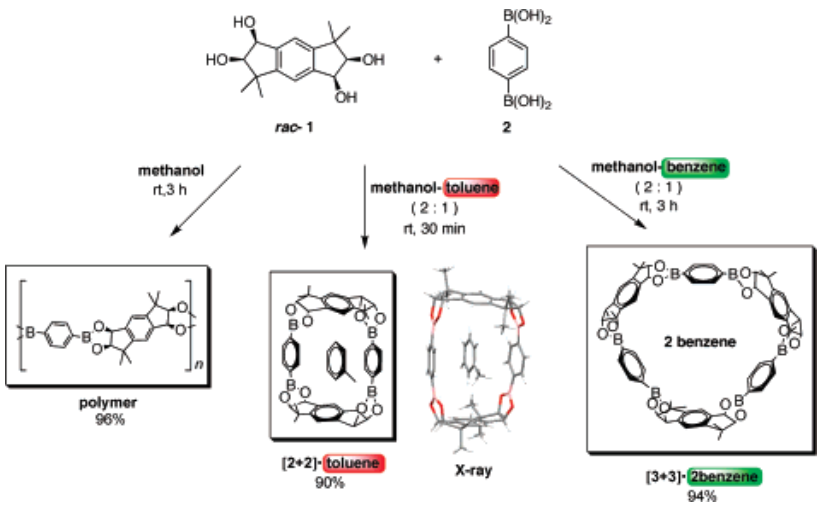

Figure 1.8 | Solvent-controlled formation of boronate esters. Figure is adapted from ref. [44].

In the field of polymer science, Guan and coworkers demonstrated that boronic ester transesterification can confer malleability, self-healing properties and reprocessability to covalent polymer networks.[45] In particular , the polymer containing 1,2-diol-moieties was dynamically cross-linking with telechelic diboronic ester via boronic ester transesterification, providing better malleability and self-healing character at mild temperature (50 °C) to the polymer network compared to the network constructed from diboronic ester without telechelic group. The dynamic materials could also recover their mechanical properties after multiple cutting-reprocess cycles. This work demonstrates that DCvC based on dynamic boronic ester bonds is promising for the development of self-healing elastomers and processable thermosets (Figure 1.9).

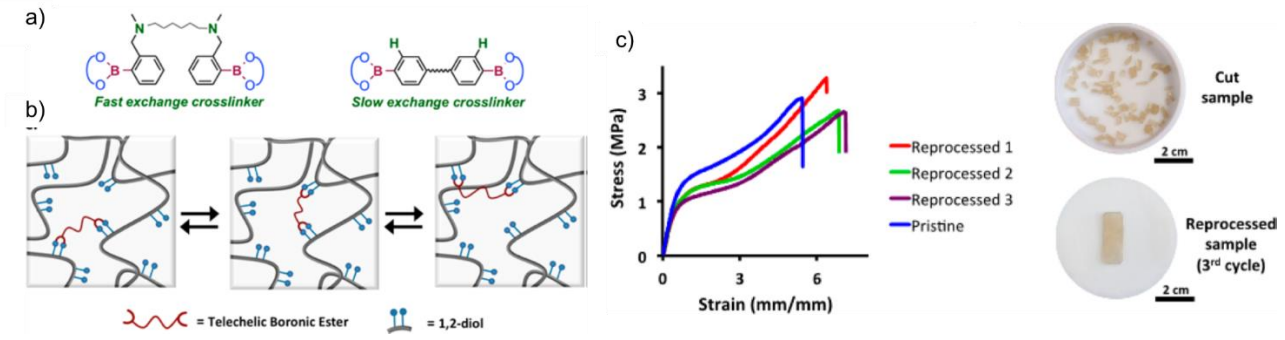

Figure 1.9 | a) Chemical structures of the 2 diboronic esters used as dynamic crosslinks (telechelic on the left); b) Representation of the dynamic network constructed by a telechelic diboronic ester and its possible rearrangement; c) Stress-strain tests on reprocessed materials and corresponding images of the polymer networks before and after reprocessing. Figure is reproduced and adapted from ref. [45].

1.1.2.5 Parameters to optimize reversible covalent reactions for DCvC

Before the birth of DCC, chemists focused on two main aspects when considering synthetic reactions: (1) performing the reaction efficiently and in high yield, and (2) driving the reaction in the forward direction to obtain the final compound. However, when considering a reaction for DCC, synthetic reactions should be considered both in the forward and reverse direction. Thus, optimizing dynamic covalent reactions necessitate to focus on particular parameters such as conditions of exchange, rate of exchange and ways to halt the exchange.

Conditions of exchange

One obvious criterion to consider for exchange reaction applied to DCC relates to the reaction conditions which ideally should be mild and favor reversibility. For example, the formation of imine from the condensation of an amine and an aldehyde is driven by the removal of water either chemically or physically but water is required to induce its hydrolysis. Nevertheless, imine metathesis occurs smoothly in the presence of a catalytic quantity of acid and the presence of a reducing agent allows to freeze its dynamic by affording the corresponding secondary amine.[46] However, one drawback of this approach is the loss of the dynamic character of the imine bond which preclude further study of the DCL. Exchange conditions can also be dictated by the targeted application. For instance, in the case of biomolecules as receptor or target, the reaction taking place in the library should ideally occur at room temperature in aqueous buffer solution. It would also be important to avoid using enzymes or conditions which would denature the biomolecules although some experimental set-up have been designed to limit possible problems.[14,47,48] So, during the methodological investigation of reaction conditions, one should keep in mind the targeted application in order to keep the integrity of the DCL.

Rate of exchange

A second parameter to look at is the rate of exchange reaction, which, in general, is expected to be as fast as possible. Typical parameters to enhance the reaction rate include, for instance, increasing the concentration of starting materials and/or the temperature. Obviously, as dynamic covalent bonds are typically characterized by high activation barriers, catalysis is often required to facilitate the equilibration for the majority of DCLs. Biological catalysts such as enzymes but also synthetic ones have been explored to facilitate exchange reactions. For instance, amide exchange between

carboxamides and amines needed 16 hours to reach equilibrium in the presence of metal catalysts, while it required more than one month in its absence.[15] However, as mentioned before, the considered catalysts should only regulate the exchange rate and not disrupt the integrity of DCLs. In some cases, significantly slow reaction rate and long equilibration time are required, such as in the folding-driven polymerization of oligo(phenylene ethynylene) imines in order to reach polymers with higher molecular weights.[49]

Ways to halt the exchange process

Analysis of the DCLs very often required to halt the dynamics of the covalent reactions involved in the process. Common approaches to freezing the exchange reaction include temperature control, pH control, removal of light input or catalysts, or kinetic trapping of the library member through oxidation or reduction. Disulfide exchange could be halted by lowering the pH and resumed by increasing the pH over 7.[31] Bowman and coworkers showed that the equilibration of transthioesterification could be halted by changing the solvent polarity from polar to non-polar.[18] As already discussed before, transesterification involving boronate esters could also be stopped by changing the solvent composition.[50]

Although the dynamic of imine can be modulated by pH, halting the dynamic process is very often achieved in an irreversible manner using reducing agents such as $NaBH_4$ (or similar derivatives) in order to completely “freeze” the dynamic bonds.[51] Similar approaches also apply for halting the dynamic nature of hemithioacetals.[52]

1.1.3 Dynamic combinatorial libraries

As mentioned in the introduction of this chapter, dynamic combinatorial libraries (DCL), composed by the combination of various building blocks hold together by reversible bonds (either covalent, non-covalent or both), are key components of DCC systems.[53] The reversible exchange of components within a DCL generates diversity (Figure 1.10). In most cases, modification of the experimental conditions leads to changes of the composition of DCLs at thermodynamic equilibrium. In particular, in the early days of DCC, the main approach consisted in introducing a target or template within the DCL in order to develop new receptors or ligands. Over the years, different types of effectors such as external physical or chemical stimuli (pressure, temperature, pH for instance) or internal templating, have emerged as new triggers to modulate the distribution of DCLs, providing them with **adaptivity**.[54]

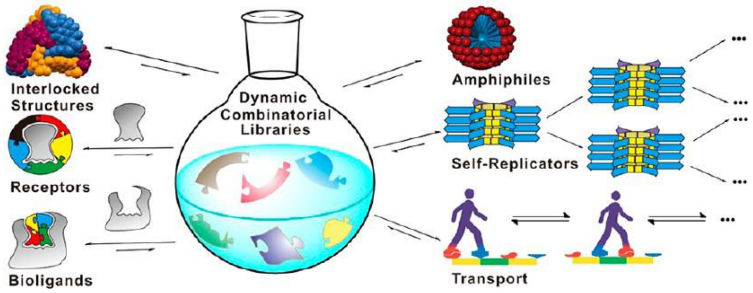

Figure 1.10 | Schematic representation of applications developed from DCLs. Figure is reproduced and adapted from ref. [53].

Several requirements are important when designing DCLs: (1) the need to possess dynamic covalent or non-covalent bonds between the library members. (2) the need to have optimal geometrical and functional space towards the targets or templates. (3) proper organization of the recognition groups for optimal binding.

Applications of DCLs involving dynamic covalent bond have initially focused on synthesizing receptors and ligands for drug discovery. Over the years, several developments have been made to design new functional materials or devices such as, for instance, catalysts, sensors, ion channels, gelators, surfactants or even polymers with unusual properties related to their dynamic character.[55–57] Advances in the field have also concerned the type of external or internal stimulus utilized to shuffle the constituents of the DCL, such as moving from templates to chemical or physical triggers such as electric field, or even to self-recognizing species.[4] Obviously, all these progress have also been made possible thanks to the use of a toolbox of analytical techniques whose performance is only improving.[58]

At the origin of the emergence of DCC, template-controlled DCLs aimed at constructing and selecting the best receptor from a large number of constituents. Targets or templates can consist in small molecules, (metal) ions, proteins, DNA/RNA or catalysts. For instance, Greaney and coworkers reported a series of glutathione (GSH) S-transferase (GST) inhibitors based on the reversible formation of acylhydrazones. In the presence of aniline as a nucleophilic catalyst, a DCL composed of one aldehyde and ten hydrazine molecules quickly reached equilibrium at pH 6.2, which is a suitable environmental set-up for biological applications (Scheme 1.5).[59] Upon the addition of two GST isozymes (hGST P1−1 and SjGST) individually in DCL, selection of the best binder for each protein target occurred. As control experiment, no selection of ligands happened using bovine serum albumin (BSA), indicating that the DCL is designed exclusively for GST enzymes.

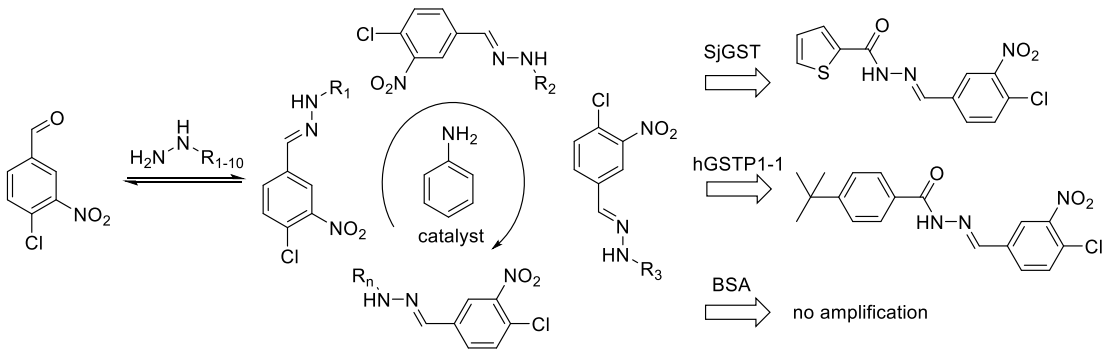

Scheme 1.5 | DCL of acylhydrazones produced in the presence of aniline and selection of the best binders for GST isozymes.

As an alternative to the use of a template, chemists have designed DCLs in which one of its members, so called replicator, can stabilize itself and possibly induce the formation of stable supramolecular structures.[60] For example, Otto and coworkers designed a DCL of dithiol-appended pentapeptides which could be oxidized into a library of tri-, tetra-, penta-, hexa- and heptameric macrocycles (Figure 1.11).[61] Due to the propensity of the alternating hydrophobic and hydrophilic amino acid residues on the pentapeptides to form β-sheets, some macrocycles could further assemble into fibers. In the absence of mechanical agitation, the smaller macrocycles were the main products for entropic reasons. However, after shaking or stirring for several days, hexameric or heptameric macrocycles became the dominant products as they can be stabilized in the form of fibers. The work demonstrated that self-replication can serve as template for DCLs by nanostructure formation and that mechanical force can act as a selection trigger between replicators.

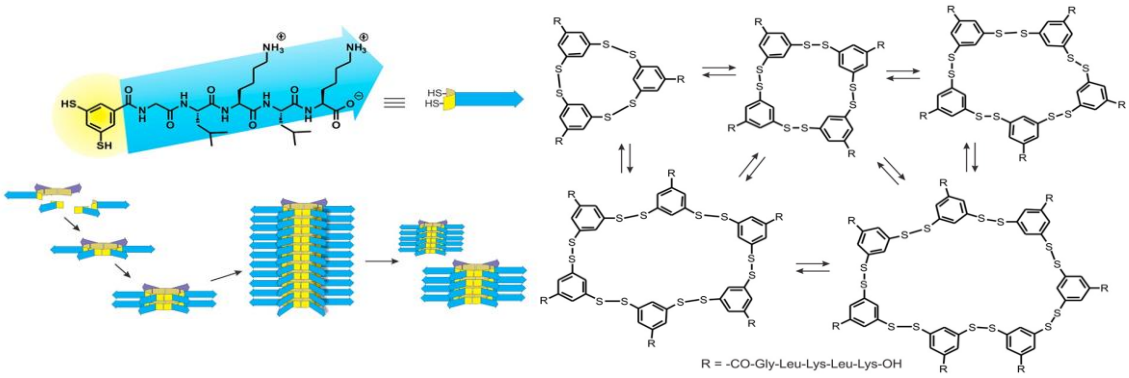

Figure 1.11 | Self-replicating behavior of a DCL made of dithiol-appended pentapeptides macrocycles. Figure is adapted from ref. [61].

In addition to a mechanical trigger, several other physical and physicochemical stimuli (solvent, light,

temperature, electric field *etc*.) have emerged as potential triggers for dynamic systems. For instance, UV irradiation at specific wavelengths can induce *cis-trans* isomerization of –C=N– bonds (imine, hydrazone) or disruption of dynamic covalent bonds such as disulfide or diselenide leading to DCLs capable of photoselection.[62,63] For example, the group of Lehn previously demonstrated that upon UV irradiation, the configuration of acyl hydrazones could be shifted from the *E*- isomer to the *Z*- one thanks to the stabilization by a hydrogen bond with the pyridine. While the *E*- isomer, which is capable of binding metal cations, leads to the formation of fiber-like supramolecular assemblies, UV irradiation induces isomerization of the acyl hydrazone leading to cation release. As DCLs are mainly prepared in solution, the addition of another non-miscible phase, leading to a so-called multiphase DCL, can also influence the behavior of dynamic systems. The group of Miller developed the concept of resin-bound DCC to figure out the identification of particular ligands. They designed a series of DCLs with various resin-bound "monomers" (octadepsipeptides), which could bind with a DNA-functional fluorescent target. Capture and exchange experiments on the resin led to the selection of a particular dimer which proved to be the best binder to DNA. Control experiments showed that single resin-bound "monomers" do not have fluorescence response. This new method overcome the limitation associated with DCLs in solution and open the door for affinity identification.[64]

Going to liquid-liquid multiphase DCL, Luning and coworkers reported the selective formation of a transport cargo (Figure 1.12), carrying $CaCl_2$ from an original water phase into an aqueous receiver phase through a layer of dichloromethane. An oligoethylene glycol diamine was dissolved with Ca^{2+} in the original water phase (left part), while a dialdehyde was solubilized in the organic phase and the receiver phase contained only water. After incubation for one week, 5 to 7% of Ca^{2+} was observed in the receiver water (right part) as monitored by NMR spectroscopy. This work confirmed the successful implementation of liquid-liquid multiphase DCL.[66] More recently, Lehn and coworkers proposed that stimuli-induced liquid-liquid separation can modify the library composition in a reversible manner upon phase reunification. The re-distribution of the DCL components was caused by the phase separation and could be reverse to its original state by the phase recombination.[67]

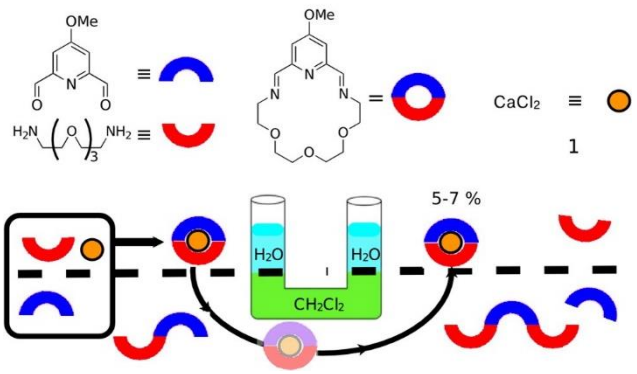

Figure 1.12 | Calcium transport experiment using a multiphase DCL of imine macrocycles. Figure is adapted from ref. [66].

Aside from DCLs performed in multiphasic environments, DCL leading to the formation of amphiphilic molecules could also generate, by themselves, mesophases such as micelles or vesicles. In these systems, the hydrophilic and hydrophobic parts of the amphiphile are connected by dynamic covalent bonds, such as imine, disulfide, *etc*. For instance, van Esch and coworkers reported a DCL of surfactants consisting in a polar aromatic aldehyde and a series of apolar aliphatic amines (Figure 1.13).[68] By changing either pH or temperature, the dynamic system was controlled between a micellar amphiphilic state and a non-micellar non-amphiphilic state. Although imine bonds can be hydrolyzed in aqueous solutions, the micellar formation could shift the system into a more stable state associated with the stabilization of the imine bond.

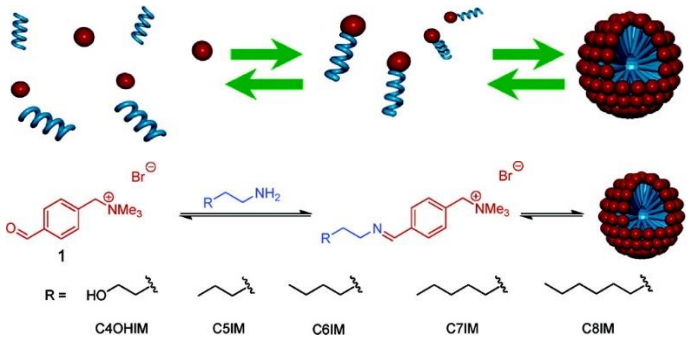

Figure 1.13 | Dynamic covalent surfactants leading to the formation of micelles. Figure is reproduced and adapted from ref. [68].

Using a library of amines with different pK_as (aliphatic, aromatic or benzylic), our group reported the formation of imine-based amphiphiles which can reversibly exchange their components and lead to the formation of either spherical or cylindrical micelles.[69] In acetonitrile, the DCL formed by a hydrophobic aldehyde (blue block) and two amines (red block) with various hydrophilic lengths reached a thermodynamic equilibrium where cylindrical micelles with short hydrophilic chain are favored. Replacing acetonitrile by water induced instability of the cylindrical micelles and their subsequent division. Over time, a dramatic evolution of the selectivity in favor of spherical micelles with longer hydrophilic chain was observed, due to the formation of more stable micellar self-assemblies (Figure 1.14). Interestingly, this example shows how selection of the best replicator at the molecular scale leads to selection of a mesophase at higher length scale.

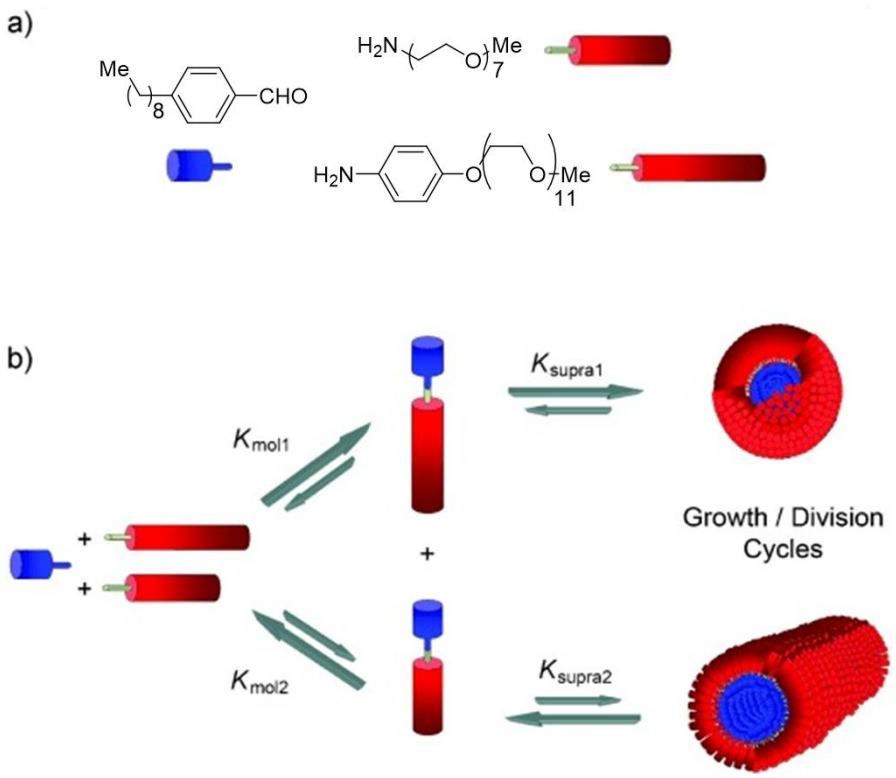

Figure 1.14 | Self-replicating DCL leading to the amplification of one mesophase depending on solvent constitution. Figure is reproduced and adapted from ref. [69].

Overall, rapid developments over the last two decades have established DCL as a reliable tool for the spontaneous discovery of new molecules with practical applications in various environments.

1.2 Emerging applications from DCvC

DCvC has found multiple applications into various research fields, leading to the formation of diverse DCLs, but also two-dimensional macrocycles and three-dimensional cages.[11] Hereafter, we will detail some examples of DCvC in the areas of drug design and filtration, biotechnology, molecular separation, light-harvesting, dynamic material, *etc*, according to the dynamic covalent bond involved.

1.2.1 Reversible imine formation

The reversible imine formation from amines and aldehydes is a historical and widespread reaction in organic chemistry. Its relative applications range from supramolecular and mechanochemical systems, to responsive dynamic polymers, and smart materials, *etc*.[70] On the supramolecular level, chemists

have used dynamic imine/hydrazone chemistry to elaborate self-sorting systems, configurational rotary switches, molecular walkers, symmetrical molecular cages, molecular capsules, and covalent organic framework.

Osowaska and Miljanić described a complex self-sorting DCL containing 25 imines formed by 5 aromatic aldehydes and 5 aniline derivatives (Figure 1.15).[70] Upon distillation, imine **1A**, the least volatile imine among all members, was collected first and all imines containing either aldehyde **1** or imine **A** were relatively eliminated from the DCL. Upon increasing the temperature of distillation, constituents **3B**, **2C**, and **4D** were successively isolated with **5E** remaining as distillation residue, while imines made of the selected constituents were depleted at the different distillation temperatures. This work highlights the efficacy of a single dynamic covalent reaction to provide five different products simultaneously with high yield and purity.

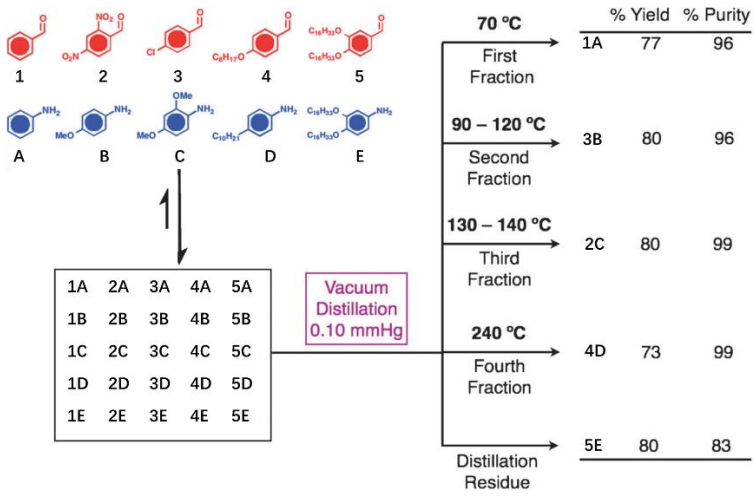

Figure 1.15 | [5×5] DCL leading to the formation of 25 possible imines and the selection of 5 of them during the course of a vacuum distillation. Figure is reproduced and adapted from ref. [70].

In 2019, Lehn reported that the generation of distribution signal by the addition of metal cations (Fe^{II}, Co^{II}, Ni^{II}, *etc*), on three different DCLs of imines, which can act as ligands for the metal cations.[71] The DCL was first studied in a single phase, typically chloroform and described as OUT phase on Figure 1.16. Upon addition of a non-miscible solvent such as water and described as IN phase, a 3D constitutional dynamic network (CDN) of imines in the biphasic mixture is formed with a distribution different from the one obtained in pure chloroform. After adding a metal cation to this initial two-phase system, the distribution of imines was again modified as a consequence of metal-ligand interactions between imines and the metal cation effector. During its adaptive process, information transfer occurs between the two phases, through the interface between the "writing" input phase (the

IN-phase, water) and the "reading" output phase (the OUT-phase). Overall, the change in the distribution of components and constituents observed in the OUT phase results from an adaptation of the DCL to a given effector, leading to the generation of a *dynamic pattern or fingerprint* which is characteristic of the presence of the effector in the two-phase system. This approach proved to be very useful for reading the response toward the effectors when data are analyzed by pattern recognition tools.

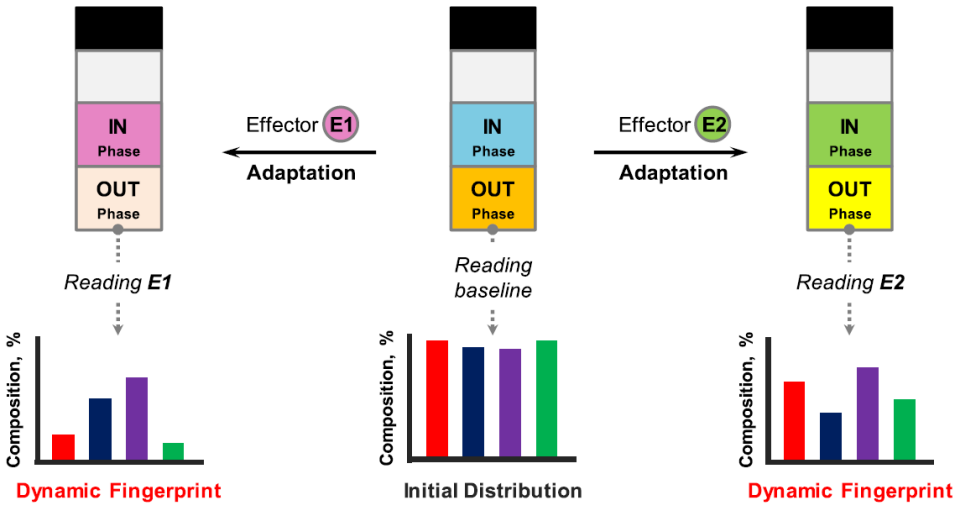

Figure 1.16 | Schematic representation of the adaptation of a DCL to different effectors E1 and E2 and leading to a distribution pattern which is characteristic of the dynamic constitutional "fingerprint" in the organic OUT-phase (e.g., a chloroform phase) for a particular effector E added to the aqueous IN phase; (center) initial distribution of constituents; (left and right) specific distributions of constituents generated in response to the addition of a given effector E1 or E2 to the IN-phase. Figure is adapted from ref. [71].

Applications of reversible imine formation to the field of polymers and at large, smart materials, has raised increasing attention over the last ten years. In 2012, Lehn and coworkers reported the synthesis of environmentally friendly dynamic polymers (dynamers)[72] with both double-degradation and self-healing properties (Figure 1.17).[73] These Green Dynamers (GDs) were fabricated from biodegradable oligomers, such as poly(butylene adipate) (PBA), poly(butylene succinate) (PBS), poly(lactic acid) (PLA), polyethylene glycol (PEG), *etc.*, incorporating reversible imine bonds. Films made of the GDs showed good mechanical properties in the bulk and could be disintegrated by the addition of water, serving as the first degree of degradation. The resulting oligomers could be further biodegraded into CO_2 and water, as a second-degree of degradation. Moreover, reversibility of the imine bonds provided the DGs with a self-healing character arising from the recombination of residual oligomers by evaporating water.

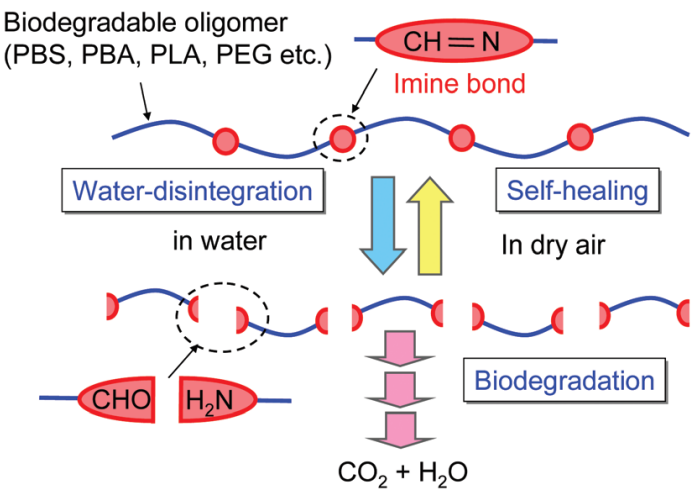

Figure 1.17 | Schematic representation of the different properties of green dynamers: water-disintegration, self-healing and biodegradable. Figure is reproduced and adapted from ref. [73]

Recently, Hecht and coworkers found out that light could influence the kinetics of imine exchange reactions on diarylethene (DAE) depending on whether they are in their ring-opened state (DAEo) or ring-closed state (DAEc).[74] As shown on Figure 1.18, after UV irradiation, the aldehyde-functionalized diarylethene is in a closed state (DAEc) which lead to the activation of aldehydes due to the extended π-conjugation of both electron-withdrawing terminal formyl groups. Conversely, in the absence of UV irradiation, the DAE is in a ring-opened state (DAEo) and aldehydes are less reactive towards amines. The activity difference between closed and opened forms for the same amines is around ten times. Based on this finding, they introduced the DAE as a difunctional crosslinker in an amino-functionalized siloxane polymer (AS). Upon UV light irradiation, closing of the DAE led to an enhanced activation of the aldehyde moieties which could more easily react with the free amine available on the polymer. Thus, DAEc@AS showed significantly faster self-healing efficiencies than DAEo@AS containing the opened DAE. This work highlights how the exchange rate of a dynamic covalent bond can affect its physical properties.

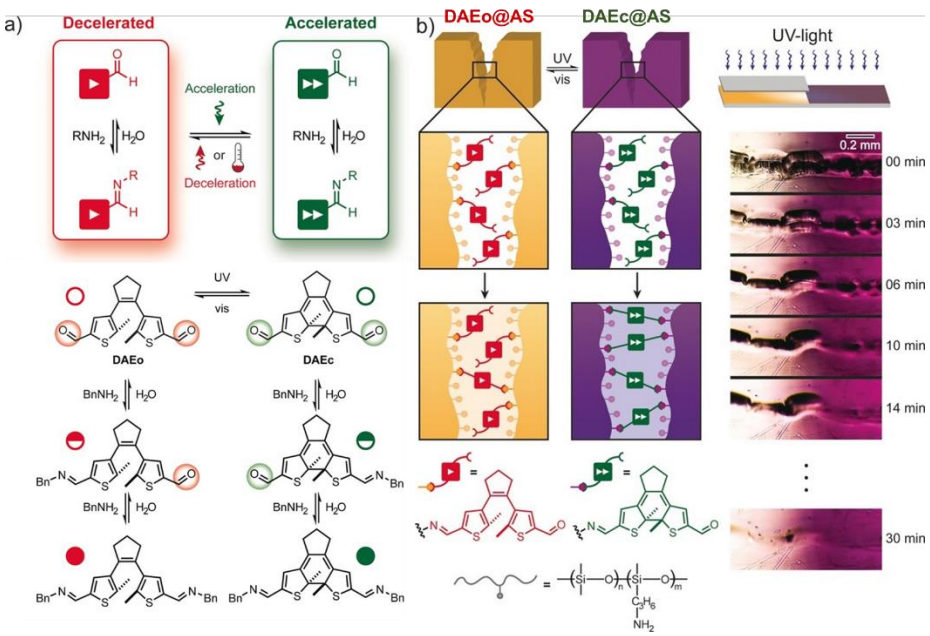

Figure 1.18 | a) Reactivity difference between ring-opened and ring-closed state of DAE towards benzylamine. Green and red colors imply accelerated and decelerated imine formation individually. b) Schematic representation of self-healing efficiencies between DAEc@AS and DAEo@AS. Figure is adapted from ref. [74].

Dynamic imine bonds have also been integrated into natural polymers to form biodynamers. For instance, the group of Barboiu synthesized hydrogel or films made of chitosans modified by dynamic imine bonds (Figure 1.19). Interestingly, the yield of imine formation on the chitosan backbones could be increased by changing from a liquid-phase reaction (with the yield of 1-12 %) to the hydrogels-induced or solid-phase-induced reaction (with the yield of 80-90 %). Such differences in efficiencies were attributed to the presence of hydrophobic aldehydes which are insoluble in water. Moreover, when two hydrogels layered one on top on the other (colorful C4 or C8 over colorless C7) were incubated for 2 weeks, a noticeable color migration occurred suggesting imine bond exchange reaction between the two parts. This result suggests the use of biodynamers for sensing and/or delivery devices. Dynamic imine exchange could also occur at the interface between a chitosan solid film (colorless C6) and a hydrogel (colorful C8) confirming the participation of dynamic covalent reactions in the biodynamer. These interesting results open the door to the innovation of more biocompatible and multifunctional materials (Figure 1.19).[75]

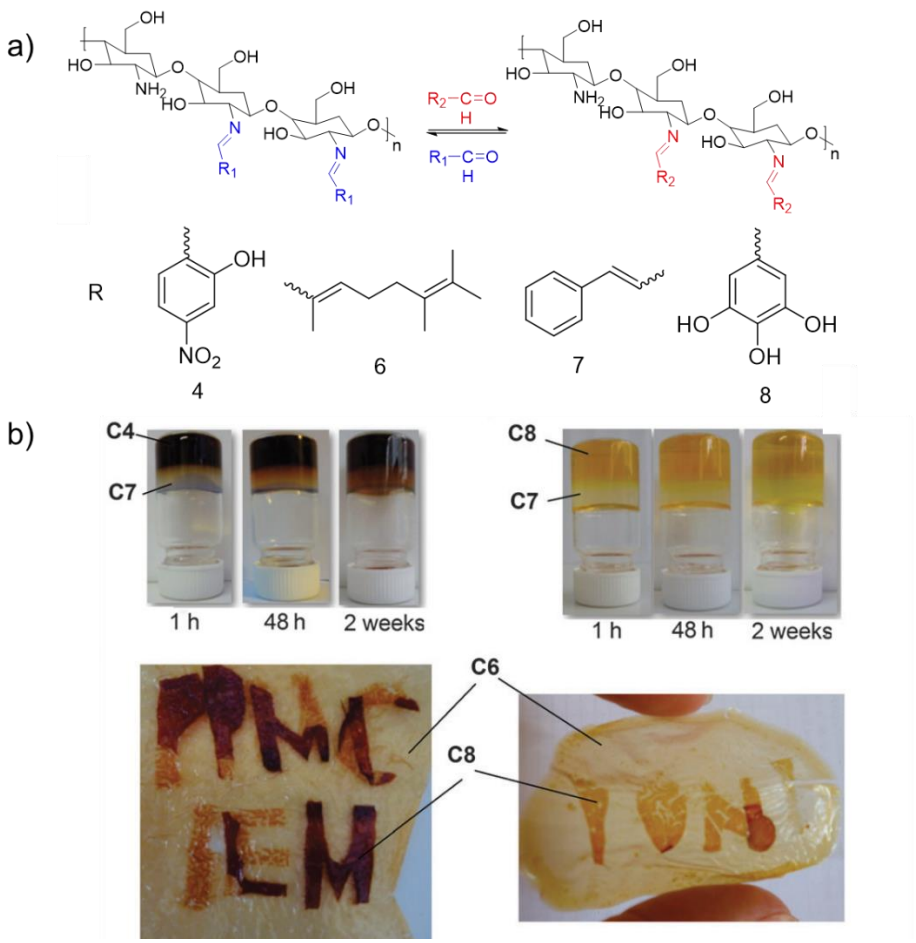

Figure 1.19 | a) Biodynamers made from imine-functionalized chitosans with different R-subunits and b) evolution with time of the color change of C4-C7 and C8-C7 hydrogels (top) and imprinting of colored slices of C8 on a film made of C6 (bottom). C4, C6, C7 and C8 represent the imine-functionalized chitosans with the R (4, 6, 7 and 8)-subunit. Figure is reproduced and adapted from ref. [75].

1.2.2 Disulfide exchange

As introduced previously, disulfide exchange is highly pH-sensitive and can be stopped by adding oxygen or lowering the pH of the mixture. Due to the easy controllability and excellent reversibility of disulfide exchange, chemists used it extensively to develop polymer hydrogels, bioconjugates, prodrugs, peptide mimetics, supramolecular structures, and nanomaterials.

DCL made from monothiol functional members could form topologically diverse structures including cages, macrocycles and linear oligomers. By combining reversible disulfide with environmental stimulus, commutation between diverse structures can be achieved. For instance, the Sanders group uses disulfide exchange reaction to synthesize various macrocycles and catenanes in water (Figure

1.20). The initial starting materials consisted in dithiol building blocks (green) made of an electron-deficient acceptor (A) aromatic unit, an alkyl chain with different lengths (n-linker: 2–9 carbons) and cysteine residues on the terminus (yellow dots). Depending on whether a cysteine-terminated and electron-rich donor (D) (red) was present or not, the DCL could adaptively produce various D-A catenanes or all-A catenane thanks to the reversibility of disulfide bonds, D-A interactions and hydrophobic effects. For instance, in the presence of dithiol acceptor, D-A [3] catenanes were produced only when the dithiol building blocks contained an alkyl chain with 2, 4, and 6 carbons (even effect), while giant macrocyclic catenanes were synthesized for linkers with 1, 3, and 5 carbons (odd effect). This phenomenon was also verified as an unexpected 'odd–even' effect in DCLs. For building blocks containing an alkyl chain above six carbons, D-A [2] catenanes were found to form with a decreasing influence of the 'odd–even' effect. In the absence of dithiol acceptor, an all-A catenane was synthesized. The selection of catenanes results from the adaptive behavior of dynamic covalent libraries to environmental stimulus, which demonstrates the importance of DCvC for the investigation of complex structures in dynamic systems.[76]

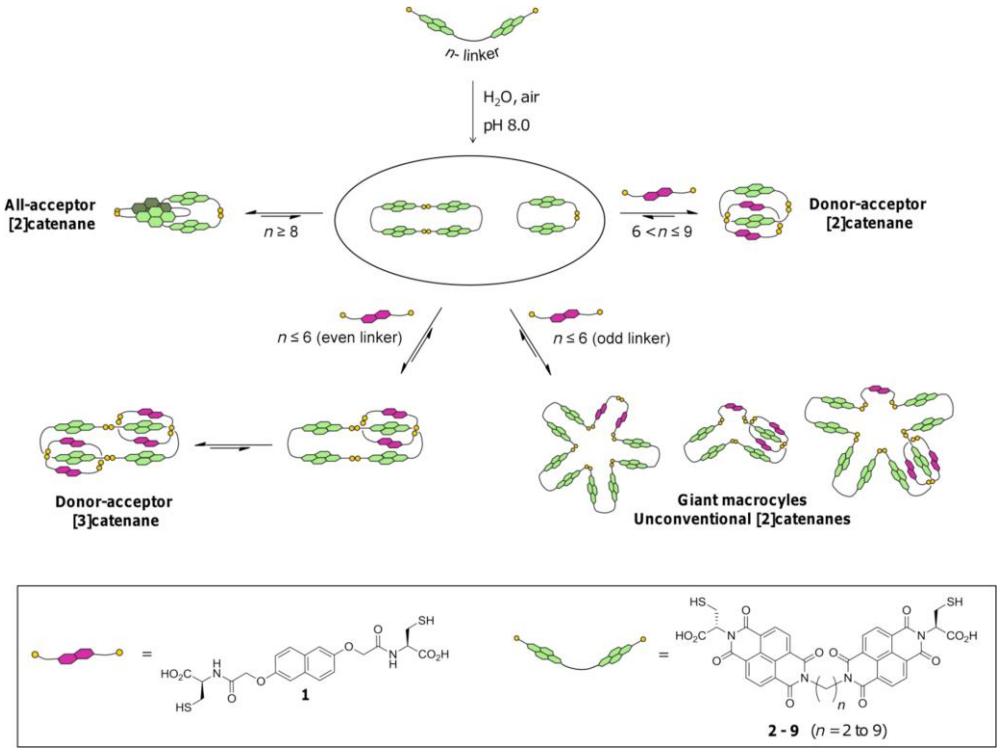

Figure 1.20 | Different catenanes formed in DCLs made of dithiol building blocks with an electron-rich donor (D) (red) 1 and an electron-deficient acceptor (A) (green) 2–9. The yellow dots represent cysteine residues on the terminus. Figure is adapted from ref. [76].

As introduced in the previous section on dynamic disulfide (section 1.1.2), disulfide exchange can be initiated by UV irradiation. Based on the work presented on Figure 1.21, Otto and coworkers found out that after UV irradiation (3 days, with a 9 W UV lamp at 365 nm) of a liquid solution containing hexameric macrocycles, disulfide bonds split into their homolytic thiol radicals. Due to the stable stacks of hexameric macrocycles, thiol radicals could attack each disulfide nearby to form cross-linked hydrogels.[62] Their work shows a new approach for the development of soft materials by DCvC.

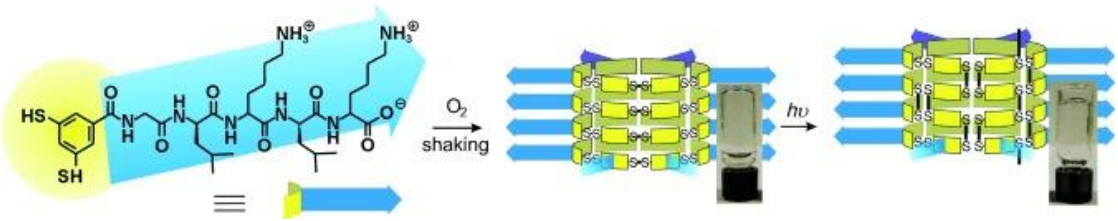

Figure 1.21 | Photochemical disulfide exchange results in the covalent capture of self-assembled structures obtained from disulfide-based DCLs, causing gelation of the aqueous solvent. Figure is adapted from ref. [62].

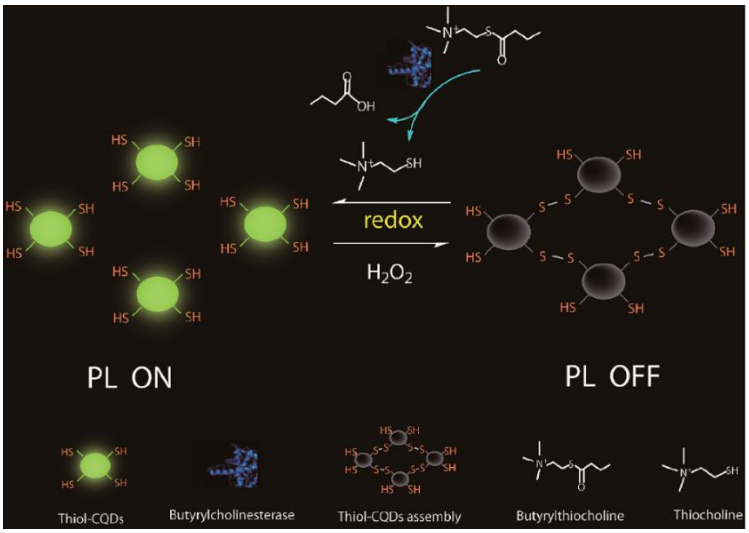

Figure 1.22 | Schematic illustration of a redox-controlled fluorescent nanoswitch as a detection strategy for BChE activity based on thiol-triggered disulfide cleavage. Figure is adapted from ref. [77].

Disulfide exchange can also be initiated by reducing reagents. Qian and coworkers published a redox-controlled fluorescence nanoswitch relying on the reversibility of covalent disulfide bonds (Figure 1.22).[77] The intense fluorescence of thiol-functionalized carbon quantum dots (thiol-CQDs) could be quenched by the addition of hydrogen peroxide (H_2O_2) which induces the formation of disulfide bonds between QCDs. However, upon the addition of butyrylcholinesterase (BChE) and butyrylthiocholine iodide (BTCh) which induce the formation of thiocholine, the fluorescence of

thiol-CQDs assembly was reversibly turned on by the breakage of disulfide bonds caused by the external redox stimuli (thiocholine). The specific thiol-triggered disaggregation-induced emission enables researchers to assay BChE activity in a fluorescence turn-on and real-time way using BTCh as the substrate.

In the last two decades, particular interests have arisen to apply DCvC to polymeric materials, leading to the formation of dynamic polymer (dynamer).[72] In 2013, Rowan and coworkers reported a new functional material, polydisulfide networks, exhibiting photo-healing, photo-reprogramming, and shape-memory properties (Figure 1.23). This cross-linked dynamer was fabricated from commercially available 1,6-hexanedithiol, 1,5-hexadiene and a tetrathiol (Figure 1.23left). The permanent shape (flat shape) of the film could be reprogrammed by exposing the film to UV light under mechanical constraint (twisting), where the disulfide bonds were cleaved and reconnected to form the new shape (helical shape). In addition, a scratched film whose depth is approximately half the thickness of the film could be recovered after UV irradiation of the scratched part. This photo-healing property is related to the photo-trigger disulfide exchange on the backbone of the polymeric material in order to reconnect the scratched parts. This multi-functional material was achieved thanks to both covalent cross-links and reversible disulfide bonds.[78]

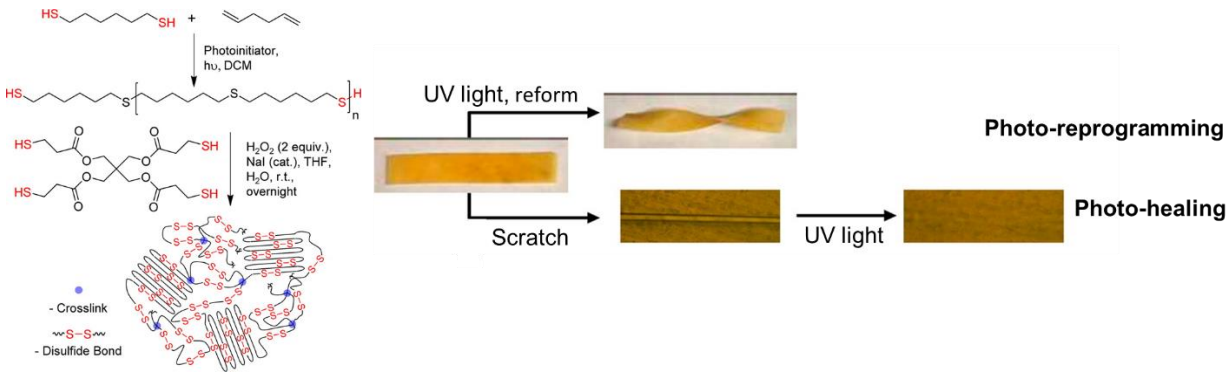

Figure 1.23 | Synthesis of polydisulfide networks and its relative light- and temperature-sensitive properties. Figure is reproduced and adapted from ref. [78].

In order to reach polymeric materials with innovative properties, chemists have designed materials which incorporate several types of dynamic covalent bonds. For instance, Chen and coworkers prepared a dynamic hydrogel with both adaptive self-healing and dual responsive sol-gel transition properties (Figure 1.24).[79] They designed and synthesized a polymeric hydrogel containing both acylhydrazone and disulfide bonds (Figure 1.24a). While acylhydrazone bonds can be activated under acidic or neutral conditions, disulfide ones can be activated under basic condition. With the

combination of these two dynamic covalent bonds, the polymeric hydrogel could undergo the self-healing process by simply bringing together the cut hydrogel, under either acidic (pH 6) or basic (pH 9) conditions, for 48 hours, and at room temperature in air (Scheme b). It is reasonable that the self-healing did not proceed at neutral condition (pH 7), as acylhydrazone and disulfide bonds are kinetically locked. However, upon addition of a catalytic amount of aniline, the acylhydrazone exchange proceeded and accelerated the self-healing efficiency (Figure 1.24b). In response to either pH or redox, the hydrogel could also undergo reversible sol-gel transition related to the disruption of either acylhydrazone or disulfide bonds, respectively.

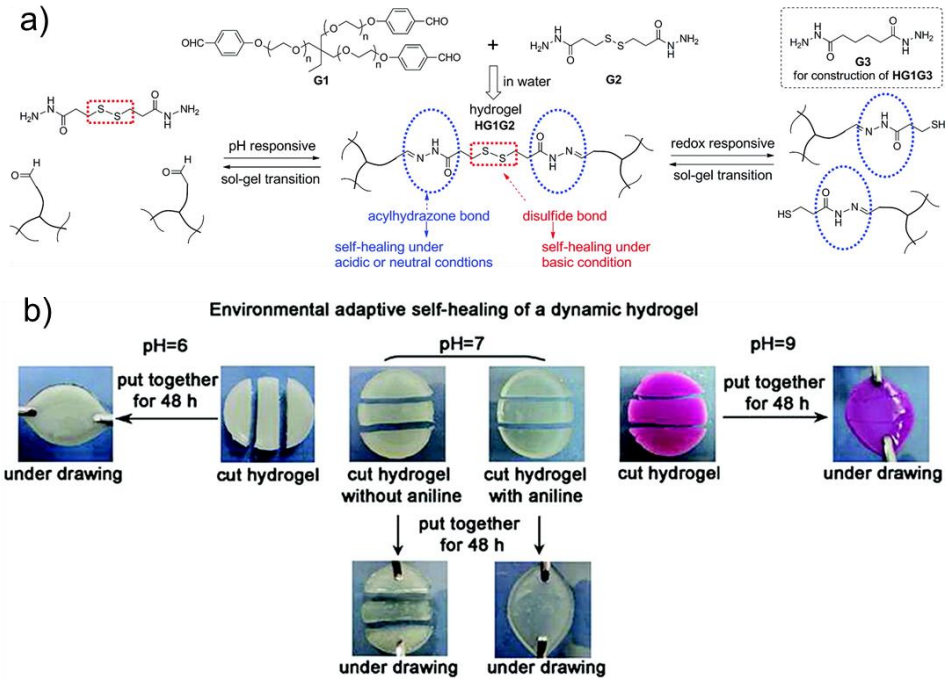

Figure 1.24 | a) Strategy for constructing a dynamic hydrogel with an environmental adaptive self-healing ability and dual responsive sol-gel transitions based on acylhydrazone and disulfide chemistry; b) Self-healing properties of the dynamic hydrogel. Figure is adapted from ref. [79].

1.2.3 Transthioesterification

The transthioesterification reaction offers an efficient stoichiometric (1:1 thiol: thioester) interchange with long-lasting reversibility, at low concentrations, at room temperature and in aqueous media (Figure 1.25 a)). The possibility to perform transthioesterification in aqueous phase makes it suitable for biomolecules and biological applications. In 1994, Kent and coworkers published a simple technique (Figure 1.25 b)) of protein total synthesis where transthioesterification directs the chemoselectivity in native chemical ligation.[80] Later, Gellman and coworkers applied

transthioesterification for evaluating higher-order structural stability in proteins (Figure 1.25 c)). After replacing the amide position in a peptide with a thioester bond, the thioester-functional molecule could perform the thiol-thioester exchange and reach their equilibrium rapidly. Based on the "backbone thioester exchange" (BTE) equilibrium constant (K_{BTE}), chemists could estimate the conformational stability of the protein analog in its native state.[81]

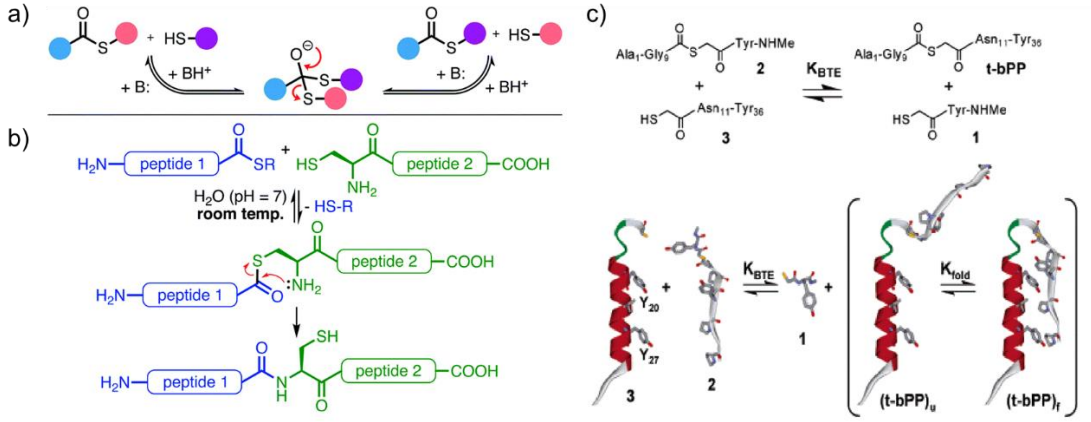

Figure 1.25 | a) Mechanism of transthioesterification; b) Mechanism of native chemical ligation related to transthioesterification; c) Equation (above) and model (below) for thermodynamic analysis of BTE. Figure is reproduced and adapted from ref. [80] [81].

Ramström and coworkers designed a DCL of thioesters with different acyl groups and thiols (sulfanylpropionic acid and thiocholine).[17] A series of five homologous acyl groups were selected for their structural similarity to the natural substrate of the enzyme, acetylcholine. The DCL at its equilibrium state was directly exposed to the catalytic domain of acetylcholinesterase (ACE), where the best substrate candidate was selectively recognized and then hydrolyzed (Figure 1.26). The self-screening process allowed the quick identification process of discrete substrates.

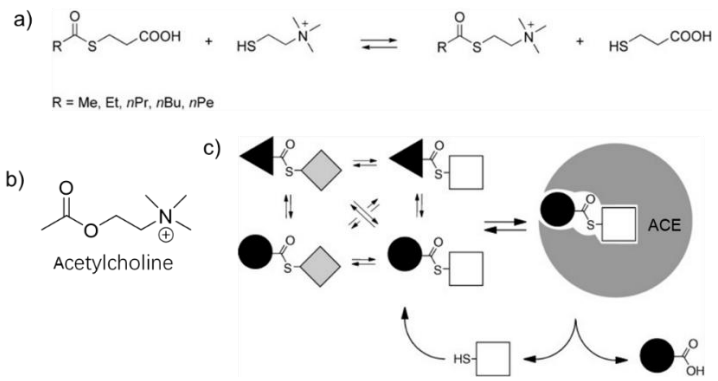

Figure 1.26 | a) DCL generation by transthioesterification; b) Acetylcholine; c) Schematic representation of the catalytic self-screening process with a DCL of thioesters. Figure is reproduced and adapted from ref. [17].

Transthioesterification has been particularly used as reversible covalent bond in material and polymer sciences. Recently, Grinstaff and coworkers published a new type of dissolvable dendritic hydrogels which could serve as sealants for second-degree burning wounds[82] This hydrogel is fabricated by the cross-linking of a lysine-based dendron and a PEG/thioester-based crosslinker with high synthetic yields. Upon the presence of a cysteine methyl ester (CME) solution to the sealants, the hydrogel which was covering wounds could dissolve rapidly *via* transthioesterification and could be removed directly. Details of the experiment is shown on Figure 1.27b). The "a" photograph shows the hydrogel covering a second-degree burning wound on a rat for 1 hour. In the photograph b, a CME-soaked gauze is applied to the left part of the hydrogel. Over time (photographs c to e), free CME-soaked gauzes were placed on the left part of the hydrogel, until complete dissolution of the hydrogel (after 30 min photograph f). The dissolution mechanism occurs through transthioesterification between the thioester bonds of the hydrogel and cysteines from the exogenous thiolate solution. The presence of thioester linkages within the hydrogel allows for an easy removal and eliminates any mechanical or surgical debridement. For biomedical applications, the efficiency of transthioesterification in aqueous solution provides new ways to develop biocompatible, multifunctional and dynamic controllable material.

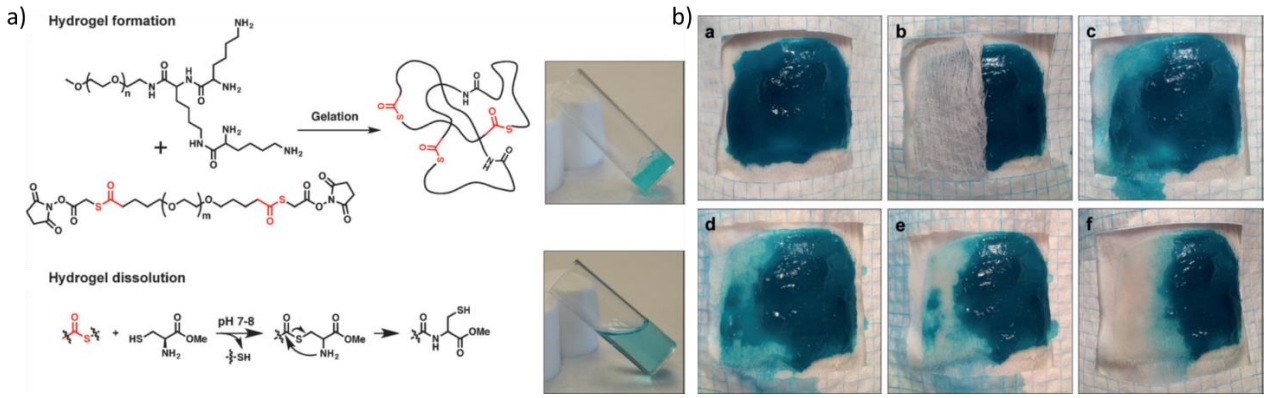

Figure 1.27 | a) Representation of a crosslinked hydrogel formed by the reaction between the dendron and a crosslinker and corresponding image of the hydrogel. And On-demand dissolution of the hydrogel relies on the transthioesterification reaction upon exposure to a cysteine methyl ester solution and corresponding image of the dissolved hydrogel. b) Photographs of the dissolution process of the hydrogel as a function of time after treatment with CME-soaked gauzes. Figure is reproduced and adapted from ref. [82].

Recently, Bowman and coworkers developed polymerization of polythioester organo- or hydrogels

via transthioesterification, in either organic phase or aqueous media, respectively.[83] Polythioester organogels were obtained from difunctional thioesters and tetra-functional thiols in DMSO at room temperature with a catalytic amount of triethylamine for 16 hours (Figure 1.28a)). Similarly, polythioester hydrogel was obtained in water under similar conditions. Oscillatory rheology on the polythioester hydrogel at a broad range of shear strain and frequency showed a change from a gel state to a solid state (Figure 1.28b) as demonstrated by the crossover of G' and G'' (G' = 1000-1100 Pa, G'' = 70-80 Pa) along with the frequency-dependent flow behavior. This behavior might be caused by transthioesterification, as similar results were found on a dynamic hydrogel containing disulfide bonds. These results open the door to extend the novel application of injectable materials and biological tissue-like sealants.

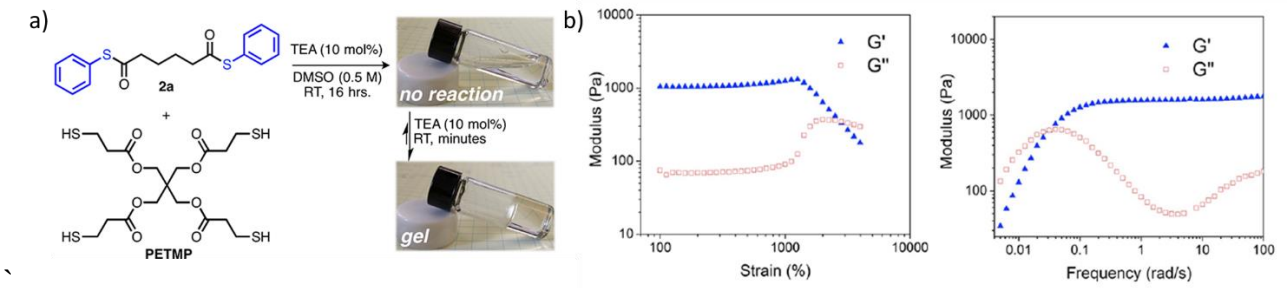

Figure 1.28 | a) Formation of a cross-linked polythioester organogel *via* transthioesterification; b) Oscillatory rheology of the polythioester hydrogel. Figure is reproduced and adapted from ref. [83].

The same group reported the synthesis of a dynamic phospholipid containing thioester-functionalized alkyl tails (**1b** with 11 carbons or **1c** with 7 carbons) *via* transthioesterification. The formation of liposomes from a mixture of a phospholipid (**1b** or **1c**) and unreacted precursors (**1a** with **3** or **2**) was confirmed by fluorescence microscopy and cryo-TEM. Upon reversible transthioesterification within stable liposomes, the presence of novel thioester-functionalized components (**2**) into previous stable phospholipid (**1b**) was observed accounting for 30% conversion of **1b** into **1c**. Fluorescence microscopy confirmed the preservation of liposomes even during the exchange process from **1b** to **1c**. These results could provide researchers with a better understanding of remodelling processes occurring in natural cell membranes which happens regularly in biological environments, furthering an inspiring example for the design and synthesis of an artificial cell.[84]

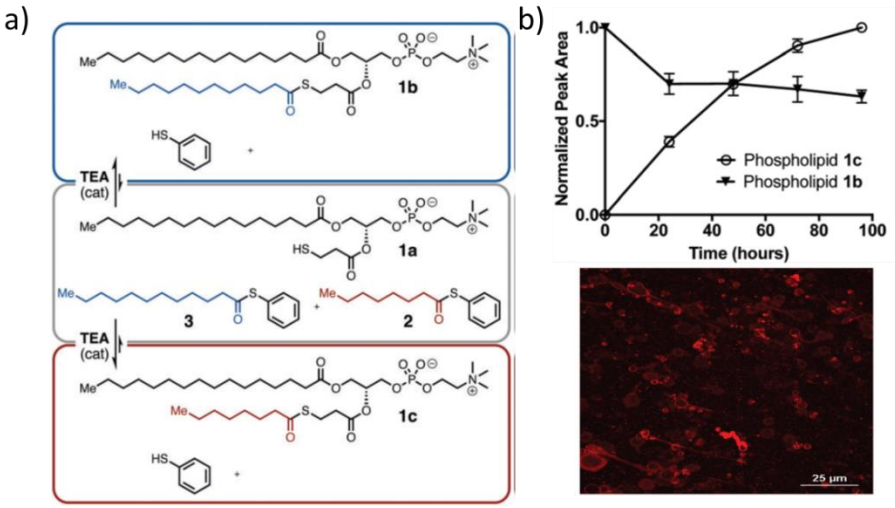

Figure 1.29 | Illustration of the formation of synthetic phospholipids using the thiol–thioester exchange reaction. Figure is reproduced and adapted from ref. [84].

1.3 Peptides and proteins in dynamic covalent chemistry

Proteins play significant roles in the structure and biological functioning of living organisms. Peptides are short proteins consisting, in general, of a short sequence (up to 50) of the 20 naturally-occurring chiral amino acids (aa) whose structure varies only at the R position located on the central carbon between the carboxylic acid and the amine units. They are chemically versatile, biodegradable, and biocompatible. The R groups and thus the sequence of amino-acids provide peptides with a particular conformation that is responsible for their function. Very often, replacement of one amino-acid in the sequence by another one results in a dysfunctioning of the corresponding biomolecule.[85] In general, proteins are obtained either biochemically by *in vivo* expression or chemically by chemical synthesis. For the latter, proteins usually arise from peptide fragments that are coupled through native chemical ligation (NCL).[80,86] In most cases, nowadays, peptides are synthesized by solid phase peptide synthesis (SPPS). Hereafter, we will first describe the basic principles of SPPS and native chemical ligation and then show how peptides and proteins have been used in DCLs.

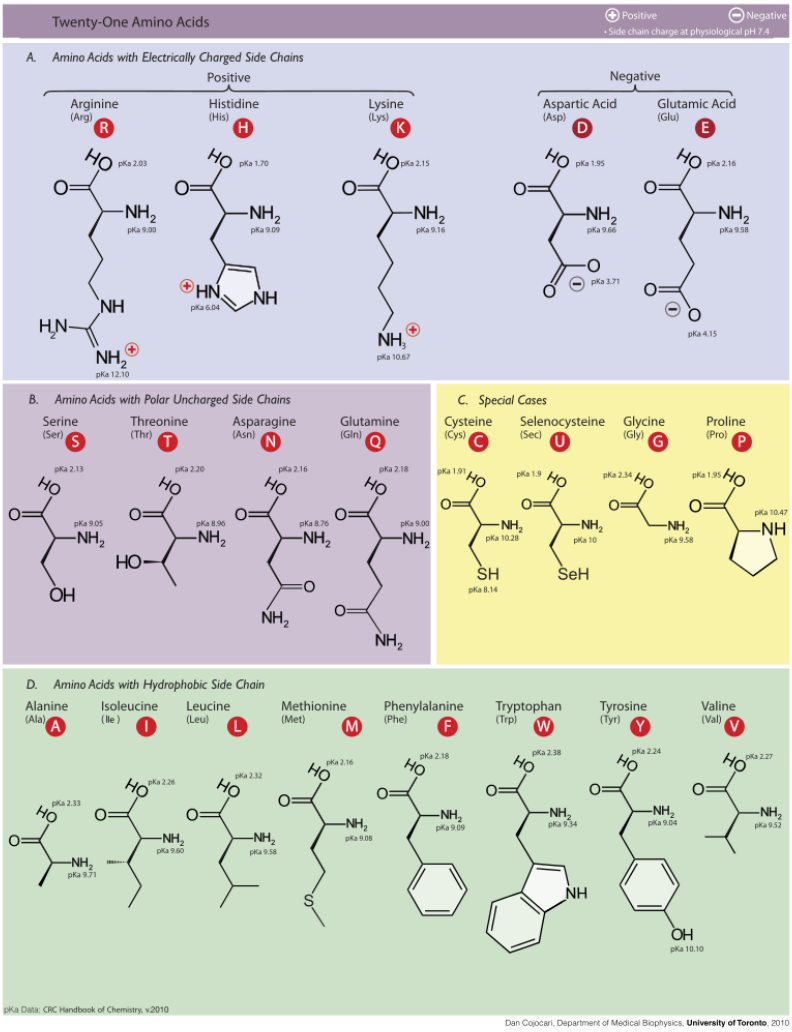

Figure 1.30 | Chemical structures of the 20 naturally-occurring L-amino acids. Amino-acids are classified according to the nature of their side chains. Their structures are drawn together with their common name, their one or three letter abbreviations and pK$_a$s of their ionizable groups. Figure is adapted from https://zh.wikipedia.org/wiki/%E6%B0%A8%E5%9F%BA%E9%85%B8#/media/File:Amino_Acids.svg.

1.3.1 Solid phase peptide synthesis (SPPS)

In 1963, Merrifield and coworkers introduced a new approach, namely solid phase peptide synthesis (SPPS) , that could provide peptide fragments with size up to 50 aa.[87] SPPS is the benchmark synthetic methods to access synthetic peptides for use in chemistry, biology, medicine, and material sciences.[88]

A general protocol for SPPS consists in the following steps. First, the free carboxylic acid group of the first aa (C-terminal part of the peptide) is covalently attached to an insoluble polymeric support-

resin with the help of an activator. Subsequently, after removal of the protecting group (generally Boc or Fmoc) at the *N*-terminal of the first aa, the second aa is loaded on the aa-functionalized resin in the presence of an excess of reagents and amino-acids. After the formation of this second peptidic bond, filtration and extensive washing of the resin from an excess of activated amino acid and soluble by-products are performed. Several cycles (coupling-washing-deprotection-washing) are repeated until the desired peptide sequence is obtained. The final step consists in cleaving the synthesized peptide from the polymeric resin under conditions which lead to the removal of protecting groups of the side chains. Finally, the crude peptide product is precipitated or extracted from the cleavage solution and a purification step, typically by reverse phase HPLC, is usually required (Figure 1.31).[86] Over the years, several parameters from this protocol have been optimized, and nowadays, microwave-assisted solid phase peptide synthesis, which consists in activating all the steps by microwave heating, has become the standard for routine peptide synthesis.[89]

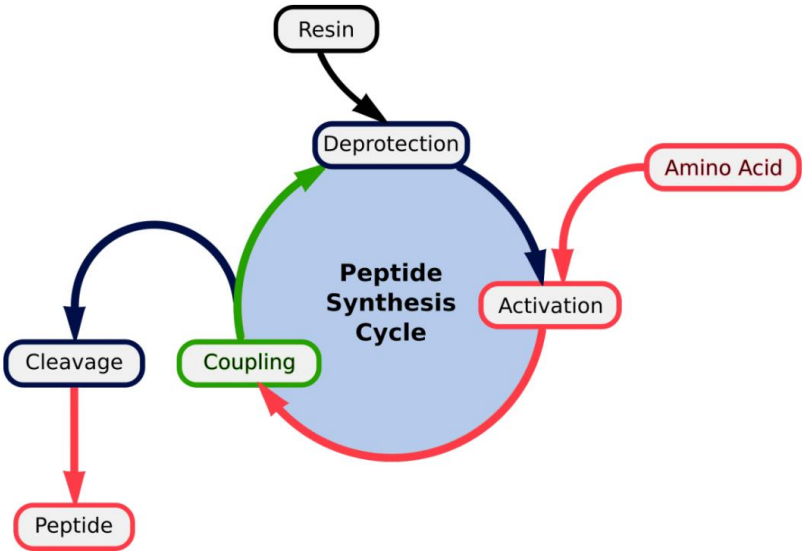

Figure 1.31 | Typical protocol for solid phase peptide synthesis (SPPS). Figure is reproduced and adapted from https://www.antibodies-online.com/resources/17/5034/peptide-synthesis-methods-and-reagents/.

When it comes to synthesis of peptides, several choices have to be made.[90] The first one consists in choosing which protecting group strategy at *N*-terminal of each aa will be followed: either the Boc one (which is typically deprotected under acidic conditions, like TFA) or the Fmoc group (which is usually deprotected in basic conditions, like piperazine). In most cases, the Fmoc strategy is preferred over the Boc one because of the milder deprotection conditions and on the possibility to follow more easily the synthesis thanks to the presence of the UV-active fluorene units. Then, selection of the solid support (resins) is required, depending on the nature of the *C*-terminus of final peptide sequences and

on the nature of the protecting group strategy chosen for SPPS (Fmoc or Boc). Wang resin is traditionally the first choice to reach peptides with a carboxylic acid at the C-terminus, although Rink acid resin or 2-chlorotrityl resin are good alternative requiring less acidic conditions for cleavage. When peptides with an amide at the C-terminus are synthesized, Rink amide resin is typically the most used.

The activation of carboxyl group of aa is also of great importance for a rapid and quantitative amide formation.[91] Nowadays, the most widely used activators are aminium slats (HATU, HBTU), and phosphonium salts (PyBOP). A great advantage of phosphonium salts over aminium salts is that the phosphonium does not react with the amino function of the incoming moiety and therefore the phosphonium does not terminate the peptide chain.[91] In SPPS, HATU is the first choice for secondary amide coupling as it is more efficient and leads to less epimerization than HBTU even if it is more expensive. The addition of HOBt can eliminate the partial racemization process and keep the chiral integrity of the aa during the amide formation. Diisopropylethylamine (DIEA), also known as Hünig's base, is necessary to deprotonate the carboxylic acid group.

The advantages of SPPS are its speed, its automatic processing, the elimination of solubility problems and its simplicity of operation. A countless number of natural or designed peptides have been produced by SPPS. However, one main limitation of SPPS is related to the maximum sequence size (< 50 aa) that can be achieved. The limitation of SPPS has stimulated the development of a more powerful tool, namely Native Chemical Ligation, to produce proteins.[86,92]

1.3.2 Native chemical ligation

In 1994, Kent and coworkers reported a new methodology, so called native chemical ligation (NCL) that allowed the direct total synthesis of native backbone proteins up to 72 aa starting from two short peptide sequences (Scheme 1.6).[80] The first step of NCL is a chemoselective reaction performed between the *N*-terminal cysteine (Cys) residue of peptide **2** and the *C*-terminal thioester of peptide **1**. This step, also known as transthioesterification, leads to the formation of a new thioester intermediate which then undergo a spontaneous intramolecular rearrangement to yield a full-length peptide with a native peptide bond at the ligation site. While the transthioesterification step is reversible, the intramolecular rearrangement of the thioester intermediate is irreversible, which totally displaces the reaction into the direction of producing peptides.

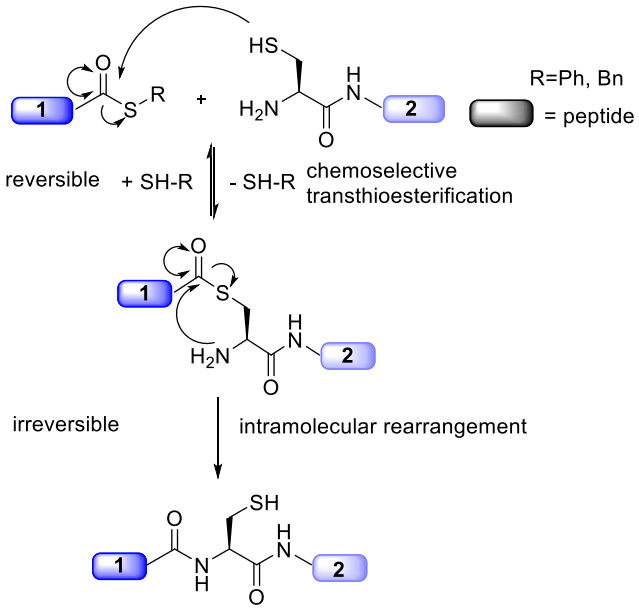

Scheme 1.6 | Detailed mechanism of NCL.

Based on the principle of NCL, chemists designed new strategies to access peptides/proteins without cysteine sites. In 2001, Dawson and coworkers reported the catalytic desulfurization (H_2/metal) of cysteines to yield the corresponding alanine.[93] This work overcome one main criticism related to the original NCL which is related to the required presence of a Cys residue within the sequence (Scheme 1.7 a). Since this seminal work, a new toolbox made of thiol-derived amino-acid have been developed which allows the synthesis of proteins without cysteine residues.[94] Alternatively, another approach to reach peptides/proteins without Cys sites consists in using an auxiliary-attached thiol that replace the Cys residue at the *N*-terminal of peptide (Scheme 1.7b).[95,96] After traditional NCL, the auxiliary (for example, 1-phenyl-2-mercaptoethyl) on the peptide segments could be removed selectively to provide the amide bond at the ligation point.

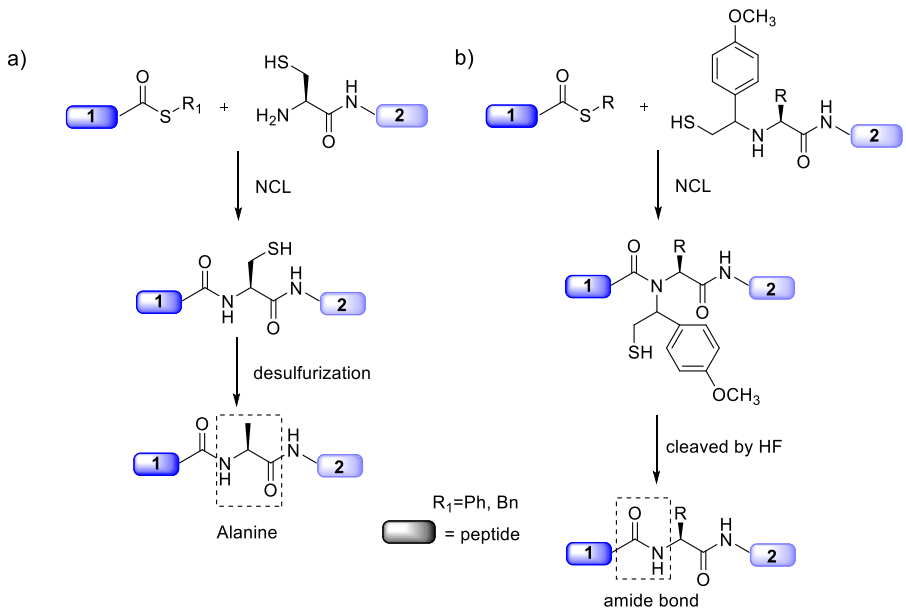

Scheme 1.7 | Chemistries that can enable NCL at non-Cys sites by a) desulfurization and b) removing auxiliaries.

The success of the NCL methodology is undeniable as its development and optimization provides nowadays access to the world of fully functional proteins and even enzymes.[86,97,98] A noticeable achievement of this methodology has been the synthesis of a 53 kDa protein made of 472 amino-acids, which constitute the largest protein synthesis to date.[99] Since its birth, NCL has emerged as the most robust and practical tool for unprotected peptide ligation strategy.

1.3.3 DCLs concerning peptide segments or proteins

Considering the robustness of the amide bond, DCLs made of peptides have first been explored using pseudopeptidic compounds and involving mainly –C=N- or disulfide exchange as dynamic covalent reactions.[100] For instance, the group of Alfonso utilized the reversibility of disulfide bonds to develop a novel strategy for the identification of cysteine or cystine in the environment by fluorescent response. (Figure 1.32) They built a dynamic chemical network of pseudopeptidic building blocks (BBs) and noticed the excess production of the heterotrimer **4a** (covalently constructed by the combination of **1-2-3a**) after mixing equimolar amounts of **1**, **2**, and **3a** in aqueous media at neutral pH. Meanwhile, with the concomitant redistribution of the constituents, fluorescent disulfide homodimer **[3b]$_2$** was released as determined by fluorescence spectroscopy. This new method with the participation of reversible disulfide bond is efficient and convenient for the detection of natural amino acid in biological conditions.[101]

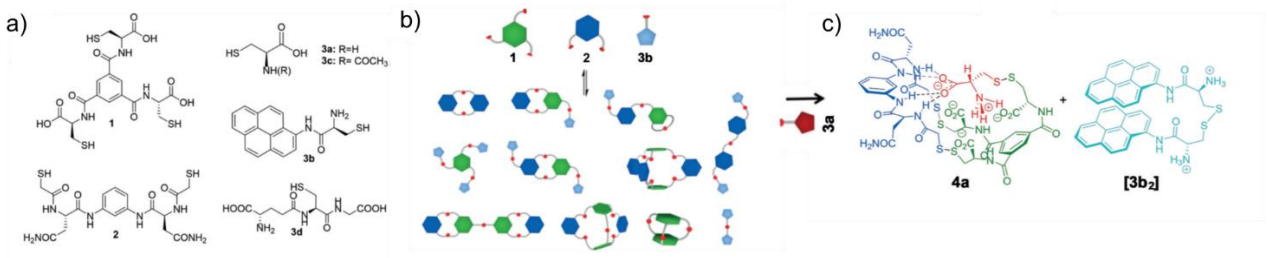

Figure 1.32 | a) Chemical structures of the cysteine/cysteine containing building blocks (BBs); b) Schematic illustration of the BBs DCL; c) The addition of 3a leads to the formation of heterotrimer 4a and the homodimer $[3b]_2$. Figure is reproduced and adapted from ref. [101].

In 2012, Lehn has reported by the first time the generation of proteoidic dynamic biopolymers (biodynamer).[102] The proteoidic biodynamer was synthesized from a dialdehyde and amino-acid hydrazides *via* acylhydrazone and imine polycondensation. During the polymerization process, the self-organization/folding of the biodynamer caused by the hydrophobic effect of amino acids, pushed the reversible reaction to the direction of continuously producing polymers. The biodynamers displayed outstandingly low dispersity (with the polydispersity index around 0.03) which is close the natural proteins. Thanks to the presence of both hydrazone and imine bonds, the stability of proteoidic biodynamer could be adjusted by the pH. This proteoidic biodynamer and the corresponding polymerization process open a wide door to the innovation of biologically-relevant dynamic materials.

One breakthrough regarding DCLs made of peptides was achieved by the group of Ulijn who focuses on using various enzymes to keep the amide bond reversible (*e.g.* amide condensation, hydrolysis, sequence exchange, *etc*) and to create dynamic peptide libraries.[103] Using proteases, one type of enzymes that catalyzes the hydrolysis of the robust amide bond, they achieved the reversible peptide bond under mild conditions. For example, they showed that thermolysin, an enzyme that has been used before in reversible amide hydrolysis[14], can induce the gelation within few minutes of a suspension of equimolar amounts of Fmoc-phenylalanine (Fmoc-Phe) and diphenylalanine (Phe_2) (Figure 1.33a)).[104] Cryo-SEM imaging of the resulting gel showed the presence of micrometer-long interwoven fibers (Figure 1.33b)). Using HPLC to monitor the evolution of the DCL with time, they demonstrated that the gelation was caused by the dynamic combination of Fmoc-Phe and Phe_2 as the peak corresponding to Fmoc-Phe decreased (< 15 minutes retention time) and the peak associated with Fmoc-Phe_3 increased (> 16 minutes retention time) (Figure 1.33c)). Furthermore, they found out that the hydrolysis direction ($K_{eq,1}$<1) was preferred for low concentrations of Fmoc-Phe_3, while increasing the mixture concentration led to continuous self-assembly of interwoven fibers ($K_{eq,2}$ >

$K_{eq,1}$). These results reported an enzyme-triggered gelation process to form nanofibrous structures.

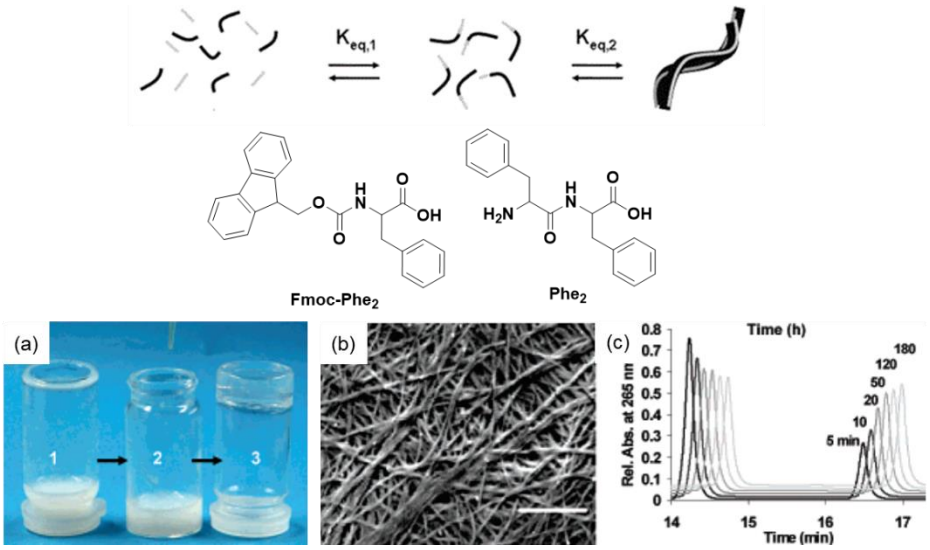

Figure 1.33 | Enzyme-triggered self-assembly of peptide hydrogels via reversed hydrolysis. a) 1: Suspension of Fmoc-Phe and $(Phe)_2$. 2: addition of 0.5 mg of thermolysin. 3: Inversion demonstrates self-supporting gel formation; b) Cryo-SEM micrograph of enzymatically prepared Fmoc-$(Phe)_3$ hydrogel obtained from 40 µmol of Fmoc-Phe and $(Phe)_2$ and 0.5 mg thermolysin. The scale bar represents 0.5 µm. c) HPLC chromatograms of peptide synthesis in the course of time in the presence of 0.5 mg thermolysin. Peaks shown represent Fmoc-Phe and Fmoc-$(Phe)_3$. Figure is reproduced and adapted from ref. [104].

Furthermore, by changing the environmental conditions (salts, solvents, and combinations), the same group showed that different peptide sequences and nanostructures can be selected out during the exchange process.[13] For that, DCLs of short peptide segments involving reversible peptide bonds were set in phosphate buffer in the presence of the nonspecific thermolysin enzyme. Under these classical conditions, the selection process was driven by the propensity of oligopeptides to form nanostructures. However, modifications of environmental conditions such as the presence of sodium salts of the Hofmeister series of anions induced the selection of different oligopeptides which are barely detected in classical conditions. For example, only low level of oligomerization was reported when ditryptophan (W_2) was placed in classical conditions while tetratryptophan (W_4) became the predominant species for phosphate buffer containing 1 M NaCl. Interestingly, starting from a 1:1 binary mixture of dipeptides (phenylalanine-serine [FS] and phenylalanine-aspartate [FD]), the octamer FDFSFDFS was the only amplified sequence in the presence of thermolysin, leading to the formation of a hydrogel consisting of an entangled fibrillar network made of β-sheet-like structures. This series of publications clearly demonstrate the existence of a relationship between molecular

sequence and selection of supramolecular nanostructure, providing inspiration for the design of novel smart materials with optimized functions under spatiotemporal control.

However, one main limitation of their results is related to the use of enzyme which is thus limited to the use of amino-acids and can be denatured under certain experimental conditions. In addition, their work is mostly limited to short peptides (max. 8 amino-acids).

1.4 Conclusions

In recent decades, DCvC has emerged as a tool capable of simultaneously producing chemical diversity, self-sorting of the building blocks, and directed binding of the targets. DCvC allows to overcome the inconvenience of weak non-covalent intermolecular interaction by taking use of robust covalent bonds. Dynamic systems based on DCvC have found their main applications in molecular separation, gas adsorption, host-guest chemistry, nanotechnology, solar energy conversion, and material science. However, the need for new or improved dynamic covalent bonds remains significant in order to target new applications.

The chemical robustness of the amide bond and its biological relevance have raised the attention of chemists to promote mild and efficient reversibility to this covalent bond. Indeed, efficient exchange of amide bonds could give rise to important applications related to drug discovery, biopolymers and even material science. However, the need for such reversible reaction remains.

1.5 References

1. Corbett PT, Leclaire J, Vial L, West KR, Wietor JL, Sanders JK, Otto S. Dynamic combinatorial chemistry. *Chem. Rev.* **106**, 3652–3711 (2006).

2. Lehn, J.-M. Dynamic combinatorial chemistry and virtual combinatorial libraries. *Chem. Eur. J,* **5**, 2455–2463 (1999).

3. Jin, Y., Yu, C., Denman, R. J. & Zhang, W. Recent advances in dynamic covalent chemistry. *Chem. Soc. Rev.* **42**, 6634-6654 (2013).

4. *Dynamic covalent chemistry: principles, reactions, and applications*. (Wiley, 2017).

5. Chakma, P. & Konkolewicz, D. Dynamic covalent bonds in polymeric materials. *Angew. Chem. Int. Ed.* **58**, 9682–9695 (2019).

6. Ramström, O. & Lehn, J.-M. Drug discovery by dynamic combinatorial libraries. *Nat. Rev.* **1**, 26–36 (2002).

7. Wilson, A., Gasparini, G. & Matile, S. Functional systems with orthogonal dynamic covalent bonds. *Chem. Soc. Rev.* **43**, 1948–1962 (2014).

8. Reuther JF, Dees JL, Kolesnichenko IV, Hernandez ET, Ukraintsev DV, Guduru R, Whiteley M, Anslyn EV. Dynamic

covalent chemistry enables formation of antimicrobial peptide quaternary assemblies in a completely abiotic manner. *Nat. Chem.* **10**, 45–50 (2018).

9. Ferrer, J.-L., Jez, J. M., Bowman, M. E., Dixon, R. A. & Noel, J. P. Structure of chalcone synthase and the molecular basis of plant polyketide biosynthesis. *Nat. Struct. Mol. Biol.* **6**, 775-784 (1999).

10. Barber, J. & Rostron, C. *Pharmaceutical Chemistry*. (OUP Oxford, 2013).

11. Jin, Y., Wang, Q., Taynton, P. & Zhang, W. Dynamic covalent chemistry approaches toward macrocycles, molecular cages, and polymers. *Acc. Chem. Res.* **47**, 1575–1586 (2014).

12. Rasmussen, B., Sørensen, A., Beeren, S. R. & Pittelkow, M. Dynamic combinatorial chemistry. in *organic synthesis and molecular engineering* (ed. Nielsen, M. B.) 393–436 (John Wiley & Sons, Inc., 2013).

13. Pappas CG, Shafi R, Sasselli IR, Siccardi H, Wang T, Narang V, Abzalimov R, Wijerathne N, Ulijn RV. Dynamic peptide libraries for the discovery of supramolecular nanomaterials. *Nat. Nanotechnol.* **11**, 960–967 (2016).

14. Swann PG, Casanova RA, Desai A, Frauenhoff MM, Urbancic M, Slomczynska U, Hopfinger AJ, Le Breton GC, Venton DL. Nonspecific protease-catalyzed hydrolysis/synthesis of a mixture of peptides: Product diversity and ligand amplification by a molecular trap. *Biopolymers* **40**, 617–625 (1996).

15. Eldred, S. E., Stone, D. A., Gellman, S. H. & Stahl, S. S. Catalytic transamidation under moderate conditions. *J. Am. Chem. Soc.* **125**, 3422–3423 (2003).

16. Ji, Q. & Miljanić, O. Š. Distillative Self-sorting of dynamic ester libraries. *J. Org. Chem* **78**, 12710–12716 (2013).

17. Larsson, R., Pei, Z. & Ramström, O. Catalytic self-screening of cholinesterase substrates from a dynamic combinatorial thioester library. *Angew. Chem. Int. Ed.* **43**, 3716–3718 (2004).

18. Worrell BT, Mavila S, Wang C, Kontour TM, Lim CH, McBride MK, Musgrave CB, Shoemaker R, Bowman CN. A user's guide to the thiol-thioester exchange in organic media: scope, limitations, and applications in material science. *Polym. Chem.* **9**, 4523–4534 (2018).

19. Nair DP, Podgorski M, Chatani S, Gong T, Xi W, Fenoli CR, Bowman CN. The Thiol-Michael addition click reaction: a powerful and widely used tool in materials chemistry. *Chem. Mater.* **26**, 724–744 (2014).

20. Stenzel, M. H. Bioconjugation using thiols: old chemistry rediscovered to connect polymers with nature's building blocks. *ACS Macro Lett.* **2**, 14–18 (2013).

21. Joshi, G. & Anslyn, E. V. Dynamic thiol exchange with β-sulfido-α,β-unsaturated carbonyl compounds and dithianes. *Org. Lett.* **14**, 4714–4717 (2012).

22. Fan, B., Zhang, K., Liu, Q. & Eelkema, R. Self-healing injectable polymer hydrogel via dynamic thiol-alkynone double addition cross-links. *ACS Macro Letters.* 776–780 (2020).

23. Giuseppone, N. & Lehn, J.-M. Constitutional dynamic self-sensing in a zinc ^{ii} /polyiminofluorenes system. *J. Am. Chem. Soc.* **126**, 11448–11449 (2004).

24. Epstein DM, Choudhary S, Churchill MR, Keil KM, Eliseev AV, Morrow JR. Chloroform-Soluble Schiff-Base Zn(II) or Cd(II) Complexes from a Dynamic Combinatorial Library. *Inorg. Chem.* **40**, 1591–1596 (2001).

25. Giuseppone, N., Schmitt, J.-L., Schwartz, E. & Lehn, J.-M. Scandium(III) catalysis of transimination reactions.

independent and constitutionally coupled reversible processes. *J. Am. Chem. Soc.* **127**, 5528–5539 (2005).

26. Zhao, D. & Moore, J. S. Reversible polymerization driven by folding. *J. Am. Chem. Soc.* **124**, 9996–9997 (2002).

27. Dirksen, A., Dirksen, S., Hackeng, T. M. & Dawson, P. E. Nucleophilic catalysis of hydrazone formation and transimination: implications for dynamic covalent chemistry. *J. Am. Chem. Soc.* **128**, 15602–15603 (2006).

28. Dirksen, A., Hackeng, T. M. & Dawson, P. E. Nucleophilic catalysis of oxime ligation. *Angew. Chem. Int. Ed.* **45**, 7581–7584 (2006).

29. Cousins, G. R. L., Poulsen, S.-A. & Sanders, J. K. M. Dynamic combinatorial libraries of pseudo-peptide hydrazone macrocycles. *Chem. Commun.* 1575–1576 (1999).

30. Dirksen, A., Yegneswaran, S. & Dawson, P. E. Bisaryl hydrazones as exchangeable biocompatible linkers. *Angew. Chem. Int. Ed.* **49**, 2023–2027 (2010).

31. Black, S. P., Sanders, J. K. M. & Stefankiewicz, A. R. Disulfide exchange: exposing supramolecular reactivity through dynamic covalent chemistry. *Chem. Soc. Rev.* **43**, 1861–1872 (2014).

32. Fairbanks, B. D., Singh, S. P., Bowman, C. N. & Anseth, K. S. Photodegradable, photoadaptable hydrogels via radical-mediated disulfide fragmentation reaction. *Macromolecules* **44**, 2444–2450 (2011).

33. Rekondo A, Martin R, de Luzuriaga AR, Cabaero G, Grande HJ, Odriozola IR. Catalyst-free room-temperature self-healing elastomers based on aromatic disulfide metathesis. *Mater. Horiz.* **1**, 237–240 (2014).

34. Lei, Z. Q., Xiang, H. P., Yuan, Y. J., Rong, M. Z. & Zhang, M. Q. Room-temperature self-healable and remoldable cross-linked polymer based on the dynamic exchange of disulfide bonds. *Chem. Mater.* **26**, 2038–2046 (2014).

35. Nevejans, S., Ballard, N., Miranda, J. I., Reck, B. & Asua, J. M. The underlying mechanisms for self-healing of poly(disulfide)s. *Phys. Chem. Chem. Phys.* **18**, 27577–27583 (2016).

36. Getz, E. B., Xiao, M., Chakrabarty, T., Cooke, R. & Selvin, P. R. A comparison between the sulfhydryl reductants tris(2-carboxyethyl)phosphine and dithiothreitol for use in protein biochemistry. *Anal. Biochem.* **273**, 73–80 (1999).

37. Fritze, U. F. & von Delius, M. Dynamic disulfide metathesis induced by ultrasound. *Chem. Commun.* **52**, 6363–6366 (2016).

38. Sobczak S, Drożdż W, Lampronti GI, Belenguer AM, Katrusiak A, Stefankiewicz AR. Dynamic covalent chemistry under high-pressure:a new route to disulfide metathesis. *Chem. Eur. J.* **24**, 8769–8773 (2018).

39. Kwart, H. & King, K. The reverse Diels-Alder or retrodiene reaction. *Chem. Rev.* **68**, 415–447 (1968).

40. Reutenauer, P., Boul, P. J. & Lehn, J.-M. Dynamic diels-alder reactions of 9,10-dimethylanthracene: reversible adduct formation, dynamic exchange processes and thermal fluorescence modulation. *Eur. J. Org. Chem.* **2009**, 1691–1697 (2009).

41. Boutelle, R. C. & Northrop, B. H. Substituent effects on the reversibility of furan–maleimide cycloadditions. *J. Org. Chem.* **76**, 7994–8002 (2011).

42. Truong TT, Thai SH, Nguyen HT, Phung DT, Nguyen LT, Pham HQ, Nguyen LT. Tailoring the hard–soft interface with dynamic Diels–Alder linkages in polyurethanes: toward superior mechanical properties and healability at mild temperature. *Chem. Mater.* **31**, 2347–2357 (2019).

43. Chakma, P. & Konkolewicz, D. Dynamic covalent bonds in polymeric materials. *Angew. Chem. Int. Ed.* **58**, 9682–9695 (2019).

44. Iwasawa, N. & Takahagi, H. Boronic esters as a system for crystallization-induced dynamic self-assembly equipped with an “on−off” switch for equilibration. *J. Am. Chem. Soc.* **129**, 7754–7755 (2007).

45. Cromwell, O. R., Chung, J. & Guan, Z. Malleable and self-healing covalent polymer networks through tunable dynamic boronic ester bonds. *J. Am. Chem. Soc.* **137**, 6492–6495 (2015).

46. Belowich, M. E. & Stoddart, J. F. Dynamic imine chemistry. *Chem. Soc. Rev.* **41**, 2003 (2012).

47. Cheeseman JD, Corbett AD, Shu R, Croteau J, Gleason JL, Kazlauskas RJ. Amplification of screening sensitivity through selective destruction: theory and screening of a library of carbonic anhydrase inhibitors. *J. Am. Chem. Soc.* 10.

48. Corbett, A. D., Cheeseman, J. D., Kazlauskas, R. J. & Gleason, J. L. Pseudodynamic combinatorial libraries: a receptor-assisted approach for drug discovery. *Angew. Chem. Int. Ed.* **43**, 2432–2436 (2004).

49. Zhao, D. & Moore, J. S. Folding-driven reversible polymerization of oligo(*m* -phenylene ethynylene) imines: solvent and starter sequence studies. *Macromolecules* **36**, 2712–2720 (2003).

50. Takahagi, H. & Iwasawa, N. Crystallization-controlled dynamic self-assembly and an on/off switch for equilibration using boronic ester formation. *Chem. Eur. J,* **16**, 13680–13688 (2010).

51. Ziach, K. & Jurczak, J. Controlling and measuring the equilibration of dynamic combinatorial libraries of imines. *Org. Lett.* **10**, 5159–5162 (2008).

52. Van Herck N, Maes D, Unal K, Guerre M, Winne JM, Du Prez FE. Covalent adaptable networks with tunable exchange rates based on reversible thiol–yne cross-linking. *Angewandte Chemie International Edition* **59**, 3609–3617 (2020).

53. Li, J., Nowak, P. & Otto, S. Dynamic combinatorial libraries: from exploring molecular recognition to systems chemistry. *J. Am. Chem. Soc.* **135**, 9222–9239 (2013).

54. Rowan, S. J., Cantrill, S. J., Cousins, G. R. L., Sanders, J. K. M. & Stoddart, J. F. Dynamic covalent chemistry. *Angew. Chem. Int. Ed.* **41**, 898–952 (2002).

55. Herrmann, A. Dynamic combinatorial/covalent chemistry: a tool to read, generate and modulate the bioactivity of compounds and compound mixtures. *Chem. Soc. Rev.* **43**, 1899–1933 (2014).

56. Moulin, E., Cormos, G. & Giuseppone, N. Dynamic combinatorial chemistry as a tool for the design of functional materials and devices. *Chem. Soc. Rev.* **41**, 1031–1049 (2012).

57. Zhang, Y. & Barboiu, M. Constitutional dynamic materials—toward natural selection of function. *Chem. Rev.* **116**, 809–834 (2016).

58. Misuraca, M. C., Moulin, E., Ruff, Y. & Giuseppone, N. Experimental and theoretical methods for the analyses of dynamic combinatorial libraries. *New J. Chem.* **38**, 3336–3349 (2014).

59. Bhat VT, Caniard AM, Luksch T, Brenk R, Campopiano DJ, Greaney MF. Nucleophilic catalysis of acylhydrazone equilibration for protein-directed dynamic covalent chemistry. *Nat. Chem.* **2**, 490–497 (2010).

60. Kosikova, T. & Philp, D. Exploring the emergence of complexity using synthetic replicators. *Chem. Soc. Rev.* **46**,

7274–7305 (2017).

61. Carnall JM, Waudby CA, Belenguer AM, Stuart MC, Peyralans JJ, Otto S. Mechanosensitive self-replication driven by self-organization. *Science* **327**, 1502–1506 (2010).

62. Li, J., Carnall, J. M. A., Stuart, M. C. A. & Otto, S. Hydrogel formation upon photoinduced covalent capture of macrocycle stacks from dynamic combinatorial libraries. *Angew. Chem. Int. Ed.* **50**, 8384–8386 (2011).

63. Vantomme, G. & Lehn, J.-M. Photo- and thermoresponsive supramolecular assemblies: reversible photorelease of k^+ ions and constitutional dynamics. *Angew. Chem. Int. Ed.* **52**, 3940–3943 (2013).

64. McNaughton, B. R. & Miller, B. L. Resin-bound dynamic combinatorial chemistry. *Org. Lett.* **8**, 4 (2006).

65. Klekota, B., Hammond, M. H. & Miller, B. L. Generation of novel DNA-binding compounds by selection and amplification from self-assembled combinatorial libraries. *Tetrahedron Lett.* **38**, 8639–8642 (1997).

66. Saggiomo, V. & Lüning, U. Transport of calcium ions through a bulk membrane by use of a dynamic combinatorial library. *Chem. Commun.* 3711–3713 (2009).

67. Hafezi, N. & Lehn, J.-M. Adaptation of dynamic covalent systems of imine constituents to medium change by component redistribution under reversible phase separation. *J. Am. Chem. Soc.* **134**, 12861–12868 (2012).

68. Minkenberg, C. B., Florusse, L., Eelkema, R., Koper, G. J. M. & van Esch, J. H. Triggered self-assembly of simple dynamic covalent surfactants. *J. Am. Chem. Soc.* **131**, 11274–11275 (2009).

69. Nguyen, R., Allouche, L., Buhler, E. & Giuseppone, N. Dynamic combinatorial evolution within self-replicating supramolecular assemblies. *Angew. Chem. Int. Ed.* **121**, 1113–1116 (2009).

70. Osowska, K. & Miljanić, O. Š. Self-sorting of dynamic imine libraries during distillation. *Angew. Chem. Int. Ed.* **123**, 8495–8499 (2011).

71. Osypenko, A., Dhers, S. & Lehn, J.-M. Pattern generation and information transfer through a liquid/liquid interface in 3d constitutional dynamic networks of imine ligands in response to metal cation effectors. *J. Am. Chem. Soc.* **141**, 12724–12737 (2019).

72. Lehn, J.-M. Dynamers: dynamic molecular and supramolecular polymers. *Prog. Polym. Sci.* **30**, 814–831 (2005).

73. Fukuda, K., Shimoda, M., Sukegawa, M., Nobori, T. & Lehn, J.-M. Doubly degradable dynamers: dynamic covalent polymers based on reversible imine connections and biodegradable polyester units. *Green Chem.* **14**, 2907-2911 (2012).

74. Kathan M, Kovaříček P, Jurissek C, Senf A, Dallmann A, Thünemann AF, Hecht S. Control of imine exchange kinetics with photoswitches to modulate self-healing in polysiloxane networks by light illumination. *Angew. Chem. Int. Ed.* **55**, 13882–13886 (2016).

75. Marin, L., Simionescu, B. & Barboiu, M. Imino-chitosan biodynamers. *Chem. Commun.* **48**, 8778-8780 (2012).

76. Cougnon, F. B. L., Ponnuswamy, N., Jenkins, N. A., Pantoş, G. D. & Sanders, J. K. M. Structural parameters governing the dynamic combinatorial synthesis of catenanes in water. *J. Am. Chem. Soc.* **134**, 19129–19135 (2012).

77. Chen G, Feng H, Jiang X, Xu J, Pan S, Qian Z. Redox-controlled fluorescent nanoswitch based on reversible disulfide and its application in butyrylcholinesterase activity assay. *Ann. Chem.* **90**, 1643–1651 (2018).

78. Michal, B. T., Jaye, C. A., Spencer, E. J. & Rowan, S. J. Inherently photohealable and thermal shape-memory

polydisulfide networks. *ACS Macro Letters* **2**, 694–699 (2013).

79. Deng G, Li F, Yu H, Liu F, Liu C, Sun W, Jiang H, Chen Y. Dynamic hydrogels with an environmental adaptive self-healing ability and dual responsive sol–gel transitions. *ACS Macro Letters* **1**, 275–279 (2012).

80. Dawson, P., Muir, T., Clark-Lewis, I. & Kent, S. Synthesis of proteins by native chemical ligation. *Science* **266**, 776–779 (1994).

81. Woll, M. G. & Gellman, S. H. Backbone thioester exchange: a new approach to evaluating higher order structural stability in polypeptides. *J. Am. Chem. Soc.* **126**, 11172–11174 (2004).

82. Konieczynska MD, Villa-Camacho JC, Ghobril C, Perez-Viloria M, Tevis KM, Blessing WA, Nazarian A, Rodriguez EK, Grinstaff MW. On-demand dissolution of a dendritic hydrogel-based dressing for second-degree burn wounds through thiol-thioester exchange reaction. *Angew. Chem. Int. Ed.* **55**, 9984–9987 (2016).

83. Wang C, Mavila S, Worrell BT, Xi W, Goldman TM, Bowman CN. Productive exchange of thiols and thioesters to form dynamic polythioester-based polymers. *ACS Macro Lett.* **7**, 1312–1316 (2018).

84. Konetski, D., Mavila, S., Wang, C., Worrell, B. & Bowman, C. N. Production of dynamic lipid bilayers using the reversible thiol–thioester exchange reaction. *Chem. Commun.* **54**, 8108–8111 (2018).

85. Stenkamp, R. E., Trong, I. L., Klumb, L., Stayton, P. S. & Freitag, S. Structural studies of the streptavidin binding loop: Streptavidin binding loop. *Protein Sci* **6**, 1157–1166 (1997).

86. Kent, S. B. H. Total chemical synthesis of proteins. *Chem. Soc. Rev.* **38**, 338–351 (2009).

87. Merrifield, R. B. Solid Phase Peptide Synthesis. I. the synthesis of a tetrapeptide. *J. Am. Chem. Soc.* **85**, 2149–2154 (1963).

88. Howl, J. *Peptide Synthesis and Applications*. (Springer Science & Business Media, 2005).

89. Vanier, G. S. Microwave-assisted solid-phase peptide synthesis based on the fmoc protecting group strategy (CEM). in *Peptide Synthesis and Applications* (eds. Jensen, K. J., Tofteng Shelton, P. & Pedersen, S. L.) 235–249 (Humana Press, 2013).

90. Palomo, J. M. Solid-phase peptide synthesis: an overview focused on the preparation of biologically relevant peptides. *RSC Adv.* **4**, 32658–32672 (2014).

91. El-Faham, A. & Albericio, F. Peptide coupling reagents, more than a letter soup. *Chem. Rev.* **111**, 6557–6602 (2011).

92. Raibaut, L., Ollivier, N. & Melnyk, O. Sequential native peptide ligation strategies for total chemical protein synthesis. *Chem Soc Rev* **41**, 7001–7015 (2012).

93. Yan, L. Z. & Dawson, P. E. Synthesis of peptides and proteins without cysteine residues by native chemical ligation combined with desulfurization. *J. Am. Chem. Soc.* **123**, 526–533 (2001).

94. Malins, L. R. & Payne, R. J. Recent extensions to native chemical ligation for the chemical synthesis of peptides and proteins. *Curr Opin Chem Biol* **22**, 70–78 (2014).

95. Low, D. W., Hill, M. G., Carrasco, M. R., Kent, S. B. H. & Botti, P. Total synthesis of cytochrome b562 by native chemical ligation using a removable auxiliary. *Proc. Nat. Acad. Sci.* **98**, 6554–6559 (2001).

96. Macmillan, D. Evolving strategies for protein synthesis converge on native chemical ligation. *Angew. Chem. Int. Ed.*

45, 7668–7672 (2006).

97. Kulkarni, S. S., Sayers, J., Premdjee, B. & Payne, R. J. Rapid and efficient protein synthesis through expansion of the native chemical ligation concept. *Nat. Rev. Chem.* **2**, (2018).

98. Agouridas V, El Mahdi O, Diemer V, Cargoët M, Monbaliu JC, Melnyk O. Native chemical ligation and extended methods: mechanisms, catalysis, scope, and limitations. *Chem. Rev.* **119**, 7328–7443 (2019).

99. Sun, H. & Brik, A. The journey for the total chemical synthesis of a 53 kDa protein. *Acc. Chem. Res.* **52**, 3361–3371 (2019).

100. Alfonso, I. From simplicity to complex systems with bioinspired pseudopeptides. *Chem. Commun.* **52**, 239–250 (2016).

101. Lafuente, M., Solà, J. & Alfonso, I. A dynamic chemical network for cystinuria diagnosis. *Angew. Chem. Int. Ed.* **57**, 8421–8424 (2018).

102. Hirsch, A. K. H., Buhler, E. & Lehn, J.-M. Biodynamers: self-organization-driven formation of doubly dynamic proteoids. *J. Am. Chem. Soc.* **134**, 4177–4183 (2012).

103. Lampel, A., Ulijn, R. V. & Tuttle, T. Guiding principles for peptide nanotechnology through directed discovery. *Chem. Soc. Rev.* **47**, 3737–3758 (2018).

104. Toledano, S., Williams, R. J., Jayawarna, V. & Ulijn, R. V. Enzyme-triggered self-assembly of peptide hydrogels via reversed hydrolysis. *J. Am. Chem. Soc.* **128**, 1070–1071 (2006).

Chapter 2. Methodological optimization of dynamic covalent native chemical ligation (dcNCL)

2.1 State of the art on dcNCL and project objectives

An early report from 1953 showed that when a Valine thioester was treated with cysteine (Cys), transthioesterification of the arylthioester with the cysteine occurred rapidly. The resulting thioester subsequently rearranged *via* a S to N acyl shift to form a dipeptide with the presence of a native peptide bond. Over the whole native chemical ligation (NCL) process, the transthioesterification step is reversible, but the irreversible intramolecular rearrangement pushes the reaction towards the formation of the native peptide bond (Scheme 2.1).[1]

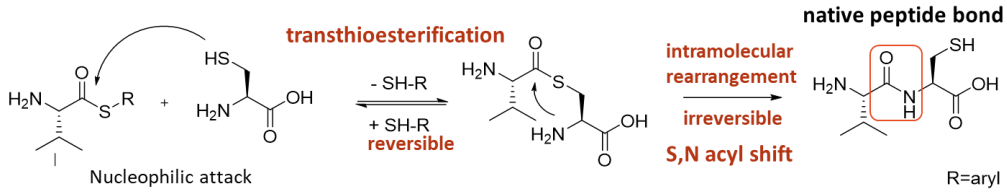

Scheme 2.1 | Irreversible native chemical ligation (NCL).

More than 50 years later, in 2013, Mootz and coworkers reported that in a folded intein, the amide bond at the *N*-alkyl Cys residue is preferentially in a *cis* or distorted conformation, thus favoring the intramolecular nucleophilic attack of the peptide bond by the free thiol of Cys residue (Scheme 2.2). This observation suggests that the intramolecular rearrangement, namely N to S acyl shift, can be reversible providing proper modification (methyl, ethyl) on the amine of the Cys residue.[2]

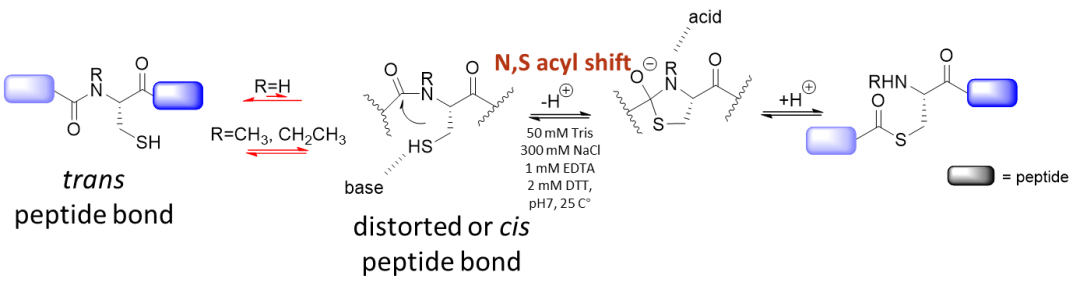

Scheme 2.2 | Key intermediates involved in the reversible native chemical ligation (reNCL).

Based on our understanding of the reversibility of the NCL and our interest in exploring dynamic covalent systems, our group focused on the reversibility of the amide bond with the purpose of designing dynamic peptide libraries able to shuffle their constituents on a practical time scale and in mild conditions (Scheme 2.3b)). Early work from our group showed that peptide fragments with *N*-alkyl Cys residue could dynamically exchange with each other.[3] Researchers firstly selected a thioethyl chain as -R group on the amide of the Cys residue. In this case, the *cis-trans* isomerization step is suppressed as there is always one thiol group correctly positioned for the intramolecular nucleophilic attack to occur.[4] The detailed mechanism is presented in Scheme 2.3a).

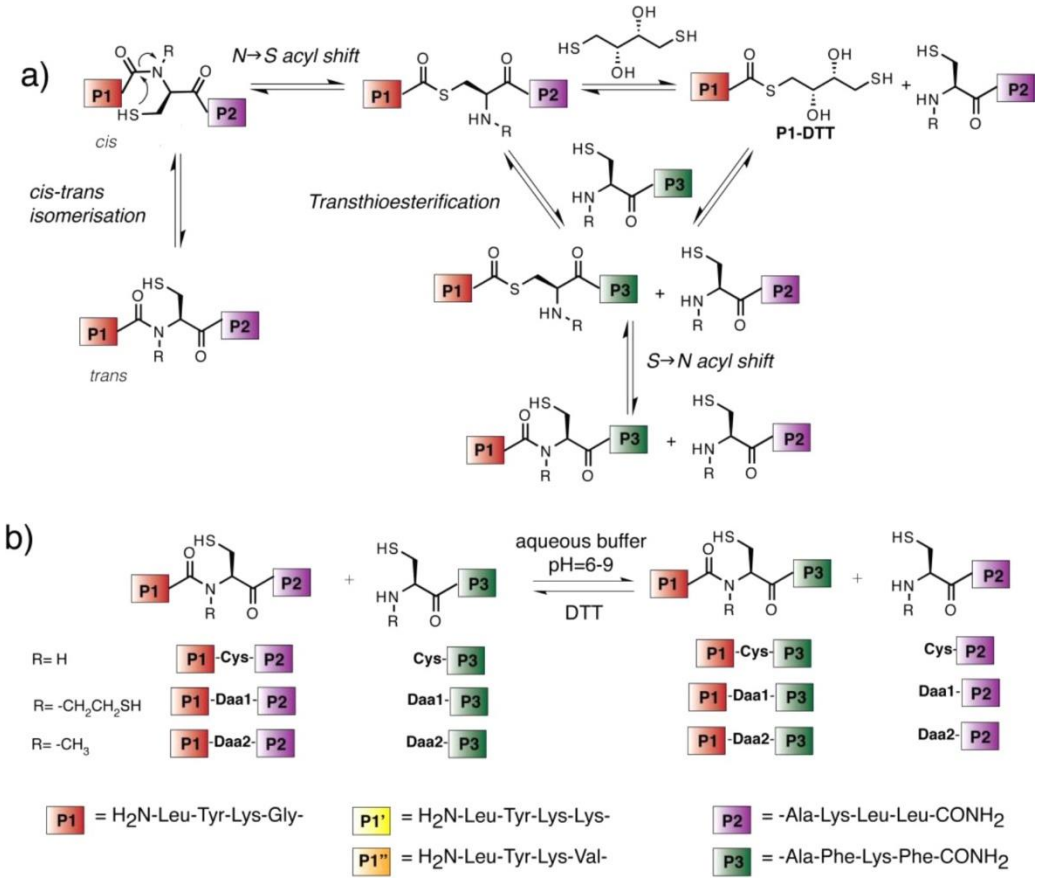

Scheme 2.3 | a) Full mechanism of dcNCL. Intermediate P1-DTT produced by the dithiothreitol additive in the present study is represented for the sake of clarity. b) Chemical structures of the peptide fragments used by our group and schematic representation of a dcNCL based on the use of cysteine (Cys), N-thioethyl-cysteine (Daa1), and N-methyl-cysteine (Daa2). Every peptide has a C-terminal carboxamide. Figure is reproduced and adapted from ref. [3].

Peptide **P1**-Daa1-**P2** with a *N*-thioethyl Cys residue (Daa1) can undergo N to S acyl shift to form the

corresponding peptide thioester. The Daa1-**P2** sequence can be replaced by the free thiol present in the environment (dithiothreitol (DTT) or Daa1-**P3**), leading to a transthioesterification, which proved to be the rate limiting step of the process. After this exchange reaction, the newly formed thioester peptide can perform S to N acyl shift leading to the exchanged product **P1**-Daa1-**P3** and Daa1-**P2**. As all intermediate steps involved in the process are reversible, we managed to determine conditions to achieve the reversible native chemical ligation. Such dynamic covalent native chemical ligation (dcNCL) could be applied potentially to build complicated dynamic covalent systems. As an alternative, regarding biocompatibility and bioactivity of the resulting dynamic peptides, our group inserted a methyl group instead of a thioethyl one onto the amide of the Cys residues. Actually, *N*-methyl-cysteines (***N*MeCys**) are non-ribosomal amino acids that can be found in natural products. They can also be transformed into alanine residues after reduction of the thiol group.[5] Similarly to peptides containing *N*-thioethyl Cys residues, the presence of ***N*MeCys** within a peptide segment allowed for exchange with each other for two main reasons. First, the presence of the methyl group on the amide position of Cys leads to a shift of the thermodynamic equilibrium between *trans* and *cis* amide bonds to energetically higher *cis* conformation and promotes the N to S acyl shift (although to a less extend compared to *N*-thioethyl Cys).[2,6] As a consequence, the ***N*MeCys** residue on the peptide fragment ensures reversibility to the robust peptide bond. Second, it requires only mild reaction conditions such as aqueous solution buffered at physiological pH and at 37 °C.

This work also demonstrated that dynamic peptide libraries (dynPL) need to be carried out under inert atmosphere and in degassed buffers to restrain the oxidation of thiol groups. More than 3 hours are required for sample preparation and the half time of equilibration is at least 10 hours. In addition, hydrolysis of thioester bonds occurs in these dynamic systems thus influencing the yield of the exchange. Considering to the potential of dcNCL for dynamic constitutional systems with possible applications as biocompatible materials, we were interested in further optimizing the exchange reaction in organic solvents or aqueous phase. The methodological part covers the dynamic control of dcNCL and the improvement of its efficiency. To strengthen the adaptability of the present reversible reaction, alkyl chain and oligo ethylene glycol were introduced to the terminal of ***N*MeCys** to increase the solubility of ***N*MeCys** derivatives in organic phase. Furthermore, the hydrolysis problem of the dcNCL could be solved by carrying out the reaction in organic solvents.

2.2 Synthesis and coupling of *N*-methyl-cysteine building blocks

The insertion of ***N*MeCys** residues into peptide sequences or small molecules can be achieved by two strategies (Scheme 2.4). The first approach, which is the most widespread, involves selective mono-

alkylation the *N*-terminal part of Cys directly on the peptide-attached resin or on small molecules.[7] This approach was employed by our group in earlier work, in order to produce ***N*MeCys**-functional peptide segments in the peptide synthesizer before removal of the side-chain protecting groups or release of the peptides from the solid support. However, this insertion strategy bears several disadvantages such as small-scale quantity, low synthetic yield, and long reaction time. To improve the procedure of dynamic peptide synthesis and simplify the synthetic route, a second strategy was envisioned, namely the synthesis of fully protected ***N*MeCys** derivatives (Scheme 2.5) and their direct introduction into peptide segments or small molecules.[8,9]

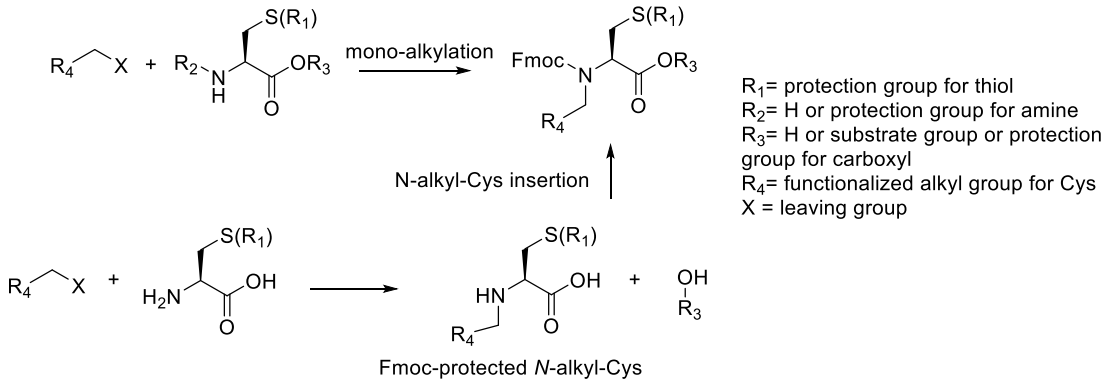

Scheme 2.4 | General routes for the preparation of N-alkyl cysteine.

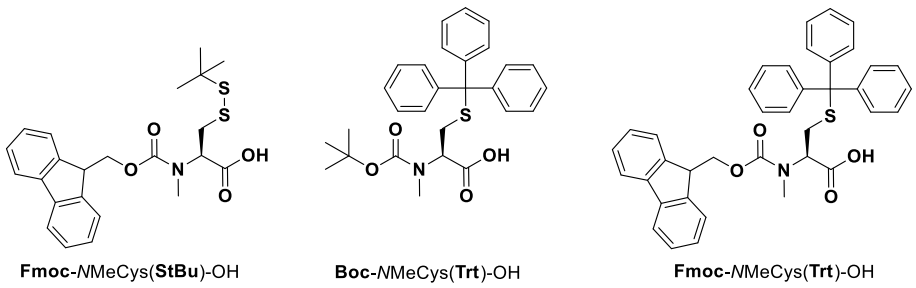

Scheme 2.5 | Three fully protected *N*MeCys considered for this work.

Most fully protected ***N*MeCys** derivatives can be synthesized in gram-scale quantities from commercially available cysteines by solution-phase synthesis. **Fmoc**-*N*MeCys(**StBu**)-OH was obtained in 2 steps (Scheme 2.6),[8] starting from **Fmoc**-Cys(**StBu**)-OH and involving at first the formation of an oxazolidinone intermediate which could be isolated by flash chromatography in excellent yield (96%). Subsequent acidic reduction of the oxazolidinone led to the **Fmoc**-

*N*MeCys(**StBu**)-OH compound in a good yield (62%). This two-step process is easy, quick, and allows gram-scale synthesis of ***N*MeCys** residues. The **StBu** protecting group, which is stable to general SPPS cleaving conditions, was chosen for a delayed release of thiol group.[10] Deprotection of the thiol from peptides incorporating *N*MeCys(**StBu**) could be occur thanks to the presence of reductants during the exchange reaction.[11]

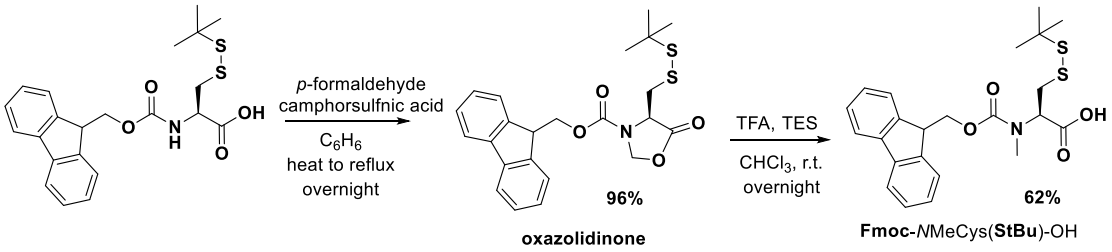

Scheme 2.6 | Synthetic route for Fmoc-*N*MeCys(StBu)-OH.

Fmoc-*N*MeCys(**Trt**)-OH could be synthesized up to 15 g scale in 4 steps (Scheme 2.7). **Boc**-*N*MeCys(**Trt**)-OH was first synthesized by methylation of commercially available **Boc**-Cys(**Trt**)-OH in high yield (90%).[9] **Boc** and **Trt** groups could then be removed simultaneously in acidic media (TFA and TES) affording *N*MeCys-OH after extraction and lyophilization. **Trt** and **Fmoc** groups could be inserted into *N*MeCys-OH in two steps according to classical procedures to form **Fmoc**-*N*MeCys(**Trt**)-OH.[7] The **Trt** protecting group can be quickly removed by global cleavage.[12]

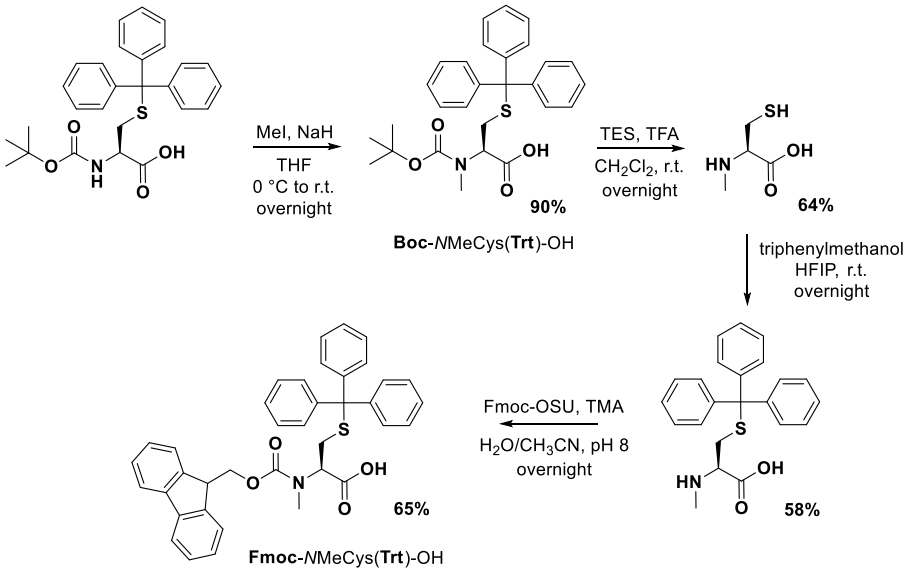

Scheme 2.7 | Synthetic route for **Boc**-*N*MeCys(**Trt**)-OH and **Fmoc**-*N*MeCys(**Trt**)-OH.

In order to synthesize peptides with a ***N*MeCys** residue either at the *N*-terminus, the *C*-terminus or within a peptide sequence, we had to optimize the coupling of the previously synthesized ***N*MeCys** amino acids on solid phase. Coupling of fully protected ***N*MeCys** (4 eq.) proceeded smoothly and with the best yield using HATU (4 eq.) and DIEA (4 eq.) as activator and base, respectively.[13] HBTU, which is cheaper than HATU, was used for amide condensation for all amino acids except ***N*MeCys**.[14] A single coupling was enough for ***N*MeCys** insertion on the peptide chain except for the initial grafting onto the resin (the *C*-terminus of the peptide chain) where double coupling (70°C, 55W) was prefered. Moreover, insertion of an amino acid after a ***N*MeCys** residue required double coupling (70°C, 35W) due to the low reactivity of the secondary amine of ***N*MeCys** (Scheme 2.8). Peptide fragments containing ***N*MeCys** could be easily synthesized by SPPS as described in section 1.3.1 with high purity and over 100 mg scale. ***N*MeCys**-attached small molecules were obtained by typical solution phase synthesis using the same reagents as for SPPS.

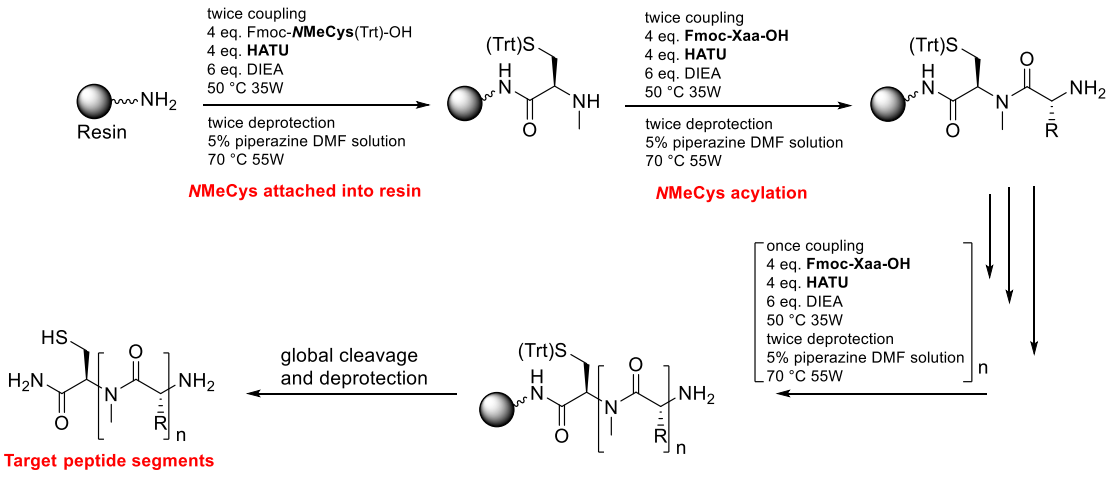

Scheme 2.8 | General procedure for Fmoc-SPPS of peptides incorporating a NMeCys residue.

2.3 General experimental protocol

An ultra-performance liquid chromatography coupled with a diode array and a mass spectrometer detector (Waters Acquity® UPLC-MS) was utilized to monitor all exchange reactions between ***N*MeCys** derivatives. The general protocol used to promote such reaction consists in adding a reductant (dithiothreitol (DTT) or tris(2-carboxyethyl) phosphine (TCEP)) in 15-fold molar excess relative to the starting materials in order to activate the thiol groups. According to the literature,[15] there is no obvious difference in the reduction efficiency between DTT and TCEP. The choice

between both depended on particular conditions. When the reactions were carried out in pure organic solvents, DTT was favored due to its good solubility in organic phase. When water-soluble solvents or milli-Q water were used as solvent for the reaction, TCEP was selected because of its considerable stability in aqueous solution for pH ranging from 1.5 up to 8.5. Standard calibration curves were established for each ***N*MeCys** derivatives under the conditions used for the exchange reactions. The kinetics of the exchange reactions were followed by UPLC-MS (UV and mass detection). By comparing the integrated area of UV peaks with the corresponding standard calibration curves, we can obtain the molar quantity of each ***N*MeCys** derivatives during the exchange reaction. Then, kinetic plots of exchange reactions were obtained by monitoring the concentration (mM) or ratio of each ***N*MeCys** derivatives present in the system *versus* reaction time (hour). According to the kinetic plots of each library, we could know its dynamic character with information on the initial reaction rate (V_0: slope of the kinetic plot at reaction time close to 0), the equilibrium constant (K = [exchange product/mM]^2 / [starting product/mM]^2) and the half time of equilibration ($t_{1/2}$). Different exchange conditions can be compared using these graphs for a same library.

2.4 dcNCL applied to model peptides

In this part, we have focused on optimizing dynPL conditions compared to our previous work.[3] After having optimized the peptidic sequence, two aspects have been studied: the influence of reducing agents and of temperature under ambient atmosphere.

2.4.1 Model peptide design

Compared to the originally reported peptide segment P1'-Daa2-P2' (NH_2-LYKG-***N*MeCys**-AKLL-$CONH_2$), **P1** (NH_2-LYRAG-***N*MeCys**) was considered as a better choice for the dynamic metathesis system.[3] It should undergo easier intramolecular rearrangement (*cis-trans* isomerization and N to S acyl shift) because of the less sterically hindered molecular structure and which could thus enhance the exchange rate. Glycine was chosen as the second C-terminal amino acid on **P1** because ligations at this site have previously been demonstrated to be fast.[16] The peptide **P2'** (***N*MeCys**-RANY-$CONH_2$) was replaced by **P2** (***N*MeCys**-RANYLA-$CONH_2$) to avoid coelution with the coupling product **P3** (NH_2-LYRAG-***N*MeCys**-RANYLA-$CONH_2$) during UPLC-MS analyses. This exchanged product was synthesized to record standard calibration curves. While the reaction solution was reserved at room temperature (r.t.) and in the presence of DTT 25 mM without the inert atmosphere of argon (Scheme 2.9), conversion of the starting peptides **P1** and **P2** was increased (X = 27 % at 48 h) with a half-time of equilibration $t_{½}$ = 12 h which is faster than the previously reported value ($t_{½}$ = 20 h [3]),

thus showing how modifications of the peptide sequences improve the exchange reaction.

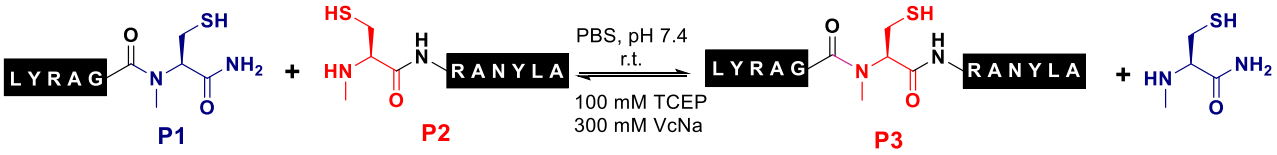

Scheme 2.9 | The optimized dynamic peptide library (dynPL). NMeCys was incorporated into model peptides at the C-terminus of P1 as an electrophilic cryptothioester (blue) and at the N-terminus of P2 as a nucleophile (red).

2.4.2 Influence of reductants

In our initial publication, 1,4-dithiothreitol (DTT) served as reductant to avoid the formation of disulfide bonds. According to the literature[15], TCEP, also a powerful reductant, has the advantages of being odorless, water-soluble, more resistant to oxidation in aerobic conditions and available as a stabilized solution from acidic to mildly basic pH value. However, in our previous publication, it resulted in a high percentage of desulfurized products for our dynPL system. Nevertheless, a recent report indicated that the addition of sodium ascorbate into protein total synthesis completely inhibits TCEP-mediated desulfurization.[17] It is also worth noting that the addition of sodium ascorbate does not slow down the rate of NCL compared with a conventional TCEP buffer. Therefore, a reducing PBS buffer (pH 7.4) containing 100 mM TCEP, 200 mM sodium ascorbate was utilized and no desulfurization has been observed during our assays.

Reductant is an essential element of our dcNCL systems in order to keep all thiol groups in their active forms. From our experiments, we noticed that in the absence of reductants, dynPL with a concentration of 1 mM could be entirely oxidized to their disulfide form within 24 hours. In comparison, the presence of DTT can preserve the reaction activity for up to 72 h at 37 °C and 96 h at 20 °C. TCEP buffer was more effective than DTT in that sense, as the system can remain active for up to 96 h at 37 °C and 120 h at 20 °C. At room temperature (20 °C) or 37 ºC, no significant difference between the two reducing buffers (Figure 2.1) was observed for the initial reaction rate (V_0). At 20 °C, the V_0 for DTT-containing dynPL was 2.01×10^{-8} M.s^{-1} while the one for TCEP buffer-containing dynPL was 4.011×10^{-8} M.s^{-1}. At 37 ºC, the V_0 for DTT-containing dynPL was 5.73×10^{-8} M.s^{-1} and that for TCEP buffer-containing dynPL was 7.19×10^{-8} M.s^{-1}. Moreover, the equilibration half-life times also showed little difference (For DTT-containing dynPL, $t_{½}$ = 12 h at 20 °C, $t_{½}$ = 8 h at 37 °C; for TCEP buffer-containing dynPL, $t_{½}$ = 7.2 h at 20 °C, $t_{½}$ = 6.75 h at 37 °C). The similar behavior of

DTT and TCEP provides us with flexibility for selecting the reducing agent. DTT has a better solubility in organic solvent than TCEP, while the reducing efficiency of DTT is limited by the pH value of the reaction environment (pH > 7). When dcNCL is conducted in a buffer with a boarder range of pH value, TCEP should be considered over DTT.

2.4.3 Influence of temperature

The experiments mentioned above also demonstrated the influence of temperature on the dcNCL. At 37 ºC, the reaction showed both higher (Figure 2.1) exchange rate and equilibrium constant (K) compared to those at 20 ºC, either with DTT (K = 0.10 at 20 °C , K = 0.99 at 37 °C) or with TCEP buffer (K = 0.24 at 20 ºC, K = 0.92 at 37 °C). However, as discussed above (in 2.4.2), increasing the temperature will limit the activity of reductants to preserve peptides in their reduced form. For instance, at 37 °C, in aerobic conditions, peptides start to oxidize to their disulfide forms, which inhibits the exchange ability of dynPL, at shorter time compared to the same system at 20 °C ($t_{oxidation}$ = 96 h for 100 mM TCEP / 200 mM sodium ascorbate, $t_{oxidation}$ = 72 h for 25 mM DTT).

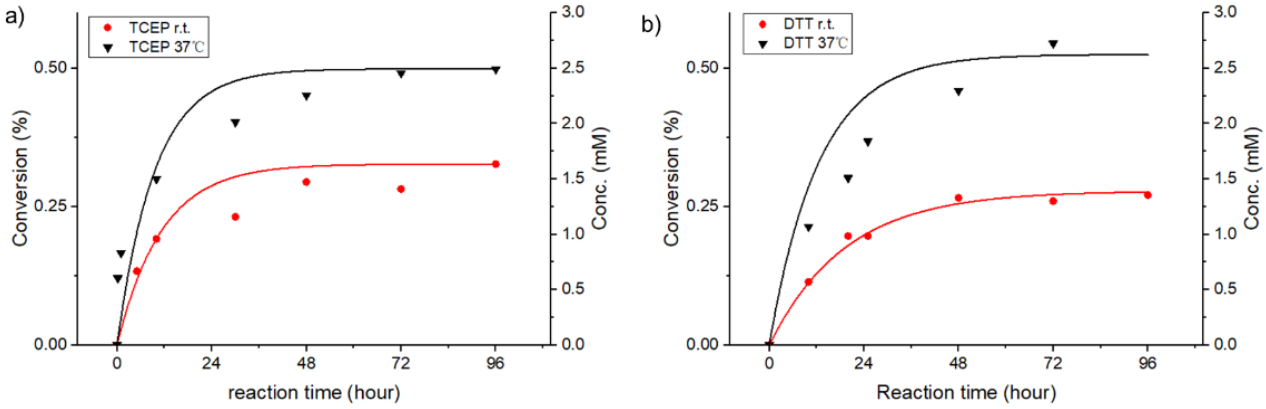

Figure 2.1 | Kinetic curves for product P3 in the presence of a) 100 mM TCEP and 200 mM ascorbate, or b) 25 mM DTT. The reaction was started from mixing equimolar amounts of P1 and P2 (2.5 mM each) in PBS buffer (pH 7.4) at 20 ºC or at 37 ºC. The trend lines are used to simply guide the reader's eye. Concentrations were calculated by standard calibration curves.

2.5 dcNCL applied to small molecules

2.5.1 Molecular design and synthetic routes

We also considered to apply our dcNCL methodology to small molecules as an alternative to peptides. Compounds **S1**-**S6** were designed considering their solubility in organic solvent and from a ***N*MeCys** mixture of alkyl chain, oligo ethylene glycol or aromatic groups.

A four-member dynamic library with internal ***N*MeCys** derivatives (**S1**, **S4**) and *N*-terminal ***N*MeCys** derivatives (**S2**, **S3**) was first prepared as a model study to investigate our dcNCL methodology in organic solvents and aqueous solutions (scheme 2.10a)). As shown in scheme 2.10b), compound **S1** bearing an internal ***N*MeCys** residue can successively undergo *cis-trans* isomerization and N to S acyl shift to form the corresponding thioester. Then, this thioester can dynamically exchange with the free thiol from compound **S2** to release **S3** and the thioester form of **S4**, in a so-called transthioesterification step. Meanwhile, the new **S4** thioester being an active intermediate can perform S to N acyl shift to produce a more stable product, i.e. **S4**. As all intermediate steps involved in this dcNCL process are reversible, this reaction should reach, in principle, thermodynamic equilibrium after proper equilibration time.

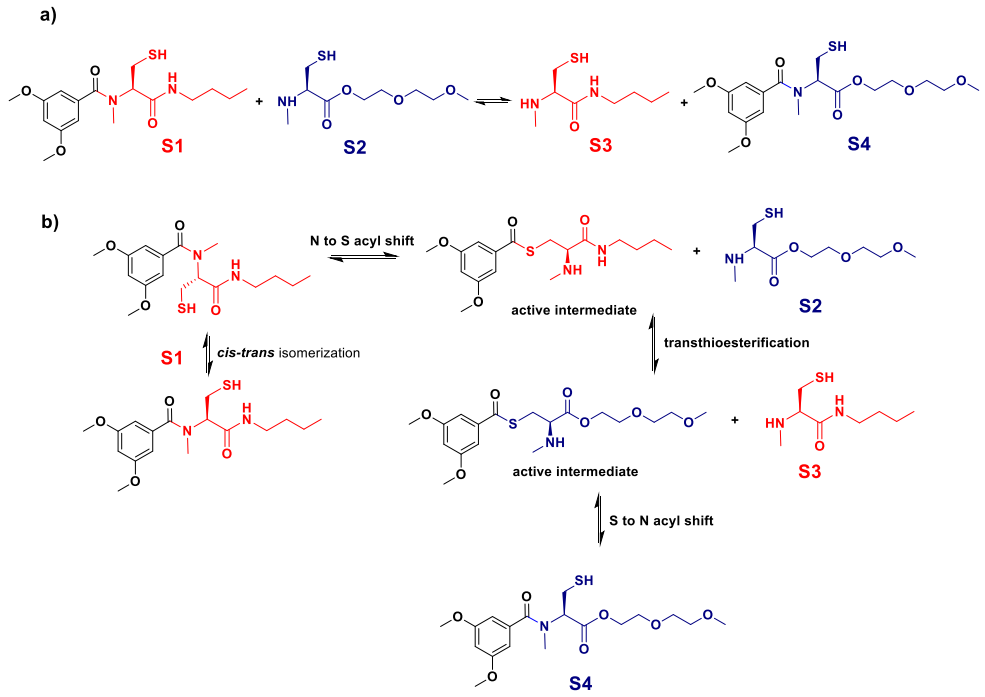

Scheme 2.10 | a) Representation of a library of small molecules with *N*MeCys residues based on the and b) its mechanism.

The reversibility of the exchange reaction could be studied starting from **S1** and **S5** (as the forward direction) or from **S6** and **S4** (as the backward direction) to reach a similar equilibrium (Scheme 2.11).

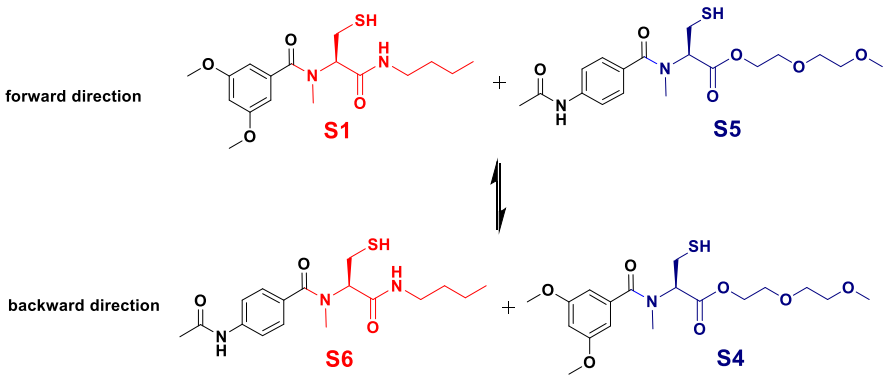

Scheme 2.11 | Reversibility of dcNCL based on the use of *N*MeCys.

The synthetic routes for all ***N*MeCys** derivatives (**S1-S6**) are shown in Scheme 2.12. Similarly, to the synthetic SPPS method to produce peptides, HATU and DIEA were used as activator and base for amide condensation, respectively. Piperazine and HOBt were used to remove the Fmoc group on the amine position of ***N*MeCys** derivatives. Acylation of the resulting secondary amine was performed using a microwave synthesizer (30 W, 70 °C), as the reaction did not proceed in classical reaction conditions even after refluxing the reaction mixture overnight. The **StBu** groups on the thiol position of ***N*MeCys** derivatives could be removed by adding thiols (for example, β-mercaptoethanol) or phosphines (for example, tributylphosphine or triphenylphosphine in TFA)[18]. Due to the long reaction time and unpleasant odor of thiols, we chose to use triphenylphosphine in TFA as deprotection reagent. The resulting side product (triphenylphosphine oxide) could be removed by filtration.[19] **Boc** and **Trt** groups on ***N*MeCys** could be simultaneously removed in few minutes using a mixture of TFA/TIPS (95/5 v/v) without the presence of any solvent.

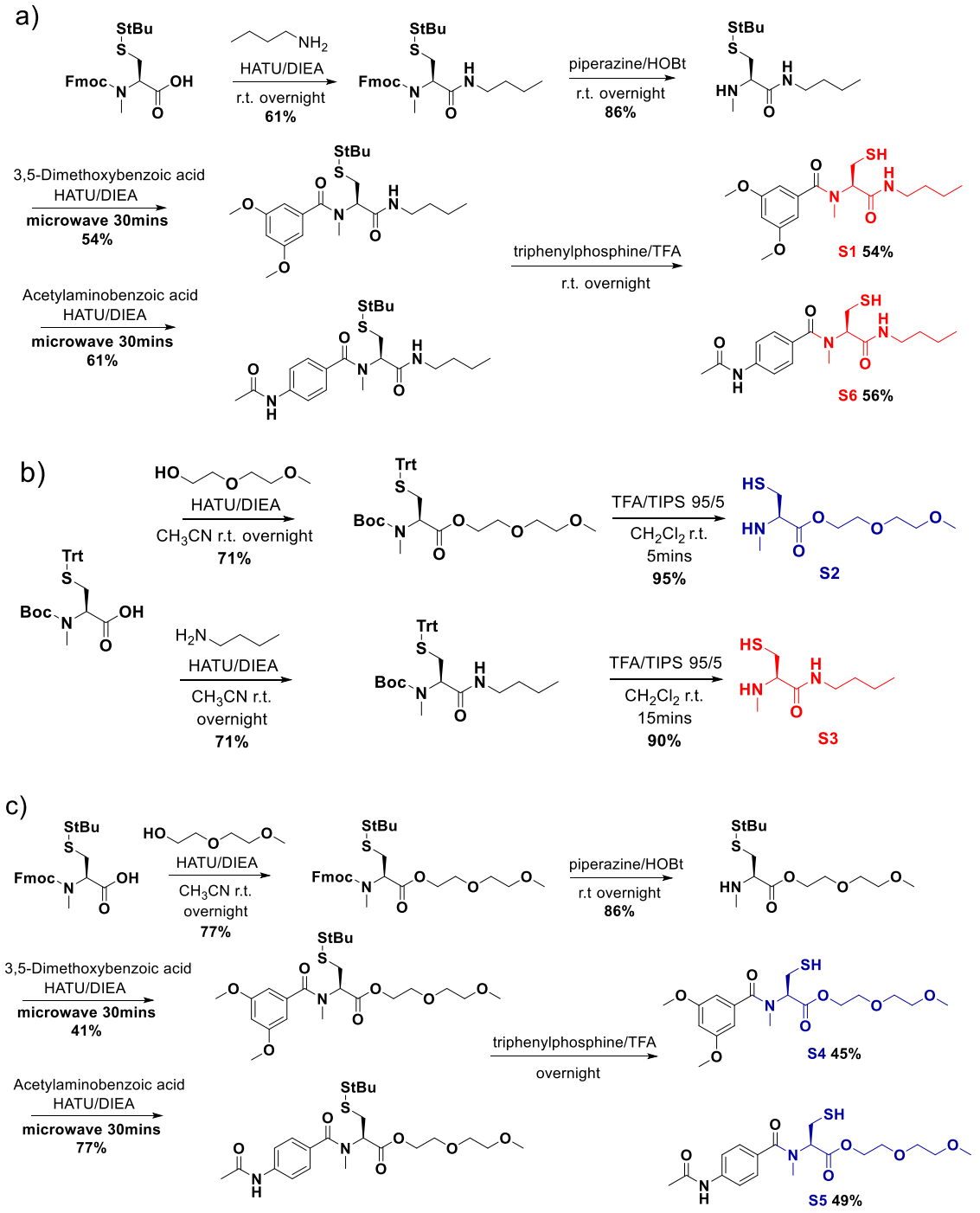

Scheme 2.12 | Synthetic routes for compounds **S1**-**S6**.

2.5.2 Influence of the reaction medium on the dcNCL

The reversible reaction (Scheme 2.10a)) between **S1** and **S2** to obtain exchange products **S3** and **S4** was first investigated. This dcNCL process is influenced by the reaction solvent (DCM, THF, MeOH) as indicated by the UV chromatograms corresponding to **S4** after mixing **S1** and **S2** for 48 h (Figure

2.2). For all solvents, at t = 0 h, only **S1**, **S2** (UV signal could not be detected because of the absence of aromatic groups) and the dimer of **S1** (small amounts) were present in the reaction mixture. After 48 h, for the library where MeOH served as the medium, the amount of exchange product **S4** was more than for the library carried out in DCM or THF.

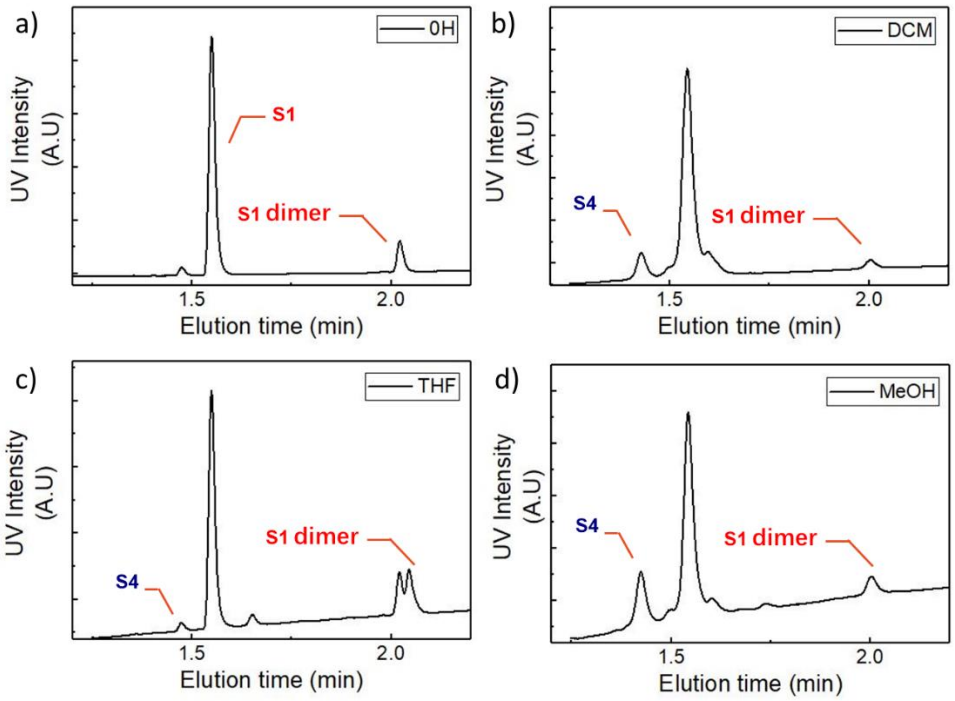

Figure 2.2 | Reverse phase UPLC chromatograms of the dcNCL between **S1** (10 mM) and **S2** (10 mM) at a) t= 0h, and at t=48 h when the solvent was b) DCM, c) THF, d) MeOH. Each solution contained 150 mM DTT.

The different behaviors observed for the dynamic library in various organic solvents (Figure 2.2) indicated that non-polar solvents including DCM and THF almost inhibited the dynamic exchange. This shall be attributed to the inability of non-polar solvents to stabilize the charged intermediates formed during the transthioesterification step. In comparison, polar organic solvents (such as methanol and acetonitrile (can)) with faster equilibration rate are more suitable for stabilizing charged intermediates. Besides, those polar solvents could also improve the solubility of our ***N*MeCys** derivatives **S1**-**S4**.[20]

As a possible approach to further accelerate the exchange rate is to strengthen the polarity of the solvent, we considered milli-Q water as a possible co-solvent. Figure 2.3 a) shows the UV chromatograms (t = 48 h) of the library in ACN and in a 1/1 (v/v) mixture of methanol and milli-Q water. When acetonitrile was used as reaction medium, **S4** was less produced compared to the reaction in the MeOH/water mixture. Kinetic

plots in this solvent system (1/1 v/v methanol and milli-Q water containing 150 mM TCEP and 300 mM sodium ascorbate, pH = 6) are presented in Scheme 2.3b), giving a half-time of equilibration $t_{1/2}$ of 5.4 h and an initial reaction rate V_0 of 1.41 × 10^{-7} M.s^{-1} which is faster than in our previous work (dynPL studied at pH 6 with a set of kinetic parameters of V_0 = 1.11 × 10^{-8} M.s^{-1} and $t_{1/2}$ =25 h).

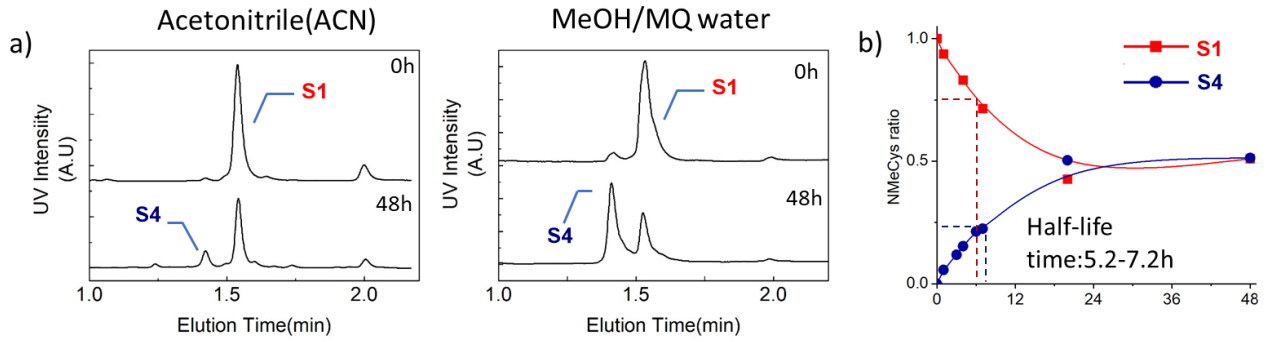

Figure 2.3| a) Reverse phase UPLC chromatograms of the dynamic library between **S1** (10 mM) and **S2** (10 mM) in acetonitrile and in a mixture of methanol and milli-Q water (1/1 v/v, 150 mM TCEP, 300 mM sodium ascorbate was contained, pH = 6) at t= 0h and t= 48h. b) Kinetic curves for *N*MeCys derivatives **S1** and **S4** as a function of reaction time in a mixture of methanol and milli-Q water. *N*MeCys ratio corresponds to [**S1**$_{reaction}$]/[**S1**$_{initial}$] and [**S4**$_{reaction}$]/[**S1**$_{initial}$]. The trend lines are used simply to guide the reader's eye.

The idea of mixing an organic polar solvent with milli-Q water can not only accelerate the exchange rate but also overcome the hydrolysis of the thioester form of the ***N*MeCys** derivatives, which shows a benefit compared to the work reported in 2014 by our group. In other words, for our dcNCL systems, inorganic polar media such as water strongly promote transthioesterification, while organic polar solvents such as methanol inhibit the hydrolysis of amino acids and increase the solubility of diverse ***N*MeCys** derivatives.

2.5.3 Influence of the pH value of the reductant on the dcNCL

Similarly, to our study with peptides, when milli-Q water is present in the dynamic system, TCEP is preferred as reductant. As it is stable in aqueous solution from pH 1.5 to 8.5,[15] we studied how the pH value of the TCEP solution affect the initial rate, the half-time of equilibration and the equilibrium constant of our library. Thus, a series of **S1**-**S2** libraries ranging from acidic (pH = 4) to mildly basic (pH = 8.5) pH were prepared. At room temperature, the dynamic recombination of **S1** and **S2** resulted in the formation of the exchange products **S3** and **S4** at all tested pH values (Figure 2.4a)), with V_0

and $t_{1/2}$ according to Table 2.1 and Figure 2.4b). Compared to our previous work[3] the 10 times increase of V_0 at pH 6 and 7 clearly show an improvement for the present exchange reaction conditions.

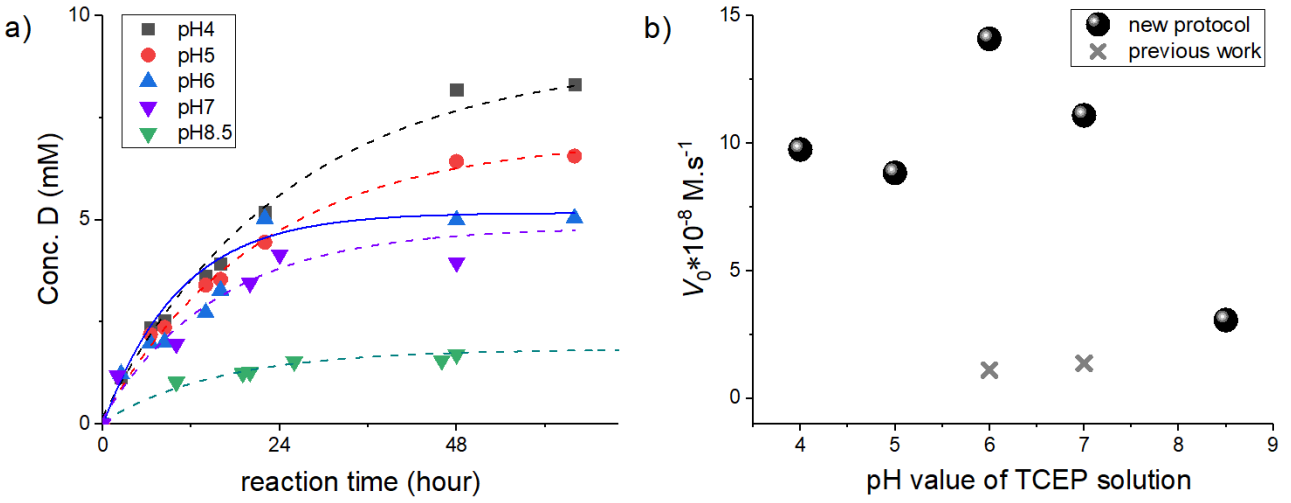

Figure 2.4 | a) Evolutional of the concentration of exchanged product **S4** as a function of reaction time for libraries at different pH. The reaction was started from **S1** (10 mM) and **S2** (10 mM) in a 1/1 (v/v) mixture of methanol and milli-Q water containing 150 mM TCEP, 300 mM sodium ascorbate at T = 298 K. The trend lines are used simply to guide the reader's eye. b) Initial rate (V_0) of the exchange reaction ($\times$ 10^{-8} M.s^{-1}) in this work and in the previous work[3] as a function of the TCEP solution's pH value. (The previous work used phosphate buffer containing 200 mM and 0.38% w/v of DTT at pH 6 and 7 at room temperature).

pH value of the reductant	V_0 (M.s^{-1}) [a]	$t_{1/2}$ (h) [b]	K[c]
4	9.76 $\times$ 10^{-8}	15	5.94
5	8.84 $\times$ 10^{-8}	12	2.50
6	1.41 $\times$ 10^{-7}	5.2	0.93
7	1.11 $\times$ 10^{-7}	11	0.92
8.5	3.07 $\times$ 10^{-8}	11	0.65

Table 2.1 | The Influence of the pH value of the reductant on the dcNCL in the dynamic character of the initial rate[a], the half-time of equilibration[b] and the equilibrium constant of our library[c].

The dependence of rate and half-time of equilibration on the pH can be rationalized according to the

mechanism (Scheme 2.10b)). Indeed, the rearrangement from **S1** to its transient thioester form by *cis-trans* isomerization and N to S acyl shift is favored at lower pH.[21] In contrast, the reversible transthioesterification is promoted by increasing the pH.[20] Faster V_0 and $t_{1/2}$ are observed for a TCEP solution at pH 6, thus indicating that geometric constraints related to *cis-trans* isomerization and N to S acyl shift are the rate limiting step. This observation is opposite what happens in pure buffer when transthioesterification is the rate limiting step.[3]

Furthermore, the equilibrium constant (K) (Figure 2.5) of the exchange reaction is greatly affected by the pH, leading to different amount of exchange products at thermodynamic equilibrium. As discussed above, during the dcNCL process between ***N*MeCys** derivatives **S1** and **S2**, the entire exchange rate is mainly influenced by the rearrangement from the free thiol form to the corresponding thioester. This intermediate thioester could be favored by increasing the acidity of the system. The pH-dependent mechanism of our dcNCL process provides remarkable flexibility to our dynamic system under the pressure of external (solvent type) and chemical (H^+) stimulus, with great potential for constructing stimuli-responsive, reversible amide materials.

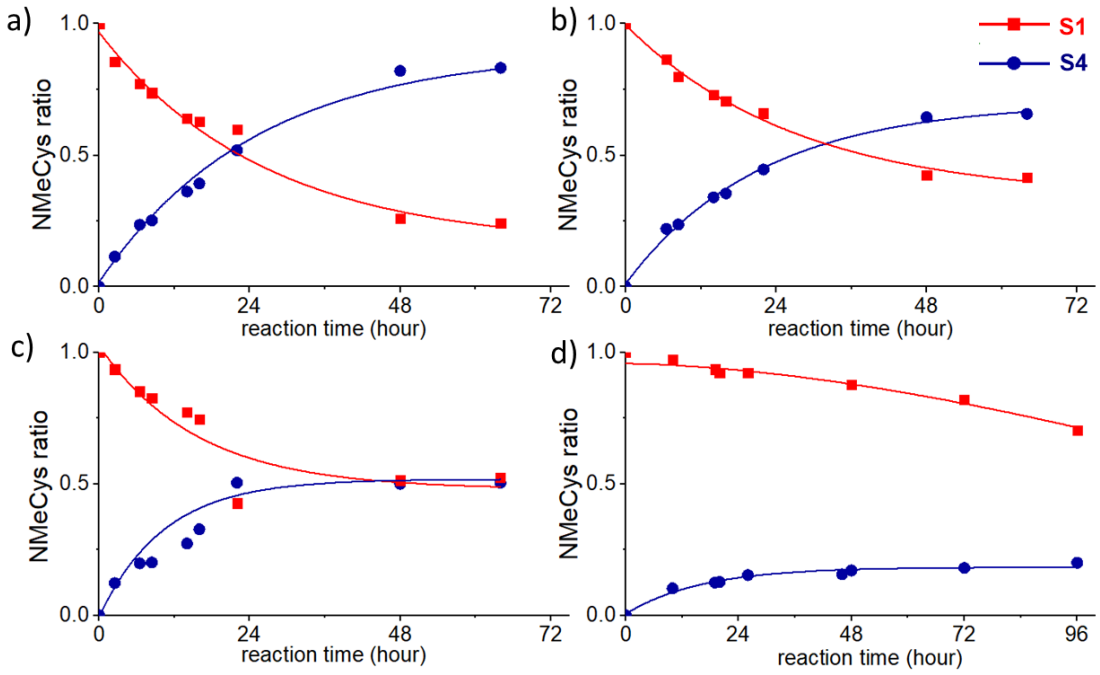

Figure 2.5 | Kinetic curves for *N*MeCys derivatives **S1** and **S4** for a library in a 1/1 (v/v) mixture of methanol and milli-Q water containing 150 mM TCEP, 300 mM sodium ascorbate) at pH = a) 4, b) 5, c) 6 and d) 8.5 as a function of reaction time. *N*MeCys ratio: [**S1**$_{reaction}$]/[**S1**$_{initial}$] and [**S4**$_{reaction}$]/[**S1**$_{initial}$].

In conclusion, the dcNCL can be conducted in aqueous solutions (1/1 v/v methanol and milli-Q water containing 150 mM TCEP, 300 mM sodium ascorbate at pH 4-7) at room temperature. In this case, the N to S acyl shift becomes the rate limiting step for the whole exchange process. Under external stimulus (acidity of the reaction environment), the dcNCL shows its adaptive behavior. (Figure 2.6)

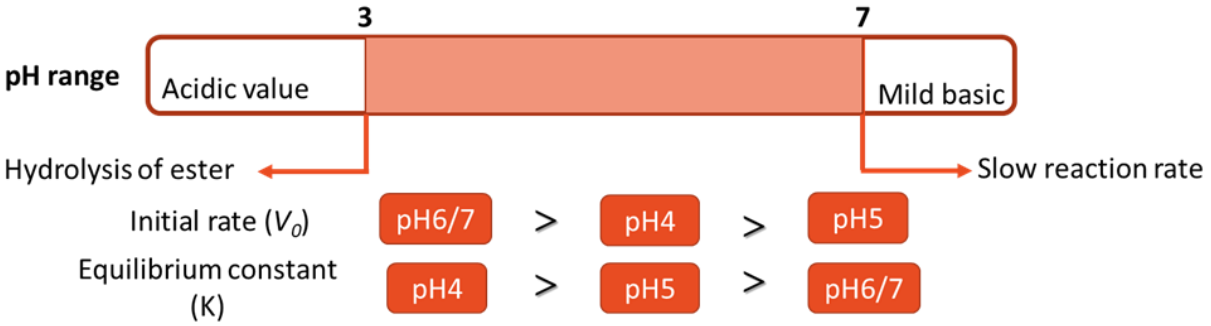

Figure 2.6 | Schematic representation of how the pH value of the TCEP solution influences the reversible amide metathesis.

2.5.4 Influence of catalysts on the dcNCL

In traditional NCL strategies, **alkyl**thioester peptides are frequently used as starting materials for total synthesis of proteins because of their easy preparation. To circumvent the low reactivity of **alkyl**thioester peptides, an excess of mild acidic thiols is often used to yield **aryl**thioester peptides by transthioesterification.[22] Once the arylthioesters were formed, they can rapidly react with the **Cys** containing peptides and thus speed up the ligation step (Scheme 2.13). Interestingly, the mild acidic thiols never accumulate in the ligation mixture and can continuously activate the NCL process, acting as efficient catalysts of these systems.

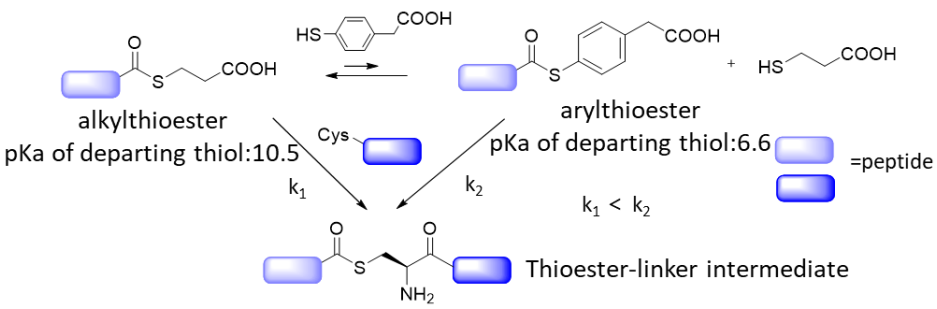

Scheme 2.13 | The catalytic mechanism of the NCL process in the presence of acidic thiols.

After comparing different NCL catalysts, we selected 4 types of thiols, namely 4-aminothiophenol, 4-mercaptopyridine, mercaptophenylacetic acid (MPAA), and trifluoroethanethiol to test their performance in our dcNCL process. 4-aminothiophenol, with a pK_a of 8.75, is a classical and effective catalyst for NCL since 1996.[23] 4-mercaptopyridine, with a pK_a of -1, is supposed to be a better leaving group compared to the thiols with higher pK_a values.[22] MPAA, with a pK_a of 6.66, is widely known as the gold-standard NCL catalyst due to its special properties: water solubility, easy-to-handle and non-malodorous. Another catalyst trifluoroethanethiol, with a pK_a of 7.30, has been demonstrated to have similar catalytic ability to thiophenol in NCL systems.[24] As it is an alkyl thiol, it is not detected by UV and thus will not perturb our UV chromatograms when following the ligation process.

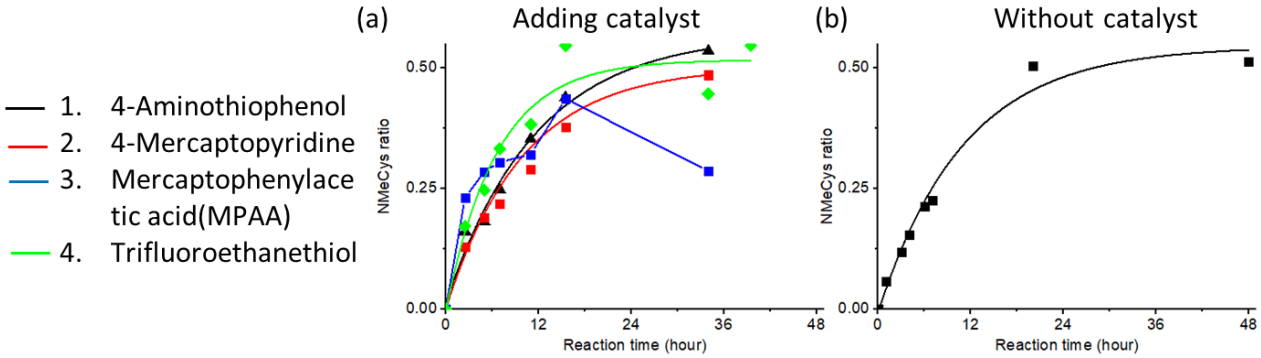

Figure 2.7 | Kinetic curves of product **S4** for the dcNCL process as a function of reaction time: a) with 100 mM 4-aminothiophenol (black), 100 mM 4-mercaptopyridine (red), 100 mM mercaptophenylacetic acid (MPAA) (blue) or 100 mM trifluoroethanethiol (green) as catalysts and b) without catalyst (black). *N*MeCys ratio: [**S4**$_{reaction}$]/[**S1**$_{initial}$]. The exchange reactions were started by mixing **S1** (10 mM) and **S2** (10 mM) in a 1/1 (v/v) mixture of methanol and milli-Q water containing 150 mM TCEP, 300 mM sodium ascorbate at pH 6 and T = 298 K.

Catalysts	V_0 (M.s^{-1}) [a]	$t_{1/2}$ (h) [b]	K[c]
4-aminothiophenol	1.32×10^{-7}	8	1.35
4-mercaptopyridine	1.39×10^{-7}	7	0.84
mercaptophenylacetic acid	2.56×10^{-7}	4	0.43
trifluoroethanethiol	2.15×10^{-7}	5.2	1.28
Without catalyst	1.41×10^{-7}	5.2	0.93

Table 2.2 | The Influence of the different catalysts on the dcNCL in the dynamic character of the initial rate[a], the half-time of equilibration[b] and the equilibrium constant of our library[c].

Unfortunately, the presence of thiol catalysts did not improve the efficiency of our exchange reaction

(Figure 2.7). All reactions had similar equilibration half-time. Only MPAA and trifluoroethanethiol slightly accelerated the exchange process (Table 2.2). These observations are in line with the ones made at different pH and confirm that the transthioesterification step is not the rate limiting step of our dcNCL process in these conditions. Thus, our reversible amide metathesis could be simply carried out without any catalyst.

2.5.5 Influence of the concentration of starting materials on the dcNCL

We then studied how the amount of starting materials influences the exchange efficiency of dcNCL systems. A series of dcNCL reactions (Figure 2.8) starting from equimolar quantities of **S1** and **S2** at different concentration (10, 2, 1, and 0.2 mM) were prepared under the same environmental conditions (1/1 v/v methanol and milli-Q water containing 150 mM TCEP, 300 mM sodium ascorbate at pH 4, T = 298 K). For concentrations of starting materials lower than 2 mM, a new UV peak showed up at t = 26 h, corresponding to the hydrolysis of active intermediates, namely **S1** and **S4** thioesters.

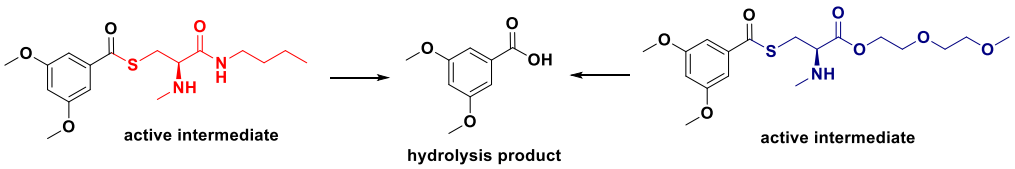

Scheme 2.14 | Hydrolytic process occurring during the dcNCL process.

Thus, lower concentrations of starting materials led to more hydrolytic products (Scheme 2.14). This observation suggests a competition between different reaction pathways in our system. Apart from all the intermediate steps involved in the dcNCL process, the oxidation of thiols and the hydrolysis of thioester derivatives can affect the efficiency of the dcNCL process and thus, the thermodynamic equilibrium. When the pH value of the TCEP solution is higher than 6 or the concentration of starting materials is high enough (> 2 mM), all side reactions are suppressed.

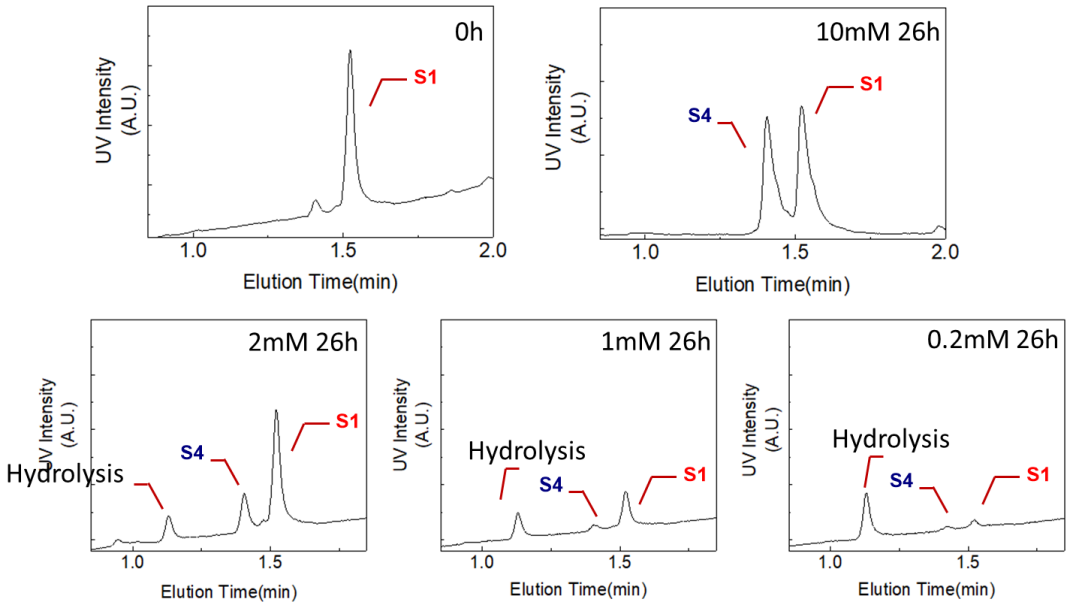

Figure 2.8 | Reversed phase UPLC chromatograms (UV traces) of the dcNCL process performed in a 1/1 (v/v) mixture of methanol and milli-Q water containing 150 mM TCEP, 300 mM sodium ascorbate at pH = 4 and T = 298 K) for different starting concentrations of **S1** and **S2**.

2.5.6 Reversibility of dcNCL

In order to further develop our methodology by expanding the scope of our ***N*MeCys** candidates, we decided to perform the dcNCL process starting from **S1** (10 mM) and **S5** (10 mM) and leading to **S6** and **S4** as exchange products (Figure 2.9a)). Both **S1**+ **S5** (10 mM each, forward) and **S6** + **S4** (10 mM each, backward) reactions were monitored on the same time scale at t = 0, 24h, and 72h (Figure 2.9b)). According to the chromatogram at t = 72h, the two reactions equilibrated to the same thermodynamic equilibrium, showing the reversibility of our dynamic covalent reaction.

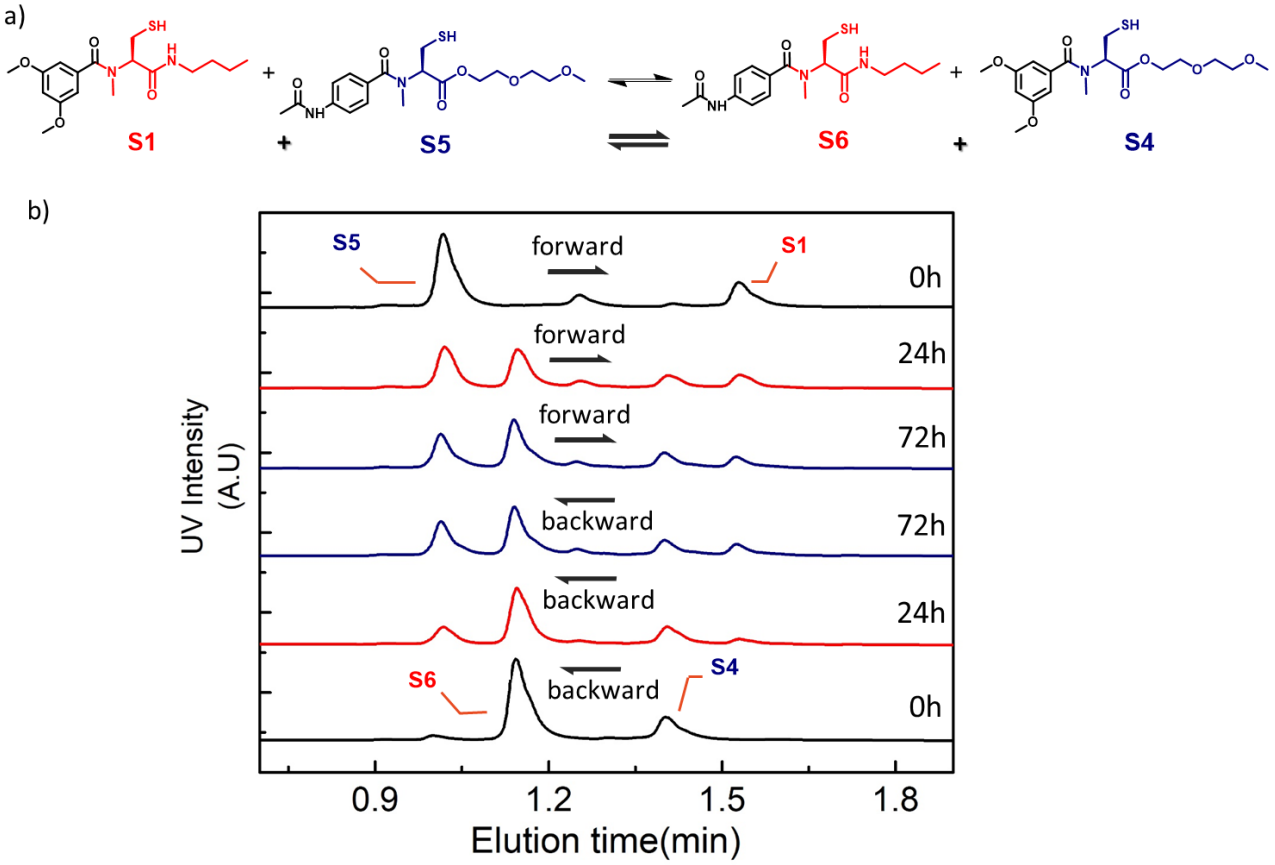

Figure 2.9 | a) Dynamic library made of **S1**, **S5**, **S6** and **S4** in organic solvents. b) Reversed phase UPLC chromatogram of both forward (**S1** + **S5**, three traces on top) and backward (**S4** + **S6**, three traces at the bottom) directions in acetonitrile (200 mM DTT) at t= 0 h, 24h, 72h.

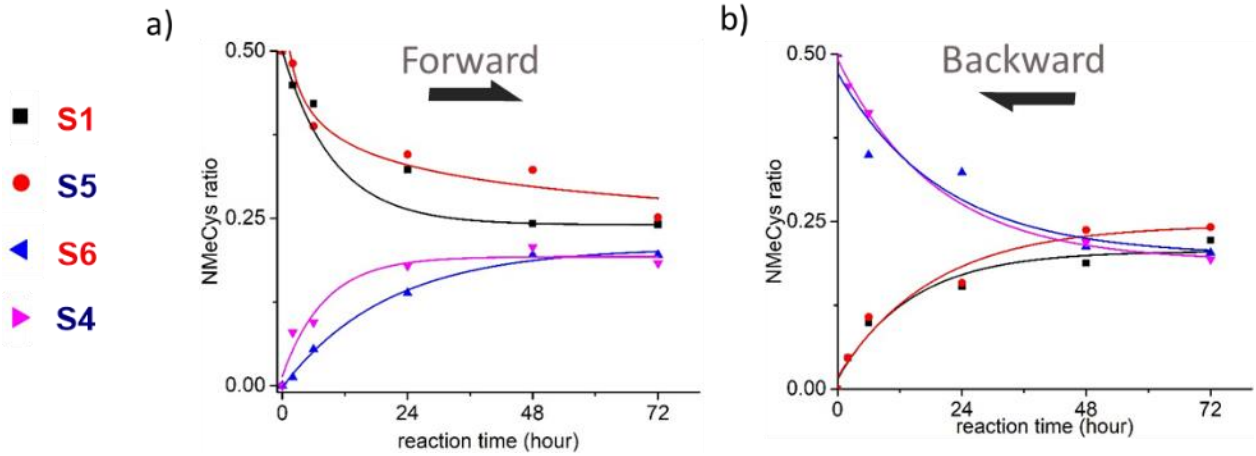

Figure 2.10 | Kinetic curves of *the four constituents* (**S1**, **S4**, **S5**, **S6**) of the library in acetonitrile (200 mM DTT) for the a) forward and b) backward direction. *N*MeCys ratio: [**S1**$_{reaction}$]/[**S1**$_{initial}$], [**S5**$_{reaction}$]/[**S1**$_{initial}$], [**S4**$_{reaction}$]/[**S1**$_{initial}$] and [**S6**$_{reaction}$]/[**S1**$_{initial}$].

We also recorded the kinetics of the four constituents **S1**, **S4, S5**, **S6** in acetonitrile at room temperature from both forward and backward direction. Although the two reactions showed different equilibration rates at the beginning, almost the same equilibrium state was reached after 72 h, which is intrinsically due to the dynamic nature of this metathesis reaction.

2.6 Conclusions

We successfully synthesized in gram-scale quantities three fully protected ***N*MeCys** derivatives, which are the main building blocks required to elaborate our dynamic covalent libraries and which are necessary for further application of our reversible amide metathesis. After careful and detailed exploration of the different parameters governing our dcNCL involving ***N*MeCys** derivatives, a suitable and convenient protocol has been optimized (see Table 2.3).

Previous work (ref.[3])	Optimized protocol of this thesis
inert atmosphere	ambient atmosphere
degassed buffers (freeze-thaw cycles)	freshly prepared buffers (no degassing) or organic solvents or organic aqueous solutions
Schlenk apparatus under argon	conventional test tube
3-4 hours for DCL preparation	less than 1 hour for DCL preparation
$t_{1/2}$ = 20 h (25 mM DTT, rt)	$t_{1/2}$ = 12 h (25 mM DTT, rt) $t_{1/2}$ = 7.2 h (0.1 M TCEP / 0.2 M asc, rt)
$t_{1/2}$ = 10 h (25 mM DTT, 37 °C)	$t_{1/2}$ = 8 h (25 mM DTT, 37 °C) $t_{1/2}$ = 6.75 h (0.1 M TCEP / 0.2 M asc, 37 °C)
$V_0 = 1.11\times10^{-7}$ M.s^{-1} (pH 6)	$V_0 = 14.1\times10^{-7}$ M.s^{-1} (pH 6)
$V_0 = 1.38\times10^{-7}$ M.s^{-1} (pH 7)	$V_0 = 11.1\times10^{-7}$ M.s^{-1} (pH 7)
significant hydrolysis for long equilibration times	no hydrolysis in all conditions

Table 2.3 | Global comparison of the dcNCL protocols before and after optimization.

The exchange reaction can efficiently equilibrate to the thermodynamic equilibrium under various conditions (different solvents, buffers, pH values and temperatures) without inert gas protection and addition of catalysts. The DTT used in the previously reported methodology to avoid disulfide formation can be substituted by a buffer containing TCEP and sodium ascorbate. The choice of reductant is related to the reaction conditions. For proper reaction conditions (solvent, pH value and concentration) hydrolysis can be totally eliminated. The solvent is also strongly influencing the dynamic metathesis reaction, mainly in terms of equilibration rate. The influence of pH value of the TCEP solution on the exchange reaction indicates its adaptivity under the pressure of chemical

stimulus. These results altogether provide us with great confidence to further develop the dcNCL process by constructing diverse dynamic constitutional systems. Furthermore, the ability of this reaction to proceed efficiently in aerobic conditions increases its intrinsic relevance for the first applications in material sciences or even in chemical biology and drug discovery.

2.7 References

1. Wieland, T., Bokelmann, E., Bauer, L., Lang, H. U. & Lau, H. Über Peptidsynthesen. 8. Mitteilung Bildung von S-haltigen Peptiden durch intramolekulare Wanderung von Aminoacylresten. *Justus Liebigs Ann. Chem.* **583**, 129–149 (1953).
2. Binschik, J. & Mootz, H. D. Chemical bypass of intein-catalyzed n-s acyl shift in protein splicing. *Angew. Chem. Int. Ed.* **52**, 4260–4264 (2013).
3. Ruff, Y., Garavini, V. & Giuseppone, N. Reversible native chemical ligation: A facile access to dynamic covalent peptides. *Journal of the American Chemical Society* **136**, 6333–6339 (2014).
4. Devaraj, N. K. & Perrin, C. L. Approach control. Stereoelectronic origin of geometric constraints on N-to-S and N-to-O acyl shifts in peptides. *Chem. Sci.* **9**, 1789–1794 (2018).
5. Yan, L. Z. & Dawson, P. E. Synthesis of peptides and proteins without cysteine residues by native chemical ligation combined with desulfurization. *J. Am. Chem. Soc.* **123**, 526–533 (2001).
6. Friedel K, Popp MA, Matern JC, Gazdag EM, Thiel IV, Volkmann G, Blankenfeldt W, Mootz HD. A functional interplay between intein and extein sequences in protein splicing compensates for the essential block B histidine. *Chem. Sci.* **10**, 239–251 (2019).
7. Hojo, H., Onuma, Y., Akimoto, Y., Nakahara, Y. & Nakahara, Y. N-Alkyl cysteine-assisted thioesterification of peptides. *Tetrahedron Lett.* **48**, 25–28 (2007).
8. Ruggles, E. L., Flemer, S. & Hondal, R. J. A viable synthesis of N-methyl cysteine. *Biopolymers* **90**, 61–68 (2008).
9. Marcucci, E., Bayó-Puxan, N., Tulla-Puche, J., Spengler, J. & Albericio, F. Cysteine- *S* -trityl a key derivative to prepare *n*- methyl cysteines. *J. Comb. Chem.* **10**, 69–78 (2008).
10. Rijkers, D. T. S., Kruijtzer, J. A. W., Killian, J. A. & Liskamp, R. M. J. A convenient solid phase synthesis of S-palmitoyl transmembrane peptides. *Tetrahedron Lett.* **46**, 3341–3345 (2005).
11. Denis, B. & Trifilieff, E. Synthesis of palmitoyl-thioester T-cell epitopes of myelin proteolipid protein (PLP). Comparison of two thiol protecting groups (StBu and Mmt) for on-resin acylation. *J. Pept. Sci.* **6**, 372–377 (2000).
12. Zheng, J.-S., Chang, H.-N., Wang, F.-L. & Liu, L. Fmoc synthesis of peptide thioesters without post-chain-assembly manipulation. *J. Am. Chem. Soc.* **133**, 11080–11083 (2011).
13. Zheng, J.-S., Tang, S., Qi, Y.-K., Wang, Z.-P. & Liu, L. Chemical synthesis of proteins using peptide hydrazides as thioester surrogates. *Nat. Protoc.* **8**, 2483–2495 (2013).
14. Dunetz, J. R., Magano, J. & Weisenburger, G. A. Large-scale applications of amide coupling reagents for the

synthesis of pharmaceuticals. *Org. Process Res. Dev.* **20**, 140–177 (2016).

15. Getz, E. B., Xiao, M., Chakrabarty, T., Cooke, R. & Selvin, P. R. A comparison between the sulfhydryl reductants tris(2-carboxyethyl) phosphine and dithiothreitol for use in protein biochemistry. *Anal. Biochem.* **273**, 73–80 (1999).
16. Hackeng, T. M., Griffin, J. H. & Dawson, P. E. Protein synthesis by native chemical ligation: Expanded scope by using straightforward methodology. *Proc. Natl. Acad. Sci.* **96**, 10068–10073 (1999).
17. Rohde, H., Schmalisch, J., Harpaz, Z., Diezmann, F. & Seitz, O. Ascorbate as an alternative to thiol additives in native chemical ligation. *ChemBioChem* **12**, 1396–1400 (2011).
18. Postma, T. M. & Albericio, F. Disulfide formation strategies in peptide synthesis: disulfide formation strategies in peptide synthesis. *Eur. J. Org. Chem.* **2014**, 3519–3530 (2014).
19. Batesky, D. C., Goldfogel, M. J. & Weix, D. J. Removal of triphenylphosphine oxide by precipitation with zinc chloride in polar solvents. *J. Org. Chem.* **82**, 9931–9936 (2017).
20. Worrell BT, Mavila S, Wang C, Kontour TM, Lim CH, McBride MK, Musgrave CB, Shoemaker R, Bowman CN. A user's guide to the thiol-thioester exchange in organic media: scope, limitations, and applications in material science. *Polym. Chem.* **9**, 4523–4534 (2018).
21. Nakamura KI, Kanao T, Uesugi T, Hara T, Sato T, Kawakami T, Aimoto S. Synthesis of peptide thioesters via an *N* - *S* acyl shift reaction under mild acidic conditions on an *N* -4,5-dimethoxy-2-mercaptobenzyl auxiliary group. *J. Pept. Sci.* **15**, 731–737 (2009).
22. Johnson, E. C. B. & Kent, S. B. H. Insights into the Mechanism and Catalysis of the Native Chemical Ligation Reaction. *J. Am. Chem. Soc.* **128**, 6640–6646 (2006).
23. Canne, L. E., Bark, S. J. & Kent, S. B. H. Extending the applicability of native chemical ligation. *J. Am. Chem. Soc.* **118**, 5891–5896 (1996).
24. Thompson RE, Liu X, Alonso-García N, Pereira PJ, Jolliffe KA, Payne RJ. Trifluoroethanethiol: An additive for efficient one-pot peptide ligation−desulfurization chemistry. *J. Am. Chem. Soc.* **136**, 8161–8164 (2014).

Chapter 3. Selectivity in dcNCL from the molecular scale to the microscopic level

3.1 Project objectives

In the previous chapter, we have optimized our protocol of dcNCL. To explore a possible extension of our methodological approach, efforts have then focused on enhancing the complexity of our libraries and on exploring how dcNCL at the molecular scale can induce changes at the microscopic level. More than 10 years ago, our group showed that the thermodynamic equilibrium of a dynamic covalent reaction could be displaced by triggering the self-replication of one specific constituent in the DCL.[1] As shown in Figure 3.1, AI_1M_1, one of the imines in the DCL could form homodimer $[AI_1M_1]_2$ through hydrogen bonds. The formation of this homodimer induces a shift of the thermodynamic equilibrium of the library towards the expression of this constituent. With no doubt, $[AI_1M_1]_2$ would be amplified with the excessive amount, along with the decrease of other constituents in the library. Because of the double reversibility in the system (hydrogen bonds and imine bonds), the final equilibrium of the library arises from a competition between kinetic and thermodynamic biases.

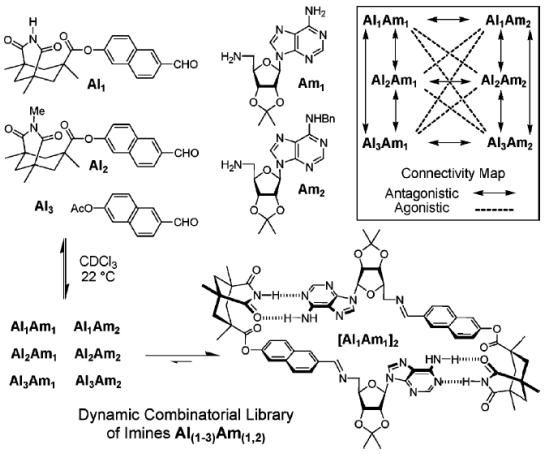

Figure 3.1 | DCL orthogonally controlled by reversible hydrogen bonding formation and imine formation. Figure is adapted from ref. [1].

Such modification of the thermodynamic equilibrium in a DCL often arises from external stimulation leading to changes at the molecular level and possibly at higher length scale. For example, our group

took advantage of the possible micellar self-assembly of amphiphiles as internal driving force to design a DCL with hydrophilic, hydrophobic, and amphiphilic building blocks based on reversible imine formation (Figure 3.2).[2,3] By investigating the reactions between amines bearing hydrophilic oligoethylene glycol chains of different lengths and a hydrophobic aldehyde, they noticed unexpected increases in equilibrium constant (*K*) of the libraries. This was attributed to the self-assembly of the amphiphilic blocks (dynablocks) into highly stable supramolecular structures.

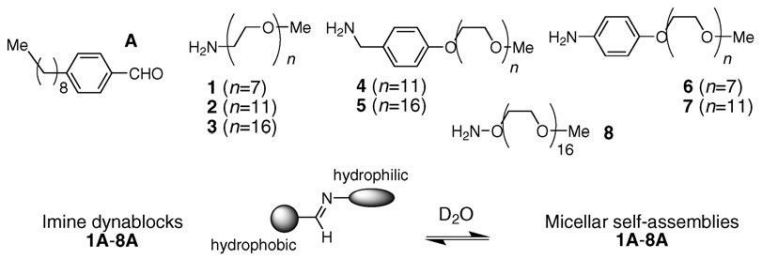

Figure 3.2 | Micellar self-assembly driven DCLs. Hydrophilic amines 1–8 react individually with the hydrophobic aldehyde A leading to imines 1A–8A. In D_2O, these dynablocks self-assembled into supramolecular micellar structures. Figure is adapted from ref. [2,3].

Based on this work and on our knowledge on DCvC, we considered to apply our ***N*MeCys**-based dcNCL to DCLs simultaneously containing hydrophilic, hydrophobic, and amphiphilic blocks (Figure 3.3). First, polyethylene glycol with an average MW of 800 Dalton (NH_2-PEG800-OMe) was inserted into the *C*-terminal of ***N*MeCys** (*N*MeCys-PEG800) to serve as a hydrophilic building block. As we intended to work with real polymers having a dispersity, we unintentionally increased the complexity of our dcNCL library. Second, a peptide segment with five lysines and five phenylalanines was introduced and inserted into the *N*-terminal of ***N*MeCys** (F_5K_5-*N*MeCys) to serve as a hydrophobic building block, but also as an internal standard for monitoring our DCL using UV spectroscopy (Figure 3.3a)). The presence of native peptide bonds was considered as a proof of concept in order to possibly apply our dcNCL into biological systems. Finally, a ***N*MeCys** derivative (C8BA-*N*MeCys-C4) with two hydrophobic chains at the C- and N- terminal was designed to enhance the scope of our dcNCL methodology with small molecules (Figure 3.3b)).

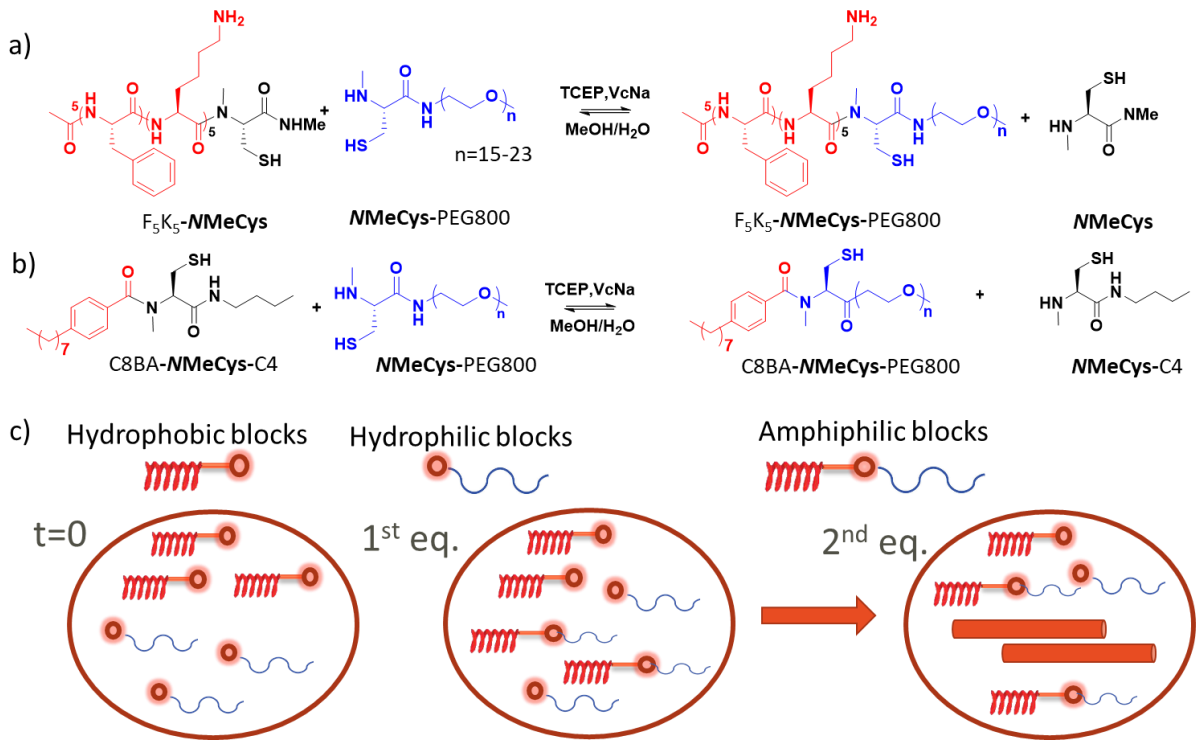

Figure 3.3 | a) DCL based on hydrophobic F_5K_5-*N*MeCys and hydrophilic *N*MeCys-PEG800 and involving dcNCL as exchange reaction. b) DCL based on hydrophobic C8BA-*N*MeCys-C4 and hydrophilic *N*MeCys-PEG800 and involving dcNCL as exchange reaction. c) Schematic representation of the DCLs combining both dynamic covalent chemistry and supramolecular self-assembly.

By combining either F_5K_5-*N*MeCys with *N*MeCys-PEG800 or C8BA-*N*MeCys-C4 with *N*MeCys-PEG800, DCLs would behave as illustrated in Figure 3.3c). In a proper solvent system and under particular environmental conditions, the hydrophilic and hydrophobic blocks should react to produce ***N*MeCys** and amphiphilic molecules (dynablocks) at a first thermodynamic equilibrium (1st eq.). However, upon changes of environmental conditions, for example an increase of water percentage in the system, the amphiphilic molecules should have a high propensity to self-assemble into noncovalent supramolecular structures. The first thermodynamic equilibrium (1st eq.) should thus be displaced towards the direction of generating more amphiphilic molecules thanks to the dynamic covalent character of the dcNCL. Finally, the DCL could be stabilized in a new equilibrium (2nd eq.) where supramolecular self-assemblies co-exist with ***N*MeCys** blocks. The detection of a supramolecular structure within a library will demonstrate the extension of dynamic covalent chemistry from the molecular scale to the microscopic level.

3.2 Molecular synthetic routes

Compound *N*MeCys-PEG800 was synthesized in two steps with high yield starting from **Boc**-*N*MeCys(**Trt**)-OH (1 eq.) and polyethylene glycol with an average MW of 800 Dalton (NH_2-PEG800-OMe) (see Scheme 3.1 as the synthetic route). In the first step, a classical amide coupling procedure[4] in the presence of HATU (1.5 eq.) and DIEA (1.8 eq.) as coupling reagents yielded Boc-*N*MeCys(Trt)-PEG800. Using a slight excess of NH_2-PEG800-OMe (1.1 eq.), side products and excess starting material could be removed easily by extraction, providing Boc-*N*MeCys (Trt)-PEG800 for direct use in the second step without further purification. Deprotection of Boc and Trt with TFA/TIPS (95/5 v/v) afforded the desired *N*MeCys-PEG800 in good yield (95%) while side products could be removed by a simple extraction step.

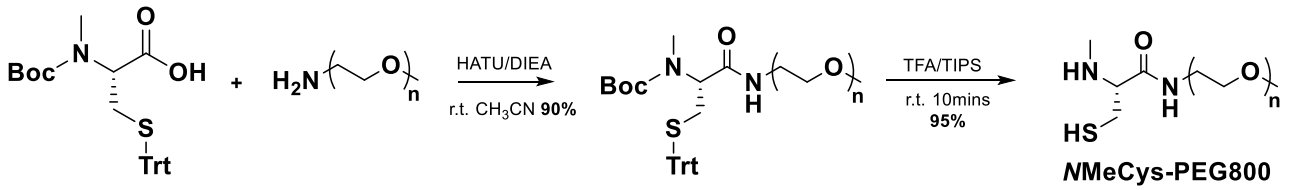

Scheme 3.1 | Synthetic route for *N*MeCys-PEG800.

F_5K_5-*N*MeCys was synthesized by SPPS as described in section 2.2.[5] Hydrophobic block C8BA-*N*MeCys-C4 (Scheme 3.2a)) and amphiphile C8BA-*N*MeCys-PEG800 (Scheme 3.2b)) were synthesized in four steps using similar synthetic procedures. In a first step, *n*-butylamine or NH_2-PEG800-OMe (2.0 eq.) was coupled with **Fmoc**-*N*MeCys(**Trt**)-OH (1.0 eq.) via a classical amide coupling procedure using HATU (1.5 eq.) and DIEA (1.8 eq.) as coupling agents. In a second step, piperazine and HOBt were used to remove the Fmoc group on the secondary amine group. Then, ***N*MeCys** residues were acylated at the secondary amine position by 4-octylbenzoic acid (C8BA) using a microwave synthesizer (30W, 70°C) yielding C8BA-*N*MeCys (**Trt**)-C4 and C8BA-*N*MeCys (**Trt**)-PEG800. Finally, Trt deprotection using TFA/TIPS (95/5 v/v) afforded the desired ***N*MeCys** derivatives C8BA-*N*MeCys-C4 and C8BA-*N*MeCys-PEG800.

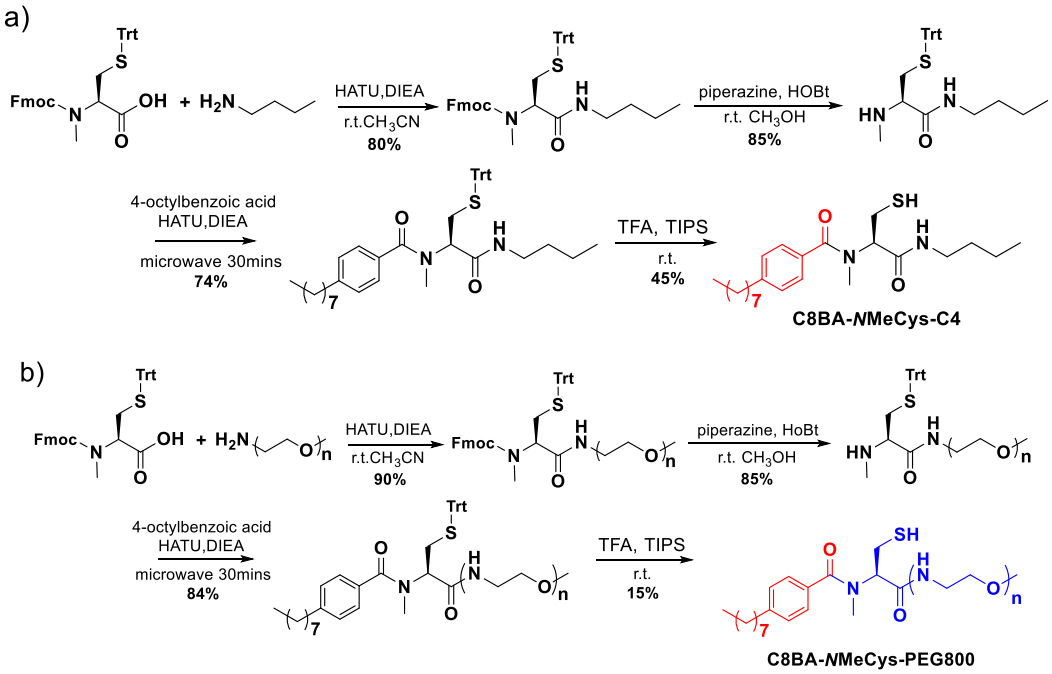

Scheme 3.2 | Synthetic routes for a) C8BA-*N*MeCys-C4 and b) C8BA-*N*MeCys-PEG800.

3.3 General experimental protocol

An ultra-performance liquid chromatography coupled with a diode array and a mass spectrometer detector (Waters Acquity® UPLC-MS) was utilized to monitor all exchange reactions between ***N*MeCys** derivatives. Unless otherwise stated, the general protocol used to promote such reaction consists in adding a reductant (tris(2-carboxyethyl) phosphine (TCEP)) in 15-fold molar excess relative to the starting materials in order to activate the thiol groups. When water-soluble solvents or milli-Q water were used as solvent for the reaction, TCEP was selected because of its considerable stability in aqueous solution for pH ranging from 1.5 up to 8.5. Standard calibration curves were established for each ***N*MeCys** derivatives under the conditions used for the exchange reactions. The kinetics of the exchange reactions were followed by UPLC-MS (UV and mass detection). By comparing the integrated area of UV peaks with the corresponding standard calibration curves, we can obtain the molar quantity of each ***N*MeCys** derivatives during the exchange reaction. Then, kinetic plots of exchange reactions were obtained by monitoring the concentration (mM) or ratio of each ***N*MeCys** derivatives present in the system *versus* reaction time (hour). According to these kinetic plots, we could know its dynamic character with information on the initial reaction rate (V_0), the equilibrium constant (K) and the half time of equilibration ($t_{1/2}$). Different exchange conditions can be compared using these graphs for a same library.

3.4 Results and discussions

3.4.1 Library involving *N*MeCys-PEG800 and F_5K_5-*N*MeCys

3.4.1.1 Stability of *N*MeCys-PEG800

Before turning to the study of libraries, we first evaluated the stability of *N*MeCys-PEG800 under the dcNCL exchange conditions. As *N*MeCys-PEG800 does not have UV-active unites, we relied on its mass signal to assess its stability. The table in Figure 3.4a) show the theoretical mass-to-charge ratio (m/z_b) for *N*MeCys-PEG800, and the theoretical m/z of its corresponding desulfurization products (m/z_c) depending on the numbers of ethylene oxide units of *N*MeCys-PEG800. On Figure 3.4b), mass chromatograms (left) and the corresponding mass spectra (right) of a stock solution of *N*MeCys-PEG800 at the concentration of 0.5 mM in a 1/1 (v/v) mixture of methanol and milli-Q water at pH 5 containing 150 mM TCEP and 300 mM sodium ascorbate for different stock time indicate that *N*MeCys-PEG800 is stable for the first 24 hours. However, after 72 hours, *N*MeCys-PEG800 undergoes total desulfurization.

a)

N^a	m/z_b	m/z_c
12	677.43	645.46
13	721.46	689.49
14	765.49	733.52
15	809.52	777.55
16	853.55	821.58
17	897.58	865.61
18	941.61	909.64
19	985.64	953.67
20	1029.67	997.70
21	1073.70	1041.73
22	1117.73	1085.76
23	1161.76	1129.79
24	1205.79	1173.82
25	1249.82	1217.85
26	1293.85	1261.88

b)

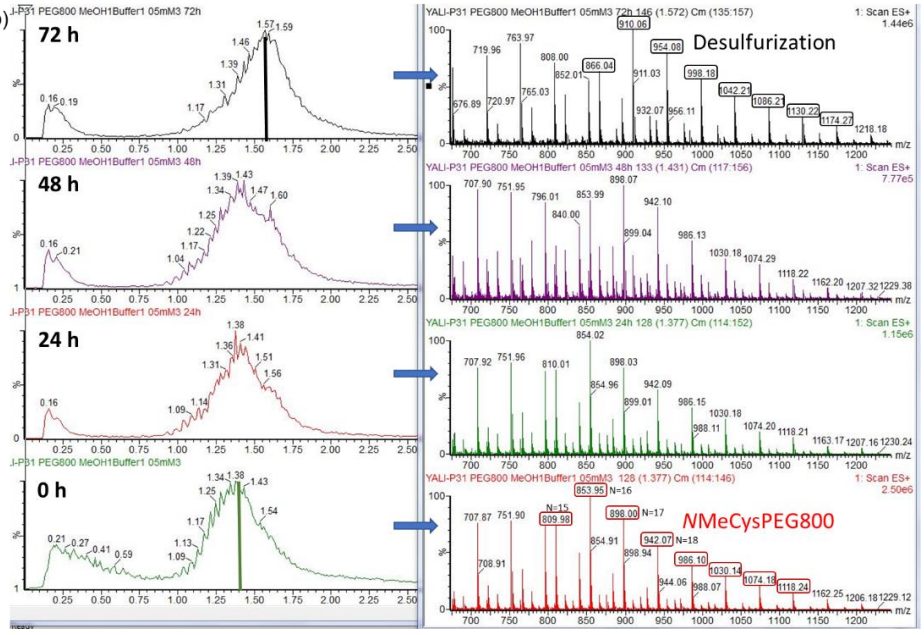

Figure 3.4 | a) Theoretical m/z_b for *N*MeCys-PEG800 and corresponding theoretical m/z_c for its desulfurization products as a function of ethylene oxide units (N^a). b) Mass chromatograms of a stock solution of *N*MeCys-PEG800 at a concentration of 0.5 mM for different stock time (from bottom to top, t = 0, 24, 48, and 72 h) and the corresponding mass spectra. The stock solution was kept in a 1/1 (v/v) mixture of methanol and milli-Q water at pH 5 containing 150 mM TCEP and 300 mM sodium ascorbate.

To overcome the desulfurization of *N*MeCys-PEG800, we tried to increase the concentration of the stock solution from 1 mM to 10 mM in order to preserve the activity of the thiol groups for up to 120 h (Figure 3.5a)). We also examined the stability of the stock solutions of *N*MeCys-PEG800 in different solvents (see Figure 3.5 b)), methanol, 1/1 (v/v) mixture of methanol and milli-Q water, and milli-Q water from bottom to top). According to the mass chromatograms, a stock solution of *N*MeCys-PEG800 at the concentration of 10 mM in either the mixture of solvent or in pure water is stable for up to 120 hours, while in pure methanol, desulfurization starts to occur.

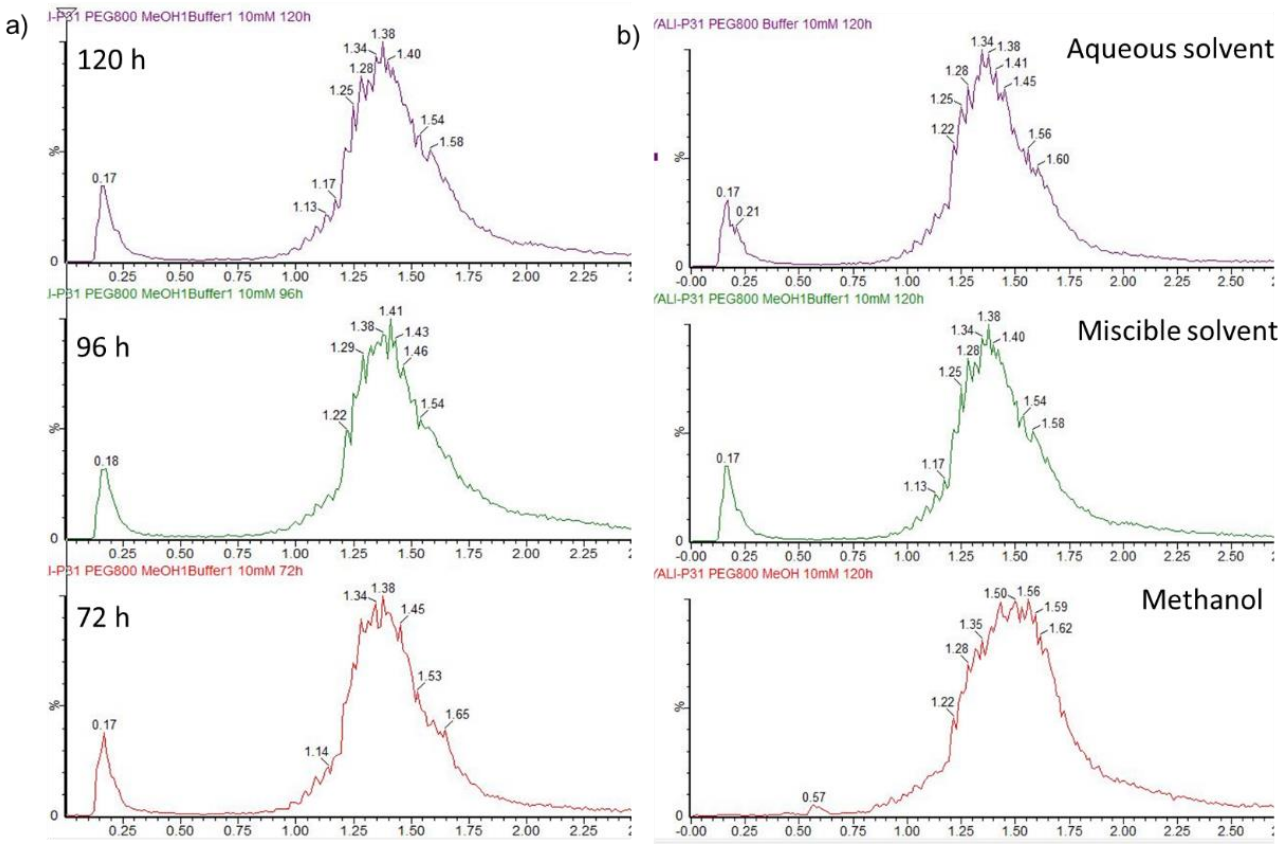

Figure 3.5 | a) MS chromatograms of a stock solution of *N*MeCys-PEG800 at the concentration of 10 mM in 1/1 (v/v) mixture of methanol and milli-Q water after 72 h, 96 h and 120 h, respectively (from bottom to top). b) MS chromatograms of the stock solution of *N*MeCys-PEG800 at the concentration of 10 mM in either methanol, or a 1/1 (v/v) mixture of methanol and milli-Q water or pure milli-Q water, respectively (from bottom to top).

3.4.1.2 Stability of F_5K_5-*N*MeCys

Similarly, to the previous section, experiments were first carried out to investigate the solubility of

F_5K_5-*N*MeCys in a 1/1 (v/v) mixture of methanol and milli-Q water. We found that the maximum concentration of F_5K_5-*N*MeCys as stock solution is 2.0 mM in this solvent mixture. In a comparable manner to experiments performed with *N*MeCys-PEG800, albeit using UV chromatograms thanks to the presence of phenylalanine units, we evaluated the stability of a stock solution of F_5K_5-*N*MeCys at 2.0 mM over 48 hours (Figure 3.6). We found that F_5K_5-*N*MeCys is stable for the first 24 hours while a new peak attributed to the hydrolytic product of F_5K_5-*N*MeCys, showed up after 48 hours. To get a better understanding of this hydrolytic process, we also evaluated the stability of F_5K_5-*N*MeCys in different solvents. Without any doubt, the hydrolysis of F_5K_5-*N*MeCys decreased together with the reduction of the water percentage in the stock solution. Based on all these results, we considered that the most suitable conditions for F_5K_5-*N*MeCys regarding its use in a DCL are a 1/1 (v/v) mixture of methanol and milli-Q water containing 150 mM TCEP, 300 mM sodium ascorbate as reaction media and 2 mM as stock concentration.

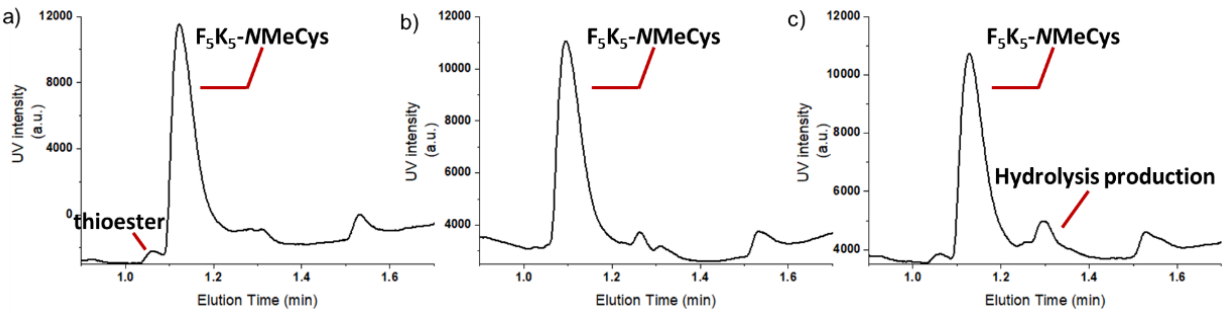

Figure 3.6 | UV Chromatograms of 2mM stock solutions of F_5K_5-*N*MeCys in a 1/1 (v/v) mixture of methanol and milli-Q water after a) 0 h, b) 24 h, and c) 48 h.

3.4.1.3 Study of the DCL between F_5K_5-*N*MeCys and *N*MeCys-PEG800

The DCL between equimolar quantities of F_5K_5-*N*MeCys (2.0 mM) and *N*MeCys-PEG800 (2.0 mM) (Scheme 3.3) was carried out in a 1/1 (v/v) mixture of methanol and milli-Q water containing 150 mM TCEP and 300 mM sodium ascorbate at different pHs (4, 5, and 6) and at room temperature (20 °C). Surprisingly, after 72 hours, no exchange products could be detected for all the pH considered. However, we found that hydrolysis of F_5K_5-*N*MeCys was enhanced by reducing the pH value of the solvent mixture.

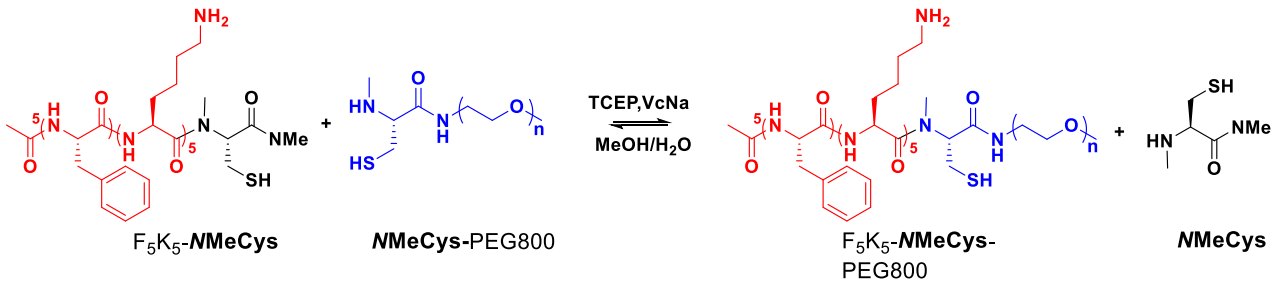

Scheme 3.3 | DCL based on hydrophobic F_5K_5-*N*MeCys and hydrophilic *N*MeCys-PEG800, and involving dcNCL as exchange reaction.

Efforts were then spent to determine suitable reaction conditions for the dynamic library. First, we modified the conditions to a pure MeOH solution containing 200 mM DTT and 2 mM acetic acid to enhance the solubility of F_5K_5-*N*MeCys. However, for 10.0 mM concentrations of the starting materials and even after 120 h, neither exchange products nor hydrolysis products were detected. Thus, we then considered to perform the dcNCL exchange in aqueous buffer containing 150 mM TCEP and 300 mM sodium ascorbate at pH= 4, 5, 6. Still, no exchange products after 96 hours were observed. In principle, the *N* to *S* acyl shift is promoted under strong acidic condition,[6–8] as the presence of an acid can improve the protonation of the free amino group, thus favoring the formation of hydroxythiazolidine intermediates and subsequently shifting the equilibrium towards the thioesters. Hence, we hypothesized that the N to S acyl shift, as well as the whole dcNCL process, could be accelerated in harsh acidic conditions. Therefore, the reaction conditions were modified to strong acidic solutions (1/1 (v/v) mixture of DMF and milli-Q water containing 150 mM TCEP, 300 mM sodium ascorbate and 4 M, 2 M, or 1 M HCl).[9] Surprisingly, for all these conditions, still no exchange products were observed after 96 hours.

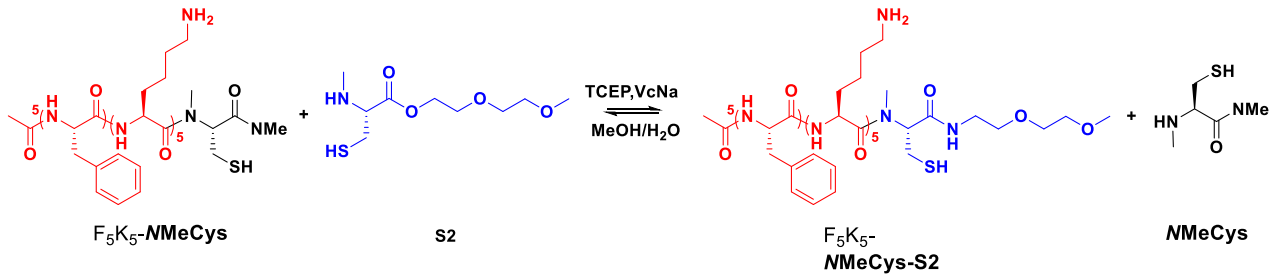

Scheme 3.4 | DCL starting from hydrophobic F_5K_5-*N*MeCys and hydrophilic S2.

In order to evaluate the ability of F_5K_5-*N*MeCys to be engaged in a dcNCL process, we replaced *N*MeCys-PEG800 by the simpler structure **S2** that was used in chapter 2. The exchange reaction

between F_5K_5-*N*MeCys (2.0 mM) and **S2** (2.0 mM) (Scheme 3.4) was carried out in a 1/1 (v/v) mixture of methanol and milli-Q water containing 150 mM TCEP and 300 mM sodium ascorbate at pH= 3, 5, or 7 and at room temperature (20 °C). After 96 hours of equilibration, the reactions at the three different pH values gave different results, as shown by UPLC analysis (Figure 3.7). At pH = 3, a new peak corresponding to the exchange product F_5K_5-*N*MeCys-S2 was observed while at pH = 5 and 7, only a small mass signal corresponding to F_5K_5-*N*MeCys-S2 was detected (no UV signal). The success of the simplified reaction at pH = 3 is in line with our hypothesis that strong acidic conditions can promote the dcNCL exchange reaction by activating the *N* to *S* acyl shift process.

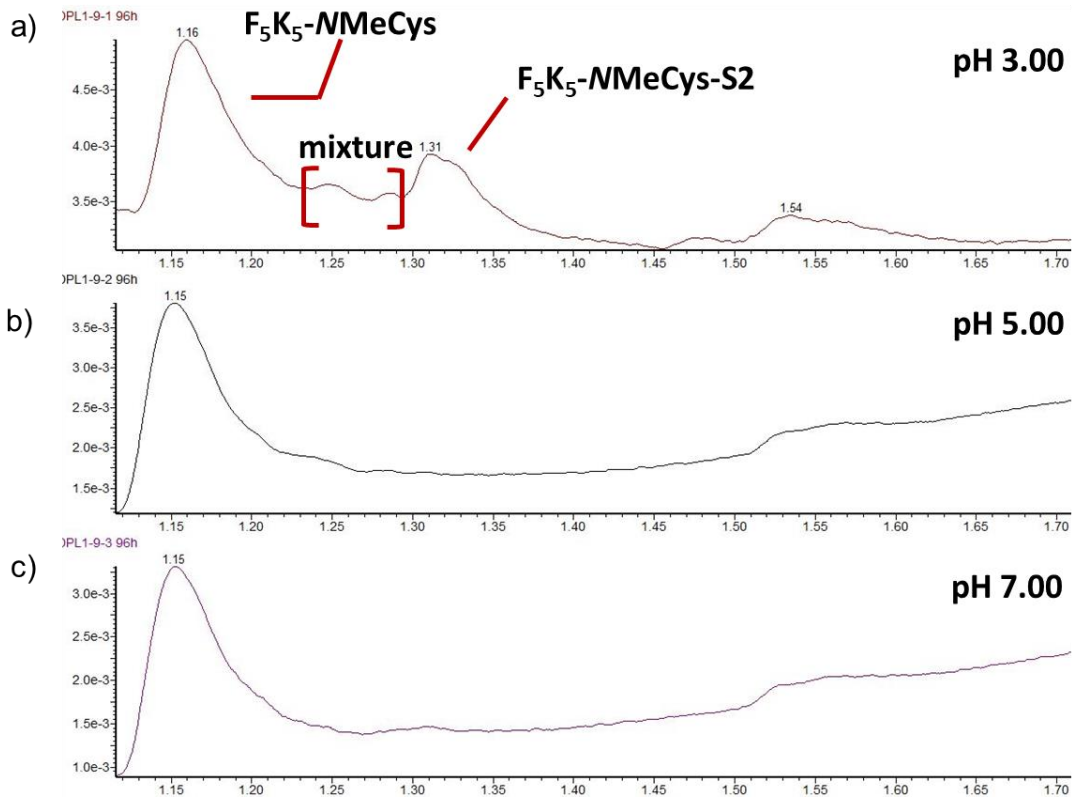

Figure 3.7 | UV chromatograms of the DCL between F_5K_5-*N*MeCys (2.0 mM) and S2 (2.0 mM) in a 1/1 (v/v) mixture of methanol and milli-Q water containing 150 mM TCEP and 300 mM sodium ascorbate at room temperature (20 °C) after 96 hours and for different pHs a) 3, b) 5, and c) 7.

We also studied the ability of *N*MeCys-PEG800 to be engaged in a dcNCL process (Scheme 3.5) by replacing F_5K_5-*N*MeCys with **S1** that was used in Chapter 2. The exchange reaction between **S1** (2.0 mM) and *N*MeCys-PEG800 (2.0 mM) was carried out in a 1/1 (v/v) mixture of methanol and milli-Q water containing 150 mM TCEP and 300 mM sodium ascorbate at pH = 3, 5 and 7 and at room temperature (20 °C).

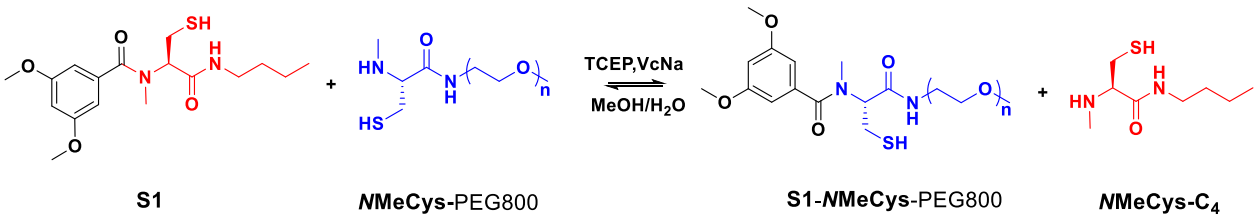

Scheme 3.5 | DCL starting from hydrophobic block S1 and hydrophilic *N*MeCys-PEG800.

After 48 hours of equilibration (the equilibration rate was faster than for the reaction between F_5K_5-*N*MeCys and **S2**), the three reactions at different pHs gave similar results (Figure 3.8). A new UPLC peak corresponding to the exchange product **S1**-*N*MeCys-PEG800 was observed and accompanied at pH = 3 by the presence of the thioester of **S1**. Compared with the dcNCL reactions performed between F_5K_5-*N*MeCys and **S2**, we found that shorter equilibration time are needed to produce the exchange product **S1**-*N*MeCys-PEG800 starting from **S1** and *N*MeCys-PEG800. This study suggests that *N* to *S* acyl migration reaction is difficult to promote when considering long peptide sequences.

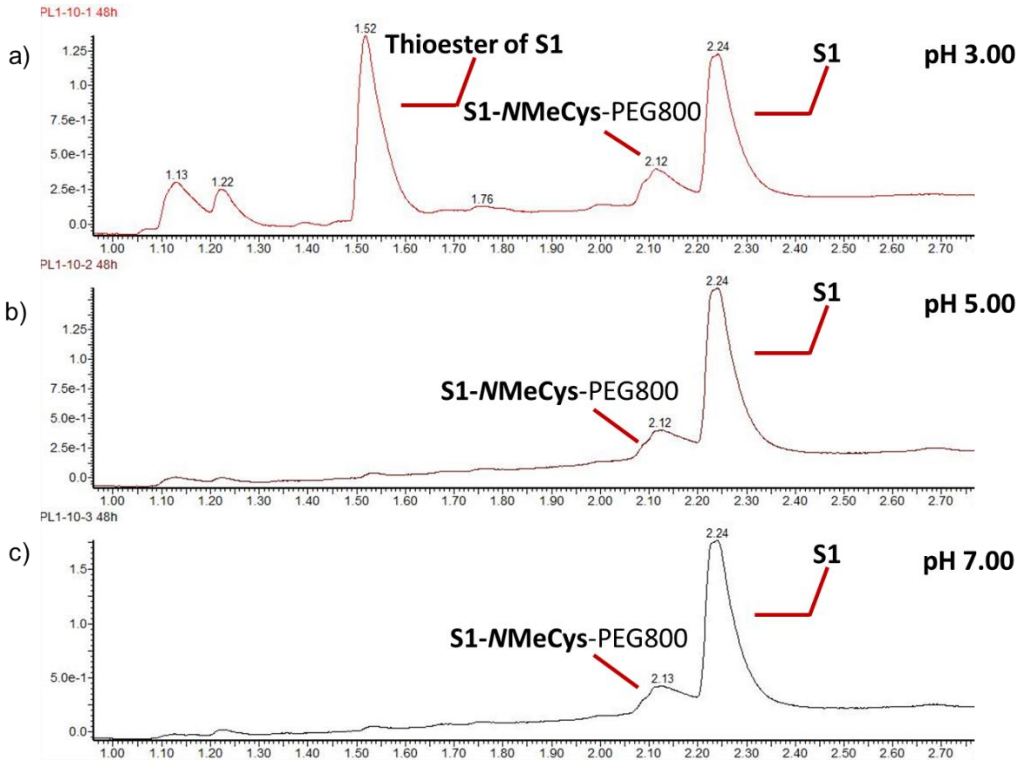

Figure 3.8 | UV chromatograms of the DCL between S1 (2.0 mM) and *N*MeCys-PEG800 (2.0 mM) in a 1/1 (v/v) mixture of methanol and milli-Q water containing 150 mM TCEP and 300 mM sodium ascorbate at room temperature (20 °C) after 48 hours and for different pHs a) 3, b) 5, and c) 7.

3.4.2 Library involving C8BA-NMeCys-C4 and NMeCys-PEG800

3.4.2.1 Study of the dcNCL between C8BA-*N*MeCys and *N*MeCys-PEG800

Considering problems faced using relatively long hydrophobic peptides, we decided to focus on a smaller hydrophobic block C8BA-*N*MeCys-C4 incorporating an internal *N*MeCys residue. Low concentration experiments of the DCL involving C8BA-*N*MeCys-C4 (1.0 mM) and *N*MeCys-PEG800 (1.0 mM) (Figure 3.9a)) were carried out in a 1/1 (v/v) mixture of methanol and milli-Q water containing 15 mM TCEP and 30 mM sodium ascorbate at pH = 6. As monitored by UPLC, after 120 hours, the library reached its thermodynamic equilibrium (Figure 3.9b)) without any trace of hydrolytic product while the oxidation product of C8BA-*N*MeCys-C4 could be detected.

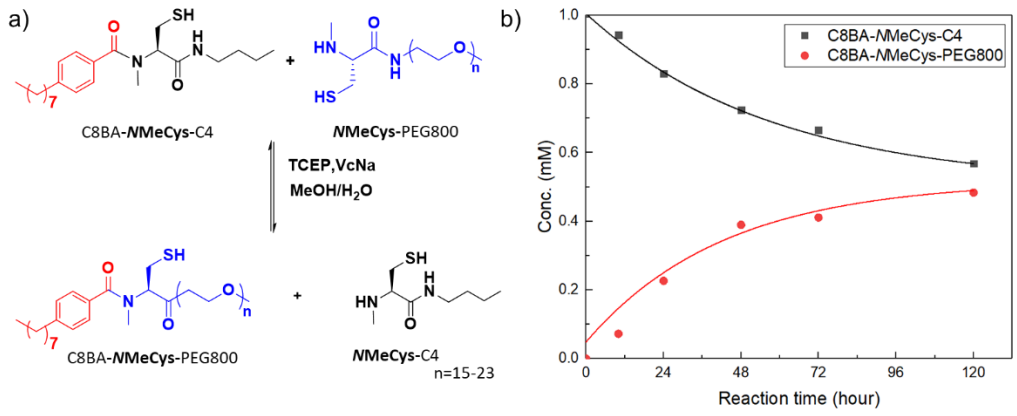

Figure 3.9 | a) DCL starting from C8BA-*N*MeCys and *N*MeCys-PEG800. b) Evolution of the concentrations of C8BA-*N*MeCys (1 mM) and C8BA-*N*MeCys-PEG800 (1 mM) as a function of reaction time in in a 1/1 (v/v) mixture of methanol and milli-Q water containing 15 mM TCEP and 30 mM sodium ascorbate at pH = 6. The trend lines are used simply to guide the reader's eye.

We then evaluated how the concentration of the library and the water percentage of the reaction mixture can affect the thermodynamic equilibrium. Exchange reactions between C8BA-*N*MeCys (5.0 mM) and *N*MeCys-PEG800 (5.0 mM) were carried out respectively in a mixture of methanol with either 40% (Figure 3.10a)) or 50% (Figure 3.10b)) milli-Q water at pH = 6 (each solution contained 15 mM TCEP and 30 mM sodium ascorbate). For the reaction performed in 40% water and 60% methanol, the library reached a thermodynamic equilibrium similar to the one recorded for initial concentrations of 1.0 mM in a 1/1 (v/v) mixture of methanol and milli-Q water. However, when the

concentration of starting materials was increased from 1 mM to 5 mM for a 1/1 (v/v) mixture of methanol and milli-Q water, the exchange product C8BA-*N*MeCys-PEG800 was largely amplified after 168 hours (Figure 3.10b)), suggesting the possible formation of supramolecular self-assemblies as also suggested when monitoring the stability of the exchange product by UPLC (see Annexes) and already observed for Dynablocks.[3] This study demonstrate how thermodynamic equilibrium can be affected by the solvent composition.

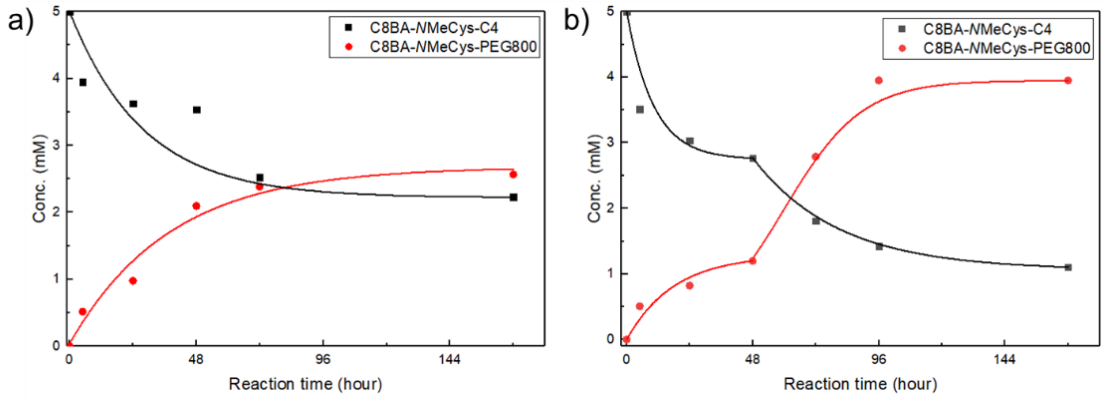

Figure 3.10 | Kinetic curves for C8BA-*N*MeCys and C8BA-*N*MeCys-PEG800 (initial concentration 5 mM each) as a function of reaction time in a mixture of methanol with either a) 40% or b) 50% water at pH = 6 (each solution contained also 15 mM TCEP and 30 mM sodium ascorbate). The trend lines are used simply to guide the reader's eye.

Finally, exchange reactions were also carried out at 10.0 mM of starting materials in a mixture of methanol with either 40% or 50% water at pH= 6 (each solution contained 150 mM TCEP, and 300 mM sodium ascorbate). After 72 hours, the library containing 40% water reached its thermodynamic equilibrium with an equilibrium constant *K* of 1.02 (Figure 3.11a)). However, at 50% water, a sigmoidal decrease of concentration of C8BA-*N*MeCys-C4 and a relevant sigmoidal growth of exchange product C8BA-*N*MeCys-PEG800 were observed, as shown in Figure 3.11b). Such sigmoid concentration-time profile suggests an evolution from random amphiphilic molecules to thermodynamically stable self-assemblies.

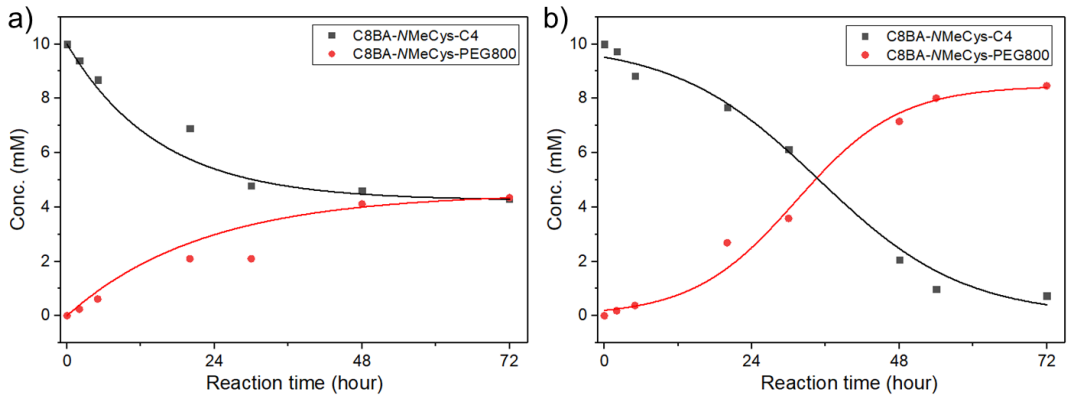

Figure 3.11 | Kinetic curves for C8BA-*N*MeCys and C8BA-*N*MeCys-PEG800 (initial concentration 10 mM each) as a function of reaction time in a mixture of methanol with either a) 40% or b) 50% water at pH= 6 (each solution contained also 150 mM TCEP and 300 mM sodium ascorbate). The trend lines are used simply to guide the reader's eye.

3.4.2.2 Study of C8BA-*N*MeCys-PEG800 by dynamic light scattering (DLS)

In order to understand the behavior of our library, we examined if C8BA-*N*MeCys-PEG800 is prompted to form supramolecular self-assemblies in the exchange reaction medium. Dynamic light scattering (DLS) is a versatile technique that can be used to determine the size distribution profile of small particles in suspensions or polymers in solutions.[10] Thus, we first studied solutions of C8BA-*N*MeCys-PEG800 at various concentrations (under 10 mM) in a mixture of methanol and water at different water percentage (0, 25%, 50%, 75%, and 100%) by DLS (Figure 3.12). When the percentage of water is comprised between 0 and 25%, no relevant DLS signal was observed for the stock solutions of C8BA-*N*MeCys-PEG800 at all the selected concentrations. When the water percentage was increased to values between 50% and 100%, a strong signal corresponding to nanometric sizes was recorded for stock solutions of C8BA-*N*MeCys-PEG800. In a 1/1 (v/v) mixture of methanol and milli-Q water, for concentration above 3 mM, stock solutions of C8BA-*N*MeCys-PEG800 yielded particles with sizes ranging from 73 to 100 nm. In a mixture with 75% water, the stock solution of C8BA-*N*MeCys-PEG800 yielded particles with an average size of ~75 nm for concentration above 0.8 mM. At 100% water, the stock solution of C8BA-NMeCys-PEG800 showed 2 DLS peaks at 10 nm and ~140 nm for concentrations above 0.5 mM, suggesting the presence of small and large aggregates. This study clearly demonstrates that increasing the water percentage decreases the minimum concentration at which supramolecular assemblies of C8BA-*N*MeCys-PEG800 are formed. This result implies that the presence of water in the system induces the formation of supramolecular structures through the self-assembly of C8BA-*N*MeCys-PEG800, which could

thus explain the shift of equilibrium observed for the afore-studied library.

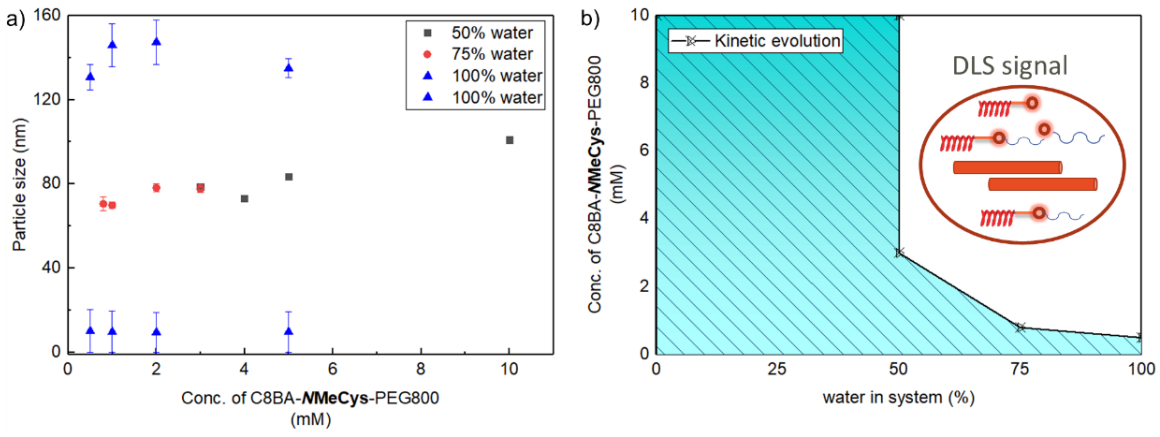

Figure 3.12 | a) Evolution of the particle size recorded for C8BA-*N*MeCys-PEG800 in methanol/water mixtures for different water contents as a function of concentration, as recorded by DLS. b) Phase diagram for C8BA-*N*MeCys-PEG800 for various water percentage and concentration in water/methanol mixtures.

Based on these DLS experiments, we built a simplified phase diagram (Figure 3.12b)) which highlights the minimal concentration of C8BA-*N*MeCys-PEG800 and water content that are necessary to produce supramolecular self-assemblies. It shows that, by changing the water percentage from low to high content, we can induce the formation of supramolecular self-assemblies made of C8BA-*N*MeCys-PEG800. This phase diagram also explains the different thermodynamic equilibria we observed previously for the DCLs made of C8BA-*N*MeCys-C4 and *N*MeCys-PEG800.

3.4.2.3 Morphological study of C8BA-*N*MeCys-PEG800 by small-angle X-ray scattering (SAXS)

In order to precisely determine the structure of our supramolecular assemblies, we studied 1 mM and 10 mM solutions of C8BA-*N*MeCys-PEG800 in a mixture of 95% milli-Q water and 5% methanol at pH = 6 with 150 mM TCEP and 300 mM sodium ascorbate by small-angle X-ray scattering (SAXS) experiments. SAXS is a powerful technique to extract reliable size and shape parameters from solvated objects in the nanometer-size range.[11] The data (q represents the scattering vector, I(q) represents the scattered intensity) displayed in Figure 3.13 show slightly different organizations for C8BA-*N*MeCys-PEG800 at low and high concentration. At 10 mM, the scattering intensity of C8BA-*N*MeCys-PEG800 displays a q^{-2} dependence at low q, which is characteristic of Gaussian chains. In

the intermediate q regime ($0.03 < q < 0.09$), a q^{-1} behavior is observed, suggesting the presence of rod-like objects. Finally, for larger q values ($q > 0.1$), we can observe a Guinier regime, which corresponds to the cross-section of the assemblies followed by a last q^{-1} regime, which is characteristic of rod-like particles. The overall SAXS pattern recorded at a concentration of 10 mM suggests the presence of quite rigid worm-like micelles with a rod-like behavior inside the micelles (q^{-1} regime at high q values).[12,13] A more quantitative analysis of the data should provide us with structural parameters such as persistence length or radius of the cross-section. Complementary small angle neutron scattering experiments and/or static light scattering experiments could provide us with additional structural parameters such as weight-average molecular weight, radius of gyration or even linear mass density.

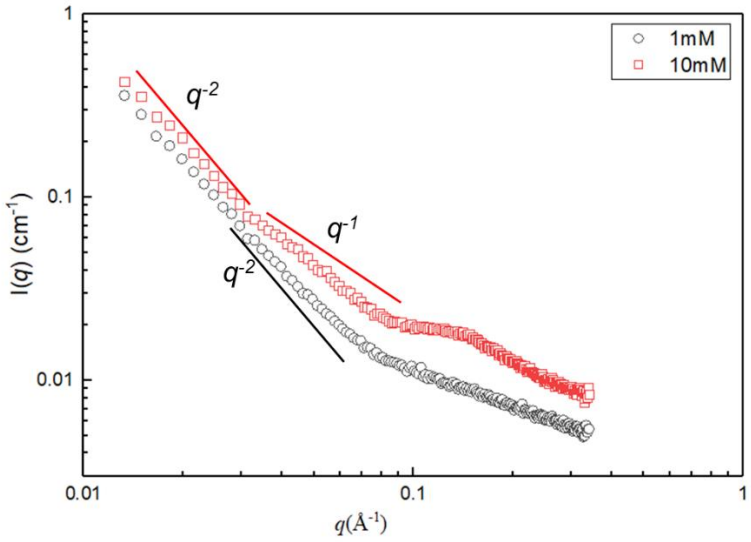

Figure 3.13 | SAXS patterns for 1 mM and 10 mM solutions of C8BA-*N*MeCys-PEG800 in a mixture of 95% milli-Q water and 5% methanol containing 150 mM TCEP and 300 mM sodium ascorbate at pH = 6.

3.4.2.4 Morphological study by transmission electron microscopy (TEM)

We then used transmission electron microscopy (TEM) in order to confirm the morphology of our amphiphilic C8BA-*N*MeCys-PEG800. Considering that the samples are dissolved in a mixture of water and methanol with a high-water percentage, the copper grid was pretreated by glow discharge in order to reach a hydrophilic surface. Furthermore, as our samples consists in a solution mostly made of water, a drop was deposited on top of the copper grid placed over a filtration paper in order to adsorb the excess of solution. This method of sample preparation avoids long waiting time and reduces variation of the morphology potentially occurring during evaporation of the solvent.

On the one hand, for the amphiphilic C8BA-*N*MeCys-PEG800 at low concentration (1 mM) in a mixture of 95% milli-Q water and 5% methanol, TEM images (Figure 3.14) showed quite mono disperse small cylinders with a size length (*L*) of 20-40 nm and a diameter (*D*) of 6-8 nm.

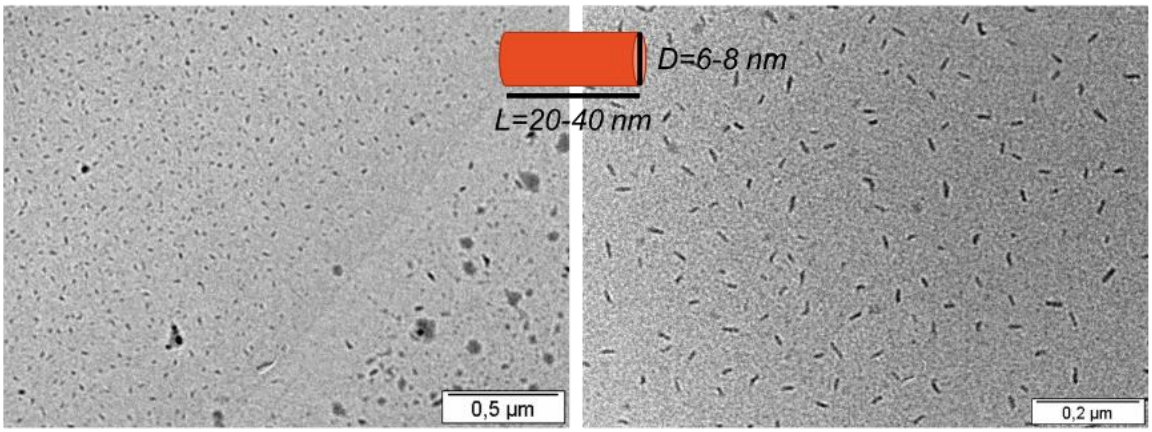

Figure 3.14 | TEM images of the amphiphilic C8BA-*N*MeCys-PEG800 at low concentration (1 mM) in a mixture of 95% milli-Q water and 5% methanol.

On the other hand, for the amphiphilic C8BA-*N*MeCys-PEG800 at high concentration (10 mM), TEM images (Figure 3.15) showed quite rigid cylindrical structures with a diameter (*D*) of 16-20 nm and micrometric length. According to molecular modeling data obtained by Avogadro software, the length of a single chain of C8BA-*N*MeCys-PEG800 ranges from 64.0 Å to 70.4 Å. Thus, we can assume that these rod-like structures are micelles formed by two molecules of C8BA-*N*MeCys-PEG800 through head-to-head arrangement with hydrophobic residues inside the structure and PEG chains outside. The short cylindrical structures observed at low concentration could correspond to premature supramolecular assemblies of C8BA-*N*MeCys-PEG800.

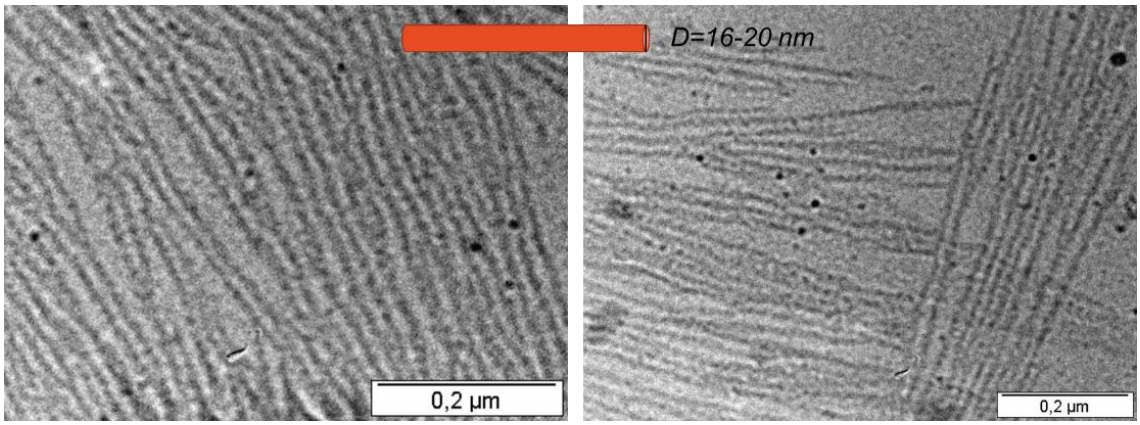

Figure 3.15 | TEM images of the amphiphilic chains C8BA-*N*MeCys-PEG800 at higher concentration (10 mM) in a mixture of 95% milli-Q water and 5% methanol.

We also analyzed the reaction solution of the DCL made of C8BA-*N*MeCys and *N*MeCys-PEG800 in a mixture of 95% milli-Q water and 5% methanol by TEM to confirm the formation of supramolecular assembly. As shown on Figure 3.16, TEM imaging showed cylindrical structures similar to the one observed for C8BA-*N*MeCys-PEG800 alone, providing an important evidence for the self-assembly driven constitutional amplification process in our dcNCL libraries.

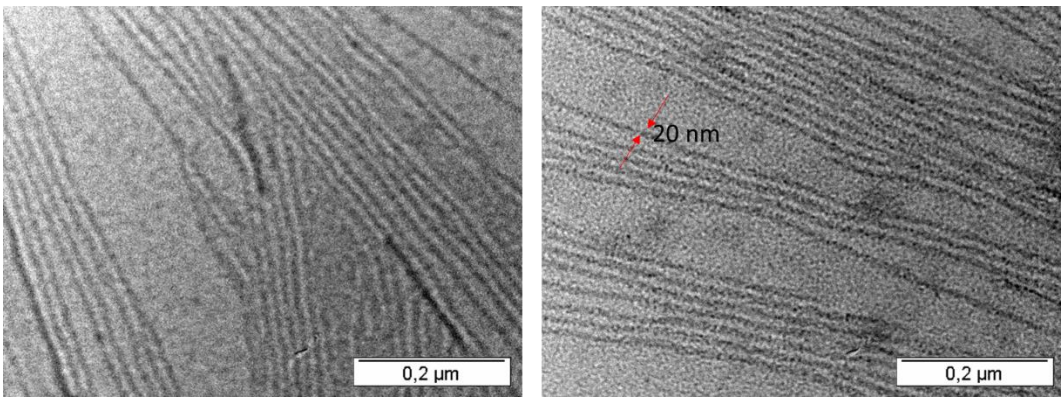

Figure 3.16 | TEM images of the structures formed in the solution containing the DCL made of C8BA-*N*MeCys and *N*MeCys-PEG800 (initially 10 mM each) in a mixture of 95% milli-Q water and 5% methanol.

3.5 Conclusions

We have studied DCLs made of *N*MeCys derivatives incorporating different hydrophilic, and hydrophobic chains at the *N*- or *C*-terminal of *N*MeCys. On one hand, the library made of F_5K_5-*N*MeCys and *N*MeCys-PEG800 did not produce any exchange product. However, two simplified DCLs involving independently *N*MeCys-PEG800 or F_5K_5-*N*MeCys led to exchange products at pH 3 and for pHs ranging from 3 to 7, respectively. This work highlighted the difficulty to perform the *N* to *S* acyl shift using relatively long peptides. On the other hand, we succeeded to establish a dcNCL library made of hydrophobic C8BA-*N*MeCys-C4 and hydrophilic *N*MeCys-PEG800 leading to amphiphilic C8BA-*N*MeCys-PEG800. Adaptivity of the dynamic constitutional library to solvent and concentration was observed during the kinetic studies (Figure 3.17). Thanks to the combination of a series of DLS, SAXS and TEM experiments, we showed that the amphiphilic species leads to the formation of supramolecular worm-like micelles. The formation of such self-assemblies under dcNCL conditions shifts the equilibrium of the DCL, demonstrating a transfer of information from

the molecular scale (exchange reaction) to the microscopic level (formation of worm-like micelles). Overall, this work extends the fundamental aspect of our dcNCL methodology into more practical aspects related to material science.

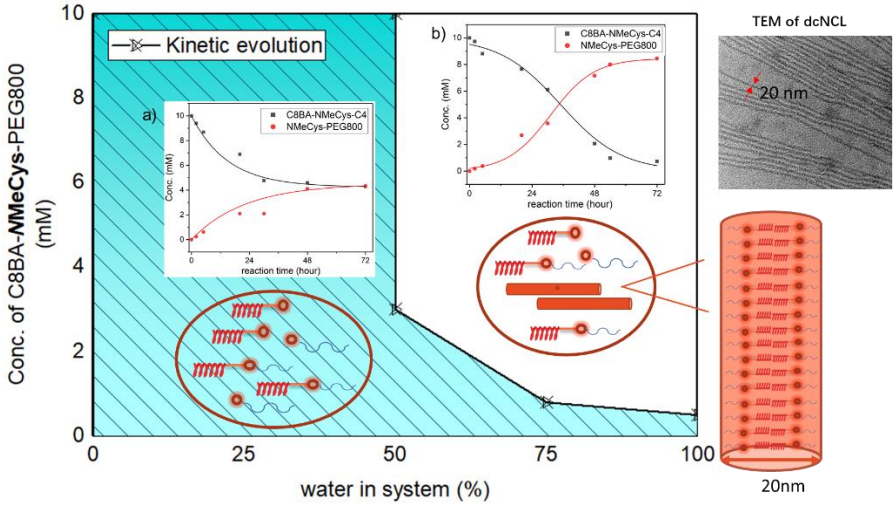

Figure 3.17 | Schematic representation of how concentration and solvent affect the DCL made of C8BA-*N*MeCys-C4 and *N*MeCys-PEG800 and leading to the formation of C8BA-*N*MeCys-PEG800.

3.6 References

1. Xu, S. & Giuseppone, N. Self-duplicating amplification in a dynamic combinatorial library. *J. Am. Chem. Soc.* **130**, 1826–1827 (2008).

2. Nguyen, R., Jouault, N., Zanirati, S., Rawiso, M., Allouche, L., Buhler, E., & Giuseppone, N. Autopoietic behavior of dynamic covalent amphiphiles. *Chem. Eur. J.* **24**, 17125–17137 (2018).

3. Nguyen, R., Allouche, L., Buhler, E. & Giuseppone, N. Dynamic combinatorial evolution within self-replicating supramolecular assemblies. *Angew. Chem. Int. Ed.* **121**, 1113–1116 (2009).

4. Dunetz, J. R., Magano, J. & Weisenburger, G. A. large-scale applications of amide coupling reagents for the synthesis of pharmaceuticals. *Org. Process Res. Dev.* **20**, 140–177 (2016).

5. Palomo, J. M. Solid-phase peptide synthesis: an overview focused on the preparation of biologically relevant peptides. *RSC Adv.* **4**, 32658–32672 (2014).

6. Shao, Y. & Kent, S. B. H. Protein splicing: occurrence, mechanisms and related phenomena. *ChemBioChem* **4**, 187–194 (1997).

7. Bandyopadhyay, A., Cambray, S. & Gao, J. Fast and selective labeling of N-terminal cysteines at neutral pH via thiazolidino boronate formation. *Chem. Sci.* **7**, 4589–4593 (2016).

8. Nakamura, K. I., Kanao, T., Uesugi, T., Hara, T., Sato, T., Kawakami, T., & Aimoto, S. Synthesis of peptide thioesters via an *N* - *S* acyl shift reaction under mild acidic conditions on an *n* -4,5-dimethoxy-2-mercaptobenzyl auxiliary group. *J. Pept. Sci.* **15**, 731–737 (2009).

9. Tsuda, S., Shigenaga, A., Bando, K. & Otaka, A. *N* → *S* acyl-transfer-mediated synthesis of peptide thioesters using anilide derivatives. *Org. Lett.* **11**, 823–826 (2009).

10. Aragón, S. R. Theory of dynamic light scattering from polydisperse systems. *J. Chem.Pys.* **64**, 2395 (1976).

11. Chu, B. & Hsiao, B. S. Small-angle x-ray scattering of polymers. *Chem. Rev.* **101**, 1727–1762 (2001).

12. Dreiss, C. A. Wormlike micelles: where do we stand? Recent developments, linear rheology and scattering techniques. *Soft Matter* **3**, 956 (2007).

13. Nguyen, R., Buhler, E. & Giuseppone, N. Dynablocks: Structural modulation of responsive combinatorial self-assemblies at mesoscale. *Macromolecules* **42**, 5913–5915 (2009).

General conclusions and perspectives

In recent decades, DCvC has evolved from a tool of structural identification to an advanced methodology in order to generate chemical diversity, select building blocks, with particular relevance to the questions related to the "origin of life". The need for new dynamic covalent bonds/reactions, being as the key elements of DCvC, is essential to expand the range of applications accessible to DCvC. Following the work initiated by our group in 2014, my PhD work describes an optimization of the dynamic covalent native chemical ligation (dcNCL) and its application for the transfer of information over several length scales.

The first chapter presents a general introduction on DCvC, the importance of dynamic covalent bonds/reactions, and their corresponding applications in DCLs applied to various fields of research including peptide- and protein-relevant areas. This background has served as a basis to comprehensively understand my PhD objective, design proper experiments and raise adequate conclusions.

In the second chapter, we synthesized three fully protected *N*MeCys derivatives in gram scale, which are the basic materials for building our dynamic covalent libraries. After careful and detailled exploration of our dcNCL between *N*MeCys derivatives with small molecules or peptide segments, a suitable and convenient protocol was developed. We found that the exchange reaction can efficiently equilibrate to the thermodynamic equilibrium in various conditions (different solvents, buffers, pH values and temperatures) without inert gas protection or addition of catalysts. The DTT used in the previously reported methodology to prevent oxidation of the thiol groups can be substituted by an aqueous buffer containing TCEP as oxidant and sodium ascorbate. This allowed us to select the reducing agent according to the solvent conditions required for the exchange reaction. In a proper reaction environment (solvent, pH value and concentration) hydrolysis can be totally suppressed. We also found that the solvent of the reaction is an important effector which influences the dynamic of the metathesis reaction, mainly its equilibration rate. The effect of the pH value of the TCEP solution regarding the exchange reaction indicates its adaptivity under the pressure of external stimulus. These results altogether provide great evidences to further develop the dcNCL methodology for constructing diverse dynamic constitutional systems. Furthermore, the ability of this reaction to proceed efficiently in aerobic conditions increases its intrinsic relevance for applications requiring biological environments.

In third chapter, we designed and investigated a series of *N*MeCys derivatives incorporating either hydrophilic or hydrophobic chains. By introducing different side chains into the *N*- or *C*-terminal of *N*MeCys, we established a DCL made of hydrophobic C8BA-*N*MeCys, hydrophilic *N*MeCys-PEG800 and amphiphilic C8BA-*N*MeCys-PEG800, thus expanding the diversity of building blocks which can be involved in the dcNCL as exchange reaction. Adaptivity of the dynamic constitutional library was observed during the kinetic studies and was found to be influenced by solvent and concentration, leading to transfer of information from the molecular scale up to the microscopic level. Formation of supramolecular self-assemblies were confirmed by DLS, SAXS and TEM analyses, providing evidences that the constitutional selection within this dcNCL library is driven by hierarchical self-assembly processes.

Overall, the work presented in this manuscript demonstrates a better understanding of the dcNCL in different environmental conditions, and highlights its potential for further applications in various fields of polymer science.

Experimental section

E1 General procedures

E1.1 Solvents and chemical reagents

Commercial reagents were used without further purification. Paraformaldehyde, triethylsilane, triisopropylsilane, (1*R*)-(-)-10-camphorsulfonic acid, sodium hydride, iodomethane, triphenylmethanol, and triethylamine were purchased from Sigma Aldrich. Trifluoroacetic acid was purchased from Fisher Scientific. Trityl chloride was purchased from Alfa Aesar. 1,1,1,3,3,3-Hexafluoro-2-propanol and 9-fluorenylmethyl N-hydroxysuccinimide ester were purchased from Fluorochem. Boc-protected and Fmoc-protected amino acids for SPPS, the polyethylene glycol with an average MW of 800 Dalton (NH_2-PEG800-OMe) were purchased from Iris Biotech. Milli-Q water was deionized by using a milli gradient system (Millipore, Molsheim, France).

All glassware was oven or flame-dried, and reactions were performed under Argon unless stated otherwise. DCM (CH_2Cl_2), chloroform and toluene were used as such. Tetrahydrofuran and N, N-dimethylformamide (DMF) were dried using a double column SolvTech purification system. Column chromatography was performed using 40-63 μm particle size silica, 230-400 mesh (Sigma Aldrich, Steinheim, Switzerland). Thin-layer chromatography (TLC) was performed on plates of 200 μm silica 60 Å-F254. The term "concentrated under reduced pressure" refers to the removal of solvents and other volatile materials using a rotary evaporator at low pressure (50-100 mbar) while maintaining the water-bath temperature at 30°C. Residual solvent was removed from samples at high vacuum. The term "high vacuum" refers to vacuum achieved by a mechanical belt-drive oil pump.

E1.2 Analytical methods and instrumentation

E 1.2.1 Nuclear Magnetic Resonance

^{1}H NMR spectra were recorded on a Bruker Avance 400 spectrometer at 400 MHz and ^{13}C spectra at 100 MHz. The spectra were internally referenced to the residual proton solvent signal ($CDCl_3$: 7.26 ppm, CD_3CN: 1.94 ppm, CD_3OD: 3.31 ppm for ^{1}H spectrum, and $CDCl_3$: 77.16 ppm and CD_3OD: 49.15 ppm for ^{13}C spectrum). For ^{1}H NMR assignments, the chemical shifts are given in ppm. Coupling constants *J* are given in Hz. Peaks are described as singlet (s), doublet (d), triplet (t), quartet

(q), multiplet (m), broad (br), broad singlet (brs) and broad multiplet (brm).

E 1.2.2 Ultra-performance liquid chromatography (UPLC®)

Ultra-Performance Liquid Chromatography (UPLC®) coupled to Mass Spectroscopy (UPLC-MS) was carried out on a Waters Acquity UPLC-SQD apparatus equipped with a PDA detector (190-500 nm, 80Hz) and a SQD spectrometer, using a reverse phase column (Waters, BEH C_{18} 1.7 µm, 2.1 × 50 mm or CSH Fluoro Phenyl Column, 130Å, 1.7 µm, 2.1 mm × 100 mm), the MassLynx 4.1 XP software.

E 1.2.3 High-performance liquid chromatography (HPLC)

Analytical and Preparative high-performance liquid chromatography (HPLC) were performed using a Waters AutoPurification® system, coupled to a Waters 2489 UV/Visible detector and Waters SQD 3100 electrospray mass detector. Details regarding the gradient and columns are given in section E 2.3.4.

E 1.2.4 Dynamic Light Scattering (DLS)

Dynamic light scattering was recorded on a Zetasizer Nano from Malvern Instruments Ltd. (UK).

E 1.2.5 Small angle X-ray scattering (SAXS)

Small angle X-ray scattering experiments were performed at the Institut Charles Sadron by using a diffractometer developed by Molecular Metrology (Elexience in France), which operates with a pinhole collimation of the X-ray beam and a two-dimensional gas-filled multiwire detector. The monochromatic (λ= 1.54 Å with Dl/l < 4%) and focused X-ray beam is obtained through a multilayer optic designed and fabricated by Osmic. The size of the incident beam on the sample was close to 600 µm. The sample to detector distance was set at 0.70 m for the Elexience, allowing to explore scattering vectors ranging from q = 0.01 $Å^{-1}$ to 0.35 $Å^{-1}$, with $q = 4\pi\sin(\theta/2)/\lambda$, where λ and θ are the wavelength of the incident beam and the scattering angle, respectively. The *q*-resolution related to the beam size on the sample and the beam divergence was close to 0.005 $Å^{-1}$. Cells of 1 mm thickness and calibrated Mica windows were used as sample holders. Measurements were performed at room temperature. All data were treated according to standard procedures for isotropic small angle X-ray scattering. After radial averaging, the spectra were corrected from electronic noise of the detector,

empty cell, absorption and sample thickness. A 55Ir source was used for the corrections of geometrical factors and detector cells efficiency as well as a Silver Behenate sample, for the *q*-calibration. After all these data treatments, the scattered intensities were corrected from the scattering of the solvent. According to such a procedure, the scattered intensity I(*q*) containing all the structural information is obtained for each solution.

E 1.2.6 Transmission Electron Microscopy (TEM)

TEM experiments were performed using a CM12 Philips microscope equipped with a MVIII (SoftImaging System) CCD camera. Samples were analyzed in Bright Field Mode with a LaB_6 cathode and 120 kV tension. Image treatments were performed by using analySIS (Soft Imaging System) software. For the sample preparation, a glow discharge was used to pre-prepare the surface of the copper grid. Then, a 5 µL drop was casted on the grid and a filter paper was used to absorb the excess solution before analysis.

E1.3 Exchange reaction procedure used in chapter 2 and 3

Libraries were prepared in Eppendorf tubes and placed on the fume hood or heating plate at the desired temperature. Libraries were prepared by mixing adequate volumes of each stock solution. The library volume was adjusted to 500 µL with the solvent containing reducing reagents to obtain a final solution with a required concentration. Libraries that required higher temperatures were incubated on a heating plate.

Sampling: Samples were collected at several timepoints (0, 12, 24, 48, 72, 96, 120 and 144 h). For each 50 µL UPLC injection, a reaction mixture aliquot (10 µL) was quenched with pure methanol (40 µL). After diluting preparation, each sample contained 10% components of the original concentration and was injected to UPLC.

Analytic experiments of all the DCLs performed by UPLC with the using of 0.1% formic acid in water (solvent A) and 0.1% formic acid in acetonitrile (solvent B) respectively as the two mobile phases.

A typical gradient is given here:

Time (min)	Flow (mL/min)	% A	% B
0	1	95	5
3.5	1	5	95
4	1	5	95
4.1	1	95	5
5.1	1	95	5

E2 Syntheses of the compounds

E2.1 *N*-(methyl)-cysteine protected by different protection group

E 2.1.1 Synthesis of **Fmoc**-*N*MeCys(**StBu**)-OH

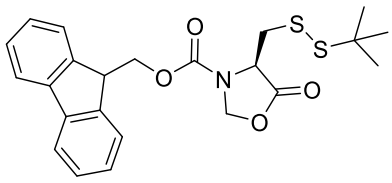

Fmoc-Cys(**StBu**)-OH (10.0 g, 23.1 mmol), paraformaldehyde (3.59 g, 120 mmol) and (1R)-(-)-10-camphorsulfonic acid (0.37 g, 15 mmol) were added to a dry 250 mL round-bottom flask and dissolved with toluene (150 mL). The reaction was heated to reflux (120 ℃) and stirred overnight. Water was removed by Dean-Stark apparatus during the reaction time. The reaction was complete as monitored by TLC (cyclohexane: ethyl acetate v/v 4:1, R_f =0.5). After cooling down to room temperature, the reaction was concentrated under reduced pressure to provide a clear oil. Flash chromatography (SiO_2, cyclohexane: ethyl acetate v/v 10:1; 8:1) was used to isolate oxazolidinone as a white solid (10 g, 96%).

^{1}H NMR (400 MHz, $CDCl_3$, 298K) δ 7.78 (d, J = 7.5 Hz, 2H), 7.56 (d, J = 8.2 Hz, 2H), 7.42 (t, J = 7.3 Hz, 2H), 7.37-7.30 (m, 2H), 5.62-5.16 (m, 2H), 4.64-4.27 (m, 2.5H), 4.27 (s, 1H), 4.02 (s, 0.5H), 3.55 (s, 0.5H), 3.24 (s, 0.5H), 2.97 (s, 0.5H), 2.68 (s, 0.5H), 1.28 (s, 9H);

^{13}C NMR (100 MHz, $CDCl_3$, 298K) δ 170.80, 152.08, 143.41, 141.37, 127.99, 127.27, 124.83, 120.13, 78.38, 77.27, 67.95, 55.44, 48.44, 47.09, 29.64;

MS (ESI+) calcd. for $C_{23}H_{26}NO_4S_2^+$ $[M+H]^+$ *m/z* = 444.13, found *m/z* = 444.31.

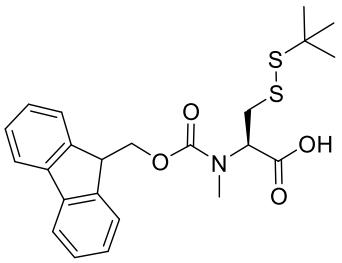

To a stirred solution of the previous oxazolidinone (5.0 g, 11.6 mmol) in chloroform (50 mL) was added triethylsilane (18 mL, 224.9 mmol) followed by the rapid addition of TFA (25 mL, 372.7 mmol). The reaction was stirred at room temperature overnight and then concentrated under reduced pressure to provide a yellow oil. The reaction was complete as monitored by TLC (cyclohexane: ethyl acetate v/v 3:2, R_f =0.5).The oil was dissolved in chloroform (100 mL) and concentrated. This step was repeated three consecutive times. Flash chromatography (SiO_2, cyclohexane: ethyl acetate v/v 8:1, with 0.1% formic acid) was used to isolate **Fmo**c-*N*MeCys(**StBu**)-OH as a white solid (3.1 g, 62%).

^{1}H NMR (400 MHz, $CDCl_3$, 298K) mixture of two rotamers δ 7.77 (d, *J* = 7.5 Hz, 1H), 7.60 (t, *J* = 7.6 Hz, 1H), 7.40 (t, *J* = 7.2 Hz, 1H), 7.32 (t, *J* = 7.5 Hz, 1H), 4.74 (dd, *J* = 10.5, 4.4 Hz, 1H), 4.56 (m, 1H), 4.44 (dd, *J* = 7.1, 4.4 Hz, 1H), 4.30 (t, *J* = 7.1 Hz, 1H), 3.35 (dd, *J* = 14.0, 4.5 Hz, 1H), 3.20-3.11 (m, 1H), 3.05 and 2.95 (s, 3H), 1.35 and 1.32 (s, 9H);

^{13}C NMR (100 MHz, $CDCl_3$, 298K) mixture of two rotamers δ 175.02 and 174.86, 156.69 and 156.28, 143.82 and 143.71, 141.26, 127.69 and 127.09, 125.10, 124.92 and 124.86, 119.95, 68.06, 59.80, 58.82, 48.19 and 47.11, 39.26 and 39.02, 33.72 and 33.02, 29.92;

MS (ESI-) calcd. for $C_{23}H_{26}NO_4S_2^-$ $[M-H]^-$ *m/z* = 444.13, found *m/z* = 444.32.

E 2.1.2 Synthesis of **Boc**-*N*MeCys(**Trt**)-OH

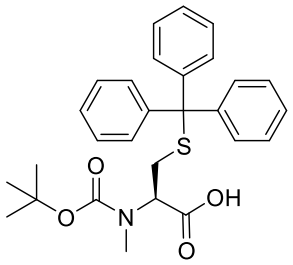

One dry schlenk tube was charged with a solution of **Boc**-MeCys(**Trt**)-OH(15 g, 13.9 mmol) in dry THF (40 mL) and placed under an atmosphere of argon gas. Another dry schlenk tube was charged with a suspension of NaH (60% in mineral oil, 3.9 g, 97.2 mmol) in dry THF (30 mL) and placed under an atmosphere of argon gas. The solution of **Boc**-MeCys(**Trt**)-OH was added slowly to the suspension of NaH with stirring under ice salt bath. The reaction was stirred overnight at room temperature and then quenched by phosphate buffer saline (50 mL, pH=7.0, Na_2HPO_4-NaOH water solution). THF was removed under reduced pressure and resulting reaction solution was acidified to pH 3 with HCl 1 M and extracted with CH_2Cl_2 (3×70 mL). The combined organic solution was concentrated under reduced pressure to provide a yellow oil. Flash chromatography (SiO_2, CH_2Cl_2: methanol v/v 100:0; 100:1) was used to isolate **Boc**-*N*MeCys(**Trt**)-OH as a white-yellow solid (10 g, 65%).

^{1}H NMR (400 MHz, $CDCl_3$, 298K) mixture of two rotamers δ 7.36 (d, J = 7.5 Hz, 6H), 7.23-7.19 (m, 6H), 7.14 (t, J = 7.2 Hz, 3H), 3.80-3.57 (m, 1H), 2.77-2.69 (m, 1H), 2.77-2.52 (m, 5H), 1.37 and 1.30 (s, 9H);

^{13}C NMR (100 MHz, $CDCl_3$, 298K) mixture of two rotamers δ 175.81 and 175.40, 156.02 and 154.81, 144.49, 129.58, 128.03, 126.83, 81.18 and 80.73, 67.06 and 66.98, 60.43 and 59.41, 53.47, 34.16 and 33.45, 31.57 and 30.91, 28.35 and 28.29;

MS (ESI-) calcd. for $C_{28}H_{30}NO_4S^-$ $[M-H]^-$ m/z = 476.19, found m/z = 476.30.

E 2.1.3 Synthesis of **Fmoc**-*N*MeCys(**Trt**)-OH

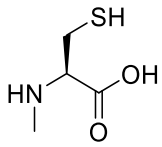

Boc-MeCys(**Trt**)-OH (10 g, 20.9 mmol) was dissolved in CH_2Cl_2 (26 mL) followed by the addition of TES (16.9 mL, 104.7 mmol) and TFA (43.6 mL, 586.2 mmol) under argon gas. The reaction was stirred at room temperature for overnight and the solvent was removed under reduced pressure. Et_2O (80 mL) was added to the crude product and the product was extracted with H_2O (3×20 mL). After freezing the sample, H_2O was removed by lyophilization and the crude *N*Me-Cys-OH obtained as a yellow oil (1.9 g, 64%). The yellow oil was put in vacuums overnight and carried over to the next step without further purification.

MS (ESI+) calcd. for $C_4H_{10}NO_2S^+$ $[M+H]^+$ *m/z* = 136.05, found *m/z* = 135.94.

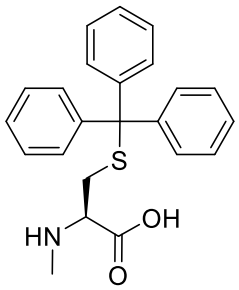

Crude *N*Me-Cys-OH (1.9 g, 14.0 mmol) was dissolved in HFIP (60 mL) given a clear solution and followed by the addition of triphenylmethanol (11.2 g, 41.9 mmol) which cannot absolutely dissolve in HFIP and the reaction solution was stirred for overnight. After TLC and phosphomolybdic acid stain solution checking (CH_2Cl_2: methanol 5:1 v: v, R_f =0.5), the reaction was quenched by sodium acetate saturated solution. The reaction mixture was evaporated to a small volume. After filtering the mixture and washing it with enough water and Et_2O separately, the crude *N*Me-Cys(**Trt**)-OH obtained as white solid (4 g, 58%). The white solid was carried over to the next step without further purification.

MS (ESI+) calcd. for $C_{23}H_{23}NO_2S^+$ $[M+H]^+$ *m/z* = 378.15, found *m/z* = 378.15.

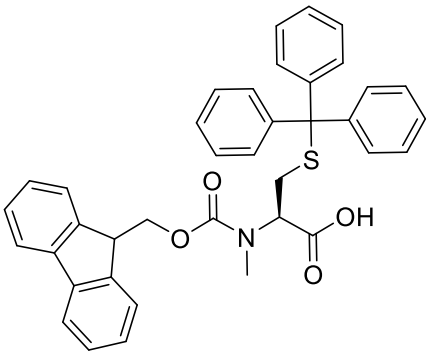

Crude *N*Me-Cys(**Trt**)-OH (4 g, 10.6 mmol) was dissolved in water/acetonitrile (28 mL/ 41 mL) followed by the addition of Fmoc-OSU (4 g, 11.7 mmol) and trimethylamine. The pH value of reaction solution was kept in 8 and the reaction solution was stirred overnight. After TLC checking, reaction was quenched by 1 M hydrochloric acid (125 mL), acetonitrile was removed under reduced pressure, extracted with ethyl acetate (3×100 mL), washed with H_2O (70 mL), brine (70 mL), dried with sodium sulfate and filtered. The combined organic solution was concentrated under reduced pressure to provide a yellow oil. Flash chromatography (SiO_2, CH_2Cl_2: methanol v/v 100:0; 100:1) was used to isolate Fmoc-*N*MeCys(Trt)-OH as a white-yellow solid (5 g, 65%).

^{1}H NMR (400 MHz, $CDCl_3$, 298K) mixture of two rotamers δ 7.75 (d, J = 7.2 Hz, 2H), 7.57 (d, J = 7.4 Hz, 2H), 7.45-7.34 (m, , 8H), 7.30-7.18 (m, 11H), 4.45 (dt, J = 6.7, 3.6 Hz, 0.8H), 4.39 (dd, J = 7.2, 2.8 Hz, 1.2H), 4.26 (t, J = 7.0 Hz, 0.6H), 4.20 (t, J = 5.9 Hz, 0.4H), 3.99 (dd, J = 10.4, 5.1 Hz, 1H), 2.86 (dd, J = 13.4, 5.1 Hz, 0.6H), 2.74 (s, 3H), 2.62 (dd, J = 13.5, 4.8 Hz, 0.4H), 2.48-2.37 (m, 0.4H);

^{13}C NMR (100 MHz, $CDCl_3$, 298K) mixture of two rotamers δ 176.45, 174.48, 144.39, 143.82, 141.31, 129.59 and 129.52, 128.03, 127.69, 127.09, 126.85, 125.08, 119.95, 77.34, 77.02, 76.70, 67.88, 67.17, 47.15, 33.08, 30.96 and 30.69, 20.59;

MS (ESI+) calcd. for $C_{38}H_{33}NO_4SNa^+$ $[M+Na]^+$ m/z = 622.19, found m/z = 622.67.

E2.2 *N*-(methyl)-cysteine derivatives

E 2.2.1 Synthesis of **S2**

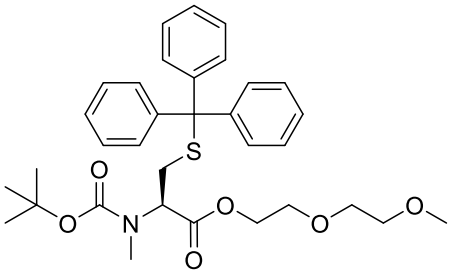

Boc-*N*MeCys(**Trt**)-OH (1000 mg, 2.1 mmol), diethylene glycol methyl ether (373.6 μL, 3.1 mmol) and DMAP (76.7 mg, 0.6 mmol) were added to a 50 mL round-bottom flask and dissolved with CH_2Cl_2 (20 mL). The mixture solution was stirring under ice bath for half hour to get a clear solution and DCC (518.4 mg, 2.5 mmol) was added to the flask. Ice bath was removed and reaction mixture was stirred at room temperature overnight. The reaction was complete detected by UPLC. After checking, the reaction solution was filtered and the reaction was concentrated under reduced pressure to provide a yellow oil. Flash chromatography (SiO_2, CH_2Cl_2: ethyl acetate v/v 0, 100:1, 50:1) was used to isolate **Boc**-*N*MeCys(**Trt**)-DME as a yellow oil (734 mg, 60%).

^{1}H NMR (400 MHz, $CDCl_3$, 298K) δ 7.47-7.39 (m, 6H), 7.28 (t, J = 7.6 Hz, 6H), 7.21 (t, J = 7.2 Hz, 3H), 4.17 (dt, J = 9.8, 5.2 Hz, 2H), 3.95 (dd, J = 9.6, 5.5 Hz, 1H), 3.66-3.59 (m, 2H), 3.57 (d, J = 9.2 Hz,20H), 3.51-3.41 (m, 2H), 3.35 (s, 3H), 2.82 (dd, J = 13.0, 5.5 Hz, 1H), 2.73-2.53 (m, 4H), 1.39 (s,

9H);

^{13}C NMR (100 MHz, $CDCl_3$, 298K) δ 144.59, 129.59, 127.96, 126.74, 77.33, 77.02, 76.70, 71.88, 70.59, 68.82, 66.91, 64.41, 64.23, 60.29, 59.06, 31.76, 31.21, 28.32;

MS (ESI+) calcd. for $C_{33}H_{41}NO_6SNa^+$ $[M+Na]^+$ *m/z* = 602.27, found *m/z* =602.72.

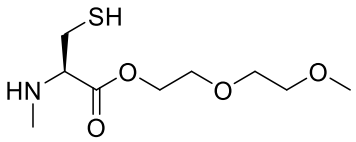

Boc-*N*MeCys(**Trt**)-DME (300 mg, 0.5 mmol), TFA (285 μL, 3.8 mmol) and triisopropylsilane (15 μL, 0.07 mmol) were added to a 25 mL round-bottom flask. The reaction was stirred at room temperature for 5 mins and followed by UPLC. After checking, the reaction was concentrated under reduced pressure to provide a yellow oil and was diluted with H_2O (50 mL) and washed with Et_2O (5×50 mL). The aqueous layer was concentrated in vacuum to provide isolate **S2** as a yellow oil (112 mg, 95%).

^{1}H NMR (400 MHz, D_2O, 298K) δ 4.51-4.31 (m, 3H), 3.77 (d, *J* = 4.4 Hz, 2H), 3.70-3.61 (m, 2H), 3.59-3.54 (m, 2H), 3.51 (d, *J* = 4.7 Hz, 0.4H), 3.37 (dd, *J* = 15.6, 5.5 Hz, 0.8H), 3.32 (s, 1H), 3.14 (d, *J* = 4.5 Hz, 0.8H), 2.77 (s, 3H);

^{13}C NMR (100 MHz, D_2O, 298K) δ 167.37, 70.92, 69.38, 68.04, 65.65, 61.75, 58.01, 31.38, 22.32 and 21.23;

MS (ESI+) calcd. for $C_9H_{20}NO_4S^+$ $[M+H]^+$ *m/z* = 238.11, found *m/z* = 238.50.

E 2.2.2 Synthesis of **S3**

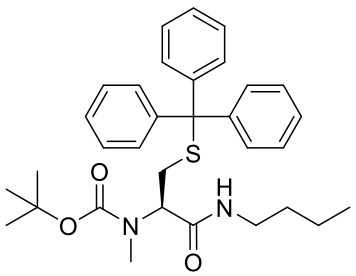

Boc-*N*MeCys(**Trt**)-OH (800 mg, 1.6 mmol), DIEA (498.3 μL, 3.0 mmol) and HATU (955.3 mg, 2.5 mmol) were added to a 100 mL round-bottom flask and dissolved with acetonitrile (50 mL). The mixture solution was stirring under ice bath for half hour to get a clear solution and butylamine (740 μL, 3.0 mmol) was added to the flask. Ice bath was removed and reaction mixture was stirred at room temperature overnight. The reaction was complete detected by UPLC. After checking, the reaction solution was filtered and the reaction was concentrated under reduced pressure to provide a yellow oil. Flash chromatography (SiO_2, CH_2Cl_2: ethyl acetate v/v 0, 100:1, 50:1) was used to isolate **Boc**-*N*MeCys(**Trt**)-C4 as a yellow oil (400 mg, 45%).

^{1}H NMR (400 MHz, $CDCl_3$, 298K) δ 7.39 – 7.32 (m, 6H), 7.24 – 7.17 (m, 6H), 7.16 – 7.10 (m, 3H), 5.99 (s, 0.5H), 4.35 – 4.07 (m, 1H), 3.17 – 2.96 (m, 2H), 2.87 – 2.34 (m, 5H), 1.38 (s, 9H), 1.26 – 1.11 (m, 2H), 0.80 (t, J = 7.2 Hz, 3H);

^{13}C NMR (100 MHz, $CDCl_3$, 298K) 144.60, 129.58, 127.93, 126.70, 77.23, 66.73, 57.44, 50.87, 38.92, 31.53, 30.09, 28.34, 19.93, 13.68;

MS (ESI+) calcd. for $C_{32}H_{40}N_2O_3S^+$ $[M+H]^+$ *m/z* = 533.28, found *m/z* =533.98.

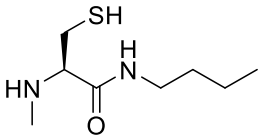

Boc-*N*MeCys(**Trt**)-DME (400 mg, 0.5 mmol), TFA (9500 μL, 127.9 mmol) and triisopropylsilane (500 μL,3.0 mmol) were added to a 25 mL round-bottom flask. The reaction was stirred at room temperature for 5 mins and followed by UPLC. After checking, the reaction was concentrated under reduced pressure to provide a yellow oil and was diluted with H_2O (50 mL) and washed with Et_2O (5×50 mL). The aqueous layer was concentrated in vacuum to provide isolate **S2** as a yellow oil (114 mg, 80%).

^{1}H NMR (400 MHz, DMSO-d_6, 298K) δ 8.54 (t, J = 5.6 Hz, 1H), 3.86 (t, J = 5.5 Hz, 1H), 3.23 – 3.05 (m, 2H), 2.96 (s, 2H), 2.52 (s, 3H), 1.43 (d, J = 6.0 Hz, 2H), 1.35 – 0.99 (m, 4H), 0.88 (t, J = 7.3 Hz, 3H).;

^{13}C NMR (100 MHz, DMSO-d_6, 298K) 165.91, 61.99, 39.06, 31.90, 31.26, 23.88, 19.93, 14.04;

MS (ESI+) calcd. for $C_8H_{19}N_2OS^+$ $[M+H]^+$ *m/z* = 191.11, found *m/z* = 191.56.

E 2.2.3 Synthesis of **S5**

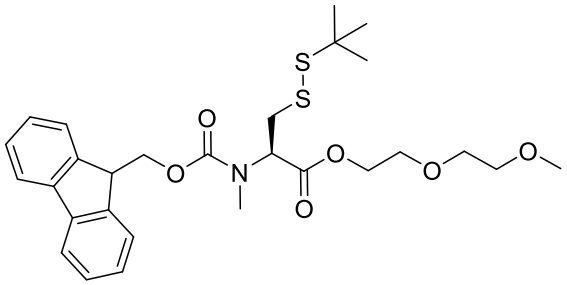

Fmoc-*N*MeCys(**StBu**)-OH (2646 mg, 5.9 mmol), diethylene glycol methyl ether (777 µL, 6.5 mmol) and DMAP (217.6 mg, 1.8 mmol) were added to a 50 mL round-bottom flask and dissolved with acetonitrile (20 mL). The mixture solution was stirring under ice bath for half hour to get a clear solution and DCC (1470 mg, 7.1 mmol) was added to the flask. Ice bath was removed and reaction mixture was stirred at room temperature overnight. The reaction was complete detected by UPLC and TLC (cyclohexane: ethyl acetate v/v 4:1, R_f =0.1). After checking, filter the solution and the reaction was concentrated under reduced pressure to provide a yellow oil. Flash chromatography (SiO_2, CH_2Cl_2: ethyl acetate v/v 0, 100:1, 50:1, 10:1) was used to isolate **Fmoc**-*N*MeCys(**StBu**)-OEG as a yellow oil (2500 mg, 77%).

^{1}H NMR (400 MHz, $CDCl_3$, 298K) δ 7.79 (d, J = 7.5 Hz, 2H), 7.63 (t, J = 6.9 Hz, 2H), 7.42 (t, J = 7.4 Hz, 2H), 7.34 (t, J = 7.9 Hz, 2H), 4.85 (dd, J = 10.5, 4.7 Hz, 1H), 4.57-4.39 (m, 2H), 4.39-4.25 (m, 2H), 4.19 (d, J = 4.3 Hz, 0.7H), 3.69 (dt, J = 16.5, 4.9 Hz, 2H), 3.64-3.56 (m, 2H), 3.51 (dd, J = 5.7, 3.2 Hz, 2H), 3.37 (s, 3H), 3.15 (dd, J = 13.8, 10.6 Hz, 1H), 3.07 (s, 3H), 2.87-2.70 (m, 0.3H), 1.37 (s, 9H);

^{13}C NMR (100 MHz, $CDCl_3$, 298K) δ 170.09, 169.84, 141.35, 141.31, 127.68, 127.07, 125.17, 119.97, 77.33, 77.01, 76.70, 71.87, 70.49, 68.88 and 68.84, 67.88, 64.49, 59.69, 59.04, 48.13, 47.19, 33.29, 29.93, 26.92;

MS (ESI+) calcd. for $C_{28}H_{38}NO_6S_2^+$ $[M+H]^+$ m/z = 548.22, found m/z = 548.76.

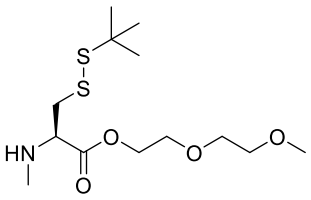

Fmoc-*N*MeCys(**StBu**)-OEG (450 mg, 0.8 mmol), piperazine (2810 mg, 32.6 mmol) and HOBt (551 mg, 4.1 mmol) were added to a 50 mL round-bottom flask and dissolved with methanol (20 mL). The reaction mixture was stirred at room temperature overnight and was complete detected by UPLC and TLC (CH_2Cl_2: methanol v/v 20:1, R_f =0.5). After checking, the mixture was diluted with ethyl acetate (100 mL) and washed with saturated $NaHCO_3$ solution (3×100 mL), saturated brine (100 mL). The organic layer was dried over Na_2SO_4, filtered and concentrated under reduced pressure. Flash chromatography (SiO_2, CH_2Cl_2: methanol v/v 0, 50:1) was used to isolate *N*MeCys(**StBu**)-OEG as a yellow oil (198 mg, 76%).

^{1}H NMR (400 MHz, $CDCl_3$, 298K) δ 4.29-4.24 (m, 2H), 3.68-3.64 (m, 2H), 3.59-3.56 (m, 2H), 3.50-3.44 (m, 3H), 3.32 (s, 4H), 3.00-2.86 (m, 2H), 2.36 (s, 3H), 1.27 (s, 9H);

^{13}C NMR (100 MHz, $CDCl_3$, 298K) δ 173.16, 71.89, 70.47, 69.05, 63.95, 62.39, 59.07, 48.04, 43.44, 34.58, 29.87;

MS (ESI+) calcd. for $C_{17}H_{38}NO_4S_2^+$ $[M+H]^+$ *m/z* = 326.15, found *m/z* = 326.45.

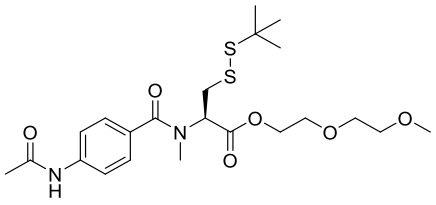

Acetylaminobenzoic acid (ABA) (100 mg, 0.6 mmol), *N*MeCys(**StBu**)-OEG (120 mg, 0.4 mmol), HATU (256 mg, 0.6 mmol) and DIEA (120 μL, 0.7mmol) were added to a 10 mL flask and dissolved with DMF (5 mL). The mixture solution was stirring under nitrogen protection in microwave synthesizer for 20mins (35 W, 70 °C). The reaction was complete detected by UPLC and TLC (ethyl acetate R_f =0.4). The mixture was diluted with ethyl acetate (100 mL) and washed with saturated $NaHCO_3$ solution (3×100 mL), saturated brine (100 mL). The organic layer was dried over Na_2SO_4, filtered and concentrated in vacuum. Flash chromatography (SiO_2, CH_2Cl_2: methanol v/v 0, 10:1, 8:1, 4:1, 2:1) was used to isolate ABA-*N*MeCys(**StBu**)-OEG as a yellow oil (136 mg, 77%).

^{1}H NMR (400 MHz, CD_3OD, 298K) δ 7.72 (d, J = 7.9 Hz, 2H), 7.47 (d, J = 8.0 Hz, 2H), 5.09 (d, J = 6.1 Hz, 2H), 4.38-4.30 (m, 2H), 3.75 (bs, 2H), 3.69-3.63 (m, 2H), 3.55 (bs, 2H), 3.36 (s, 3H), 3.29-3.10(m, 1H), 3.04 (s, 3H), 2.17 (s, 3H), 1.34 (s, 9H);

^{13}C NMR (100 MHz, $CDCl_3$, 298K) δ 171.81, 169.72, 160.82, 137.65, 137.39, 71.87, 70.46, 68.92, 64.76, 64.43, 59.00, 58.56, 55.47, 48.21, 48.09, 38.60, 37.08, 29.90, 29.74, 29.14;

MS (ESI+) calcd. for $C_{22}H_{35}N_2O_6S_2^+$ $[M+H]^+$ m/z = 487.20, found m/z = 487.56.

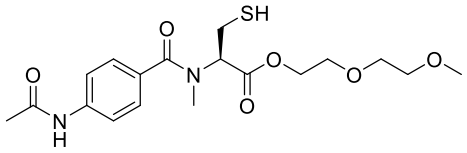

ABA-*N*MeCys(**StBu**)-OEG (100 mg, 0.2 mmol) and triphenylphosphine (539 mg, 2.0 mmol) were added to a 50 mL flask and dissolved with TFA (10 mL). The reaction mixture was stirred at room temperature overnight and was complete detected by UPLC and TLC (CH_2Cl_2: ethyl acetate v/v 1:1, R_f =0.3). After checking, the mixture was diluted with ethyl acetate (50 mL) and washed with saturated $NaHCO_3$ solution (3×50 mL), saturated brine (50 mL). The organic layer was dried over Na_2SO_4, filtered and concentrated in vacuum. Flash chromatography (SiO_2, CH_2Cl_2: methanol v/v 0, 10:1, 1:1) was used to isolate **S5** as a yellow oil (39 mg, 49%).

^{1}H NMR (400 MHz, CD_3OD, 298K) δ 7.70 (d, J = 7.4 Hz, 2H), 7.43 (d, J = 8.8 Hz, 2H), 4.86 (s, 3H), 4.36 (bs, 2H), 3.74 (t, J = 4.6 Hz, 2H), 3.69-3.60 (m, 2H), 3.54 (bs, 2H), 3.33 (s, 2H), 3.08 (bs, 2H), 2.97 (bs, 2H), 2.16 (s, 3H);

^{13}C NMR (100 MHz, $CDCl_3$, 298K) δ 169.33, 162.60, 140.34, 130.12, 128.06, 119.42, 77.47, 77.15, 76.83, 71.80, 70.38, 70.35, 68.78, 64.00, 58.97, 36.55, 31.47, 24.31;

MS (ESI+) calcd. for $C_{18}H_{27}N_2O_6S^+$ $[M+H]^+$ m/z = 399.16, found m/z = 399.42.

E 2.2.4 Synthesis of **S1**

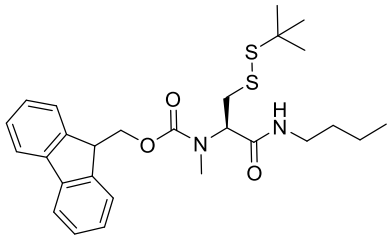

Fmoc-*N*MeCys(**StBu**)-OH (1000 mg, 2.2 mmol), HATU (1054 mg, 2.6 mmol) and DIEA (470 μL, 3.0 mmol) were added to a 100 mL flask and dissolved with acetonitrile (30 mL). The mixture solution was stirring under ice bath for half hour to get a clear solution and butylamine (340 μL, 3.4 mmol) was added to the flask. Ice bath was removed and reaction mixture was stirred at room temperature overnight. The reaction was complete detected by UPLC and TLC (cyclohexane: ethyl acetate v/v 4:1, R_f =0.2). After checking, the mixture was diluted with ethyl acetate (100 mL) and washed with saturated $NaHCO_3$ solution (3×100 mL), saturated brine (100 mL). The organic layer was dried over Na_2SO_4, filtered and concentrated in vacuum. Flash chromatography (SiO_2, CH_2Cl_2: methanol v/v 0, 100:1, 50:1, 25:1) was used to isolate **Fmoc**-*N*MeCys(**StBu**)-C4 as a yellow oil (680 mg, 61%).

^{1}H NMR (400 MHz, $CDCl_3$, 298K) δ 7.78 (d, J = 7.6 Hz, 2H), 7.65-7.57 (m, 2H), 7.41 (dd, J = 8.3, 6.7 Hz, 2H), 7.32 (t, J = 7.4 Hz, 2H), 6.13-6.05 (m, 0.5H), 5.38 (bs, 0.5H), 4.87 (dd, J = 9.5, 6.0 Hz, 1H), 4.60-4.51 (m, 1H), 4.44 (dd, J = 10.7, 7.0 Hz, 1H), 4.28 (t, J = 6.9 Hz, 1H), 3.30-3.20 (m, 4H), 2.82 and 2.80 (s, 3H), 1.49-1.42 (m, 2H), 1.33 and 1.30 (s, 9H), 0.90 (t, J = 7.3 Hz, 3H);

MS (ESI+) calcd. for $C_{27}H_{37}N_2O_3S_2^+$ $[M+H]^+$ m/z = 501.23, found m/z = 501.50.

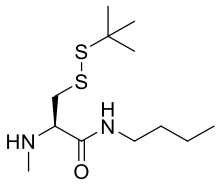

Fmoc-*N*MeCys(**StBu**)-C4 (700 mg, 0.8 mmol), piperazine (5418 mg, 62.9 mmol) and HOBt (944 mg, 6.9 mmol) were added to a 50 mL round-bottom flask and dissolved with methanol (30 mL). The reaction mixture was stirred at room temperature overnight and was complete detected by UPLC and TLC (cyclohexane: ethyl acetate v/v 1:1, R_f =0.3). After checking, the mixture was diluted with ethyl acetate (100 mL) and washed with saturated $NaHCO_3$ solution (3×100 mL), saturated brine (100 mL).

The organic layer was dried over Na_2SO_4, filtered and concentrated in vacuum. Flash chromatography (SiO_2, CH_2Cl_2: methanol v/v 0, 10:1) was used to isolate *N*MeCys(**StBu**)-C4 as a yellow oil (290 mg, 74%).

^{1}H NMR (400 MHz, $CDCl_3$, 298K) δ 3.33-3.13 (m, 4H), 2.70 (dd, J = 14.4, 10.4 Hz, 1H), 2.38 (s, 3H), 1.90 (s, 1H), 1.56-1.42 (m, 2H), 1.33 (s, 11H), 0.92 (t, J = 7.3 Hz, 3H);

^{13}C NMR (100 MHz, $CDCl_3$, 298K) δ 172.08, 77.34, 77.22, 77.02, 76.70, 63.49, 48.36, 43.13, 38.76, 35.19, 31.71, 29.89, 20.09, 13.74;

MS (ESI+) calcd. for $C_{12}H_{27}N_2OS_2^+$ $[M+H]^+$ m/z = 279.16, found m/z = 279.49.

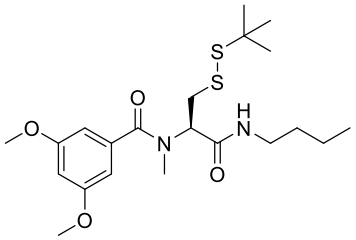

3,5-dimethoxybenzoic acid (DBA) (136 mg, 0.7 mmol), *N*MeCys(**StBu**)-C4 (140 mg, 0.5 mmol), HATU (356 mg, 0.9 mmol) and DIEA (165 μL, 1.0 mmol) were added to a 10 mL flask and dissolved with DMF (5 mL). The mixture solution was stirring under nitrogen protection in microwave synthesizer for 20mins (35 W, 70 ℃). The reaction was complete detected by UPLC and TLC (cyclohexane: ethyl acetate v/v 2:1, R_f =0.5). The mixture was diluted with ethyl acetate (50 mL) and washed with saturated $NaHCO_3$ solution (3×50 mL), saturated brine (50 mL). The organic layer was dried over Na_2SO_4, filtered and concentrated in vacuum. Flash chromatography (SiO_2, CH_2Cl_2: methanol v/v 0, 10:1, 8:1, 4:1, 2:1) was used to isolate DBA-*N*MeCys(**StBu**)-C4 as a yellow oil (119 mg, 54%).

^{1}H NMR (400 MHz, $CDCl_3$, 298K) δ 6.70 (t, J = 4.9 Hz, 0.5H), 6.54 (d, J = 2.0 Hz, 1.5H), 6.46 (s, 1H), 5.17 (dd, J = 10.2, 5.9 Hz, 1H), 3.74 (s, 6H), 3.29-3.04 (m, 4H), 2.92 and 2.85 (s, 3H), 1.47-1.39 (m 2H), 1.33-1.15 (m, 11H), 0.86 (t, J = 7.3 Hz, 3H);

^{13}C NMR (100 MHz, $CDCl_3$, 298K) δ 173.16, 169.24, 160.83, 137.13, 105.43, 102.46, 77.22, 56.51, 55.52, 48.18, 39.13, 34.06, 31.55, 29.90, 19.99, 13.73;

MS (ESI+) calcd. for $C_{21}H_{35}N_2O_4S_2^+$ $[M+H]^+$ m/z = 443.21, found m/z = 443.59.

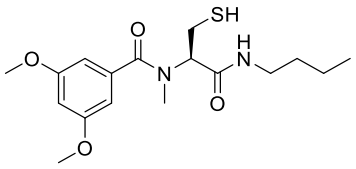

DBA-*N*MeCys(**StBu**)-C4(76 mg, 0.2 mmol) and triphenylphosphine (539 mg, 2.0 mmol) were added to a 50 mL flask and dissolved with TFA (10 mL). The reaction mixture was stirred at room temperature overnight and was complete detected by UPLC and TLC (cyclohexane: ethyl acetate v/v 2:1, R_f =0.2). After checking, the mixture was diluted with ethyl acetate (50 mL) and washed with saturated $NaHCO_3$ solution (3×50 mL), saturated brine (50 mL). The organic layer was dried over Na_2SO_4, filtered and concentrated in vacuum. Flash chromatography (SiO_2, CH_2Cl_2: methanol v/v 0, 10:1, 1:1) was used to isolate **S1** as a yellow oil (32 mg, 54%).

^{1}H NMR (400 MHz, $CDCl_3$, 298K) δ 6.51 (bs, 2H), 6.45 (s, 1H), 4.99 (t, J = 7.8 Hz, 1H), 3.74 (s, 6H), 3.17 (m, 3H), 2.97-2.68 (m, 4H), 1.44 (dq, J = 14.6, 7.1 Hz, 2H), 1.31-1.23 (m, 2H), 0.86 (t, J = 7.3 Hz, 3H);

^{13}C NMR (100 MHz, $CDCl_3$, 298K) δ 173.04, 168.79, 160.92, 137.07, 105.28, 102.22, 59.40, 55.49, 39.12, 33.37, 31.56, 22.44, 19.97, 13.69;

MS (ESI-) calcd. for $C_{17}H_{25}N_2O_4S^-$ $[M-H]^-$ m/z = 353.15, found m/z = 353.37.

E 2.2.5 Synthesis of **S4**

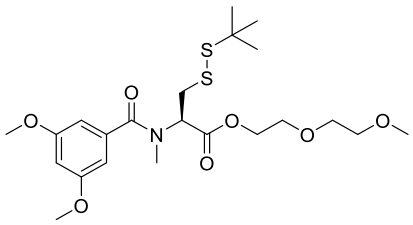

3,5-dimethoxybenzoic acid (DBA) (335 mg, 1.8 mmol), *N*MeCys(StBu)-OEG (400 mg, 1.2 mmol), HATU (867 mg, 2.2 mmol) and DIEA (407 μL, 2.5 mmol) were added to a 10 mL flask and dissolved with DMF (5 mL). The mixture solution was stirring under nitrogen protection in microwave synthesizer for 20 mins (35 W, 70 ℃). The reaction was complete detected by UPLC and TLC (CH_2Cl_2: ethyl acetate v/v 1:1, R_f =0.4). The mixture was diluted with ethyl acetate (100 mL) and washed with saturated $NaHCO_3$ solution (3×100 mL), saturated brine (100 mL). The organic layer

was dried over Na_2SO_4, filtered and concentrated in vacuum. Flash chromatography (SiO_2, CH_2Cl_2: methanol v/v 0, 10:1, 8:1, 4:1, 2:1) was used to isolate DBA-*N*MeCys(**StBu**)-OEG as a yellow oil (244 mg, 41%).

^{1}H NMR (400 MHz, $CDCl_3$, 298K) δ 6.61 (s, 2H), 6.49 (s, 1H), 4.97 (dd, J = 10.9, 4.5 Hz, 0.5H), 4.76 (dd, J = 9.5, 5.1 Hz, 0.5H), 4.43- 4.26 (m, 2H), 3.80 (s, 6H), 3.72 (t, J = 5.0 Hz, 2H), 3.63 (dd, J = 5.7, 3.6 Hz, 2H), 3.55- 3.50 (m, 2H), 3.47 (dd, J = 13.8, 4.6 Hz, 1H), 3.36 (s, 3H), 3.32-3.17 (m, 1H), 3.00 (d, J = 31.3 Hz, 3H), 1.35 (d, J = 11.8 Hz, 6H), 1.26 (s, 3H);

^{13}C NMR (100 MHz, $CDCl_3$, 298K) δ 171.81, 169.72, 160.82, 137.51, 104.99, 101.95, 71.87, 70.46, 68.92, 64.60, 59.00, 58.56, 55.47, 48.21, 38.60, 37.08, 29.90;

MS (ESI+) calcd. for $C_{22}H_{36}NO_7S_2^+$ $[M+H]^+$ m/z = 490.20, found m/z = 490.50.

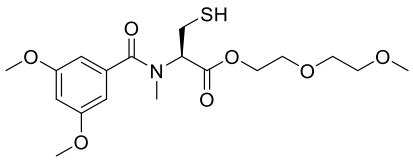

DBA-*N*MeCys(**StBu**)-OEG (144 mg, 0.3 mmol) and triphenylphosphine (539 mg, 2.0 mmol) were added to a 50 mL flask and dissolved with TFA (10 mL). The reaction mixture was stirred at room temperature overnight and was complete detected by UPLC and TLC (methanol : ethyl acetate v/v 1:10, R_f =0.5). After checking, the mixture was diluted with ethyl acetate (50 mL) and washed with saturated $NaHCO_3$ solution (3×50 mL), saturated brine (50 mL). The organic layer was dried over Na_2SO_4, filtered and concentrated in vacuum. Flash chromatography (SiO_2, CH_2Cl_2: methanol v/v 0, 10:1, 1:1) was used to isolate **S4** as a yellow oil (54 mg, 45%).

^{1}H NMR (400 MHz, $CDCl_3$, 298K) δ 6.62- 6.48 (m, 2H), 6.43 (s, 1H), 4.97 (s, 0.5H), 4.53 (d, J = 7.1 Hz, 0.5H), 4.36- 4.20 (m, 2H), 3.73 (s, 6H), 3.65 (s, 2H), 3.56 (dd, J = 5.9, 3.2 Hz, 2H), 3.50-3.42 (m, 2H), 3.29 (s, 3H), 2.91 (d, J = 9.5 Hz, 5H);

^{13}C NMR (100 MHz, $CDCl_3$, 298K) δ 169.33, 160.86, 137.48, 105.00, 101.96, 101.85, 71.87, 70.47, 68.89, 64.77 and 64.45, 63.71, 59.03, 55.50, 35.58, 23.95 and 23.40;

MS (ESI+) calcd. for $C_{18}H_{27}NO_7S^+$ $[M+H]^+$ m/z = 402.48, found m/z = 402.45.

E 2.2.6 Synthesis of **S6**

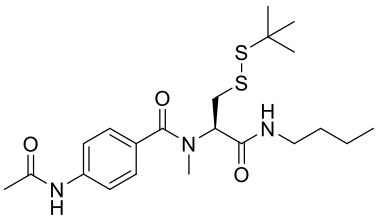

Acetylaminobenzoic acid (ABA) (579 mg, 3.2 mmol), *N*MeCys(**StBu**)-C4 (600 mg, 2.2 mmol), HATU (1520 mg, 3.9 mmol) and DIEA (641 μL, 3.9 mmol) were added to a 10 mL flask and dissolved with DMF (5 mL). The mixture solution was stirring under nitrogen protection in microwave synthesizer for 20 mins (35 W, 70 ℃). The reaction was complete detected by UPLC and TLC (CH_2Cl_2: ethyl acetate v/v 1:10, R_f =0.4). The mixture was diluted with ethyl acetate (50 mL) and washed with saturated $NaHCO_3$ solution (3×50 mL), saturated brine (50 mL). The organic layer was dried over Na_2SO_4, filtered and concentrated in vacuum. Flash chromatography (SiO_2, CH_2Cl_2: methanol v/v 0, 10:1, 8:1, 4:1, 2:1) was used to isolate ABA-*N*MeCys(**StBu**)-C4 as a yellow oil (442 mg, 50%).

^{1}H NMR (400 MHz, $CDCl_3$, 298K) δ 7.72 (s, 1H), 7.55 (d, J = 8.2 Hz, 2H), 7.46 (d, J = 8.3 Hz, 2H), 6.85 (s, 1H), 3.33-3.16 (m, 4H), 2.93 (s, 3H), 2.18 (s, 3H), 1.56-1.43 (m, 2H), 1.36-1.25 (m, 12H), 0.92 (t, J = 7.3 Hz, 3H);

^{13}C NMR (100 MHz, $CDCl_3$, 298K) δ 173.16, 169.24, 160.83, 137.13, 105.43, 102.46, 77.22, 56.51, 55.52, 48.18, 39.13, 34.06, 31.55, 29.90, 19.99, 13.73;

MS (ESI+) calcd. for $C_{21}H_{34}N_3O_3S_2^+$ $[M+H]^+$ m/z = 440.20, found m/z = 440.55.

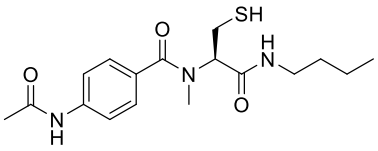

ABA-*N*MeCys(**StBu**)-C4 (442 mg, 1.0 mmol) and triphenylphosphine (539 mg, 2.0 mmol) were added to a 50 mL flask and dissolved with TFA (10 mL). The reaction mixture was stirred at room temperature overnight and was complete detected by UPLC and TLC (CH_2Cl_2: ethyl acetate v/v 1:2, R_f =0.4). After checking, the mixture was diluted with ethyl acetate (50 mL) and washed with

saturated $NaHCO_3$ solution (3×50 mL), saturated brine (50 mL). The organic layer was dried over Na_2SO_4, filtered and concentrated in vacuum. Flash chromatography (SiO_2, CH_2Cl_2: methanol v/v 0, 10:1, 1:1) was used to isolate **S6** as a yellow oil (196 mg, 56%).

^{1}H NMR (400 MHz, $CDCl_3$, 298K) δ 8.02 (s, 1H), 7.58 (d, J = 8.2 Hz, 2H), 7.44 (d, J = 8.1 Hz, 2H), 6.90 (s, 1H), 5.32 (d, J = 6.8 Hz, 1H), 3.41- 3.03 (m, 4H), 2.96 (s, 3H), 2.19 (s, 3H), 1.57- 1.44 (m, 2H), 1.36 (dq, J = 9.6, 7.3 Hz, 2H), 0.94 (t, J = 7.3 Hz, 3H);

^{13}C NMR (100 MHz, $CDCl_3$, 298K) δ 173.17, 169.40, 169.13, 140.62, 129.93, 128.63, 119.47, 60.41, 53.44, 41.31, 31.45, 29.65, 24.40, 20.00, 13.71;

MS (ESI-) calcd. for $C_{17}H_{24}N_3O_3S^-$ $[M-H]^-$ m/z = 350.15, found m/z = 350.41.

E 2.2.7 Synthesis of C8BA-*N*MeCys-C4

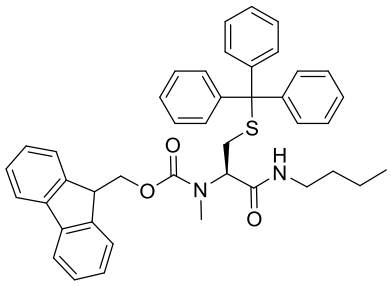

Fmoc-*N*MeCys(**Trt**)-OH(1000 mg, 1.7 mmol), HATU (1054 mg, 2.6 mmol) and DIEA (470 μL, 3.0 mmol) were added to a 100 mL flask and dissolved with acetonitrile (30 mL). The mixture solution was stirring under ice bath for half hour to get a clear solution and butylamine (330 μL, 3.3 mmol) was added to the flask. Ice bath was removed and reaction mixture was stirred at room temperature overnight. The reaction was complete detected by UPLC and TLC (cyclohexane: ethyl acetate v/v 4:1, R_f =0.3). After checking, the mixture was diluted with ethyl acetate (100 mL) and washed with saturated $NaHCO_3$ solution (3×100 mL), saturated brine (100 mL). The organic layer was dried over Na_2SO_4, filtered and concentrated in vacuum. Flash chromatography (SiO_2, CH_2Cl_2: methanol v/v 0, 100:1, 50:1, 25:1, 10:1) was used to isolate **Fmoc**-*N*MeCys(**Trt**)-C4 as a yellow oil (890 mg, 80%).

^{1}H NMR (400 MHz, $CDCl_3$, 298K) δ 7.77 (d, J = 7.6 Hz, 2H), 7.58 (dd, J = 7.6, 3.7 Hz, 2H), 7.51--7.34 (m, 8H), 7.33- 7.17 (m, 11H), 4.50 (dd, J = 10.6, 6.6 Hz, 1H), 4.37 (ddd, J = 12.7, 10.4, 6.3 Hz, 1H), 4.27 (t, J = 7.0 Hz, 1H), 3.20- 2.95 (m, 2H), 2.79- 2.56 (m, 5H), 1.36 (dp, J = 18.2, 8.8, 8.2 Hz, 2H), 0.87 (t, J = 7.2 Hz, 3H);

^{13}C NMR (100 MHz, $CDCl_3$, 298K) δ 169.28, 157.13, 144.52, 143.88, 141.35, 129.64, 127.99, 127.77, 127.10, 126.78, 124.98, 120.03, 67.85, 66.97, 58.18, 47.22, 39.11, 31.53, 30.15, 29.83, 19.97, 13.72;

MS (ESI+) calcd. for $C_{42}H_{42}N_2O_3S^+$ $[M+H]^+$ *m/z* = 655.30, found *m/z* = 655.84.

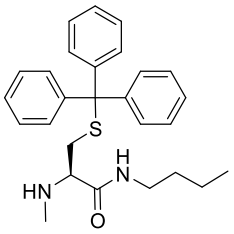

Fmoc-*N*MeCys(**Trt**)-C4 (890 mg, 1.4 mmol), piperazine (5267 mg, 62.0 mmol) and HoBt (918 mg, 6.8 mmol) were added to a 50 mL round-bottom flask and dissolved with methanol (30 mL). The reaction mixture was stirred at room temperature overnight and was complete detected by UPLC and TLC (CH_2Cl_2: ethyl acetate v/v 4:1, R_f =0.2). After checking, the mixture was diluted with ethyl acetate (100 mL) and washed with saturated $NaHCO_3$ solution (3×100 mL), saturated brine (100 mL). The organic layer was dried over Na_2SO_4, filtered and concentrated in vacuum. Flash chromatography (SiO_2, CH_2Cl_2: methanol v/v 0, 10:1) was used to isolate *N*MeCys(**Trt**)-C4 as a yellow oil (511 mg, 85%).

^{1}H NMR (400 MHz, $CDCl_3$, 298K) δ 7.40-7.33 (m, 5H), 7.26- 7.11 (m, 10H), 6.89 (s, 1H), 3.11 (ddt, *J* = 10.2, 6.1, 3.9 Hz, 2H), 2.58 (ddd, *J* = 23.4, 9.6, 3.3 Hz, 2H), 2.37 (ddd, *J* = 11.9, 8.6, 2.8 Hz, 1H), 2.09 (dd, *J* = 8.8, 2.8 Hz, 4H), 1.35 (td, *J* = 7.4, 5.0 Hz, 2H), 1.28-1.16 (m, 2H), 0.82 (td, *J* = 7.3, 2.8 Hz, 3H);

^{13}C NMR (100 MHz, $CDCl_3$, 298K) δ 172.06, 144.55, 129.59, 127.98, 126.78, 66.89, 63.32, 38.66, 35.18, 34.96, 31.65, 20.05, 13.74;

MS (ESI+) calcd. for $C_{27}H_{33}N_2OS^+$ $[M+H]^+$ *m/z* = 433.23, found *m/z* = 433.82.

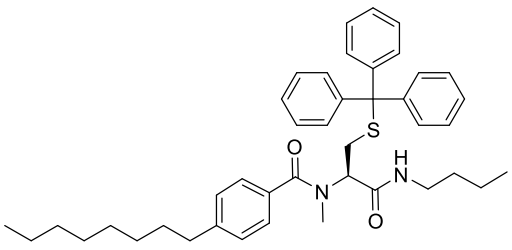

4-octylbenzoic acid(C8BA) (414 mg, 1.7 mmol), *N*MeCys(Trt)-C4 (510 mg, 1.8 mmol), HATU (1008 mg, 2.6 mmol) and DIEA (526 μL, 3.2 mmol) were added to a 10 mL flask and dissolved with DMF (5 mL). The mixture solution was stirring under nitrogen protection in microwave synthesizer for 20 mins (35 W, 70 ℃). The reaction was complete detected by UPLC and TLC (cyclohexane: ethyl acetate v/v 1:1, R_f =0.1). The mixture was diluted with ethyl acetate (50 mL) and washed with saturated $NaHCO_3$ solution (3×50 mL), saturated brine (50 mL). The organic layer was dried over Na_2SO_4, filtered and concentrated in vacuum. Flash chromatography (SiO_2, CH_2Cl_2: methanol v/v 0, 10:1, 8:1, 4:1, 2:1) was used to isolate C8BA -*N*MeCys(**Trt**)-C4 as a yellow oil (890 mg, 74%).

^{1}H NMR (400 MHz, $CDCl_3$, 298K) δ 7.47 (d, J = 7.7 Hz, 5H), 7.38-7.26 (m, 8H), 7.25-7.15 (m, 6H), 6.58 (t, J = 6.0 Hz, 1H), 4.67 (dd, J = 9.7, 6.3 Hz, 1H), 3.24-3.06 (m, 2H), 2.79- 2.67 (m, 5H), 2.62 (t, J = 7.7 Hz, 2H), 1.61 (p, J = 7.6 Hz, 2H), 1.47-1.37 (m, 2H), 1.36-1.18 (m, 12H), 0.89 (td, J = 7.2, 4.0 Hz, 6H);

^{13}C NMR (100 MHz, $CDCl_3$, 298K) δ 173.40, 169.39, 145.85, 145.85, 144.51, 132.38, 132.38, 129.58, 128.41, 128.01, 127.89, 126.77, 66.90, 56.29, 38.91, 35.87, 33.56, 31.88, 31.51, 31.25, 29.59, 29.44, 29.24, 22.67, 19.94, 14.11, 13.70;

MS (ESI+) calcd. for $C_{42}H_{53}N_2O_2S^+$ $[M+H]^+$ m/z = 649.38, found m/z = 649.99.

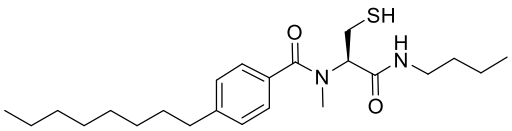

C8BA -*N*MeCys(**Trt**)-C4 (850 mg, 1.3 mmol) and triisopropylsilane (0.5 mL, 3.0 mmol) were added to a 50 mL flask and dissolved with TFA (10 mL). The reaction mixture was stirred at room temperature for one hour and was complete detected by UPLC and TLC (CH_2Cl_2: ethyl acetate v/v 10:1, R_f =0.2). After checking, the mixture was diluted with ethyl acetate (50 mL) and washed with saturated $NaHCO_3$ solution (3×50 mL), saturated brine (50 mL). The organic layer was dried over Na_2SO_4, filtered and concentrated in vacuum. Flash chromatography (SiO_2, CH_2Cl_2: methanol v/v 0, 10:1, 1:1) was used to isolate C8BA-*N*MeCys-C4 as a yellow oil (237 mg, 45%).

^{1}H NMR (400 MHz, $CDCl_3$, 298K) δ 7.44-7.36 (m, 2H), 7.23 (d, J = 8.1 Hz, 2H), 6.76 (s, 1H), 5.06 (t, J = 8.0 Hz, 1H), 3.35-3.10 (m, 3H), 2.92 (s, 4H), 2.68-2.57 (m, 2H), 1.67-1.56 (m, 2H), 1.49 (dtd, J = 8.6, 7.3, 5.9 Hz, 2H), 1.40-1.20 (m, 12H), 0.90 (dt, J = 18.7, 7.2 Hz, 6H);

^{13}C NMR (100 MHz, $CDCl_3$, 298K) δ 173.67, 146.00, 132.23, 128.53, 127.73, 39.08, 35.86, 33.65, 31.86, 31.58, 31.23, 30.92, 29.43, 29.25, 29.23, 22.66, 22.42, 19.98, 14.09, 13.71;

MS (ESI+) calcd. for $C_{23}H_{39}N_2O_2S^+$ $[M+H]^+$ *m/z* =407.28, found *m/z* = 407.86.

E 2.2.8 Synthesis of *N*MeCys-PEG800

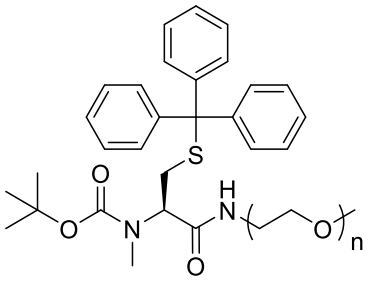

Boc-*N*MeCys(**Trt**)-OH (800 mg, 1.0 mmol), HATU (598 mg, 1.5 mmol) and DIEA (280 μL, 1.8 mmol) were added to a 50 mL flask and dissolved with acentonitrile (20 mL). The mixture solution was stirring under nitrogen protection for 60 mins and NH_2-PEG800-OMe (376 mg, 1.1 mmol) was added to the flask. The reaction was complete detected by UPLC and the mixture was diluted with ethyl acetate (100 mL) and washed with saturated $NaHCO_3$ solution (3×100 mL), saturated brine (100 mL). The organic layer was dried over Na_2SO_4, filtered and concentrated in vacuum. This crude product **Boc**-*N*MeCys(**Trt**)-PEG800 was used directly in the next step without any further purification.

^{1}H NMR (400 MHz, $CDCl_3$, 298K) δ 7.46-7.36 (m, 6H), 7.36-7.29 (m, 6H), 7.29-7.22 (m, 3H), 6.54 (s, 0.5H), 4.30 (d, *J* = 97.6 Hz, 1H), 3.59-3.52 (m, 37H), 3.50 (s, 2H), 3.49-3.44 (m, 1.5H), 3.40 (q, *J* = 6.5, 6.1 Hz, 1.5H), 3.29 (s, 2H), 3.19 (dd, *J* = 9.8, 4.0 Hz, 1H), 2.73-2.51 (m, 4H), 1.46-1.25 (m, 9H).

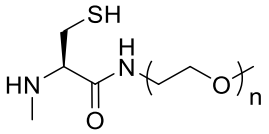

Boc-*N*MeCys(**Trt**)-PEG800 (150 mg, 0.03 mmol), TFA (9500 μL, 12.8 mmol) and triisopropylsilane (500 μL, 3.0 mmol) were added to a 25 mL round-bottom flask. The reaction was stirred at room temperature for 20 mins and complete detected by UPLC. After checking, the reaction was

concentrated under reduced pressure to provide a yellow oil and was diluted with H_2O (50 mL) and washed with Et_2O (5×50 mL). The aqueous layer was concentrated in vacuum to provide isolate *N*MeCys-PEG800 (112 mg, 95%).

^{1}H NMR (400 MHz, CD_3OD, 298K) δ 4.00 (t, J = 5.4 Hz, 1H), 3.84-3.38 (m, 74H), 3.36 (s, 3H), 3.06 (dd, J = 5.5, 3.0 Hz, 1H), 2.75 (d, J = 8.5 Hz, 3H);

^{13}C NMR (100 MHz, $CDCl_3$, 298K) δ 165.91, 61.99, 39.06, 31.90, 31.26, 23.88, 19.93, 14.04;

MS (ESI+) see 3.4.1.1.

E 2.2.9 Synthesis of C8BA-*N*MeCys-PEG800

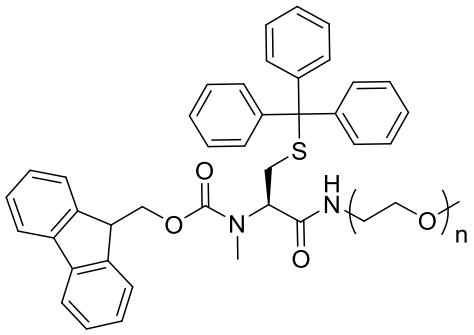

Fmoc-*N*MeCys(**Trt**)-OH (604 mg, 1.0 mmol), HATU (518 mg, 1.4 mmol) and DIEA (256 μL, 1.6 mmol) were added to a 50 mL flask and dissolved with acentonitrile (20 mL). The mixture solution was stirring under nitrogen protection for 60mins and Polyethylene glycol 800 (PEG800) (641 mg, 0.8 mmol) was added to the flask. The reaction was complete detected by UPLC and the mixture was diluted with CH_2Cl_2 (100 mL) and washed with saturated $NaHCO_3$ solution (3×100 mL), saturated brine (100 mL). The organic layer was dried over Na_2SO_4, filtered and concentrated in vacuum. Flash chromatography (SiO_2, CH_2Cl_2: methanol v/v 0, 10:1, 1:1) was used to isolate **Fmoc**-*N*MeCys(**Trt**)-PEG800 as a (1.24 g, 90%).

^{1}H NMR (400 MHz, $CDCl_3$, 298K) δ 7.75 (d, J = 7.6 Hz, 2H), 7.57 (dt, J = 7.6, 4.5 Hz, 2H), 7.49-7.33 (m, 8H), 7.32-7.16 (m, 11H), 6.19 (t, J = 5.0 Hz, 0.6H), 5.98-5.86 (m, 0.4H), 4.48 (dd, J = 10.2, 6.7 Hz, 1H), 4.41 (dd, J = 10.6, 5.2 Hz, 1H), 4.36-4.21 (m, 2H), 3.85-3.49 (m, 63H), 3.47 (s, 3H), 3.44 (q, J = 4.2, 3.1 Hz, 2H), 3.37 (s, 3H), 3.36-3.25 (m, 1H), 2.92-2.70 (m, 1H), 2.67 (s, 3H), 2.61 (s, 0.5H), 2.52-2.36 (m, 0.2H).

^{13}C NMR (100 MHz, $CDCl_3$, 298K) δ 144.48, 141.30, 129.60, 127.97, 127.74, 127.15, 127.10, 126.76, 125.12, 125.07, 125.01, 119.98, 77.36, 77.04, 76.72, 71.95, 70.62, 70.58, 70.54, 70.48, 70.29, 69.61, 67.88, 59.04, 58.14, 58.13, 50.84, 47.17, 39.21, 30.27.

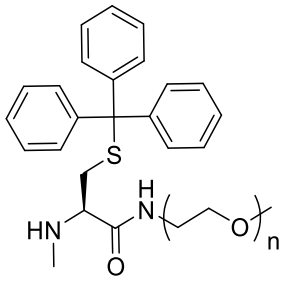

Fmoc-*N*MeCys (**Trt**)-PEG800 (1.24 g, 1.0 mmol), piperazine (4.06 g, 47.0 mmol) and HOBt (707 mg, 5.2 mmol) were added to a 25 mL round-bottom flask with methanol (10 mL). The reaction was stirred at room temperature for 2 hours and complete detected by UPLC. After checking, the mixture was diluted with ethyl acetate (100mL) and washed with saturated $NaHCO_3$ solution (3×100 mL), saturated brine (100mL). The organic layer was dried over Na_2SO_4, filtered and concentrated in vacuum. Flash chromatography (SiO_2, CH_2Cl_2: methanol v/v 0, 10:1) was used to isolate *N*MeCys(**Trt**)-PEG800 as a yellow oil (511 mg, 85%).

^{1}H NMR (400 MHz, $CDCl_3$, 298K) δ 7.38-7.33 (m, 6H), 7.25-7.18 (m, 7H), 7.16 (t, J = 1.3 Hz, 1H), 7.15-7.11 (m, 2H), 3.77-3.72 (m, 1H), 3.68-3.53 (m, 61H), 3.52-3.45 (m, 6H), 3.44-3.39 (m, 2H), 3.39-3.32 (m, 1H), 3.31 (s, 3H), 3.30-3.22 (m, 1H), 2.59 (dd, J = 12.2, 3.9 Hz, 1H), 2.52 (dd, J = 8.5, 4.0 Hz, 1H), 2.40 (dd, J = 12.2, 8.5 Hz, 1H), 2.08 (s, 3H);

^{13}C NMR (100 MHz, $CDCl_3$, 298K) δ 172.30, 144.54, 129.58, 127.97, 126.78, 77.38, 77.06, 76.74, 71.94, 70.60, 70.56, 70.51, 70.30, 69.92, 66.87, 63.22, 59.03, 38.77, 35.00, 34.79.

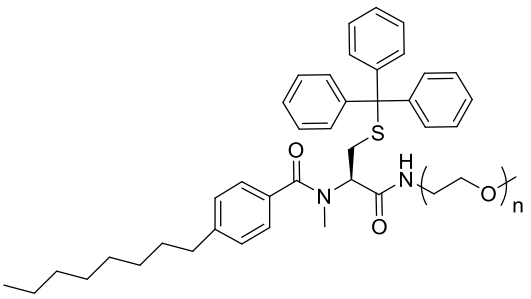

4-octylbenzoic acid(C8BA) (210 mg, 0.9 mmol), *N*MeCys (**Trt**)-PEG800 (630 mg, 0.6 mmol), HATU (515 mg, 1.35 mmol) and DIEA (268 μL, 1.62 mmol) were added to a 10 mL flask and

dissolved with DMF (5 mL). The mixture solution was stirring under nitrogen protection in microwave synthesizer for 20 mins (35 W, 70 ℃). The reaction was complete detected by UPLC and the mixture was diluted with ethyl acetate (50 mL) and washed with saturated $NaHCO_3$ solution (3×50 mL), saturated brine (50 mL). The organic layer was dried over Na_2SO_4, filtered and concentrated in vacuum. Flash chromatography (SiO_2, CH_2Cl_2: methanol v/v 0, 10:1, 8:1) was used to isolate C8BA-*N*MeCys(**Trt**)-PEG800 as a yellow oil (700 mg, 84%).

^{1}H NMR (400 MHz, $CDCl_3$, 298K) δ 7.45 (d, J = 7.7 Hz, 4H), 7.41-7.11 (m, 15H), 6.82 (t, J = 3.8 Hz, 1H), 4.76 (dd, J = 10.0, 5.4 Hz, 1H), 3.82-3.68 (m, 1H), 3.69-3.55 (m, 63H), 3.55-3.50 (m, 2H), 3.47 (t, J = 5.7 Hz, 2H), 3.36 (s, 3H), 3.35 (d, J = 3.8 Hz, 1H), 2.86-2.71 (m, 2H), 2.69 (d, J = 13.8 Hz, 3H), 2.63-2.56 (m, 2H), 1.59 (t, J = 3.8 Hz, 2H), 1.53-1.12 (m, 12H), 0.86 (t, J = 6.8 Hz, 3H);

^{13}C NMR (100 MHz, $CDCl_3$, 298K) δ 173.19, 169.55, 145.68, 144.48, 132.44, 129.54, 128.36, 127.99, 127.79, 126.77, 77.39, 77.07, 76.75, 71.89, 70.53, 70.48, 70.45, 70.31, 69.71, 66.85, 59.01, 56.25, 50.73, 39.13, 35.86, 33.57, 31.86, 31.25, 29.75, 29.43, 29.23, 22.65, 14.10.

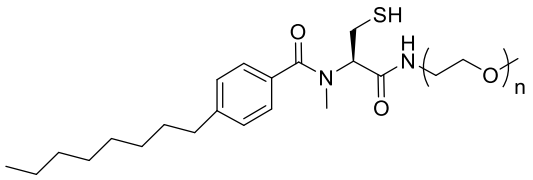

C8BA-*N*MeCys (**Trt**)-PEG800 (700 mg, 1.1 mmol), TFA (1800 μL, 18% solvent) and (200 μL, 2% solvent) were added to a 25 mL round-bottom flask with CH_2Cl_2 (10 mL). The reaction was stirred at room temperature for 10 mins and complete detected by UPLC. After checking, the reaction was concentrated under reduced pressure to provide a yellow oil and was diluted with H_2O (50 mL) and washed with Et_2O (5×50 mL). The aqueous layer was concentrated in vacuum to provide isolate C8BA-*N*MeCys-PEG800 (42 mg, 15%).

^{1}H NMR (400 MHz, $CDCl_3$, 298K) δ 7.35 (d, J = 7.8 Hz, 2H), 7.14 (d, J = 7.8 Hz, 2H), 5.07 (s, 1H), 3.78-3.44 (m, 64H), 3.40 (s, 4H), 3.30 (s, 3H), 3.15 (dd, J = 12.3, 6.3 Hz, 1H), 2.90 (s, 3H), 2.55 (t, J = 7.8 Hz, 2H), 1.53 (q, J = 7.4 Hz, 2H), 1.29-1.12 (m, 10H), 0.85-0.75 (m, 3H);

^{13}C NMR (100 MHz, $CDCl_3$, 298K) δ 173.54, 169.46, 145.78, 132.08, 128.34, 127.74, 127.58, 77.40, 77.08, 76.77, 71.66, 70.17, 70.11, 70.00, 69.71, 59.75, 58.92, 39.18, 35.84, 33.87, 31.84, 31.22, 29.40, 29.26, 29.21, 22.63, 14.08.

E2.3 Synthesis, isolation and purification of *N*MeCys peptide segments

E 2.3.1 Fmoc-SPPS general procedures

Standard solid phase peptide synthesis (SPPS) was performed using standard Fmoc/*tert*-butyl chemistry and using Microwave assisted solid phase peptide synthesis with a CEM Liberty 1^{TM} microwave synthesizer starting with a Fmoc-Rink-amide MBHA resin (0.74 mmol/g). A typical synthesis was done on a 0.5 mmol scale. For each amino acid, double couplings were performed at 70 °C and 35 W (microwave power) for 5 min using 4-fold molar excess of each Fmoc L-aa (10 mL of a 0.2 M solution in DMF), HBTU (4 mL of a 0.5 M solution in DMF) and DIEA (2 mL of a 2 M solution in NMP). Fmoc groups were deprotected with 2 successive treatments with 20 vol% piperidine solution in DMF (15 mL, 70 °C for 3 min, 55 W).

E 2.3.2 *N*-methyl cysteine coupling

N-methyl cysteine residues were attached by preparing the activated carboxylic acid manually: **Fmoc**-*N*MeCys(**Trt**)-OH (4 eq.), HATU (4 eq.), DIPEA (6 eq.) in DMF (4 mL). This mixture was then added to the reaction vessel and coupled using a two-step microwave program previously described for cysteine residues.

E 2.3.3 Peptide cleavage from solid phase-resin

The resin was suspended in a 10mL solution of TFA/TIS/2-2` ethyldioxy)diethanethiol/H2O: 92.5/2.5/2.5/2.5 vol%. After 1h, the resin was filtered and washed with TFA (5 mL). The combined filtrates were concentrated in vacuo and then added to cold diethylether (200 mL) to precipitate the crude peptides. The solids were separated by centrifugation, washed with cold diethylether (2 x 40 mL) and dried under argon to afford crude peptides.

E 2.3.4 Peptide purification

Crude peptides were then purified by High-Performance Liquid Chromatography (HPLC) Waters AutoPurification® system, coupled to a Waters 2489 UV/Visible detector and Waters SQD 3100 electrospray mass detector. Purification was performed using 0.1 % formic acid in water (A) and 0.1 % formic acid in methanol (B) as the two mobile phases on either a preparative SunFire® Prep C18

QBD™ 5 µm 19 x150 mm column from Waters or a preparative XBridge® Prep C18 5 µm QBD™ 19 x150 mm column from Waters.

A typical gradient is given here:

Time (min)	Flow (mL/min)	% A	% B
0	24.5	95	5
0.95	24.5	95	5
25	24.5	5	95
33	24.5	5	95
34	24.5	95	5
34.9	24.5	95	5

Model peptide P1: Fmoc MW-SPPS on H-Rink Amide ChemMatrix® resin at 0.10 mmol scale. Arg-3, Gly-5 and MeCys-6 were attached by double coupling. FmocMeCys(Trt)-OH was used for the incorporation of the MeCys residue. Analytical HPLC-MS was performed at a flow rate of 2 mL/min using a gradient of 5-40% solvent A in solvent B over 16 min, retention time 9.6 min. The crude peptide was purified by preparative HPLC-MS yielding a purity of >95% after lyophilization. MS-ESI (m/z): calcd. for $C_{30}H_{51}N_{10}O_7S^+$ $[M+H]^+$ 695.36, found 695.58.

Model peptide P2: Fmoc MW-SPPS on H-Rink Amide ChemMatrix® resin at 0.10 mmol scale. Arg-2 and Ala-7 were attached by double coupling. FmocMeCys(Trt)-OH was used for the incorporation of the MeCys residue. Analytical HPLC-MS was performed at a flow rate of 2 mL/min using a gradient of 5-40% solvent A in solvent B over 16 min, retention time 6.2 min. The crude peptide was purified by preparative HPLC-MS yielding a purity of >84% after lyophilization. MS-ESI (m/z): calcd. for $C_{35}H_{58}N_{12}O_9S^+$ $[M+H]^+$ 823.42, found 823.32.

Model peptide P2': Fmoc MW-SPPS on H-Rink Amide ChemMatrix® resin at 0.10 mmol scale. Arg-2 and Tyr-5 were attached by double coupling. FmocMeCys(StBu)-OH was used for the incorporation of the MeCys residue and the peptide was deprotected using 20% β-mercaptoethanol in DMF containing 0.1 M NMM prior to cleavage. Analytical HPLC-MS was performed at a flow rate of 2 mL/min using a gradient of 5-30% solvent A in solvent B over 16 min, retention time 5.1 min. The crude peptide was purified by preparative HPLC-MS yielding a purity of >86% after

lyophilization. MS-ESI (m/z): calcd. for $C_{26}H_{43}N_{10}O_7S^+$ $[M+H]^+$ 639.30, found 639.45

Model peptide P3: Fmoc MW-SPPS on H-Rink Amide ChemMatrix® resin at 0.10 mmol scale. Arg-3, Gly-5, Arg-7 and Ala-12 were attached by double coupling. FmocMeCys (Trt)-OH was used for the incorporation of the MeCys residue. Analytical HPLC-MS was performed at a flow rate of 2 mL/min using a gradient of 5-30% solvent A in solvent B over 16 min, retention time 9.6 min. The crude peptide was purified by preparative HPLC-MS yielding a purity of >97% after lyophilization. MS-ESI (m/z): calcd. for $C_{61}H_{99}N_{20}O_{15}S^+$ $[M+H]^+$ 1383.72, found 1384.67.

Annex

Annex 1. NMR Characterization of the *N*-(methyl)-cysteine derivatives utilized on the manuscript

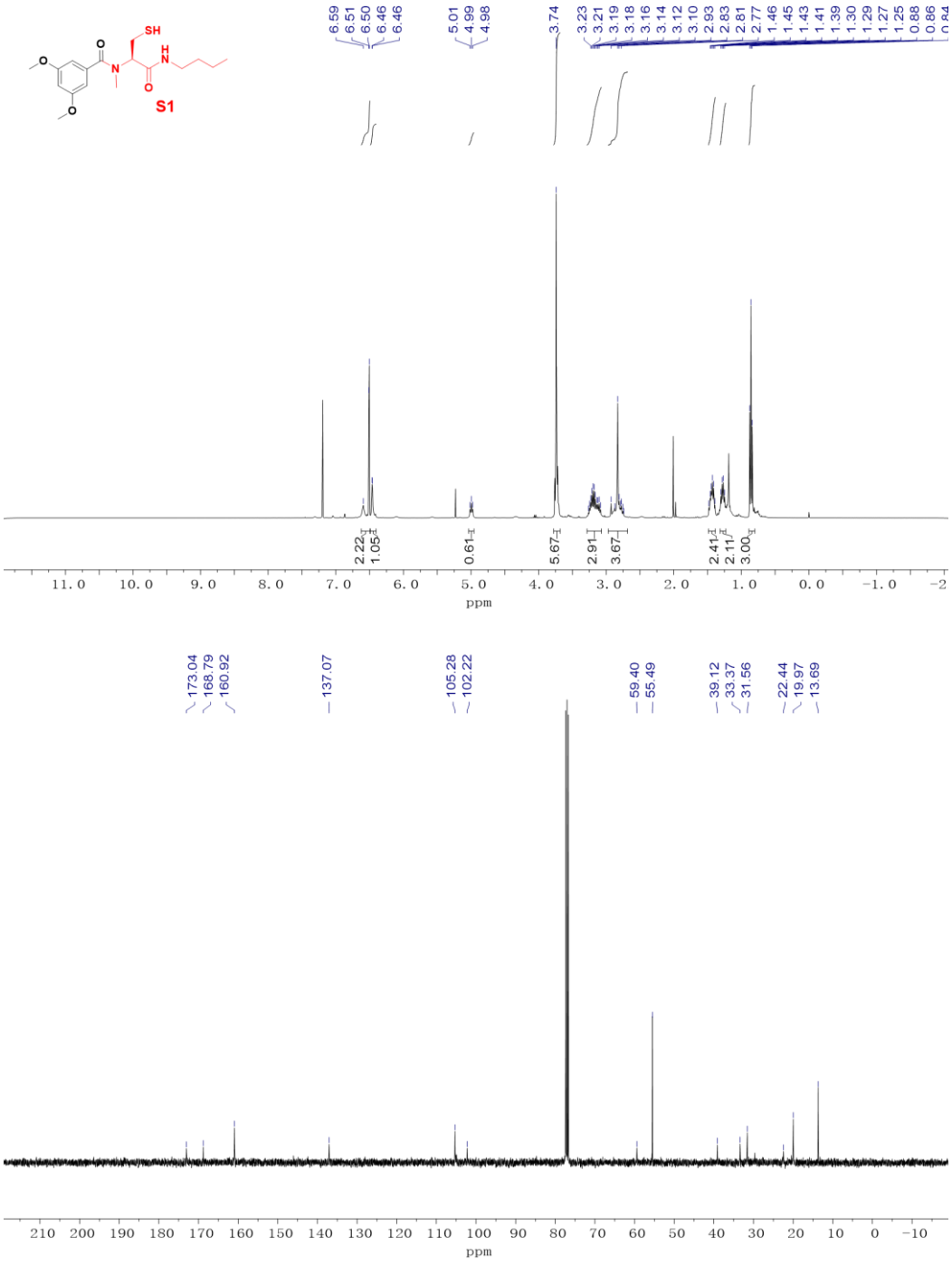

Figure A1 | ^{1}H-NMR (above) and ^{13}C-NMR spectra (below) of S1.

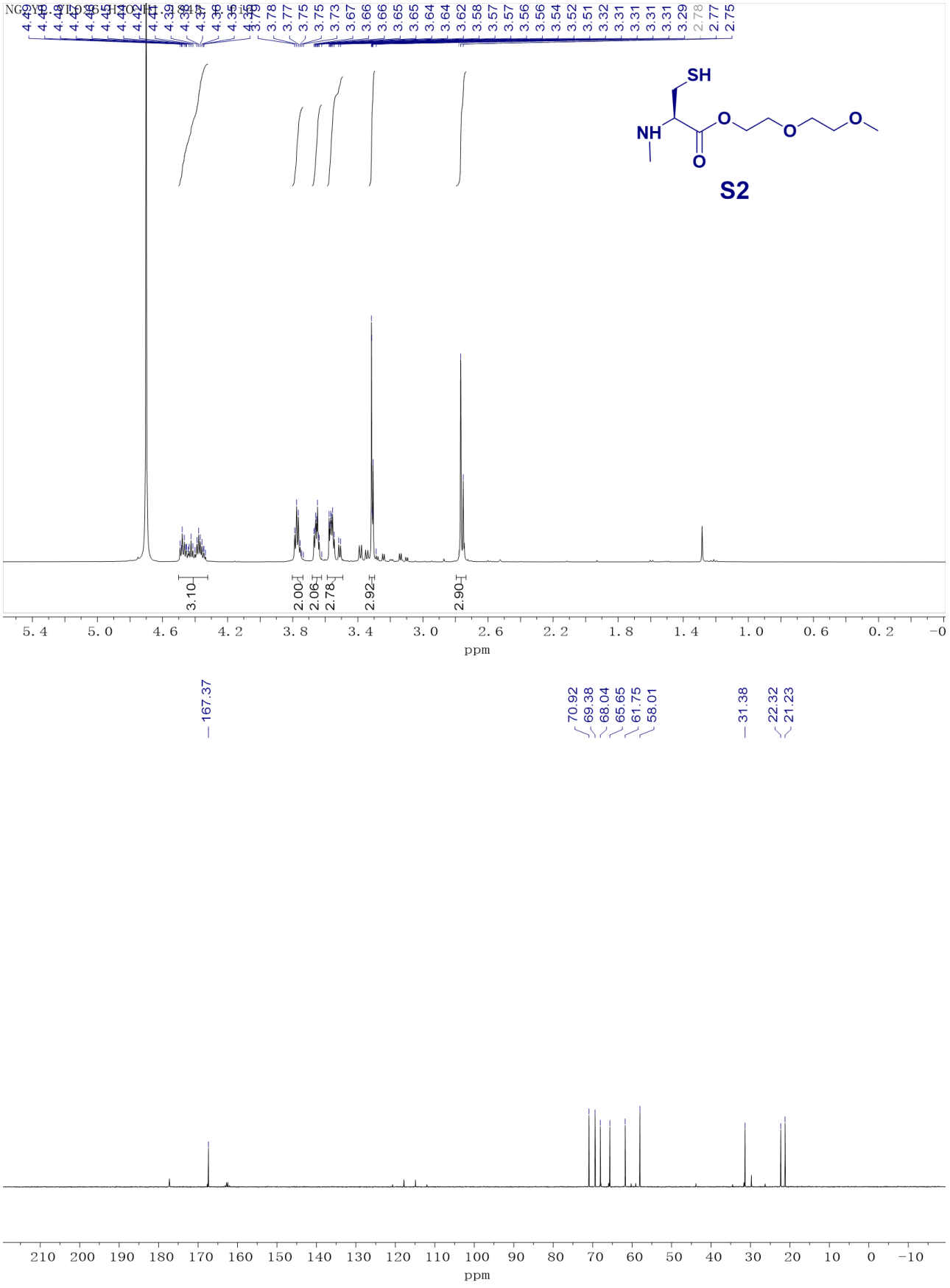

Figure A2 | ^{1}H-NMR (above) and ^{13}C-NMR spectra (below) of S2.

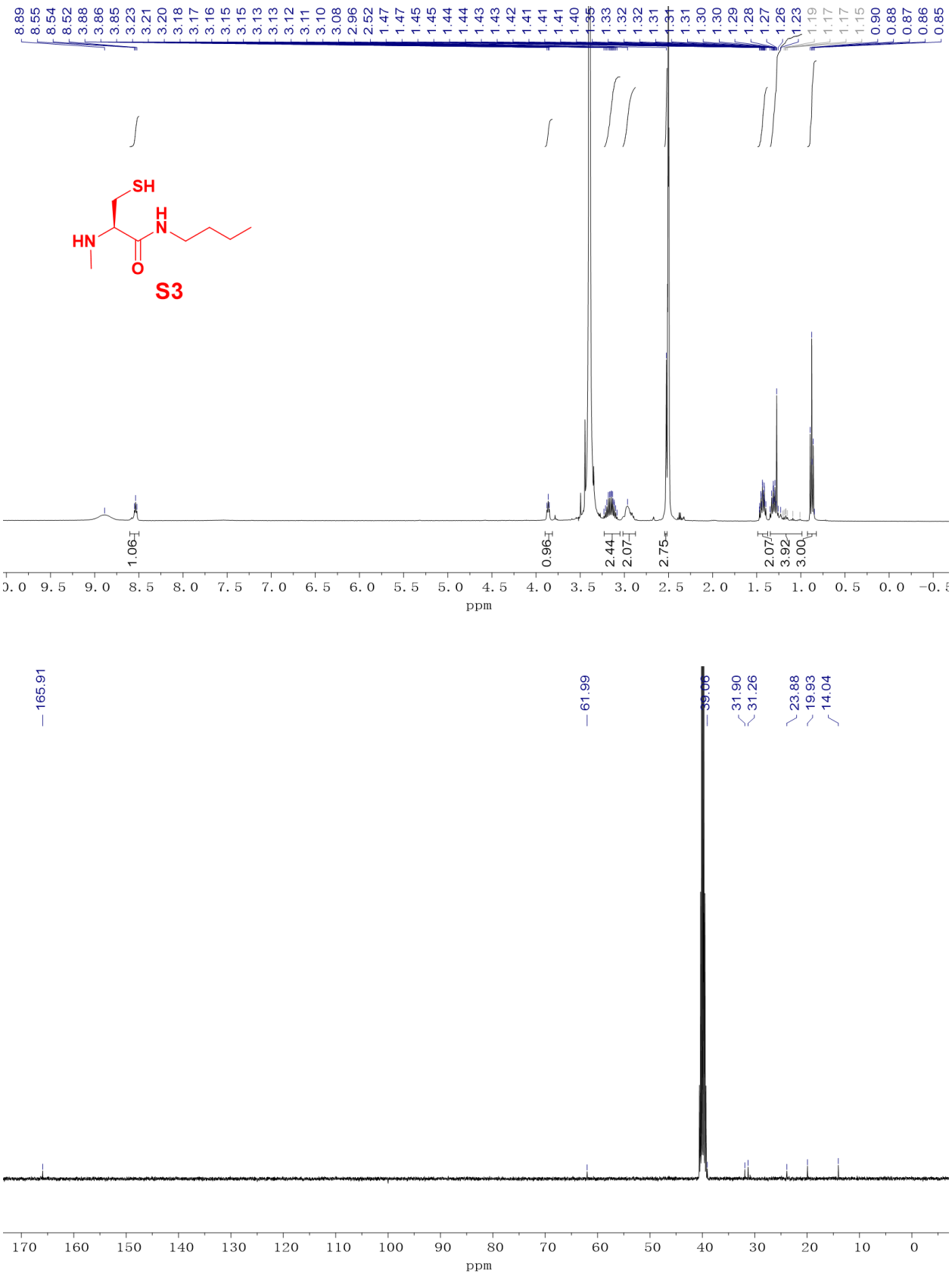

Figure A3 | ^{1}H-NMR (above) and ^{13}C-NMR spectra (below) of S3.

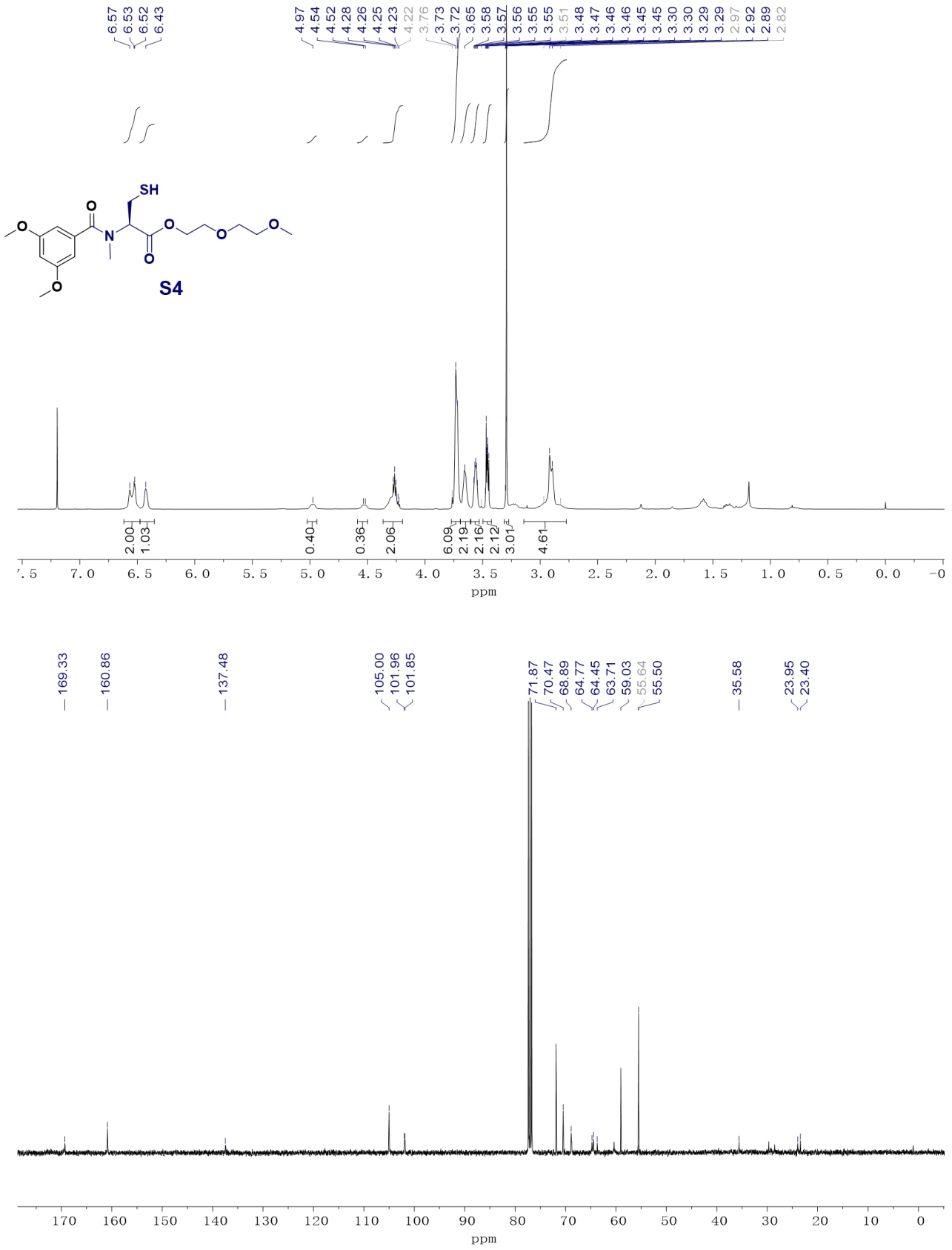

Figure A4 | ^{1}H-NMR (above) and ^{13}C-NMR spectra (below) of S4.

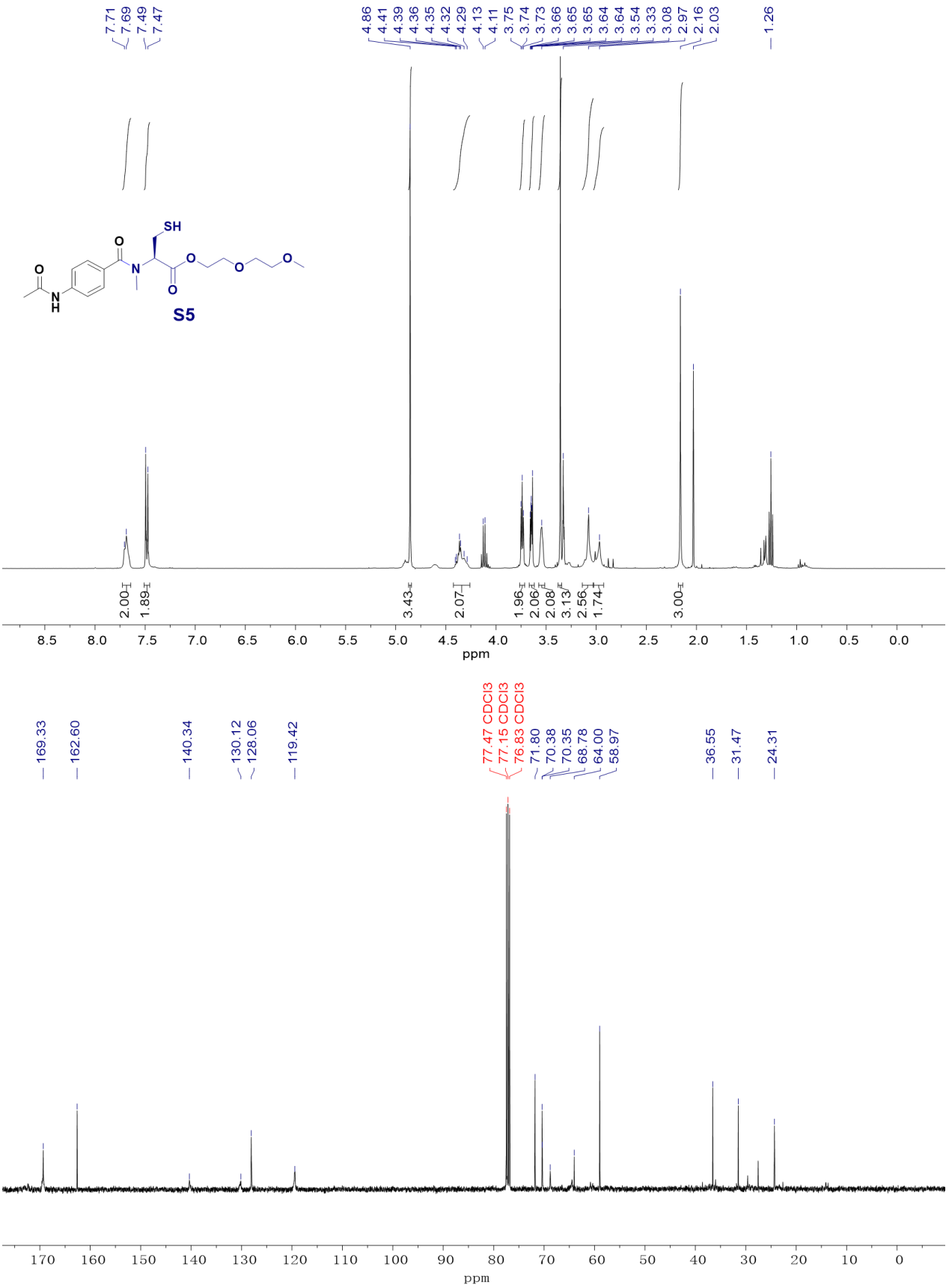

Figure A5 | ^{1}H-NMR (above) and ^{13}C-NMR spectra (below) of S5.

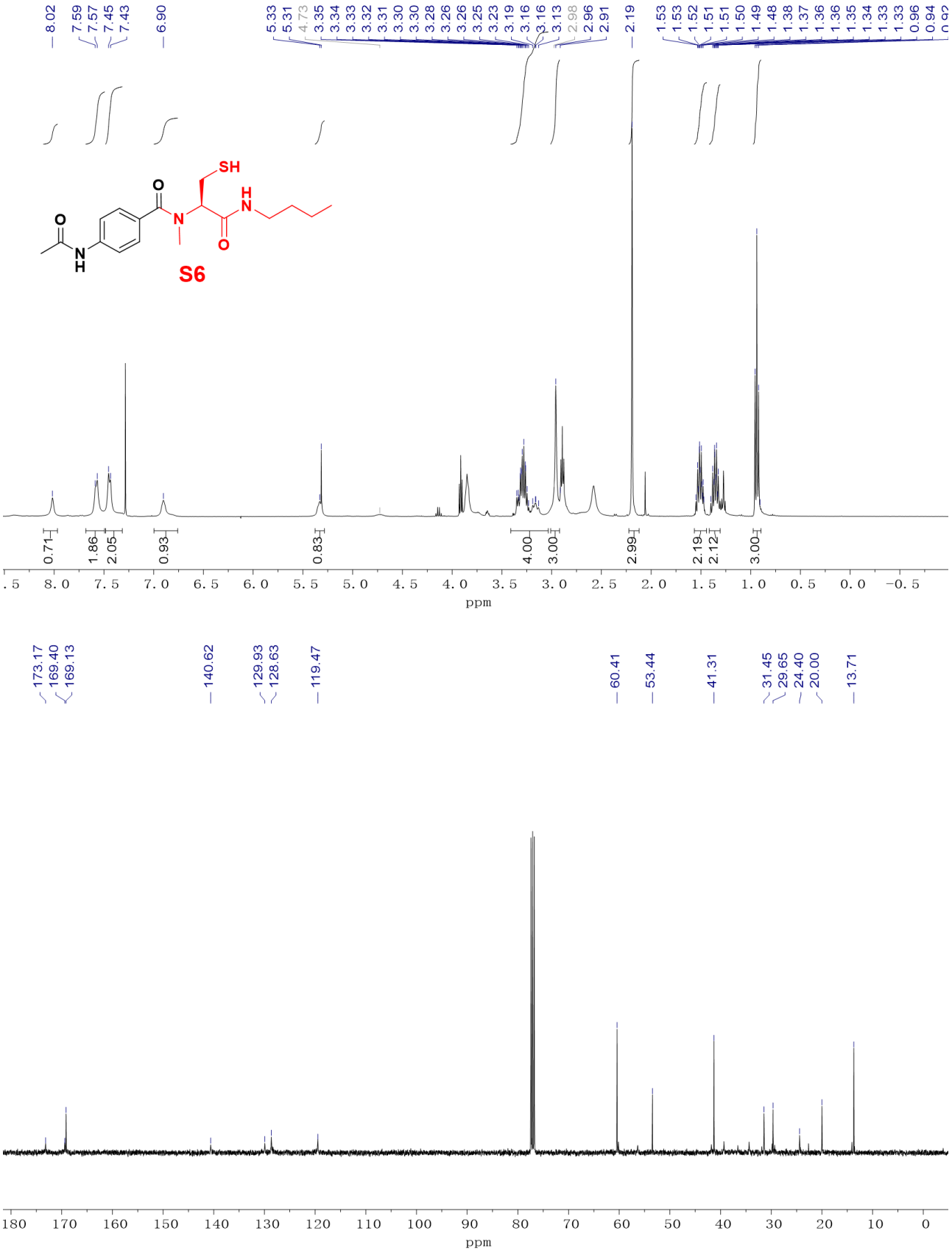

Figure A6 | ^{1}H-NMR (above) and ^{13}C-NMR spectra (below) of S6.

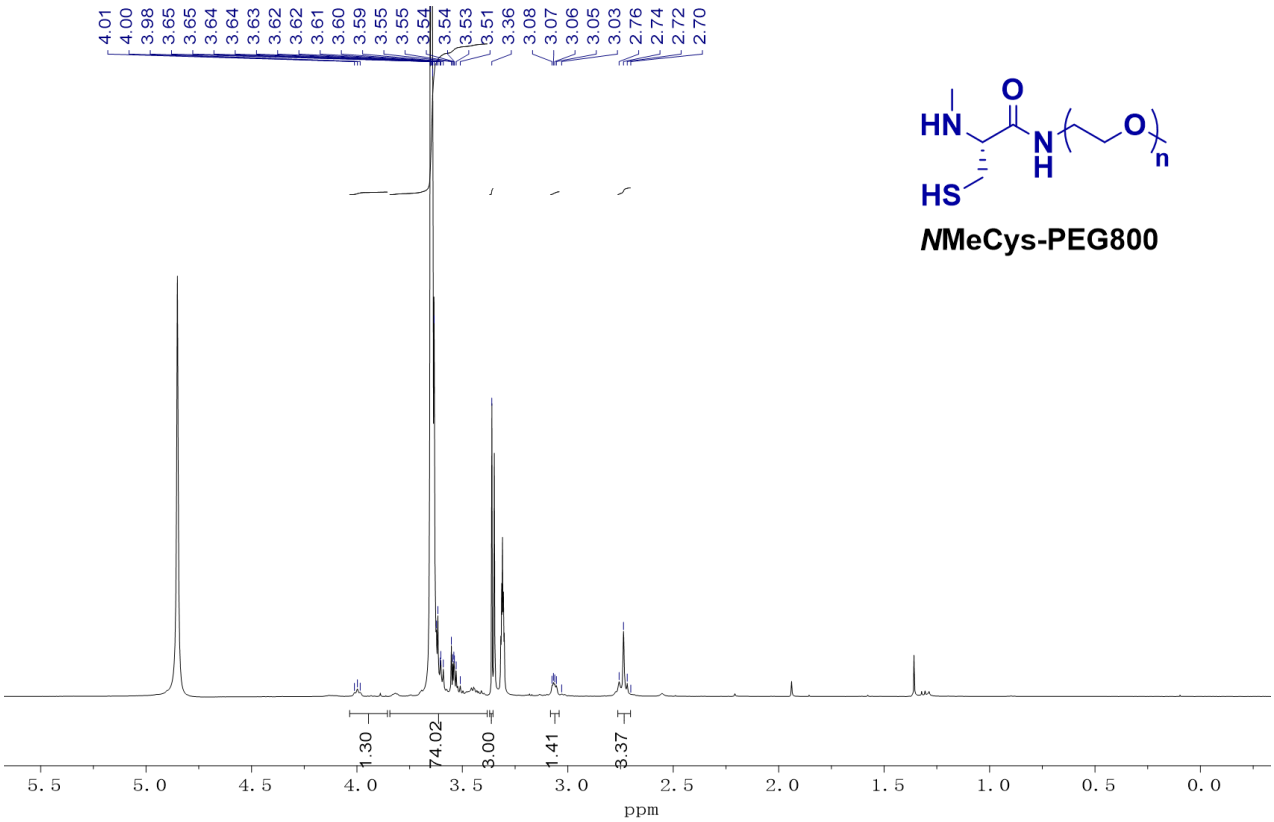

Figure A7 | ^{1}H-NMR spectrum of *N*MeCys-PEG800.

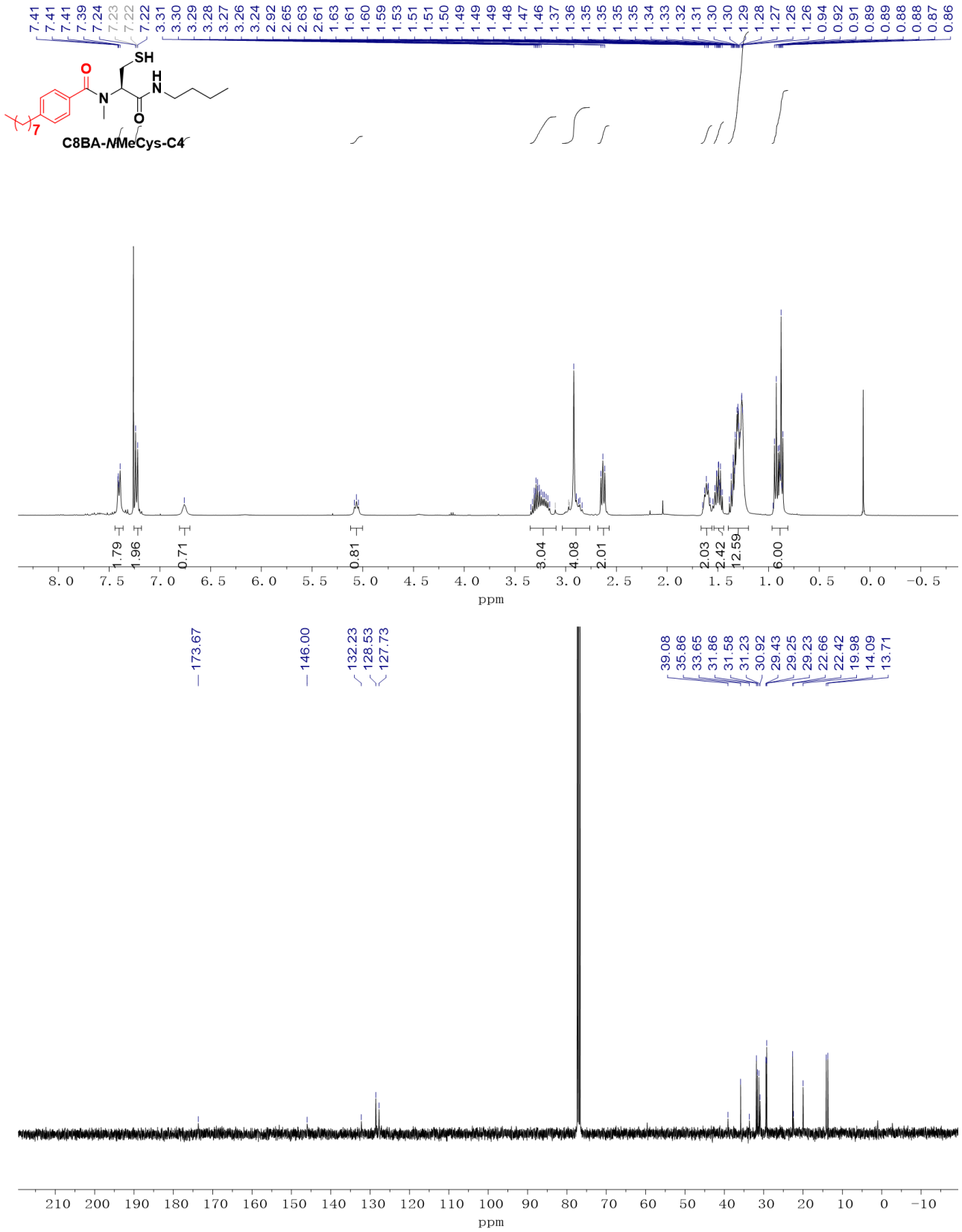

Figure A8 | ^{1}H-NMR (above) and ^{13}C-NMR spectra (below) of C8BA-*N*MeCys-C4.

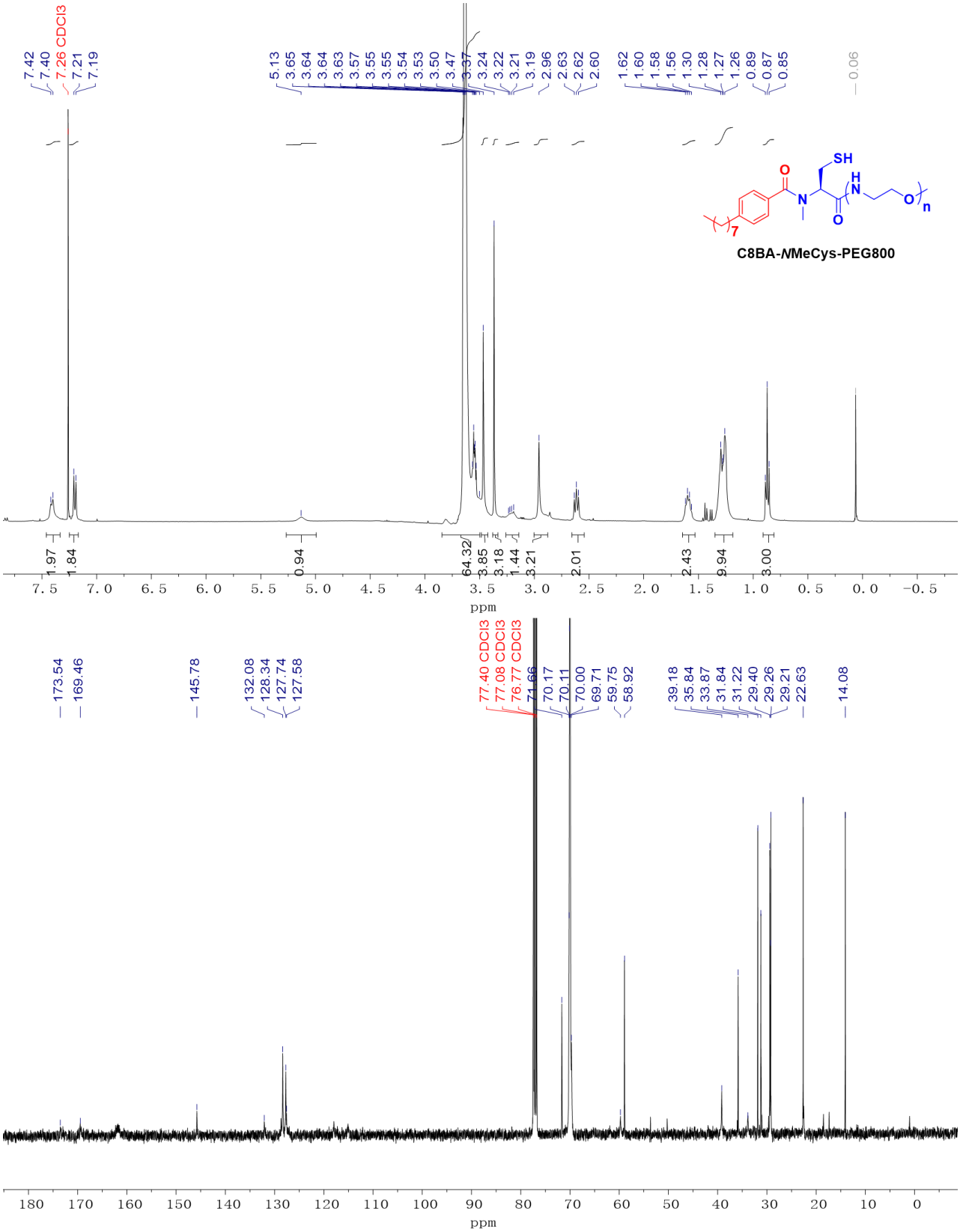

Figure A9 | ^{1}H-NMR (above) and ^{13}C-NMR spectra (below) of C8BA-*N*MeCys-PEG800.

Annex 2. Stability of C8BA-*N*MeCys-PEG800 by UPLC

We independently evaluated the stability of C8BA-*N*MeCys-PEG800 under the dcNCL exchange conditions (Figure A10a)) by using both the UV and mass traces recorded on UPLC. The table in Figure A10b) shows their theoretical mass-to-charge ratio for $z = 1$ (m/z_b), and $z = 2$ (m/z_c) depending on the numbers of ethylene oxide units of C8BA-*N*MeCys-PEG800. Calibration curves for C8BA-*N*MeCys-PEG800 were established based on the integrated area of the UV peak at known concentrations under conditions identical as the ones used for exchange reactions.

a)

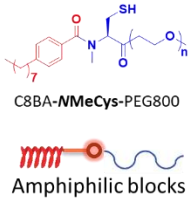

b)

N[a]	m/z_b	m/z_c
15	1025.67	513.34
16	1069.7	535.355
17	1113.73	557.37
18	1157.76	579.385
19	1201.79	601.4
20	1245.82	623.415
21	1289.85	645.43
22	1333.88	667.445
23	1377.91	689.46
24	1421.94	711.475

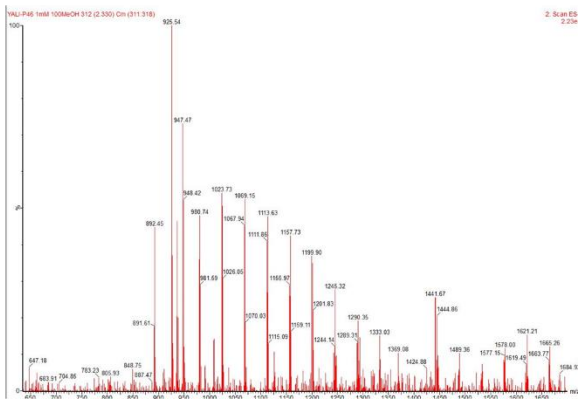

Figure A10 | a) Molecular structure and schematic representation of C8BA-*N*MeCys-PEG800. b) Theoretical mass-to-charge ratio for $z = 1$ (m/z_b), and $z = 2$ (m/z_c) depending on the numbers of ethylene oxide units of C8BA-*N*MeCys-PEG800. c) mass spectrum of the stock solution of C8BA-*N*MeCys-PEG800. The stock solution as kept in a 1/1 (v/v) of methanol and milli-Q water containing 150 mM TCEP and 300 mM sodium ascorbate.

Interestingly, when increasing the water percentage of the stock solution of C8BA-*N*MeCys-PEG800 at 1 mM, UPLC peaks became broader and weaker (Figure A911a)), although no linear relationship between the UV peak area and the water percentage was found. This trend could be explained by the decrease amount of dispersed C8BA-*N*MeCys-PEG800 in solution when the water percentage increases. This could be caused by the self-assembly (or micelle formation) of this amphiphilic compound. In order to overcome this problem, reaction solutions were diluted with MeOH to 5%/95% water/MeOH before injection in the UPLC, as there is no obvious difference between the calibration curves of stock solutions in 100% Methanol and in 95% Methanol.

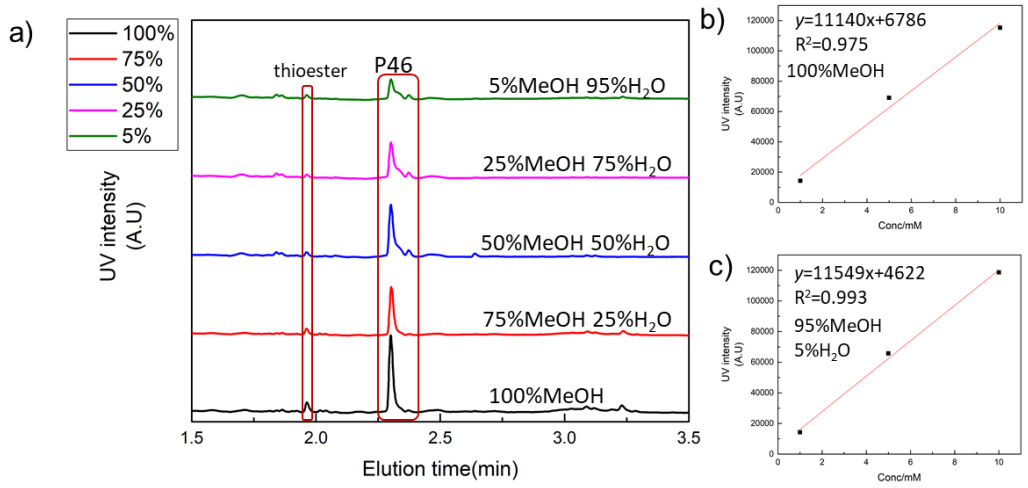

Figure A11 | a) UPLC chromatograms (UV traces) of 1 mM solutions of C8BA-*N*MeCys-PEG800 starting from different water percentage of the stock solution. b-c) Calibration curve obtained by linear regression for C8BA-*N*MeCys-PEG800 in b) pure methanol and c) in a 95/5 (v/v) of methanol and milli-Q water containing 150 mM TCEP and 300 mM sodium ascorbate.

Annex 3. UPLC data for F_5K_5-*N*MeCys

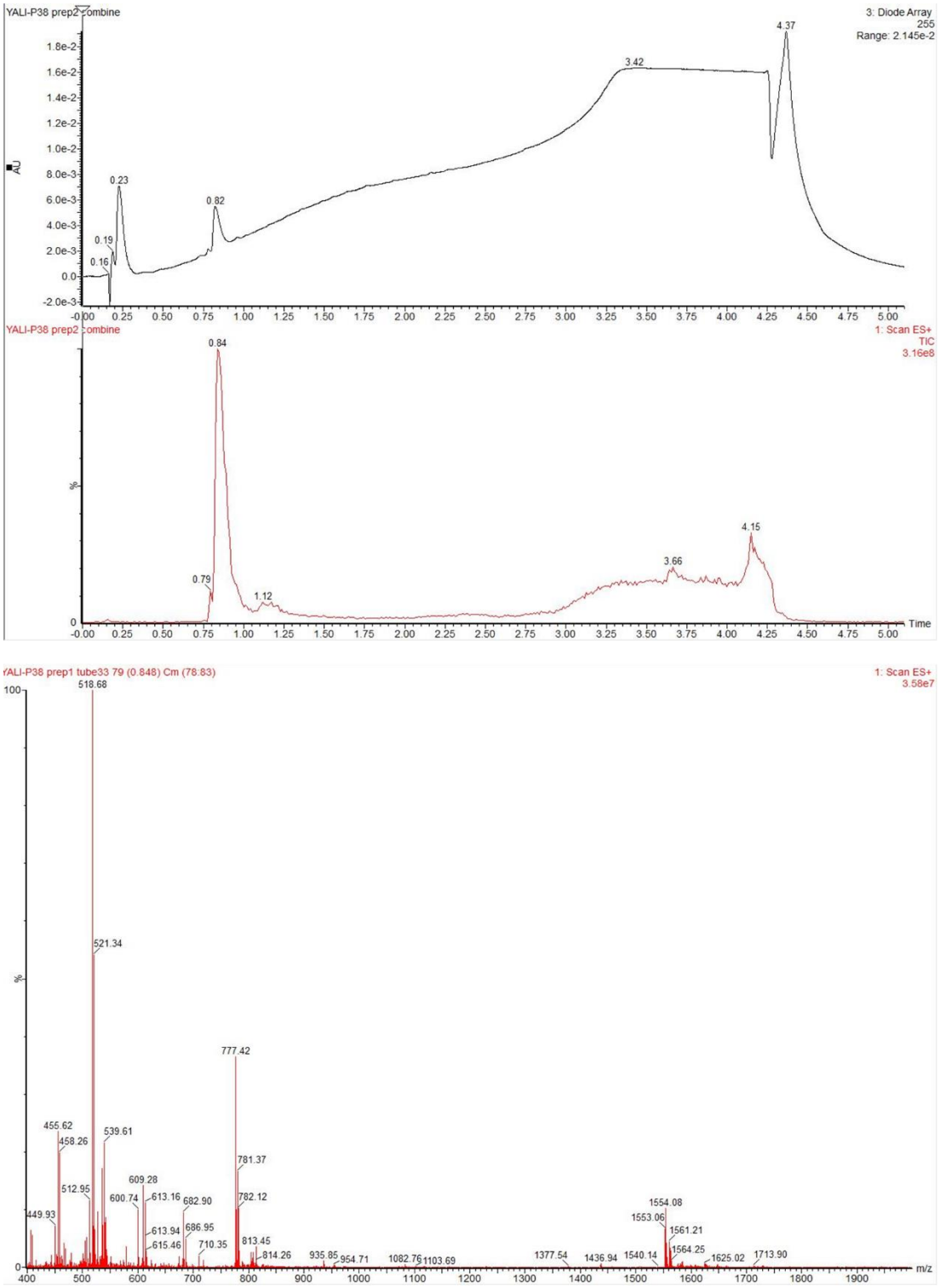

Figure A12| UPLC chromatograms (UV and Mass traces) of F_5K_5-*N*MeCys in pure methanol.

Yali ZENG

Vers une efficace mise en œuvre de la ligation chimique native dynamique

Résumé

La chimie covalente dynamique (DCvC) trouve des applications dans divers domaines de recherche, tels que la découverte de médicaments, la biotechnologie, la science des matériaux, *etc.* Cependant, le développement de nouvelles réactions covalentes dynamiques a été limité par divers facteurs. A partir d'une réaction réversible d'échange d'amide décrite récemment, ce doctorat avait pour objectif d'optimiser la méthodologie de ligation chimique native covalente dynamique (dcNCL), afin de construire des bibliothèques covalentes dynamiques basées sur la dcNCL et pouvant conduire à la formation d'un auto-assemblage après amplification de constituants spécifiques.

Dans le premier chapitre, nous présentons une introduction générale sur la DCvC, qui identifie les réactions covalentes dynamiques les plus utilisées. Nous décrivons ensuite leurs applications au sein de bibliothèques combinatoires dynamiques (DCLs) en se focalisant particulièrement sur les systèmes impliquant des peptides et des protéines.

Dans le deuxième chapitre, nous rappelons les principes de la dcNCL. En étudiant divers paramètres qui gouvernent la dcNCL sur des peptides modèles ou des petites molécules, nous proposons une optimisation du protocole de dcNCL dans diverses conditions environnementales.

Le troisième chapitre décrit la première application de notre approche méthodologique à des DCLs complexes contenant simultanément des constituants hydrophiles, hydrophobes et amphiphiles, conduisant à l'amplification d'un auto-assemblage supramoléculaire unique.

En résumé, cette thèse décrit l'optimisation méthodologique de la dcNCL et son application à des DCLs capables de sélectionner des nanostructures auto-assemblées. Ces travaux permettent d'envisager d'étendre cette nouvelle liaison covalente dynamique à diverses applications.

Mots clés: Chimie covalente dynamique, ligation chimique native covalente dynamique, peptides, amphiphiles

Résumé en anglais

Dynamic covalent chemistry (DCvC) has found various applications in diverse research areas, such as drug discovery, biotechnology, material science, *etc*, over the last twenty years. However, the development of new dynamic covalent reactions has been limited by several factors. Based on a recent reversible amide exchange reaction, this PhD project aims at optimizing the methodology of the dynamic covalent native chemical ligation (dcNCL), in order to construct dcNCL-based dynamic covalent libraries (DCLs), which could undergo self-assembly at the mesoscopic scale by forcing the library to amplify specific constituents.

In the first chapter, we give a general introduction on DCvC, and highlight the most important dynamic covalent reactions. We then describe their corresponding applications in dynamic combinatorial libraries with a particular focus on biosystems involving peptides and proteins.

In the second chapter, we first recall the principles of dcNCL as initially reported by our group in 2014. Then, we focus on the various parameters which govern dcNCL in order to optimize the reaction conditions first on some model peptides and then on small molecules. Overall, this chapter provides an optimum protocol to achieve dcNCL in various environmental conditions.

In the third chapter, we describe the first application of our methodological approach to complex dynamic libraries containing simultaneously hydrophilic and hydrophobic building blocks, leading to the amplification of a particular type of supramolecular self-assembly.

Overall, this thesis describes the methodological optimization of dcNCL and its use in DCLs for the selection of self-assembled nanostructures. It provides experimental evidences for the extension of this new dynamic covalent bond into various applications.

Keywords: Dynamic covalent chemistry, dynamic covalent native chemical ligation, peptides, amphiphiles